

NONLINEAR PANEL FLUTTER AND ITS  
INTERACTION WITH FORCING EXCITATIONS

by

CHING-CHIANG KUO

B.S., Cheng Kung University, Taiwan

(1965)

M.S., University of Iowa, Iowa City, Iowa

(1968)

SUBMITTED IN PARTIAL FULFILLMENT

OF THE REQUIREMENTS FOR THE

DEGREE OF DOCTOR OF PHILOSOPHY

at the

MASSACHUSETTS INSTITUTE OF TECHNOLOGY

February 1972



Signature of Author \_\_\_\_\_

Department of  
Aeronautics and Astronautics,  
September, 1971

Certified by \_\_\_\_\_

Thesis Supervisor

Accepted by \_\_\_\_\_

Chairman, Departmental Graduate Committee

NONLINEAR PANEL FLUTTER AND ITS  
INTERACTION WITH FORCING EXCITATION

by

CHING-CHIANG KUO

Submitted to the Department of Aeronautics and Astro-  
nautics on September 27, 1971, in partial fulfillment of the  
requirements for the degree of Doctor of Philosophy.

ABSTRACT

This thesis consists of two parts, the first part is concerned with nonlinear panel flutter and the second part concentrates on the interaction of panel flutter with forcing excitation. In both parts von Karman's plate vibration theory and linear Piston Theory are used to represent the elastic forces and aerodynamic forces respectively.

The effect of aerodynamic damping  $\mu/M$ , membrane forces  $R_x$ , viscous structural damping  $g_s$  and hysteretic structural damping  $g_b$ , on the flutter response are studied for both two-dimensional simply-supported plate and three-dimensional clamped-clamped plate. The effect of the length-width ratio  $a/b$  is also studied for three-dimensional plates. Among these parameters  $a/b$  and  $\mu/M$  are favorable both in stabilizing the panel and limiting the amplitude of flutter. Membrane force is unfavorable in destabilizing the panel. Both viscous and hysteretic structural damping are unfavorable in both destabilizing the panel and making the flutter explosive once the critical dynamic pressure  $\lambda_c$  is exceeded.

Forcing excitation tends to increase the flutter stability boundary. Over a certain range of forcing frequency  $\Omega$ , pure forced response may exist for a dynamic pressure  $\lambda$  well above  $\lambda_c$ . Coexistence of both the pure forced response and forcing-flutter interaction are found over a certain range of  $\Omega$  and  $\lambda$ . For some fixed  $\Omega$ , a jump in the response resembling the on-set of flutter may be found at a  $\lambda$  much less than  $\lambda_c$ .

Thesis Advisors:

John Dugundji

Professor of Aeronautics and Astronautics, M.I.T.

Pin Tong

Associate Professor of Aeronautics and Astronautics,  
M.I.T.

Luigi Morino

Associate Professor of Aerospace Engineering, Boston  
University

#### ACKNOWLEDGEMENTS

I wish to express my deepest appreciation to Professor John Dugundji, my thesis adviser, for his continuous guidance and invaluable suggestions during this work. I also wish to thank Professors Luigi Morino and Pin Tong, my thesis committee members, for their constant criticism and many helpful discussions. I wish to express my gratitude to my wife, Ju-pi, for her thoughtfulness and constant encouragement during my stay at M.I.T. and for her typing of the first draft of this thesis. Thanks should also go to Miss Frances Moy for the excellent typing of this manuscript.

This work was supported in part by NASA under Grant No. NGR 22-009-387 administered by Mr. Robert W. Hess and in part by the U. S. Air Force under Contract No. F44620-69-C-0091 administered by Dr. Jacob Pomerantz.

TABLE OF CONTENTS

| <u>Chapter</u> |  | <u>Page</u> |
|----------------|--|-------------|
| 1.             | Introduction                               | 12          |
| 2.             | Nonlinear Panel Flutter--Theory            | 19          |
| 2.1            | Introduction                               | 19          |
| 2.2            | Formulation of Problem                     | 21          |
| 2.2.1          | Two-Dimensional Simply-Supported Panel     | 21          |
| 2.2.2          | Three-Dimensional Clamped-Clamped<br>Panel | 24          |
| 2.3            | Method of Solution                         | 28          |
| 2.3.1          | Two-Dimensional Simply-Supported Panel     | 29          |
| 2.3.2          | Three-Dimensional Clamped-Clamped<br>Panel | 31          |
| 2.4            | Steady State Solution                      | 34          |
| 2.5            | Stability of Steady State Solutions        | 37          |
| 2.6            | Transient Solutions                        | 40          |
| 2.7            | Static Buckling Solutions                  | 42          |
| 3.             | Nonlinear Panel Flutter--Results           | 45          |
| 3.1            | Two-Dimensional Simply-Supported Plates    | 46          |
| 3.1.1          | Critical Dynamic Pressure                  | 47          |
| 3.1.2          | Critical Flutter Frequency                 | 49          |
| 3.1.3          | Limit-Cycle Amplitude                      | 50          |
| 3.1.4          | Frequency of Flutter                       | 52          |
| 3.1.5          | Static Buckling Solutions                  | 52          |
| 3.1.6          | Transient Envelope Solution of Flutter     | 53          |
| 3.2            | Three-Dimensional Clamped-Clamped Panels   | 54          |
| 3.2.1          | Critical Dynamic Pressure                  | 54          |

|          |   |     |
|----------|---|-----|
| 3.2.2    | Critical Flutter Frequency  | 55  |
| 3.2.3    | Limit-Cycle Amplitude   | 56  |
| 3.2.4    | Frequency of Flutter  | 57  |
| 4.       | Nonlinear Interaction of Panel Flutter and<br>Forcing Excitation--Theory  | 58  |
| 4.1      | Introduction  | 58  |
| 4.2      | Formulation of Problems   | 59  |
| 4.3      | Forced Response of Panel Below Flutter                                    | 62  |
| 4.3.1    | Linear System   | 63  |
| 4.3.2    | Nonlinear System  | 64  |
| 4.4      | Interaction of Forcing-Flutter Response                                   | 68  |
| 5.       | Nonlinear Interaction of Panel Flutter and<br>Forcing Excitation--Results | 72  |
| 5.1      | Forced Response of Panel Below Flutter                                    | 73  |
| 5.1.1    | Linear Systems  | 73  |
| 5.1.2    | Nonlinear Systems   | 74  |
| 5.2      | Forcing-Flutter Interaction   | 76  |
| 5.3      | Examples of Numerical Integration   | 80  |
| 5.4      | Comparison of Two-Mode Results with Six-<br>Mode Results                  | 81  |
| 6.       | Conclusions   | 82  |
| Appendix |   |     |
| A.       | Galerkin's Technique for Three-Dimensional<br>Clamped-Clamped Panels      | 86  |
| B.       | Harmonic Balanced Method for Forcing Response<br>Below Flutter            | 96  |
| C.       | Harmonic Balance Method for Forcing-Flutter<br>Interaction                | 123 |

LIST OF TABLES

| <u>No.</u> |   | <u>Page</u> |
|------------|---|-------------|
| 1.         | Effect of Applied Membrane Force $R_y$ on Panel Flutter | 129         |

LIST OF FIGURES

| <u>No.</u> |  | <u>Page</u> |
|------------|--|-------------|
| 1.         | Two-Dimensional Panel Configuration for a Simply-Supported Plate   | 130         |
| 2.         | Three-Dimensional Panel Configuration with Clamped Edges   | 131         |
| 3.         | Convergence of Harmonic Balance Solutions for a Two-Dimensional Simply-Supported Flat Plate  | 132         |
| 4.         | Comparison of Limit-Cycle Deflection Vs. Distance for a Two-Dimensional Simply-Supported Flat Plate  | 133         |
| 5.         | Effect of Membrane Force $R_x$ and Mass Ratio $\mu/M$ on the Critical Dynamic Pressure $\lambda_c$ for Two-Dimensional Simply-Supported Plates     | 134         |
| 6.         | Effect of the Viscous Type Structural Damping $g_s$ on the Critical Dynamic Pressure $\lambda_c$ for Two-Dimensional Simply-Supported Plates       | 135         |
| 7.         | Effect of the Hysteretic Type Structural Damping $g_s$ on the Critical Dynamic Pressure $\lambda_c$ for Two-Dimensional Simply-Supported Panels    | 136         |
| 8.         | Effect of the Membrane Force $R_x$ and Mass Ratio $\mu/M$ on the Critical Flutter Frequency $\omega_c$ for Two-Dimensional Simply-Supported Plates | 137         |

9. Effect of the Viscous Type Structural Damping  $g_s$  on the Critical Flutter Frequency  $\omega_c$  for Two-Dimensional Simply-Supported Plates at Different Values of  $\mu/M$  138
10. Effect of the Hysteretic Type Structural Damping  $g_b$  on the Critical Flutter Frequency  $\omega_c$  for Two-Dimensional Simply-Supported Plates at Different Values of  $\mu/M$  139
11. Effect of Applied Membrane Force  $R_x$  on the Limit-Cycle Amplitudes of Two-Dimensional Simply-Supported Flat Plates 140
12. Effect of Mass Ratio  $\mu/M$  on the Limit-Cycle Amplitudes of Two-Dimensional Simply-Supported Flat Plates 141
13. Effect of Viscous Structural Damping on the Limit-Cycle Amplitudes of Two-Dimensional Simply-Supported Plates 142
14. Variation of Flutter Frequency  $\omega$  with Dynamic Pressure  $\lambda$  at Different Values of Membrane Force  $R_x$  for a Two-Dimensional Simply-Supported Plate 143
15. Variation of Flutter Frequency  $\omega$  with Dynamic Pressure  $\lambda$  At Different Values of  $\mu/M$  for a Two-Dimensional Simply-Supported Plate 144
16. Variation of Flutter Frequency  $\omega$  with Dynamic Pressure  $\lambda$  At Different Values of  $\mu/M$  for a Two-Dimensional Simply-Supported Plate 145
17. Static Buckling Solutions for Two-Dimensional Simply-Supported Flat Plates 146
18. Example Envelope of Transient Response for a Two-Dimensional Simply-Supported Flat Plate 147



19. Effects of Varying  $a/b$  and  $R_x$  Upon the Critical Dynamic Pressure to Produce Flutter of a Three-Dimensional Clamped-Clamped Flat Plate 148
20. Effect of  $\mu/M$  on  $\lambda_c$  for Three-Dimensional Clamped-Clamped Panel with  $a/b=1.0$  149
21. Effect of the Viscous Type Damping  $g_s$  on the critical Dynamic Pressure  $\lambda_c$  for Three-Dimensional Clamped-Clamped Panel with  $a/b=1.0$  and Different Values of  $\mu/M$  150
22. Effect of Membrane Force  $R_x$  and Length-to-Width Ratio  $a/b$  on the Critical Flutter Frequency  $\omega_c$  for Three-Dimensional Clamped-Clamped Panel 151
23. Effect of  $\mu/M$  on  $\omega_c$  For Three-Dimensional Panels with  $a/b=1.0$  and Various Values of  $g_s$  152
24. Effect of Viscous Type Structural Damping  $g_s$  on the Critical Flutter Frequency  $\omega_c$  for Three-Dimensional Clamped-Clamped Panels with Different Values of  $\mu/M$  153
25. Effect of Length to Width Ratio  $a/b$  on the Limit-Cycle Amplitude for a Three-Dimensional Clamped-Clamped Flat Plate with  $R_x=R_y=0$  154
26. Effect of Applied Membrane Force  $R_x$  (For  $R_y=0$ ) on the Limit-Cycle Amplitude of a Three-Dimensional Clamped-Clamped Flat Plate with  $a/b=1.0$  155
27. Effect of Mass Ratio  $\mu/M$  on the Limit-Cycle Amplitude for a Three-Dimensional Clamped-Clamped Flat Plate with  $R_x=R_y=0$ . 156

|     |   |     |
|-----|---|-----|
| 28. | Effect of Viscous Structural Damping $g_s$ on the Limit Cycle Amplitude of Three-Dimensional Panels with $a/b=1.0$  | 157 |
| 29. | Variation of Flutter Frequency $\omega$ with Dynamic Pressure $\lambda$ for Three-Dimensional Plate with Different Values of $a/b$  | 158 |
| 30. | Variation of Flutter Frequency $\omega$ with Dynamic Pressure $\lambda$ for a Three-Dimensional Clamped-Clamped Plate at Different Values of Membrane Force $R_x$             | 159 |
| 31. | Variation of Flutter Frequency $\omega$ with Dynamic Pressure $\lambda$ for Three-Dimensional Plates with $a/b=1.0$ and Various Values of $\mu/M$                             | 160 |
| 32. | Variation of Flutter Frequency $\omega$ with Dynamic Pressure $\lambda$ for a Three-Dimensional Clamped-Clamped Plate at Different Values of Viscous Structural Damping $g_s$ | 161 |
| 33. | Linear Forced Response of Panel Below Flutter   | 162 |
| 34. | Nonlinear Forced Response of a Plate without Air Flow   | 163 |
| 35. | Nonlinear Forced Response of a Plate at $\lambda=\frac{3}{4}\lambda_c$  | 164 |
| 36. | Nonlinear Forced Response of a Plate at $\lambda=\lambda_c$ with Large Forcing Excitation   | 165 |
| 37. | Nonlinear Forced Response of a Panel at $\lambda=\lambda_c$ with Small Forcing Excitations  | 166 |
| 38. | Actual Critical Dynamic Pressure $\bar{\lambda}_c$ at Different Forcing Amplitudes  | 167 |
| 39. | Forcing Flutter Interaction--Amplitude of the Flutter Component for Different Values of Forcing Frequency $\Omega$  | 168 |

|     |   |     |
|-----|---|-----|
| 40. | Forcing-Flutter Interaction--Amplitude of the Forcing Component for Different Values of Forcing Frequency $\Omega$                | 169 |
| 41. | Forcing Flutter Interaction--Variation of Flutter Frequency with Dynamic Pressure for Different Forcing Frequency $\Omega$        | 170 |
| 42. | Nonlinear Forced Response of a Panel at $\lambda \geq \lambda_c$ .  | 171 |
| 43. | Nonlinear Forced Response of a Panel at Different Forcing Frequencies   | 172 |
| 44. | Direct Integration--Pure Forced Response at $\lambda=285$ , $\Omega=20$ , $F_R=40$  | 173 |
| 45. | Direct Integration--Forcing Flutter Interaction at $\lambda=292$ , $\Omega=20$ , $F_R=40$   | 174 |
| 46. | Direct Integration--Forcing-Flutter Interaction at $\lambda=295.9$ , $\Omega=20$ , $F_R=40$                                       | 175 |
| 47. | Direct Integration--Coexistence of Pure Forced Response and Forcing Flutter Interaction at $\lambda=340$ , $\Omega=40$ , $F_R=40$ | 176 |
| 48. | A Six-Mode Example of Forced Response of a Panel at $\lambda=\lambda_c=344.2$   | 177 |

CHAPTER 1

INTRODUCTION

This thesis consists of two parts. The first part concentrates on the study of nonlinear panel flutter and the second part is concerned with the nonlinear interactions of panel flutter and forcing excitations.

Panel flutter is a self excited oscillation of a plate when supersonic airflow passes by one side of it while the air on the other side remains stationary. People became interested in this problem when sustained and sometimes destructive, vibrations were observed on certain skin sections of the German V-2 rocket. This problem was first studied theoretically by Miles<sup>1</sup>, followed by Shen<sup>2</sup> and dozens of authors in the last two decades.

Panel flutter results from the interaction of the inertia force of panel, the elastic force associated with the panel deformation and the aerodynamic pressure brought about by the motion of the panel. The last one extracts energy from the airflow and causes instability of the panel at its undeformed position when a certain critical dynamic pressure is exceeded. Hence an initial disturbance would result in a growing amplitude oscillation. This growing, however, is limited by the

membrane force induced by the large deformation of the panel and the constraints at the boundary. The balance of destabilizing dynamic pressure and stabilizing membrane force results in a sustained limit-cycle motion.

In all the published papers, two expressions of the elastic forces have been used. The first is the linear plate vibration theory. This expression is simpler and used by most of the earlier investigators<sup>1-7</sup>. Theoretically, this analysis can predict the flutter boundary (critical dynamic pressure) correctly. But because this theory is good only for infinitesimal displacements, it is difficult to compare this analytical results with experiments since during the transient response, the deflection could be so large that the linear theory is no longer valid. Another drawback of this analysis is that, it cannot predict the panel behavior after the critical dynamic pressure is exceeded. The second expression of elastic forces, which has been employed by many investigators recently<sup>8-12</sup>, is the nonlinear plate vibration theory or the von Karman large deflection theory. By introducing the nonlinear terms, the problem becomes much more complicated and only approximate solutions can be obtained. Because this analysis can remedy the two drawbacks mentioned above, it is employed in this thesis.

Five aerodynamic theories have been used in the previous analysis. The first and the simplest one is the two-dimensional static aerodynamic theory employed by Hedgepeth<sup>6</sup> and others. The second one is the two-dimensional quasi-static aerodynamic

theory employed by Dugundji<sup>7</sup> and others. The third one is the linear Piston Theory<sup>13</sup> employed by Dowell<sup>10</sup> and others. The last two differ from the first one in taking into account the angle of attack caused by the velocity of the plate motion. Hence some sort of aerodynamic damping is included. The third one differs from the second by approximating  $M^2-1 \approx M^2$ ,  $M^2-2 \approx M^2$ , where  $M$  is the Mach Number of the airflow. The fourth one is the three-dimensional linearized, invicid aerodynamic theory<sup>11,14-16</sup>. This takes care of three-dimensional effect but results in a much more complicated calculation of the aerodynamic forces. The fifth one is the nonlinear piston theory employed by Bolotin<sup>8</sup>. This nonlinearity introduces some destabilizing effect. Because this nonlinearity is not likely to be important as pointed out by Dowell<sup>10</sup> and because of the complexity involved, it is seldom used. As shown by Dixon<sup>17</sup> and others, the first three theories yield good results for high Mach Number,  $M > 1.6$ , and low initial angle of attack, and because of their simplicity, they are the most often used ones. Since the third one takes care of the aerodynamic damping, and is simpler than the second one, it is employed in this study.

The compressive membrane forces caused by aerodynamic heating always make the panel more prone to flutter as shown by Hedgepeth<sup>6</sup> and others. Failure to define and control the membrane forces in earlier experimental work have been regarded as one of the major causes of the discrepancy between experimental and analytical results. The aerodynamic damping parameter, represented by mass ratio  $\mu/M$ , always makes the panel more stable

and limits the flutter amplitudes once the critical dynamic pressure is exceeded, as has been shown by Dowell<sup>11</sup>, Morino, Kuo and Dugundji<sup>12</sup>. The strange role of the structural damping on the stability boundary has been studied by Dugundji<sup>7\*</sup> and others for simply-supported panels. Because the actual amount of structural damping is difficult to determine and because a small amount of structural damping changes the stability boundary substantially, some of the discrepancy between experimental and analytical work could be attributed to the failure to measure the structural damping correctly. The effects of these parameters, along with that of length-width ratio, on the flutter behavior have been carefully studied in this thesis.

The flutter of buckled panels have been studied by Fung<sup>18,19</sup>, Eisely<sup>20</sup>, Houbolt<sup>21</sup> and Fralich<sup>22</sup>. In these studies, only the stability boundary is sought. The flutter of curved plates and shells are studied by Olson<sup>23</sup>, Evensen<sup>24</sup>, Dowell<sup>25,26</sup> and etc. The effect of flow direction on the flutter response has been studied by Kordes and Noll<sup>27</sup> and Friedmann<sup>28</sup>. The effect of boundary layer on panel flutter has been studied by Dowell<sup>29</sup>. Some excellent summaries of panel flutter have been done by Johns<sup>30,31</sup>, Fung<sup>32,33</sup>, Dowell<sup>34</sup> and Dugundji<sup>7</sup>. Some experiments on panel flutter have been performed by Sylvester<sup>35</sup>, Dixon<sup>36</sup>, Stearman<sup>37</sup>, Anderson<sup>38</sup>, Kappus and el<sup>39</sup>.

Several methods can be used to investigate panel flutter problems. In linear solution, only the critical dynamic pressure and the normal modes of vibration are of interest, one can solve

---

\*See also "Errata and Addendum," AIAA J., Vol. 7, No. 8, August 1969, pp. 1663-1664.

the problem exactly, see Goland<sup>3</sup> and Dugundji<sup>7</sup>. In nonlinear systems, exact solution to the partial differential equation is a matter of art. The approximate technique most often used is to assume normal-mode representation of the deflection, then apply Galerkin's Technique to reduce the system to a set of nonlinear ordinary differential equations. Various methods can be used to solve this set of nonlinear differential equations. First and the most straightforward method is the direct integration of the equations of motion from given initial conditions. This has been used with considerable success by Dowell<sup>10,11</sup> and Ventres<sup>40</sup>, see also Evensen and Olson<sup>24</sup>. Secondly, the equations of motion can be placed on an analog computer with nonlinear components, and the response observed. Kobayashi<sup>9</sup> and Bolotin<sup>8</sup> have used this method. Thirdly, the harmonic balance method can be used to determine the steady limit cycles; see for example Kobayashi<sup>9</sup>, Bolotin<sup>8</sup>, Eastep and McIntosh<sup>41</sup>, Morino, Kuo and Dugundji<sup>12</sup>. Fourthly, the Kryloff and Bogoliuboff method can be used to find both the transient and limit-cycle solution, see Olson and Fung<sup>42</sup>. Fifthly, perturbation methods can be used to obtain neighboring solutions to the linear problem; see Morino<sup>43</sup>, Morino and Kuo<sup>44</sup>. Finally, Lyapunov stability criteria can be used to study qualitatively the nonlinear behavior of the response. Such a technique has been employed by Librescu<sup>45</sup>.

In the first part of this thesis, the problem of panel flutter of both two-dimensional simply-supported plates and three-dimensional clamped-clamped panels has been studied. The



harmonic balance method has been employed in a systematic way so that one can include as many modes as a good convergency requires. Because this approach takes much less time than the direct integration method, it enables one to go through a thorough study of the problem at a reasonable amount of computation cost, hence proves to be a good alternative to the direct integration method.

As one knows, the frame of a flight vehicle, on which the panel (skin) is mounted, is not rigid. Hence during the flight, vibration of the frame due to elastic deformation or noise from the engine is possible. This vibration induces some inertia loading on the panel. This inertia loading and the gust loading make the panel constantly exposed to external excitations besides that due to passing air. So in order to understand the behavior of the panel during a flight, a forcing excitation should be considered in the formulation of the problem. Dzygadło<sup>46</sup> studied the forcing response of a quasi-linear system at the dynamic pressure approximately equal to the critical dynamic pressure of the panel. Some bubble-shape solutions were obtained at  $\lambda > \lambda_c$  and very small nonlinearity. Because of the small nonlinearity included in this study, the lack of data for  $\lambda < \lambda_c$ , and because only one-frequency solutions were sought, the study does not give a complete picture of the behavior, and does not predict the existence of flutter response besides the forcing response. In the second part of this thesis, the interaction of panel flutter with a harmonic forcing excitation is studied for the

whole range of dynamic pressure  $\lambda=0$  to  $\lambda \gg \lambda_c$ : The existence of the flutter components as well as the forcing components are sought. Harmonic balance method is the main tool used in this investigation. Some of the results are checked by the direct integration solutions obtained by this author. It is hoped that this study would contribute a better understanding of the panel behavior during the flight.

## CHAPTER 2

### NONLINEAR PANEL FLUTTER - THEORY

#### 2.1 Introduction

In this chapter, the problem of panel flutter is studied. As mentioned in Chapter 1, panel flutter is a self-excited motion. When the speed of the air flowing over one face of the panel is low, the plate motion will subside after an initial disturbance. However, when the speed is increased and reaches a certain critical value, some sustained motion can be observed. Linear plate theory can predict this critical speed by the classical stability analysis. This linear analysis cannot give us the relation between the speed of the air and the amplitude of vibration of the panel after the critical air speed is exceeded. So, in order to obtain meaningful panel flutter response, nonlinear plate vibration theory has to be employed. A brief derivation of the nonlinear plate vibration is given in sub-section 2.2.1 for a two-dimensional simply-supported plate and in sub-section 2.2.2 for a three-dimensional clamped-clamped plate. These two cases are studied here because the former is the classical formulation, more data are available to check the results obtained by the method employed in this study and the latter a more realistic representation of

of the real problem. Since Mach Number  $M \gg 1$  and the slope of the vibrating plate is small, linear Piston Theory<sup>13</sup> is used to calculate the aerodynamic pressure exerted on the plate. The complete equations of motion, Eq. 2.7 for the two-dimensional plate and Eqs. 2.22 and 2.23 for the three-dimensional plate, are nonlinear partial differential equations.

In order to avoid the complexity of the problem, Galerkin's Technique is used to eliminate the spatial variables and reduce the equations to nonlinear ordinary differential equations. A brief description of the Galerkin's technique is given in Section 2.3. The application of Galerkin's technique to the two-dimensional simply-supported panel and the three-dimensional clamped-clamped panel are given in sub-sections 2.3.1 and 2.3.2 and the spatial series representation are given in Eqs. 2.33 and 2.37 respectively for the two types of panels.

The resulting equations, Eqs. 2.34 and 2.48, are studied in Sections 2.4, 2.6 and 2.7. In Section 2.4, attention is focused on finding the steady state or limit cycle solutions. Since wind tunnel experiments shows that periodic vibration exists for the dynamic pressure  $\lambda$  greater than a critical value  $\lambda_c$ , and because direct integration method takes a lot of computation time, the Harmonic Balance method is employed here. The steady state solution is assumed to take the form shown in Eq. 2.49. Employing this equation in either Eq. 2.34 or Eq. 2.48, and balancing the first harmonic, one obtains a set of simultaneous nonlinear algebraic equations shown in

Eqs. 2.50 and 2.51. These equations are solved by Newton-Raphson's iteration technique to obtain the steady state solution. Because this Harmonic Balance method gives both stable and unstable solutions, a stability analysis of these solution is given in Section 2.5 by giving a perturbation to the limit cycle solution and studying the behavior of the perturbation function.

Section 2.6 is concerned with the transient response. The time required to reach the steady state is of major interest, so only the envelope of the transient response is sought. Section 2.7 is concerned with the static buckling solution. An exact two-mode solution of a two-dimensional, simply-supported plate is given to illustrate the conditions for the existence of the static buckling solutions.

The results of the panel flutter solution are discussed in Chapter 3 and are shown in figure form at the end of this thesis.

## 2.2 Formulation of Problem

### 2.2.1 Two-Dimensional Simply-Supported Panel

The problem studied in this section is a simply-supported two-dimensional plate with air flowing over one of its faces, while the air on the other face remains stationary. The configuration of the plate is shown in Fig. 1, where  $a$  is the length of the plate,  $h$  is the thickness of the plate,  $k$  is the spring constant at one end of the plate and it is assumed to be equal to infinity in the calculation,  $U$  is the speed of the air-

flow,  $x$  is the direction of the airflow. Let  $w$  denote the out of plane displacement of the plate, then the equation of motion of the plate can be represented by\*

$$\frac{\partial^2}{\partial x^2} \left[ D \left( 1 + \bar{g}_s \frac{\partial}{\partial t} + \frac{1}{\omega} \bar{g}_b \frac{\partial}{\partial t} \right) \frac{\partial^2 w}{\partial x^2} \right] - \frac{\partial}{\partial x} \left[ N_x \frac{\partial w}{\partial x} \right] = \rho_m h \frac{\partial^2 w}{\partial t^2} + p(w) + \Delta P \quad (2.1)$$

where  $\bar{g}_s$  - the viscous type structural damping coefficient,  
 $\bar{g}_b$  - the hysteretic type structural damping coefficient,  
 both are associated with bending,  
 $\rho_m$  - the density of the material of the plate,  
 $N_x$  - the membrane force,  
 $p(w)$  - the pressure difference between the lower surface and upper surface of the plate caused by the deflection of the plate,  
 $\Delta p$  - the static pressure difference.

$N_x$  may consist of two parts, one is the applied membrane force  $N_x^a$  and the other is that caused by the deflection of the plate  $N_x^w$ . So one can write

$$N_x = N_x^a + N_x^w \quad (2.2)$$

where

$$N_x^w = d \frac{Eh}{2a} \int_0^a \left( \frac{\partial w}{\partial x} \right)^2 dx \quad (2.3)$$

and

$$d = ka / (ka + Eh) \quad (2.4)$$

Since the plate is originally parallel to the airflow,

---

\* $\omega$  associated with  $\bar{g}_b$  represents the frequency of vibration. This device is commonly used for hysteretic type structural damping.

and the displacement  $w$  is small compared to the length of the plate, the linear Piston Theory<sup>13</sup>, can be used to determine  $p(w)$ , i.e.

$$p(w) = \frac{2\mathcal{B}}{M} \left[ \frac{\partial w}{\partial x} + \frac{1}{U} \frac{\partial w}{\partial t} \right] \quad (2.5)$$

where  $M$  is the Mach Number of the airflow and  $q$  is the dynamic pressure, which can be expressed as

$$q = \frac{1}{2} \rho_a U^2 \quad (2.6)$$

where  $\rho_a$  is the density of the air.

If the plate has uniform thickness,  $D$  is constant. If there is no body forces acting on the plate in the  $x$ -direction,  $N_x^a$  is constant. Using relations 2.2 to 2.5, Eq. 2.1 becomes

$$\begin{aligned} D \left( 1 + \bar{g}_s \frac{\partial}{\partial t} + \frac{1}{\omega} \bar{g}_b \frac{\partial}{\partial t} \right) \frac{\partial^4 w}{\partial x^4} - \left[ N_x^a + \alpha \frac{Eh}{2a} \int_0^a \left( \frac{\partial w}{\partial x} \right)^2 dx \right] \frac{\partial^2 w}{\partial x^2} \\ = \rho_m h \frac{\partial^2 w}{\partial t^2} + \frac{2\mathcal{B}}{M} \left[ \frac{\partial w}{\partial x} + \frac{1}{U} \frac{\partial w}{\partial t} \right] + \Delta p \end{aligned} \quad (2.7)$$

Use the following nondimensional parameters

$$\begin{aligned} \xi = x/a \quad \tau = t \left[ D / \rho_m h a^4 \right]^{1/2} \\ W = w/h \quad \lambda = 2\mathcal{B} a^3 / MD \quad \mu = \rho_a a / \rho_m h \\ R_x = N_x^a a^2 / D \quad P = \Delta p a^4 / D h \\ \bar{g}_s = \bar{g}_s \left[ D / \rho_m h a^4 \right]^{1/2} \quad \bar{g}_b = \bar{g}_b \quad \omega = \bar{\omega} \left[ D / \rho_m h a^4 \right]^{1/2} \end{aligned} \quad (2.8)$$

Eq. 2.7 becomes

$$\left(1 + g_s \frac{\partial}{\partial z} + \frac{1}{\omega} g_b \frac{\partial}{\partial t}\right) \frac{\partial^4 W}{\partial \xi^4} - 6\alpha(1-\nu^2) \left[ \int_0^1 \left(\frac{\partial W}{\partial \xi}\right)^2 d\xi \right] \frac{\partial^2 W}{\partial \xi^2} - R_x \frac{\partial^2 W}{\partial \xi^2} + \frac{\partial^2 W}{\partial \tau^2} + \lambda \frac{\partial W}{\partial \xi} + \left(\frac{\lambda \mu}{M}\right)^{1/2} \frac{\partial W}{\partial \tau} = P \quad (2.9)$$

Eq. 2.9 is the nondimensional form of the equation for panel flutter. The boundary conditions for a two-dimensional, simply-supported plate, written in nondimensional form, are

$$W = \frac{\partial^2 W}{\partial \xi^2} = 0 \text{ at } \xi=0 \text{ and } \xi=1 \quad (2.10)$$

Solving Eq. 2.9 subject to the boundary conditions, Eq. 2.10, for  $\lambda$  greater than a certain critical value, one can obtain the flutter amplitude and the corresponding frequency as functions of  $\nu$ ,  $R_x$ ,  $\mu/M$ ,  $g_s$ ,  $g_b$  etc.

### 2.2.2 Three-Dimensional Clamped-Clamped Panel

The problem studied in this section is a three-dimensional clamped-clamped plate, subject to airflow on one side of its surface while the air on the other side remains stationary. The geometrical configuration of the plate is shown in Fig. 2, where  $a$ ,  $h$ .  $U$  represent the same physical properties as those for a two-dimensional simply-supported plate,  $b$  is the width of the plate. Note that if  $b \rightarrow \infty$ , we have a two-dimensional panel. The equation of motion in the out-of-plane direction can be written as

$$D \left(1 + \bar{g}_s \frac{\partial}{\partial t} + \frac{1}{\omega} \bar{g}_b \frac{\partial}{\partial t}\right) \left[ \frac{\partial^4 W}{\partial x^4} + 2 \frac{\partial^4 W}{\partial x^2 \partial y^2} + \frac{\partial^4 W}{\partial y^4} \right] + \rho_m h \frac{\partial^2 W}{\partial t^2} \quad (2.11)$$

$$= N_x \frac{\partial^2 W}{\partial x^2} + N_y \frac{\partial^2 W}{\partial y^2} + 2 N_{xy} \frac{\partial^2 W}{\partial x \partial y} + p(W) + \Delta P$$



where  $D$ ,  $\bar{g}_s$ ,  $\bar{g}_b$ ,  $\rho_m$ ,  $N_x$ ,  $p(w)$  and  $\Delta p$  are the same as those defined in subsection 2.2.2,  $N_y$  is the membrane force in the y direction and  $N_{xy}$  is the in-plane torsional force.

The equilibrium equations of the in-plane forces<sup>8</sup> are

$$\frac{\partial}{\partial x} N_x + \frac{\partial}{\partial y} N_{xy} = 0 \quad (2.12)$$

$$\frac{\partial}{\partial x} N_{xy} + \frac{\partial}{\partial y} N_y = 0 \quad (2.13)$$

Introducing a stress function  $\phi$ , such that

$$\begin{aligned} N_x &= \frac{\partial^2 \phi}{\partial y^2} + N_x^a \\ N_y &= \frac{\partial^2 \phi}{\partial x^2} + N_y^a \\ N_{xy} &= -\frac{\partial^2 \phi}{\partial x \partial y} + N_{xy}^a \end{aligned} \quad (2.14)$$

where  $N_x^a$  and  $N_y^a$  are applied membrane forces in the x and y direction and substituting relation 2.14 into Eqs. 2.12 and 2.13, one can see that these two equations are satisfied automatically.

Another condition that has to be satisfied is the compatibility condition. The compatibility condition is briefly derived in the following: for large deflection  $w$ ,  $\epsilon_x$ ,  $\epsilon_y$ , and  $\epsilon_{xy}$  should include the quadratic terms in  $w$  and its derivatives, that is

$$\begin{aligned}\epsilon_x &= \frac{\partial u}{\partial x} + \frac{1}{2} \left( \frac{\partial w}{\partial x} \right)^2 \\ \epsilon_y &= \frac{\partial v}{\partial y} + \frac{1}{2} \left( \frac{\partial w}{\partial y} \right)^2 \\ \epsilon_{xy} &= \frac{1}{2} \left( \frac{\partial v}{\partial x} + \frac{\partial u}{\partial y} \right) + \frac{1}{2} \frac{\partial w}{\partial x} \frac{\partial w}{\partial y}\end{aligned}\tag{2.15}$$

The stress-strain relations for plane stress problems are

$$\begin{aligned}\epsilon_x &= \frac{1}{Eh} (N_x - \nu N_y) \\ \epsilon_y &= \frac{1}{Eh} (N_y - \nu N_x) \\ \epsilon_{xy} &= \frac{1+\nu}{Eh} N_{xy}\end{aligned}\tag{2.16}$$

Combining Eqs. 2.15 and 2.16, one obtains

$$\frac{\partial u}{\partial x} = \frac{1}{Eh} (N_x - \nu N_y) - \frac{1}{2} \left( \frac{\partial w}{\partial x} \right)^2\tag{2.17}$$

$$\frac{\partial v}{\partial y} = \frac{1}{Eh} (N_y - \nu N_x) - \frac{1}{2} \left( \frac{\partial w}{\partial y} \right)^2\tag{2.18}$$

$$\frac{1}{2} \left( \frac{\partial u}{\partial y} + \frac{\partial v}{\partial x} \right) = \frac{1+\nu}{Eh} N_{xy} - \frac{1}{2} \frac{\partial w}{\partial x} \frac{\partial w}{\partial y}\tag{2.19}$$

Differentiating Eq. 2.17 with respect to  $y$  twice, Eq. 2.18 with respect to  $x$  twice and Eq. 2.19 with respect to  $x$  and  $y$ , then adding up the first two equations and subtracting two times the last equation, one obtains

$$\begin{aligned}\frac{1}{Eh} \left[ \frac{\partial^2 N_x}{\partial y^2} - \nu \frac{\partial^2 N_x}{\partial x^2} + \frac{\partial^2 N_y}{\partial x^2} - \nu \frac{\partial^2 N_y}{\partial y^2} - 2(1+\nu) \frac{\partial^2 N_{xy}}{\partial x \partial y} \right] \\ = \left( \frac{\partial w}{\partial x} \right)^2 - \frac{\partial^2 w}{\partial x^2} \frac{\partial^2 w}{\partial y^2}\end{aligned}\tag{2.20}$$

Equation 2.20 is the compatibility condition to be satisfied. Using Eq. 2.14, the nondimensional parameters defined in Eq. 2.8 and letting

$$R_y = N_y^a a^2/D \quad (2.21)$$

$$A = a/b \quad \eta = y/b$$

eqs. 2.11 and 2.20 can be rewritten as \*

$$\begin{aligned} & (1 + g_s \frac{\partial}{\partial z} + \frac{1}{\omega} g_b \frac{\partial}{\partial t}) \left[ \frac{\partial^4 W}{\partial z^4} + 2A^2 \frac{\partial^4 W}{\partial z^2 \partial \eta^2} + A^4 \frac{\partial^4 W}{\partial \eta^4} \right] + \frac{\partial^2 W}{\partial z^2} \\ & = R_x \frac{\partial^2 W}{\partial z^2} + R_y A^2 \frac{\partial^2 W}{\partial \eta^2} - \lambda \frac{\partial W}{\partial z} + \left( \frac{\lambda M}{M} \right)^{1/2} \frac{\partial W}{\partial z} + P \\ & + \frac{A^2}{D} \left\{ \frac{\partial^2 \Phi}{\partial \eta^2} \frac{\partial^2 W}{\partial z^2} + \frac{\partial^2 \Phi}{\partial z^2} \frac{\partial^2 W}{\partial \eta^2} - 2 \frac{\partial^2 \Phi}{\partial z \partial \eta} \frac{\partial^2 W}{\partial z \partial \eta} \right\} \end{aligned} \quad (2.22)$$

$$\begin{aligned} \frac{\partial^4 \Phi}{\partial z^4} + 2A^2 \frac{\partial^4 \Phi}{\partial z^2 \partial \eta^2} + A^4 \frac{\partial^4 \Phi}{\partial \eta^4} = 12(1-\nu^2) DA^2 \left\{ \left( \frac{\partial^2 W}{\partial z \partial \eta} \right)^2 \right. \\ \left. - \frac{\partial^2 W}{\partial z^2} \frac{\partial^2 W}{\partial \eta^2} \right\} \end{aligned} \quad (2.23)$$

These are the two governing differential equations to be solved.

The out-of-plane boundary conditions for a clamped-clamped plate are

$$W = \frac{\partial W}{\partial z} = 0 \text{ at } \xi=0 \text{ and } \xi=1 \quad (2.24)$$

$$W = \frac{\partial W}{\partial \eta} = 0 \text{ at } \eta=0 \text{ and } \eta=1$$

For convenience, one requires the inplane boundary conditions to be satisfied in an average sense, i.e. instead of

\* $N_{xy}^a$  is set to zero.

requiring  $\Delta x = \frac{1}{ER} (N_x^a - \nu N_y^a)$  and  $\Delta y = \frac{1}{Eh} (N_y^a - \nu N_x^a)$ , one requires

$$\int_0^1 \Delta x d\eta = \int_0^1 \int_0^1 \frac{\partial u}{\partial \xi} d\xi d\eta = \frac{1}{ER} (N_x^a - \nu N_y^a) \quad (2.25)$$

$$\int_0^1 \Delta y d\xi = \int_0^1 \int_0^1 \frac{\partial v}{\partial \eta} d\eta d\xi = \frac{1}{ER} (N_y^a - \nu N_x^a) \quad (2.26)$$

$$N_{xy}^{ave.} = 0 \quad (2.27)$$

Using Eqs. 2.14, 2.17, 2.18, 2.19 and the nondimensional parameters expressed in Eqs. 2.8 and 2.21, Eqs. 2.25 and 2.26 can be rewritten as

$$\iint_0^1 \left[ \frac{1}{ER^3} (A^2 \frac{\partial^2 \Phi}{\partial \eta^2} - \nu \frac{\partial^2 \Phi}{\partial \xi^2}) - \frac{1}{2} \left( \frac{\partial W}{\partial \xi} \right)^2 \right] d\xi d\eta = 0 \quad (2.28)$$

$$\int_0^1 \int_0^1 \left[ \frac{1}{ER} \left( \frac{\partial^2 \Phi}{\partial \xi^2} - \nu A^2 \frac{\partial^2 \Phi}{\partial \eta^2} \right) - \frac{1}{2} A^2 \left( \frac{\partial W}{\partial \eta} \right)^2 \right] d\xi d\eta = 0 \quad (2.29)$$

Eqs. 2.24, 2.27, 2.28 and 2.29 are the boundary conditions to be satisfied when we solve Eqs. 2.22 and 2.23.

### 2.3 Method of Solution

Galerkin's Technique will be used to reduce Eqs. 2.9, 2.22 and 2.23 to a set of equations having time  $\tau$  as the only independent variable. This process involves expressing the transverse deflection  $W$  in the following form

$$W = \sum_{m=1}^{\infty} \sum_{n=1}^{\infty} W_{mn}(\tau) \varphi_m(\xi) \varphi_n(\eta) \quad (2.30)$$

where  $\zeta_m(\xi)\zeta_n(\eta)$  is the assumed mode-shape of deflection and must individually satisfy the out-of-plane boundary conditions. In order to represent  $W$  exactly,  $\zeta_m(\xi)\zeta_n(\eta)$  must form a complete set throughout the whole plate. After choosing the set  $\zeta_m(\xi)\zeta_n(\eta)$ , one substitutes Eq. 2.30 into the governing differential equation

$$D(W) = 0 \quad (2.31)$$

then use the assumed mode shape as a weight function, satisfy Eq. 2.31 by setting the weighted residual to zero<sup>47</sup>, i.e.

$$\int_0^1 \int_0^1 \varphi_m(\xi) \varphi_n(\eta) D(W) d\xi d\eta = 0 \quad (2.32)$$

This will yield  $M \times N$  ordinary differential equations for  $W_{mn}$ .  $M$  and  $N$  are the upper limits of  $m$  and  $n$  respectively. After solving these ordinary differential equations, one has the complete picture of the response.

Application of this technique to our present problems are discussed in the following two sub-sections.

### 2.3.1 Two-Dimensional Simply-Supported Panel

Because the plate is infinitely long in the  $y$ -direction and the air is flowing in the  $x$ -direction, it is reasonable to assume that the lateral deflection is not a function of  $y$ . From the previous statement of this section, one would assume a deflection mode shape which will satisfy the boundary conditions stated in Eq. 2.10. Hence one assumes

$$W = \sum_{n=1}^{\infty} W_n \sin n\pi z \quad (2.33)$$

where  $W_n$  is a function of the time factor  $\tau$ . Note that sine series is a complete set, it can represent any function of  $\xi$  except at the point of discontinuity.

Placing Eq. 2.33 into Eq. 2.9, multiplying it by  $\sin m\pi\xi$  then integrating it from  $\xi=0$  to  $\xi=1$ , one obtains the following set of equations\*

$$\sum_{n=1}^N [M_{mn}\ddot{W}_n + G_{mn}\dot{W}_n + \frac{1}{\omega}GB_{mn}\dot{W}_n + \lambda E_{mn}W_n + K_{mn}W_n] + \sum_{n,p,q=1}^N C_{mnpq} W_n W_p W_q = 0 \quad (2.34)$$

where the coefficients are defined as follows

$$\begin{aligned} M_{mn} &= \delta_n^m \\ G_{mn} &= \left[ \left( \frac{\lambda\mu}{M} \right)^{1/2} + g_s m^4 \pi^4 \right] \delta_n^m = \lambda^{1/2} \tilde{G}_{mn} + g_s \tilde{\tilde{G}}_{mn} \\ GB_{mn} &= g_b m^4 \pi^4 \delta_n^m \\ K_{mn} &= m^2 \pi^2 [m^2 \pi^2 + R_x] \delta_n^m \\ E_{mn} &= \frac{2mn [1 - (-1)^{m+n}]}{m^2 - n^2} \\ C_{mnpq} &= 3(1-\nu^2) (n\pi)^2 (g\pi)^2 \delta_n^m \delta_q^p \end{aligned} \quad (2.35)$$

So the partial differential equation, Eq. 2.9, has been reduced to a set of ordinary differential equations, Eq. 2.34, having  $\tau$  as the only independent variable. According to different objectives, equation 2.34 will be solved in sections

---

\*P is set to zero.

2.4, 2.6 and 2.7.

2.3.2 Three-Dimensional Clamped-Clamped Panel

A simple set of functions that can satisfy the out-of-plane boundary conditions of a clamped-clamped plate, i.e. Eq. 2.24 can be written in the following form\*

$$W = \sum_{m,n=1}^{\infty} W_{mn} [\cos(m-1)\pi\zeta - \cos(m+1)\pi\zeta] [\cos(n-1)\pi\eta - \cos(n+1)\pi\eta] \quad (2.36)$$

Because the airflow has no velocity component in the y direction and the strain energy is roughly proportional to  $n^4$ , where n is number of the mode shape, higher modes are not likely to become important in the y direction unless there are some special constraints at the boundaries, i.e. high in-plane loadings, etc. So it is reasonable to assume that the deflection shape in the y-direction can fairly well be represented by the first mode shape. Hence Eq. 2.34 can be rewritten as

$$W = \sum_{m=1}^N W_m [\cos(m-1)\pi\zeta - \cos(m+1)\pi\zeta] (1 - \cos 2\pi\eta) \quad (2.37)$$

Note that the particular solution  $f_p$  for a function f which satisfies the following equation

$$\frac{\partial^4 f}{\partial \zeta^4} + 2A^2 \frac{\partial^2 f}{\partial \zeta^2 \partial \eta^2} + A^4 \frac{\partial^4 f}{\partial \eta^4} = f_0 \cos m\pi\zeta \cos n\pi\eta \quad (2.38)$$

is

$$f_p = \frac{f_0}{(m^2 + A^2 n^2)^2} \cos m\pi\zeta \cos n\pi\eta \quad (2.39)$$

for m and n not equal to zero at the same time.

Substituting Eq. 2.37 into Eq. 2.23 and using Eq. 2.39, one can find the particular solution of  $\Phi$

---

\*This is a complete set since it is a linear combination of the cosine series, which is a complete set.

$$\begin{aligned}
 \bar{\Phi}_p = & [ P + \bar{A} \cos 4\pi\eta + G \cos 2\pi\eta ] \cos (\rho-\theta)\pi \} \\
 & + [ Q + B \cos 4\pi\eta + H \cos 2\pi\eta ] \cos (\rho-\theta-2)\pi \} \\
 & + [ R + C \cos 4\pi\eta + I \cos 2\pi\eta ] \cos (\rho-\theta+2)\pi \} \\
 & + [ S + D \cos 4\pi\eta + J \cos 2\pi\eta ] \cos (\rho+\theta)\pi \} \\
 & + [ T + E \cos 4\pi\eta + M \cos 2\pi\eta ] \cos (\rho+\theta-2)\pi \} \\
 & + [ U + F \cos 4\pi\eta + N \cos 2\pi\eta ] \cos (\rho+\theta+2)\pi \}
 \end{aligned} \tag{2.40}$$

where the coefficients  $\bar{A}, B, \dots$  are defined in Appendix A with details of the calculations.

In order to satisfy the boundary conditions, Eq. 2.27, 2.28 and 2.29, a homogeneous solution of  $\bar{\Phi}$  is needed. For simplicity, one assumes

$$\bar{\Phi}_{\text{homo}} = \frac{1}{2} [ \bar{N}_x \eta^2 + \bar{N}_y \zeta^2 + 2 \bar{N}_{xy} \zeta \eta ] \tag{2.41}$$

where  $\bar{N}_x, \bar{N}_y,$  and  $\bar{N}_{xy}$  are constants to be determined.

Note that the total solution of  $\bar{\Phi}$  is  $\bar{\Phi} = \bar{\Phi}_{\text{homo.}} + \bar{\Phi}_{\text{parti}}$ : Eqs. 2.27, 2.40, 2.41 and 2.14 yields

$$\bar{N}_{xy} = 0 \tag{2.42}$$

Substituting Eqs. 2.37, 2.40 and 2.41 into Eqs. 2.28 and 2.29, one obtains

$$\bar{N}_x = \frac{1}{(1-\nu^2)A^2} ( I_1 + A^2 \nu I_2 ) \tag{2.43}$$



$$\bar{N}_y = \frac{1}{1-\nu^2} (I_1 \nu + I_2 A^2) \quad (2.44)$$

where

$$I_1 = \frac{q}{2} (1-\nu^2) \pi^2 D \sum_{p=1}^N \sum_{g=1}^N W_p W_g [2(pg+1) \delta_g^p - (p+1)(g-1) \delta_g^{p+2} - (p-1)(g+1) \delta_{g+2}^p] \quad (2.45)$$

$$I_2 = 6(1-\nu^2) \pi^2 D \sum_{p=1}^N \sum_{g=1}^N W_p W_g [2\delta_g^p + \delta_2^{p+g} - \delta_{g+2}^p - \delta_g^{p+2}] \quad (2.46)$$

So the total solution of  $\bar{\Phi}$  is

$$\bar{\Phi} = \bar{\Phi}_p + \frac{1}{2(1-\nu^2)} \left[ \frac{1}{A^2} (I_1 + A^2 \nu I_2) \eta^2 + (I_1 \nu + I_2 A^2) \zeta^2 \right] \quad (2.47)$$

where  $\bar{\Phi}_p$ ,  $I_1$  and  $I_2$  are defined in Eqs. 2.40, 2.45 and 2.46 respectively.

Substituting Eq. 2.37 and 2.47 into Eq. 2.22 and applying Galerkin's Technique, one again obtains

$$\sum_{n=1}^N [M_{mn} \ddot{W}_n + G_{mn} \dot{W}_n + \frac{1}{\omega} GB_{mn} \dot{W}_n + K_{mn} W_n + \lambda E_{mn} W_n] + \sum_{n,p,g=1}^N C_{mnpq} W_n W_p W_g = 0 \text{ for } m=1,2,\dots,N \quad (2.48)$$

where the coefficients  $M_{mn}$ ,  $G_{mn}$ ,  $GB_{mn}$ ,  $K_{mn}$ ,  $E_{mn}$  and  $C_{mnpq}$  are defined in Appendix A. Eq. 2.48 constitutes a set of ordinary differential equations. The upper limit  $N$  is determined by the convergence of the modal representation. Eq. 2.48 will be

solved in Section 2.4, 2.6 and 2.7 respectively according to different objectives.

## 2.4 Steady State Solution

In this section, the steady state solutions of both Eqs. 2.34 and 2.48 are obtained. Since they appear in the same general form, only one discussion is given for both equations.

Wind tunnel experiments<sup>15,37</sup> and results from direct integration methods show that a periodic solution generally exists when the panel reaches its steady state motion for the dynamic pressure  $\lambda$  greater than a certain critical value  $\lambda_c$ . So one can assume, for  $\lambda > \lambda_c$ , that

$$W_n = a_n \sin \omega \tau + b_n \cos \omega \tau \quad (2.49)$$

where  $a_n$  and  $b_n$  are constants to be determined. Once  $a_n$  and  $b_n$  are determined, the whole solution of panel flutter is obtained.

Substituting Eq. 2.49 into either Eq. 2.34 or Eq. 2.48, and balancing the first harmonic, one obtains the following two sets of equations.

$$f_{2m-1}(\mathcal{X}) = \sum_{n=1}^N [(-M_{mn}\omega^2 + K_{mn} + \lambda E_{mn})a_n - (\omega G_{mn} + G B_{mn})b_n] \quad (2.50)$$

$$+ \frac{1}{4} \sum_{n,p,q=1}^N C_{mnpq} [3a_n a_p a_q + a_n b_p b_q + b_n a_p b_q + b_n b_p a_q] = 0$$

$$f_{2m}(\mathcal{X}) = \sum_{n=1}^N [(-M_{mn}\omega^2 + K_{mn} + \lambda E_{mn})b_n + (\omega G_{mn} + G B_{mn})a_n] \quad (2.51)$$

$$+ \frac{1}{4} \sum_{n,p,q=1}^N C_{mnpq} [3b_n b_p b_q + b_n a_p a_q + a_n b_p a_q + a_n a_p b_q] = 0$$

Equations 2.50 and 2.51 constitute a set of  $2N$  simultaneous algebraic equations. So, instead of solving a set of ordinary nonlinear differential equations, one has to solve a set of nonlinear algebraic equations. Giving a value of  $\lambda > \lambda_c$ , both  $\omega$  and the amplitude of vibration, hence  $a_n$ 's and  $b_n$ 's, are fixed. Because  $\lambda_c$  is not known beforehand and the relation between  $\lambda$  and  $\omega$  is not known, one assumes both  $\lambda$  and  $\omega$  as unknowns in solving Eqs. 2.50 and 2.51 and at the same time let  $a_1$  equal to zero and  $b_1$  equal to a certain number. The value of  $b_1$  will determine the level of the amplitude of the vibration and the value  $\lambda$  and  $\omega$ . Rewrite Eqs. 2.50 and 2.51 in vectorial form

$$\underset{\sim}{f}(\underset{\sim}{x}) = \begin{pmatrix} f_1 \\ f_2 \\ \vdots \\ f_{2N} \end{pmatrix} = 0 \quad (2.52)$$

where  $\underset{\sim}{x}$  is the unknown vector to be found, or

$$\underset{\sim}{x} = \begin{pmatrix} \lambda \\ \omega \\ a_2 \\ b_2 \\ a_3 \\ \vdots \\ b_N \end{pmatrix} \quad (2.53)$$

Eq. 2.52 is solved by Newton-Raphson iteration technique. The iteration formula is

$$\underset{\sim}{x}^{i+1} = \underset{\sim}{x}^i - J^{-1}(\underset{\sim}{x}^i) \underset{\sim}{f}(\underset{\sim}{x}^i) \quad (2.54)$$

where  $\tilde{x}^{i+1}$  is the  $i + 1$ st iteration value of the unknown vector  $\tilde{x}$ ,  $\tilde{x}^i$  the  $i$ th iteration value of  $\tilde{x}$  and  $J(\tilde{x}^i)$  is the Jacobian of the vector  $\underline{f}(\tilde{x})$  calculated for  $\tilde{x} = \tilde{x}^i$ . The Jacobian  $J(\tilde{x})$  is obtained by the partial differentiation of the vector  $\underline{f}(\tilde{x})$ . With the unknown vector chosen in Eq. 2.53, the Jacobian of the vector  $\underline{f}$  is defined as

$$\begin{aligned}
 J_{2m-1,1} &= \sum_{n=1}^N E_{mn} a_n - \frac{1}{2} \lambda^{-1/2} \omega \sum_{n=1}^N \tilde{G}_{mn} b_n \\
 J_{2m-1,2} &= -2\omega \sum_{n=1}^N M_{mn} a_n - \sum_{n=1}^N G_{mn} b_n \\
 J_{2m-1,2l-1} &= -\omega^2 M_{me} + K_{me} + \lambda E_{me} + \frac{1}{4} \sum_{n,p,q=1}^N C_{mnpq} [ (3a_p a_q \\
 &\quad + b_p b_q) \delta_e^n + (3a_n a_q + b_n b_q) \delta_e^p + (3a_n a_p + b_n b_p) \delta_e^q ] \\
 J_{2m-1,2l} &= -\omega G_{me} - GB_{me} + \frac{1}{4} \sum_{n,p,q=1}^N C_{mnpq} [ (a_p b_q + a_q b_p) \delta_e^n \\
 &\quad + (b_n a_q + a_n b_q) \delta_e^p + (b_n a_p + a_n b_p) \delta_e^q ] \\
 J_{2m,1} &= \sum_{n=1}^N E_{mn} b_n + \frac{1}{2} \lambda^{-1/2} \omega \sum_{n=1}^N \tilde{G}_{mn} a_n \\
 J_{2m,2} &= -\sum_{n=1}^N 2\omega M_{mn} b_n + \sum_{n=1}^N G_{mn} a_n \\
 J_{2m,2l-1} &= G_{me} + GB_{me} + \frac{1}{4} \sum_{n,p,q=1}^N C_{mnpq} [ (a_p b_q + b_p a_q) \delta_e^n \\
 &\quad + (a_n b_q + b_n a_q) \delta_e^p + (a_n b_p + b_n a_p) \delta_e^q ] \quad (2.55) \\
 J_{2m,2l} &= -\omega^2 M_{me} + K_{me} + \lambda E_{me} + \frac{1}{4} \sum_{n,p,q=1}^N C_{mnpq} [ 3b_p b_q \\
 &\quad + a_p a_q) \delta_e^n + (3b_n b_q + a_n a_q) \delta_e^p + (3b_n b_p + a_n a_p) \delta_e^q ]
 \end{aligned}$$

for  $m=1,2,\dots,N$

where  $\tilde{G}_{mn}$  represents the part of  $G_{mn}$  that contains  $\lambda^{1/2}$  as shown in Eq. A.9.2.

Equation 2.52 is solved by using the iteration formula shown in Eq. 2.54. The iteration stops when the absolute value of the ratio of the correction value  $J^{-1}(\tilde{x}^i)F(\tilde{x}^i)$  to  $\tilde{x}^i$  is smaller than  $10^{-4}$ . Some results obtained are shown in figure form and are discussed in Chapter 3.

### 2.5 Stability of Steady State Solutions

The method described in Section 2.4 yields both stable and unstable solutions; hence each limit cycle solution must be checked for stability by giving a small perturbation to the limit cycle solution (steady state solution). Let

$$W_n(\tau) = [a_n + \xi_n(\tau)] \mu \sin \omega \tau + [b_n + \zeta_n(\tau)] c_{20} \omega \tau \quad (2.56)$$

where  $\xi_n$  and  $\zeta_n$  are the perturbed values of  $a_n$  and  $b_n$  respectively,  $a_n$  and  $b_n$  are the limit cycle solution and satisfy Eqs. 2.50 and 2.51. Stability is to be studied in the vicinity of the limit cycle solution, hence one assumes

$$|\xi_n(\tau)| \ll |a_n| \quad |\zeta_n(\tau)| \ll |b_n| \quad (2.57)$$

Since  $\xi_n$  and  $\zeta_n$  are only small perturbations, it is also reasonable to assume that they are only slowly varying functions of  $\tau$ , i.e.

$$\begin{aligned} \frac{2\pi}{\omega} \left| \frac{\dot{\eta}_n}{\eta_n} \right| \ll 1 & \quad \frac{2\pi}{\omega} \left| \frac{\dot{\zeta}_n}{\zeta_n} \right| \ll 1 \\ \frac{2\pi}{\omega} \left| \frac{\ddot{\eta}_n}{\dot{\eta}_n} \right| \ll 1 & \quad \frac{2\pi}{\omega} \left| \frac{\ddot{\zeta}_n}{\dot{\zeta}_n} \right| \ll 1 \end{aligned} \quad (2.58)$$

So one can neglect  $\dot{\zeta}_n$ ,  $\dot{\xi}_n$ ,  $\ddot{\zeta}_n$  and  $\ddot{\xi}_n$  in comparison with  $\zeta_n$ ,  $\xi_n$ ,  $\dot{\zeta}_n$  and  $\dot{\xi}_n$  respectively.

Placing Eq. 2.56 into either Eq. 2.34 or Eq. 2.48, balancing the first harmonic, subtracting the limit cycle solution, neglecting the higher order terms of  $\xi_n$  and  $\zeta_n$  and the higher order derivatives of  $\xi_n$  and  $\zeta_n$  according to the smallness and slowly varying characteristics of  $\xi_n$  and  $\zeta_n$ , one obtains the following two sets of linear differential equations for  $\xi_n$  and  $\zeta_n$ ,

$$\begin{aligned} \sum_{n=1}^N \left[ -2\omega M_{mn} \dot{\eta}_n + G_{mn} \dot{\zeta}_n + \frac{G_{mn}}{\omega} \right] + \sum_{n=1}^N \left[ (\omega G_{mn} + GB_{mn}) \eta_n + (K_{mn} \right. \\ \left. - \omega^2 M_{mn} + \lambda E_{mn}) \zeta_n + \frac{1}{4} \sum_{n,p,q=1}^N C_{mnpq} [(3b_n b_p + a_n a_p) \zeta_p + (3b_n b_q \right. \\ \left. + a_n a_q) \zeta_q + (3b_p b_q + a_p a_q) \zeta_n + (a_n b_p + b_n a_p) \eta_p \right. \\ \left. + (a_n b_q + b_n a_q) \eta_q + (b_p a_q + a_p b_q) \eta_n \right] = 0 \end{aligned} \quad (2.59)$$

$$\begin{aligned}
 & \sum_{n=1}^N [-2\omega M_{mn} \dot{\xi}_n + G_{mn} \dot{Y}_n] - \sum_{m=1}^N [\omega G_{mn} + G B_{mn}] \xi_n + \sum_{n=1}^N (K_{mn} - \omega^2 M_{mn} \\
 & + \lambda E_{mn}) Y_n + \frac{1}{4} \sum_{n,p,q=1}^N C_{mnpq} [(3a_n a_p + b_n b_p) Y_q + (3a_n a_q \\
 & + b_n b_q) Y_p + (3a_p a_q + b_p b_q) Y_n + (a_n b_p + a_p b_n) \xi_p \\
 & + (a_n b_q + b_n a_q) \xi_p + (a_p b_q + a_q b_p) \xi_n] + \sum_{n=1}^N \frac{G B_{nn}}{\omega} \dot{Y}_n = 0
 \end{aligned} \tag{2.60}$$

for  $m=1, 2, \dots, N$

Let

$$\begin{aligned}
 Y_n(\tau) &= q_{2n-1} e^{\alpha \tau} \\
 \xi_n(\tau) &= q_{2n} e^{\alpha \tau} \quad n=1, 2, \dots
 \end{aligned} \tag{2.61}$$

where  $q_{2n-1}$ ,  $q_{2n}$  and  $\alpha$  are constants.

Placing Eq. 2.61 into eqs. 2.59 and 2.60, dividing the former by  $-2\omega$ , the latter by  $2\omega$  and writing the resulting equations in matrix form, one obtains

$$\{ Q - \alpha N \} \underline{q} = 0 \tag{2.62}$$

where  $\underline{Q}$  and  $\underline{N}$  are defined as follows

$$\begin{aligned}
 N_{2m-1, 2\ell-1} &= M_{me} & N_{2m-1, 2\ell} &= \frac{1}{2\omega} G_{m\ell} + \frac{1}{2\omega^2} GB_{mn} \\
 N_{2m, 2\ell-1} &= -\frac{1}{2\omega} G_{m\ell} - \frac{1}{2\omega^2} GB_{mn} & N_{2m, 2\ell} &= M_{m\ell} \\
 Q_{2m-1, 2\ell-1} &= -\frac{1}{2\omega} \left\{ \omega G_{m\ell} + GB_{m\ell} + \frac{1}{4} \sum_{n,p,g=1}^N C_{mnp_g} [(a_n b_p \right. \\
 &\quad \left. + b_n a_p) S_\ell^g + (a_n b_g + b_n a_g) S_\ell^p + (b_g a_p + a_g b_p) S_\ell^n] \right\} \\
 Q_{2m-1, 2\ell} &= -\frac{1}{2\omega} \left\{ K_{m\ell} - \omega^2 M_{m\ell} + \lambda E_{m\ell} + \frac{1}{4} \sum_{n,p,g=1}^N C_{mnp_g} [(3b_n b_p \right. \\
 &\quad \left. + a_n a_p) S_\ell^g + (3b_n b_g + a_n a_g) S_\ell^p + (3b_p b_g + a_p a_g) S_\ell^n] \right\} \\
 Q_{2m, 2\ell-1} &= \frac{1}{2\omega} \left\{ K_{m\ell} - \omega^2 M_{m\ell} + \lambda E_{m\ell} + \frac{1}{4} \sum_{n,p,g=1}^N C_{mnp_g} [(3a_n a_p \right. \\
 &\quad \left. + b_n b_p) S_\ell^g + (3a_n a_g + b_n b_g) S_\ell^p + (3a_p a_g + b_p b_g) S_\ell^n] \right\} \\
 Q_{2m, 2\ell} &= \frac{1}{2\omega} \left\{ -\omega G_{m\ell} - GB_{m\ell} + \frac{1}{4} \sum_{n,p,g=1}^N C_{mnp_g} [(a_n b_p + a_p b_n) S_\ell^g \right. \\
 &\quad \left. + (a_n b_g + b_n a_g) S_\ell^p + (a_p b_g + a_g b_p) S_\ell^n] \right\}
 \end{aligned} \tag{2.63}$$

In order to obtain nontrivial solution of  $q$  from Eq. 2.62, one has to set

$$| \underline{Q} - \alpha \underline{N} | = 0 \tag{2.64}$$

This is an eigenvalue problem. One can find  $\alpha$  by power method. If all real parts of  $\alpha$  are negative or equal to zero, the limit cycle solution is a stable one. If any of the real parts of  $\alpha$  is greater than zero, the limit cycle solution is an unstable one.

## 2.6 Transient solutions

The time required to reach the steady state is of interest. Of immediate concern is the transient response of the envelope



of the panel flutter. For simplicity, the fluttering frequency is assumed to be constant at its final steady state value, throughout the process of reaching the steady state. Assume

$$W_n(\tau) = a_n(\tau) \sin \omega \tau + b_n(\tau) \cos \omega \tau \quad (2.65)$$

where  $a_n(\tau)$  and  $b_n(\tau)$  are assumed to be slowly varying function of time. Note that  $a_n(\tau)$  and  $b_n(\tau)$  may bring some frequency correction for the transient response. Again, using the properties of slowly varying function, one finds that

$$\dot{W}_n = (\dot{a}_n - \omega b_n) \sin \omega \tau + (\dot{b}_n + \omega a_n) \cos \omega \tau \quad (2.66)$$

$$\ddot{W}_n \approx (-2\omega \dot{b}_n - \omega^2 a_n) \sin \omega \tau + (2\omega \dot{a}_n - \omega^2 b_n) \cos \omega \tau$$

Substituting these relations into either Eq. 2.34 or Eq. 2.48 and balancing the first harmonic, one obtains

$$\begin{aligned} & 2\omega \sum_{n=1}^N M_{mn} \dot{a}_n + \sum_{n=1}^N \left( G_{mn} + \frac{1}{\omega} G B_{mn} \right) \dot{b}_n + \sum_{n=1}^N \left( \omega G_{mn} + G B_{mn} \right) a_n \\ & + \sum_{n=1}^N \left( K_{mn} + \lambda E_{mn} - \omega^2 M_{mn} \right) b_n + \frac{1}{4} \sum_{n,p,q=1}^N C_{mnpq} [3b_n b_p b_q \\ & + b_n a_p a_q + b_p a_n a_q + b_q a_n a_p] = 0 \end{aligned} \quad (2.67)$$

$$\begin{aligned} & -2\omega \sum_{n=1}^N M_{mn} \dot{b}_n + \sum_{n=1}^N \left( G_{mn} + \frac{1}{\omega} G B_{mn} \right) \dot{a}_n - \sum_{n=1}^N \left( \omega G_{mn} + G B_{mn} \right) b_n \\ & + \sum_{n=1}^N \left( K_{mn} + \lambda E_{mn} - \omega^2 M_{mn} \right) a_n + \frac{1}{4} \sum_{n,p,q=1}^N C_{mnpq} [3a_n a_p a_q \\ & + a_n b_p b_q + a_p b_n b_q + a_q b_n b_p] = 0 \end{aligned} \quad (2.68)$$

for  $m=1, 2, \dots, N$

Eqs. 2.67 and 2.68 are first order nonlinear differential equations for  $a_n$  and  $b_n$ . Integrate these two equations by either Runge-Kutta method or Predictor-Corrector method, one can obtain the transient response of the envelope of the panel flutter.

### 2.7 Static Buckling Solutions

Under certain combinations of the dynamic pressure and the in-plane loading, the panel could undergo static buckling instead of fluttering. In order to find the static buckling solutions, one sets  $\ddot{W}_n(\tau)$  and  $\dot{W}_n(\tau)$  to zero. Then the governing differential equations become

$$\sum_{n=1}^N (K_{mn} + \lambda E_{mn}) W_n + \sum_{n,p,q=1}^N C_{mnpq} W_n W_p W_q = 0 \quad (2.69)$$

This can be programmed for solution by the Newton-Raphson iteration technique in the same way as the previous flutter equations, i.e. Eq. 2.34 or Eq. 2.48, only now, the unknown vector is taken as  $\underline{x} = (w_1, w_2, \dots, w_n)$  and  $\lambda$  is assumed known. The Jacobian for Eq. 2.69 with the  $x$  vector taken here is

$$J_{m,e} = K_{me} + \lambda E_{me} + \sum_{n,p,q=1}^N C_{mnpq} [W_n W_p \delta_e^q + W_n W_q \delta_e^p + W_p W_q \delta_e^n] \quad (2.70)$$

One has to note, however, that there is a limit on  $\lambda$  beyond which no static buckling solution exists. This point can be visualized by solving the two-mode solution of a two-

dimensional, simply-supported panel exactly. The governing equations are

$$K_{11} W_1 + \lambda E_{12} W_2 + (C_{11} W_1^2 + 4 C_{11} W_2^2) W_1 = 0 \quad (2.71)$$

$$K_{22} W_2 - \lambda E_{12} W_1 + (4 C_{11} W_1^2 + 16 C_{11} W_2^2) W_2 = 0 \quad (2.72)$$

where

$$C_{11} = C_{1111}$$

Taking  $4 \times W_2 \times$  Eq. 2.71 -  $W_1 \times$  Eq. 2.72, and dividing by  $\lambda E_{12}$  gives

$$W_1^2 + 4 W_2^2 = - \frac{1}{\lambda E_{12}} (4 K_{11} - K_{22}) W_1 W_2 \quad (2.73)$$

Employing Eq. 2.73 in Eq. 2.71 gives

$$W_2 = - \frac{K_{11} \lambda E_{12} W_1}{\lambda^2 E_{12}^2 - (4 K_{11} - K_{22}) C_{11} W_1^2} \quad (2.74)$$

Substituting Eqs. 2.73 and 2.74 into Eq. 2.72, using the relation  $4K_{11} - K_{22} = -12\pi^4$  and solving for  $W_1$  one obtains

$$W_1^2 = \frac{1}{12\pi^4 C_{11}} \left\{ K_{11} [-6\pi^4 \pm \sqrt{36\pi^8 - 4\lambda^2 E_{12}^2}] - \lambda^2 E_{12}^2 \right\} \quad (2.75)$$

then

$$W_2^2 = \frac{-\lambda^2 E_{12}^2 \left\{ K_{11} [6\pi^4 \mp \sqrt{36\pi^8 - 4\lambda^2 E_{12}^2}] + \lambda^2 E_{12}^2 \right\}}{12\pi^4 C_{11} [-6\pi^4 \pm \sqrt{36\pi^8 - 4\lambda^2 E_{12}^2}]^2} \quad (2.76)$$

$W_1$  must be real, and since  $\sqrt{36\pi^8 - 4\lambda^2 E_{12}^2} < 6\pi^4$ , the first requirement is

$$K_{11} < 0 \quad \text{or} \quad R_x < -\pi^2 \quad (2.77)$$

This condition is the conventional plate buckling condition.

The second requirement is that

$$36\pi^8 - 4\lambda^2 E_{12}^2 \geq 0 \quad \text{or} \quad \lambda^2 \leq 9\pi^8 / E_{12}^2 \quad (2.78)$$

This gives one of the upper bounds of  $\lambda$ .

Note that:

(a) If  $K_{11}[-6\pi^4 + \sqrt{36\pi^8 - 4\lambda^2 E_{12}^2}] > \lambda^2 E_{12}^2$

there are two solutions

(b) If  $K_{11}[-6\pi^4 + \sqrt{36\pi^8 - 4\lambda^2 E_{12}^2}] < \lambda^2 E_{12}^2 < K_{11}[-6\pi^4 - \sqrt{36\pi^8 - 4\lambda^2 E_{12}^2}]$  there is one solution

(c) If  $K_{11}[-6\pi^4 - \sqrt{36\pi^8 - 4\lambda^2 E_{12}^2}] < \lambda^2 E_{12}^2$  there is no solution.

Case (c) gives another upper bound for  $\lambda$ , usually this upper bound is more restrictive than that in Eq. 2.78. This illustrates that there is an upper limit on  $\lambda$  for static buckling solution to exist.

CHAPTER 3

NONLINEAR PANEL FLUTTER--RESULTS

A computer program has been written to solve the steady state panel flutter equations, Eq. 2.34 or Eq. 2.48, subject to different boundary conditions. Three other programs have also been written for solving the static buckling equations, Eq. 2.69, the transient equations, Eqs. 2.67 and 2.68, and the stability analysis, Eqs. 2.62. All these programs have a common sub-program to generate the coefficients  $M_{mn}$ ,  $G_{mn}$ ,  $GB_{mn}$ ,  $E_{mn}$ ,  $K_{mn}$  and  $C_{mnpq}$ .

For the two-dimensional plate, the harmonic balance method takes less than 1/12 of a minute on the IBM 360/65 computer to get one point for the 6-mode analysis and less than 3/10 of a minute for a 20-mode analysis. For the three-dimensional clamped-clamped plate, it takes approximately 1/10 of a minute to obtain one point for a 6-mode analysis. These mean quite a lot of computer time savings when compared to Dowell's<sup>10</sup> and Ventres'<sup>39</sup> direct integration method which takes 2 to 10 minutes for two-dimensional plates and more for three-dimensional clamped-clamped plates.

The panel flutter response is affected by a few parameters. First, there are influences from the panel such as the length to

width ratio  $a/b$ , the viscous type structural damping  $g_s$  and the hysteretic type structural damping  $g_b$ . Secondly, there are influences from the airflow such as the dynamic pressure  $\lambda$ , the aerodynamic damping coefficient  $\mu/M$ . Thirdly, there are influences from the boundary conditions such as the applied membrane force  $R_x$  and  $R_y$  and the spring constant  $K$ . Influence of these parameters are discussed in the next two sections where the various properties of panel flutter are presented for two-dimensional simply-supported panels and three-dimensional clamped-clamped panels.

### 3.1 Two-Dimensional Simply-Supported Plates

Consider, first, the question of convergence. The series representation for  $W$ , Eq. 2.33, is a complete set only when infinite terms are used. In practice, using infinite terms is out of question, hence truncation is inevitable. So a good understanding of the convergence of the series is important. Fig. 3 is a typical chart showing the convergence of the solution. It is clear from the figure that a 6-mode solution gives good convergence for the range of amplitude of vibration and dynamic pressure of interest here. It is also clear that convergence is better for a limit-cycle of low amplitude than for one of high amplitude. This is true because the high dynamic pressure associated with high amplitude response tends to blow the peak of the deflection to the rear, hence the deflection shape deviates more from the shapes of the first few modes. It has been found that the presence of the viscous type damping,  $g_s$  terms, damps out the higher modes and moves

the peak towards the center of the plate. Another parameter affecting the convergence of the solution is the membrane force  $R_x$ . It has been found that for  $R_x = -4\pi^2$ ,  $\mu/M = .01$ , only four modes are needed for **good convergence** whereas six modes are required for  $R_x = 0$ ,  $\mu/M = .01$ . Again, the explanation is that the larger the compressive membrane force is, the smaller the dynamic pressure is needed for the same amplitude of deflection, hence the peak is not blown so far back to the rear. Fig. 4 gives a comparison of the deflection shapes for different values of  $g_s$  and  $R_x$ . Because in panel flutter all the points do not reach the maximum amplitude at the same time, the deflection shapes shown in Fig. 4 indicate the maximum deflection of all the points for a given x-coordinate, rather than the deflection shapes of a certain instant.

### 3.1.1 Critical Dynamic Pressure

It is important for a flight vehicle designer to know under what circumstance the panel he designs will start to flutter. It is also important for him to know how many factors affect, and how they affect, the on-set of the flutter so that he can have a clear picture to avoid the occurrence of the flutter, if required to do so. This sub-section is devoted to the study of the pertinent factors that affect the stability boundary. In this sub-section, the influence of the mass ratio  $\mu/M$ , the membrane stress  $R_x$ , the viscous type structural damping  $g_s$  and the hysteretic type structural damping  $g_b$  on the critical dynamic pressure  $\lambda_c$  is explored.

First, consider the influence due to the membrane force  $R_x$ , Fig. 5 shows the effect of  $R_x$  on  $\lambda_c$  for different values of  $\mu/M$ . Only compressive membrane force is considered here. It is clear that the compressive membrane force always makes the panel less stable. A linear relation holds quite well for the range of  $R_x$  investigated here.  $R_x = -\pi^2$  is the classical buckling load of the plate, but because of the effect due to the passing air, the plate is not buckled in the range of  $R_x$  and  $\lambda$  shown\*. Next, consider the effect of  $\mu/M$  on  $\lambda_c$ . From Fig. 5, one can see that  $\mu/M$  always makes the panel more stable. For these particular values of  $g_s$  and  $g_b$ , a linear relation between  $\mu/M$  and  $\lambda_c$  also holds quite well. It can also be seen that the stabilizing effect of  $\mu/M$  is greater for smaller compressive membrane forces.

Fig. 6 shows the effect of the viscous type structural damping  $g_s$  on  $\lambda_c$  for different values of  $\mu/M$ . It can be seen that for small  $\mu/M$ , existence of small viscous damping drastically destabilizes the panel. Minimum  $\lambda_c$  occurs around  $g_s = .025$ . After this point, increase in  $g_s$  tends to make the panel more stable. With higher  $\mu/M$ , however, the destabilizing effect of  $g_s$  is not so pronounced. The curve corresponding to  $\mu/M=0$  serves as an asymptote only since some aerodynamic damping always exists. So the limiting value of  $\lambda_c$  for both  $g_s$  and  $\mu/M$  approaching zero is the upper limit in the figure, i.e.  $\lambda_c \approx 344$ . From this figure, it is also clear that increase

---

\*A discussion of the static buckling solution is given in subsection 3.1.5. One is also referred to Dowell<sup>10</sup>, for a detailed discussion.



in  $\mu/M$  has a greater stabilizing effect if  $g_s$  is at the range of .002 to .02. Since small amount of viscous type structural damping has great destabilizing effect and its exact value is very difficult to determine, this figure may well explain some of the discrepancy between the results of experiments and that of analytical work.

Fig. 7 shows the effect of the hysteretic structural damping  $g_b$  on  $\lambda_c$ . It can be seen that these two type of structural dampings have similar effect on  $\lambda_c$  except that the viscous type damping effect is magnified by the critical flutter frequency  $\omega_c$ , hence the minimum  $\lambda_c$  is reached at a  $g_s$  smaller than the corresponding value of  $g_b$ .\*

### 3.1.2 Critical Flutter Frequency

As one knows that the natural frequency of a plate determines the nonlinear forced response of the plate, so we devote this sub-section to study the variation of the critical flutter frequency as various parameters change. Coupled with the second part of this thesis, hopefully this study will enable the designer of space vehicles to avoid resonance peak when the panel is on the verge of fluttering. Fig. 8 shows the combined effect of  $R_x$  and  $\mu/M$  on the critical flutter frequency  $\omega_c$ . Presence of compressive  $R_x$  tends to reduce  $\omega_c$  whereas  $\mu/M$  tends to increase  $\omega_c$ . For both  $g_s$  and  $g_b$  equal to zero, the influence on  $\omega_c$  due to  $R_x$  seems to be much greater

---

\*Comparing structural damping coefficients  $g_s$  and  $g_b$  with the usual critical damping ratio  $\zeta_{cr}$  as measured from decaying measurements for the first mode with no airforces or mid-plane forces present gives  $g_s = 2/\pi^2 \zeta_{cr}$  and  $g_b = 2/\pi^2 \zeta_{cr}$ .

than that due to  $\mu/M$ . Fig. 9 shows the effect of  $g_s$  on  $\omega_c$  for different values of  $\mu/M$ . As one can see, the presence of small amount of  $g_s$  reduces  $\omega_c$  drastically. For  $g_s$  greater than .04, further increase of  $g_s$  doesn't seem to have much influence on  $\omega_c$ . It is also clear that  $\mu/M$  has a great influence on  $\omega_c$  when a small amount of  $g_s$  presents. Fig. 10 shows the effect of  $g_b$  on  $\omega_c$ . Again the effect is similar to that due to  $g_s$  but the rate of change of  $\omega_c$  is slower here. So examination of both lower critical frequency and lower critical speed than predicted can help ascertain whether significant  $g_s$  or  $g_b$  is present.

### 3.1.3 Limit-Cycle Amplitude

According to the classical estimation of the fatigue life of materials, the number of cyclic loading an aluminum material can take before fatigue failure<sup>45</sup> is

$$N_c = (2 \times 10^5 / \sigma_x)^6 \quad (3.1)$$

and the fatigue life  $T$  is equal to  $N_c$  divided by the frequency  $f = \frac{\omega}{2\pi}$ , or

$$T = \frac{N_c}{f} = \frac{2\pi N_c}{\omega} = \frac{2\pi}{\omega} (2 \times 10^5 / \sigma_x)^6 \quad (3.2)$$

where  $\sigma_x$  is roughly proportional to the maximum out of plane deflection. So if flutter is inevitable in the flight, it is desirable to keep amplitude of flutter as low as possible. Hence it is important to understand how the panel will behave after the critical dynamic pressure  $\lambda_c$  is exceeded and how the parameters discussed before affect the flutter response. All

the limit-cycle amplitudes in the following discussion are measured at  $\xi=x/a=.75$  for  $g_s=0$  and  $\xi=.6$  for  $g_s=0$ , since for  $g_s=0$ , the maximum deflection point occurs near  $\xi= .75$  and presence of  $g_s$  tends to damp out higher modes and hence moves the peak towards the center. The results obtained by Harmonic Balance Method agree quite well with both the Direct Integration Method and the Multiple Time Scale Technique, see Ref. 12. The third order approximation by Multiple Time Scale Technique, Ref. 41, gives

$$w/h = c (\lambda - \lambda_c)^{1/2} + h.o.t. \quad (3.3)$$

so all the response curves shown latter are very close to a parabola with  $w=0$  as its axis. And  $c$  is a measurement of the opening of the parabola.

Fig. 11 shows the effect of  $R_x$  on the limit cycle amplitude of flutter. A careful study will reveal that compressive membrane force not only reduces  $\lambda_c$  but also increases the value  $c$  hence causes the amplitude grow faster once  $\lambda_c$  is exceeded. Fig. 12 shows the effect of  $\mu/M$  on the flutter response curve. It is quite clear that  $\mu/M$  tends to reduce the opening of the  $\lambda-w/h$  curve. Fig. 13 shows the effect of  $g_s$  on the flutter response. It can be seen that small  $g_s$  cause the panel to start flutter at smaller  $\lambda_c$  and once flutter starts, the amplitude increases very fast with increasing  $\lambda$ . So the presence of  $g_s$  is highly undesirable. One should also note that with  $g_s = .15$ , although  $\lambda_c$  is greater than that of  $g_s=0$ , the opening of the  $\lambda-w/h$  curve is still much greater for  $g_s=.15$  than for  $g_s=0$ .

So the opening of the curve, or the value of  $c$ , is not just a function of  $\lambda_c$  as one may conclude from the last two figures.\*

#### 3.1.4 Frequency of Flutter

From Eq. 3.2, one knows that the fatigue life is inversely proportional to the frequency of vibration, so it is of interest to see the variation of the flutter frequency  $\omega$ . Fig. 14 shows the effect of membrane force  $R_x$  on the  $\lambda$ - $\omega$  relation. Compressive  $R_x$  reduces flutter frequency  $\omega$  over a certain range of  $\lambda$ , but the effect is not great. All the curves approach that for  $R_x=0$  as  $\lambda$  increases. Fig. 15 shows the variation of  $\omega$  with  $\lambda$  for different value of  $\mu/M$ . It is quite clear that  $\mu/M$  always reduces  $\omega$  for a fixed value of  $\lambda$ . It can also be seen that a linear relation between  $\omega$  and  $\lambda$  holds quite well, this shows that the perturbation expansion used by Morino<sup>41</sup> is quite good. The variation of  $\omega$  with  $\lambda$  for different values of  $g_s$  is shown in Fig. 16. Effect of  $g_s$  is not quite clear, first it reduces  $\omega$ , then increases it and finally reduces it again.

#### 3.1.5 Static Buckling Solutions

The static buckling solution are shown in Fig. 17. Since the panel is not vibrating and  $\lambda$  is small, higher modes are not

---

\*In the above discussion, one should keep in mind that  $\xi$  is kept constant (i.e. either  $\xi=.6$  or  $\xi=.75$ ) for the whole response curve and does not always coincide with the maximum deflection point, so the response curve will change slightly if one plots the maximum deflection versus  $\lambda$ . Then the discussion of the variation of  $c$  would be more meaningful. But it's quite academic to locate the maximum deflection point for every  $\lambda$ .

likely to be important, so only two-mode results are shown. It can be seen that higher compressive membrane forces exaggerate the deflection. For higher compressive membrane forces,  $R_x < -3\pi^2$ , two solutions exist over a certain range of  $\lambda$ . Stability analysis shows that the lower branch is unstable. The figure also shows that there is an upper limit for static buckling solution to exist. For  $R_x > -3\pi^2$ , this limit is lower than that given by Eq. 2.78, so the upper limit is governed by that stated in Case C following that equation.

### 3.1.6 Transient Envelope Solution of Flutter

Fig. 18 is a typical curve of the transient envelope solution of flutter. Experience here shows that the analysis given in Section 2.6 yields good convergence for a two-mode solution. The time increment can be set very large (about 1/4 of the period of the limit cycle solution). But as one increases the mode number to six, one has to decrease the time increment to such a small size (about 1/120 of the period of steady state oscillation) that this envelope analysis doesn't have great advantage over the direct integration analysis. One explanation is that during the transient period amplitudes of higher modes are not necessary small and they vibrate at their own frequencies which are not necessary close to that of the steady state solution; hence the assumption of slowly varying character of  $a_n$ 's and  $b_n$ 's are no longer valid\*.

---

\*If  $W_6(t) = \bar{A}_6 e^{(-\alpha + i\omega_6)t} = A_6(t) e^{i\omega t}$  where  $\omega$  is the steady state frequency,  $\bar{A}_6$  is a constant and  $A_6(t)$  is a damped oscillating function. Then  $A_6(t) = \bar{A}_6 e^{[-\alpha + i(\omega_6 - \omega)]t}$ , and when  $\alpha \ll 1$ ,  $\omega_6 \gg \omega$ ,  $A_6(t)$  is no longer a slowly varying function.

### 3.2 Three Dimensional Clamped-Clamped Panels

As in the two-dimensional simply-supported case, the convergence of the series representation of  $w$ , i.e. Eq. 2.37, is of immediate concern. The present analysis shows that for  $a/b = 1$ ,  $R_x = g_s = g_b = 0$  and  $\mu/M = .1$ , an eight-mode solution can contribute a few percents of improvement over a six-mode solution. Whereas with  $R_x = -4\pi^2$ , the improvement is not appreciable unless the amplitude of vibration is very high. As discussed at the beginning of Section 3.1, both  $g_s$  and compressive  $R_x$  improve the convergence of the series representation. The present analysis also shows that the length to width ratio  $a/b$  is a very important factor in deciding the convergence. For  $a/b=3$ , as many as sixteen modes are required for good convergence. Since computation time goes up very fast with the number of modes used, if long panel are used very often and computer time is a matter of concern, some other modal representation with peak near the rear part of the panel may be used. But use of such modes would increase much more mathematical manipulation to the already complicated one required in this work.

#### 3.2.1 Critical Dynamic Pressure

The influence of a few parameters on the critical dynamic pressure is discussed in this sub-section. Fig. 19 shows the combined effect of  $R_x$  and the length to width ratio  $a/b$  on the critical dynamic pressure  $\lambda_c$ . As in the two-dimensional case, compressive membrane force always makes the panel more

unstable. Also a linear relation between  $\lambda_c$  and  $R_x$  seems to hold quite well. The increase in length to width ratio  $a/b$  makes the panel more stable and the rate of increase is higher at higher  $a/b$ . Fig. 20 shows the effect of  $\mu/M$  on  $\lambda_c$ . As before  $\mu/M$  always stabilizes the panel. Fig. 21 shows the effect of the viscous type structural damping  $g_s$  on  $\lambda_c$  for different values of  $\mu/M$ . The characteristics of these curves are similar to those shown in Fig. 6 for two-dimensional plate, only now minimum  $\lambda_c$  occurs around  $g_s = .0035$  instead of  $g_s = .025$ . One should also note that for  $\mu/M > .15$ , presence of  $g_s$  only stabilizes the panel. So for  $a/b = 1^*$ , if one can keep  $\mu/M > .1$ , one would be quite safe even if he does not take  $g_s$  into account.

### 3.2.2 Critical Flutter Frequency

Fig. 22 shows the combined effect of  $a/b$  and  $R_x$  on the critical flutter frequency. These curve look like parabolas with its axis coincide with  $\omega_c$  axis. It is clear that increase in  $a/b$  always increases  $\omega_c$  and increase in the compressive membrane force causes a decrease in  $\omega_c$ . Fig. 23 shows the  $\mu/M - \omega_c$  relation, one can see that increase of  $\mu/M$  always increases the critical flutter frequency. Fig. 24 shows the effect of  $g_s$  on  $\omega_c$  for different values of  $\mu/M$ . The characteristics is similar to that of two dimensional case: presence of  $g_s$  first reduces  $\omega_c$  drastically, then as  $g_s$  increases,  $\omega$  approaches a certain limiting value.

---

\*Results for  $a/b=.1$ , however, shows that the destabilizing effect of  $g_s$  at  $\mu/M=.15$  is still quite appreciable.

### 3.2.3 Limit-Cycle Amplitude

Fig. 25 shows the effect of  $a/b$  on the  $\lambda$ - $w/h$  relation. It can be seen that increase in  $a/b$  decreases the opening of the  $\lambda$ - $w/h$  curves as well as increases the critical dynamic pressure. So increase in  $a/b$  is desirable both in preventing flutter and in prolonging the fatigue life of the panel. Fig. 26 shows the effect of  $R_x$  on the response curve. If one moves all the curves horizontally so that all the starting points fall on that for  $R_x=0$  curve, one can see that all the curves coincide with that for  $R_x=0$  quite well up to  $w/h=1$ , so one can conclude that for this length to width ratio  $a/b$ , the major effect of  $R_x$  is to change  $\lambda_c$ , while its effect on the opening of the  $\lambda$ - $w/h$  curve is secondary. Fig. 27 shows the effect of  $\mu/M$  on the opening of the  $\lambda$ - $w/h$  curve. It can be seen that  $\mu/M$  not only increases the critical dynamic pressure, but also makes the opening of the  $\lambda$ - $w/h$  smaller, hence limits the flutter amplitude once  $\lambda_c$  is exceeded. The effect of  $g_s$  on the opening of the  $\lambda$ - $w/h$  curve is not quite definite as can be seen in Fig. 28. For  $g_s=.001$ , the opening of the curve is smaller than that corresponding to  $g_s=0$ , whereas the curves with greater  $g_s$  have larger opening than that with  $g_s=0$ . The reason for the smaller opening for  $g_s=.001$  may be because  $\xi=.6$  is too far away from the actual peak of the deflection curve, so the deflection shown here is much less than the maximum deflection of the plate.

The effect of the membrane force  $R_y$  is small for small  $a/b$  as can be expected since every  $R_y$  is associated with  $(a/b)^2$



in the differential equation, Eq. 2.22. The effect of  $R_y$  is also small for  $a/b=1.0$  as can be seen in Table 1. This may result from the lack of coupling between the aerodynamic force and the deflection mode in  $y$  direction as pointed out by Hedgepeth<sup>6</sup> in his study of the three-dimensional simply-supported panel flutter. One should be aware of the result shown by Fralich<sup>22</sup> that at higher compressive  $R_x$ , if  $R_y=0$ , the first mode representation in  $y$  direction is no longer good and additional spanwise modes have to be included.

### 3.2.4 Frequency of Flutter

The variation of the flutter frequency  $\omega$  with dynamic pressure  $\lambda$  for different values of  $a/b$  is shown in Fig. 29. It can be seen that a linear relation between  $\lambda$  and  $\omega$  holds quite well. Increase of  $a/b$  increases the value of  $\omega$  for a fixed  $\lambda$ , but the shape of the  $\lambda$ - $\omega$  curve is not changed significantly. Fig. 30 shows the effect of  $R_x$  on the  $\lambda$ - $\omega$  relation. Compressive  $R_x$  always increase  $\omega$  for a fixed  $\lambda$ , however, increment is not great and the shape remains the same. Fig. 31 shows the effect of  $\mu/M$  on the  $\lambda$ - $\omega$  relation. Again linear relation holds quite well for all range of  $\mu/M$  studied here, so the only effect of  $\mu/M$  is to decrease the value of  $\omega$  for a fixed  $\lambda$ . Fig. 32 shows the effect of  $g_s$  on  $\lambda$ - $\omega$  relation. Presence of  $g_s$  tends to reduce the flutter frequency. As before, the effect of  $g_s$  on the  $\lambda$ - $\omega$  curve is secondary.

CHAPTER 4

NONLINEAR INTERACTION OF PANEL FLUTTER AND FORCING  
EXCITATION--THEORY

4.1 Introduction

The problem studied in this chapter is the interaction of aerodynamic forces, elastic forces, inertia forces and external forcing excitations. In Chapter 2, the interaction of the first three forces has been thoroughly studied. The results obtained there are good enough if one assumes that during the flight, the vehicle will not encounter any strong external excitations from the air, or from the body vibrating as a flexural structure. However, gust loading is inevitable during the flight and the vehicle is a flexural structure. So external forcing excitations due to the gust or vibration of wings or some other flexural components of the structures always exist. Hence in order to better understand the behavior of the panel during the flight, one should include the external excitations. For simplicity, however, only simple harmonic excitation is considered here.

Section 4.2 gives the formulation of the problem. Galerkin's technique is also used here to reduce the partial differential equation to a set of ordinary differential equations with time,

$\tau$ , the only independent variable. The resulting equation, Eq. 4.6, is similar to those for panel flutter, i.e. Eqs. 2.34 and 2.48, except for the forcing terms on the right hand side. Section 4.3 is concerned with the solution of Eq. 4.6 for the dynamic pressure  $\lambda$  smaller than the critical dynamic pressure  $\lambda_c$ . At this stage, the panel is not fluttering, so the response frequencies will be that of the forcing frequency or a multiple or fraction of it. In order to obtain a clear picture on the effect of aerodynamic force on the forcing response, both the linear and nonlinear analyses are given. Section 4.4 is concerned with the solution of Eq. 4.6 with  $\lambda$  greater than  $\lambda_c$ . Since the panel might be fluttering, both the responses with forcing frequency and with flutter frequency have to be considered. Hence a series representation of  $w$  like that shown in Eq. 4.23 has to be used. This enables one to see both the effect of forcing excitations on the flutter and the effect of the flutter on the forcing response. The results of these studies are discussed in Chapter 5, and are shown in figure form at the end of this thesis.

#### 4.2 Formulation of Problem

The problem studied in this chapter is a plate subject to both the aerodynamic force described in Section 2.2 and a harmonic varying uniform pressure loading. This loading could come from either a gust loading, the noise from the engine, or the inertial loading due to the vibration of the supporting frame caused either by the response of the airplane

to gust or by the vibration of the wing if the panel is located at or near the wing tips. Attention is focused on a uniform loading. Other types of spatially varying loading can be similarly incorporated. The equation of motion of a plate is briefly derived in Section 2.2 and is not repeated here. The equation of motion corresponds to Eq. 2.7 for a two-dimensional simply-supported plate is

$$D \left( 1 + \bar{g}_s \frac{\partial}{\partial t} + \bar{g}_b \frac{1}{\omega} \frac{\partial}{\partial t} \right) \frac{\partial^4 w}{\partial x^4} - \left[ N_x^a + \alpha \frac{Eh}{2a} \int_0^a \left( \frac{\partial w}{\partial x} \right)^2 dx \right] \frac{\partial^2 w}{\partial x^2} \quad (4.1)$$

$$= \rho_m h \frac{\partial^2 w}{\partial t^2} + \frac{2\mathcal{E}}{M} \left[ \frac{\partial w}{\partial x} + \frac{1}{U} \frac{\partial w}{\partial t} \right] + \Delta P + \bar{F}_0 \cos \bar{\Omega} t$$

where  $F_0$  and  $\bar{\Omega}$  are the amplitude and frequency of the forcing excitation. The boundary conditions are the same as those shown in Eq. 2.10.

The equations of motion corresponding to Eqs. 2.22 and 2.23, i.e. for three-dimensional clamped-clamped plate, are

$$\begin{aligned} & \left( 1 + g_s \frac{\partial}{\partial t} + g_b \frac{1}{\omega} \frac{\partial}{\partial t} \right) \left[ \frac{\partial^4 W}{\partial z^4} + 2A^2 \frac{\partial^4 W}{\partial z^2 \partial \eta^2} + A^4 \frac{\partial^4 W}{\partial \eta^4} \right] \\ & + \frac{\partial^2 W}{\partial z^2} = R_x \frac{\partial^2 W}{\partial z^2} + R_y A^2 \frac{\partial^2 W}{\partial \eta^2} - \lambda \frac{\partial W}{\partial z} - \left( \frac{\lambda M}{M} \right)^{1/2} \frac{\partial W}{\partial t} \end{aligned} \quad (4.2)$$

$$+ P + \bar{F}_0 A^4 / D_R \cos \Omega t$$

$$\begin{aligned} & \frac{\partial^4 \Phi}{\partial z^4} + 2A^2 \frac{\partial^4 \Phi}{\partial z^2 \partial \eta^2} + A^4 \frac{\partial^4 \Phi}{\partial \eta^4} = 12(1-\nu^2) D A^2 \\ & \times \left\{ \left( \frac{\partial^2 W}{\partial z \partial \eta} \right)^2 - \frac{\partial^2 W}{\partial z^2} \frac{\partial^2 W}{\partial \eta^2} \right\} \end{aligned} \quad (4.3)$$

with the same boundary conditions as those shown in Eqs. 2.24,

2.27, 2.28 and 2.29.

In both Eqs. 4.1 and 4.2, only simple harmonic forcing excitation is considered. One should also note that if the dynamic pressure  $q$  in Eq. 4.1 and  $\lambda$  in Eq. 4.2 were set to zero, one obtains the equations for forcing vibration of a plate.

Here again Galerkin's Technique is employed to eliminate the spatial variables and reduce the equations to ordinary differential equations. For the two-dimensional simply-supported plate, substituting Eq. 2.33 into Eq. 4.1 for  $w$ , using the non-dimensional parameters shown in Eq. 2.35, applying Galerkin's Technique, one obtains

$$\sum_{n=1}^N \left[ M_{mn} \frac{\partial^2 W}{\partial \tau^2} + G_{mn} \frac{\partial W_n}{\partial \tau} + GB_{mn} \frac{1}{\omega} \frac{\partial W_n}{\partial \tau} + \lambda E_{mn} W_n + K_{mn} W_n \right] \quad (4.4)$$

$$+ \sum_{n,p,q=1}^N C_{mnpq} W_n W_p W_q = F_m \cos \Omega \tau$$

for  $m=1,2,\dots,N$

where  $M_{mn}$ ,  $G_{mn}$ ,  $GB_{mn}$ ,  $E_{mn}$ ,  $K_{mn}$  and  $C_{mnpq}$  are the same as those defined in Eq. 2.35, and

$$\Omega = \bar{\Omega} [D/\rho_m h a^4]^{1/2}$$

$$F_m = \int_0^1 \frac{\bar{F}_0 a^4}{Dh} \sin m\pi \xi d\xi = \frac{\bar{F}_0 a^4}{Dh} \frac{1}{m\pi} [1 - (-1)^m] = \frac{F_R}{2m} [1 - (-1)^m] \quad (4.5)$$

For the three-dimensional clamped-clamped plate, using the deflection mode, Eq. 2.37, for  $w$  in Eq. 4.2 and 4.3, going through the same procedures as in sub-section 2.3.2, one obtains,

$$\sum_{n=1}^N \left[ M_{mn} \frac{\partial^2 W_n}{\partial \tau^2} + G_{mn} \frac{\partial W_n}{\partial \tau} + GB_{mn} \frac{1}{\omega} \frac{\partial W_n}{\partial \tau} + \lambda E_{mn} W_n + K_{mn} W_n \right] \quad (4.6)$$

$$+ \sum_{n,p,q=1}^N C_{mnpq} W_n W_p W_q = F_m \cos \Omega \tau$$

for  $m=1,2,\dots,N$

where  $M_{mn}$ ,  $G_{mn}$ ,  $GB_{mn}$ ,  $E_{mn}$ ,  $K_{mn}$  and  $C_{mnpq}$  are defined in appendix A, Eqs. A.9.1 to A.9.6 and

$$F_m = \int_0^1 \int_0^1 \frac{\bar{F}_0 a^4}{D h} [\cos(m-1)\pi\zeta - \cos(m+1)\pi\zeta] [1 - \cos 2\pi\eta] d\zeta d\eta$$

$$= \frac{\bar{F}_0 a^4}{D h} S_1^m \quad (4.7)$$

Eqs. 4.4 and 4.6 are the subjects of study in the next two sections. Section 4.3 concerns with forcing excitation before the classical flutter dynamic pressure  $\lambda_c$  is reached. At this state, the panel is not fluttering, so the response frequency will be that of the forcing frequency or multiples or fractions of the forcing frequency. Hence the interaction is a one-way influence, i.e. the aerodynamic force affects the forcing response of the plate. Section 3.4 concerns with the forcing excitation with  $\lambda$  greater than the conventional critical dynamic pressure. At this state, the plate may be fluttering, so the response solution should include a component which has a frequency the same as the flutter frequency. Because Eqs. 4.6 and 4.4 have the same general form, only one discussion will be given in both sections 4.3 and 4.4.

### 4.3 Forced Response of Panel Below Flutter

In this section, the effect of the aerodynamic force on the forced response characteristics of a plate is studied. With appropriate amount of aerodynamic damping present, it is well known that when the dynamic pressure increases and approaches its critical value, i.e. the value that causes the

panel to flutter, the frequencies of the first two modes approaches each other. In some cases, i.e. in the absence of structural damping, they even merge together and cause the so-called frequencies coalescence. How the response curves corresponding to these first two frequencies pile up is the matter to study in this section. As mentioned at the end of the last section, at the range of dynamic pressure interested here, the panel is not fluttering, and the plate responds only with frequencies equal to or multiple or fraction of the forcing frequency. We focus our attention on the following two response characteristics: (a) Response characteristics of the linear system and (b) response characteristics of non-linear system.

#### 4.3.1 Linear System

Setting  $C_{mnpq}$  equal to zero in either Eqs. 4.4 or 4.6, one obtains the linear system

$$\sum_{n=1}^N \left[ M_{mn} \frac{\partial^2 W_n}{\partial \tau^2} + G_{mn} \frac{\partial W_n}{\partial \tau} + GB_{mn} \omega \frac{\partial W_n}{\partial \tau} + \lambda E_{mn} W_n + K_{mn} W_n \right] = F_m \cos \Omega \tau \quad (4.8)$$

Since this is a linear system, the only response is the one with frequency  $\Omega$ , so assume

$$W_n = c_n \sin \Omega \tau + d_n \cos \Omega \tau \quad (4.9)$$

substituting this into Eq. 4.8 and setting the coefficients of  $\sin \Omega \tau$  and  $\cos \Omega \tau$  to zero, one obtains,

$$\sum_{n=1}^N \left[ (-\Omega^2 M_{mn} + \lambda E_{mn} + K_{mn}) c_n - (\omega G_{mn} + GB_{mn}) d_n \right] = 0 \quad (4.10)$$

$$\sum_{n=1}^N [(-\Omega^2 M_{mn} + \lambda E_{mn} + K_{mn}) d_n + (\omega G_{mn} + GB_{mn}) C_n] = F_m$$

for  $m=1, 2, \dots, N$  (4.11)

Solving Eqs. 4.10 and 4.11 simultaneously for  $c_n$ 's and  $d_n$ 's, one obtains the solution to this problem. Solutions for different value of  $\lambda$  have been obtained, discussed in subsection 5.1 and shown in figure form at the end of this thesis.

#### 4.3.2 Nonlinear System

In order to find the nonlinear response characteristics, the whole equation of either equation 4.4 or equation 4.6 has to be considered. For the convenience of later discussion, the following new time scale is used, let

$$\Omega \tau = k t, \tag{4.12}$$

and rewrite either Eq. 4.4 or Eq. 4.6 in the following form,

$$\sum_{n=1}^N \left[ \bar{M}_{mn} \frac{d^2 W_n}{dt_1^2} + \bar{G}_{mn} \frac{dW_n}{dt_1} + GB_{mn} \frac{1}{\bar{\omega}} \frac{dW_n}{dt_1} + \lambda E_{mn} W_n + K_{mn} W_n \right] + \sum_{p, q=1}^N C_{mnpq} W_n W_p W_q = F_m \cos k t,$$

for  $m=1, 2, \dots, N$  (4.13)

where

$$\begin{aligned} \bar{M}_{mn} &= \frac{\Omega^2}{k^2} M_{mn} \\ \bar{G}_{mn} &= \frac{\Omega}{k} G_{mn} \\ \bar{\omega} &= \frac{k}{\Omega} \omega \end{aligned} \tag{4.14}$$



Because nonlinear terms are present in Eq. 4.13, subharmonic and superharmonic responses might occur as well as simple harmonic solution. To explore their existence, one assumes

$$W_n = [d_{n0} + \sum_{r=1}^3 (C_{nr} \sin rt_1 + d_{nr} \cos rt_1)] \quad (4.15)$$

Employing this expression in Eq. 4.13 and balancing constant term and the first to the third harmonics, one obtains; constant terms

$$\sum_{n=1}^N (\lambda E_{mn} + K_{mn}) d_{n0} + \sum_{n,p,q=1}^N C_{mnpq} P_1 = 0 \quad (4.16)$$

$\sin t_1$  terms:

$$\begin{aligned} \sum_{n=1}^N (-\bar{M}_{mn} + \lambda E_{mn} + K_{mn}) C_{n1} - \sum_{n=1}^N (\bar{G}_{mn} + GB_{mn}) d_{n1} \\ + \sum_{n,p,q=1}^N C_{mnpq} P_2 = 0 \end{aligned} \quad (4.17)$$

$\cos t_1$  terms:

$$\begin{aligned} \sum_{n=1}^N (-\bar{M}_{mn} + \lambda E_{mn} + K_{mn}) d_{n1} + \sum_{n=1}^N (\bar{G}_{mn} + GB_{mn}) C_{n1} \\ + \sum_{n,p,q=1}^N C_{mnpq} P_3 = F_m \delta_1^k \end{aligned} \quad (4.18)$$

$\sin 2t_1$  terms:

$$\begin{aligned} \sum_{n=1}^N (-4\bar{M}_{mn} + \lambda E_{mn} + K_{mn}) C_{n2} - \sum_{n=1}^N (2\bar{G}_{mn} + GB_{mn}) d_{n2} \\ + \sum_{n,p,q=1}^N C_{mnpq} P_4 = 0 \end{aligned} \quad (4.19)$$

cos2t<sub>1</sub> terms:

$$\begin{aligned} \sum_{n=1}^N (-4\bar{M}_{mn} + \lambda E_{mn} + K_{mn}) d_{n2} + \sum_{n=1}^N (2\bar{G}_{mn} + GB_{mn}) C_{n2} \\ + \sum_{n,p,q=1}^N C_{mnpq} P_5 = F_m S_2^* \end{aligned} \quad (4.20)$$

sin3t<sub>1</sub> terms:

$$\begin{aligned} \sum_{n=1}^N (-9\bar{M}_{mn} + \lambda E_{mn} + K_{mn}) C_{n3} - \sum_{n=1}^N (3\bar{G}_{mn} + GB_{mn}) d_{n3} \\ + \sum_{n,p,q=1}^N C_{mnpq} P_6 = 0 \end{aligned} \quad (4.21)$$

cos3t<sub>1</sub> terms:

$$\begin{aligned} \sum_{n=1}^N (-9\bar{M}_{mn} + \lambda E_{mn} + K_{mn}) d_{n3} + \sum_{n=1}^N (3\bar{G}_{mn} + GB_{mn}) C_{n3} \\ + \sum_{n,p,q=1}^N C_{mnpq} P_7 = F_m S_3^* \end{aligned} \quad (4.22)$$

where all the p's are functions of c<sub>ni</sub>'s and d<sub>ni</sub>'s. The definitions of p's along with the details of the calculation are given in appendix B. According to different objectives, the solutions of Eqs. 4.16 to 4.22 are discussed in the following:

Case A: Simple harmonic response

In order to obtain the simple harmonic response, one sets k=1 in Eq. 4.12. Note that if one sets d<sub>n0</sub>, c<sub>n2</sub> and d<sub>n2</sub> to zero, Eqs. 4.16, 4.19 and 4.20 are satisfied identically. So

there are only four equations left, i.e. Eqs. 4.17, 4.18, 4.21 and 4.22. Results obtained here show that inclusion of  $c_{n3}$  and  $d_{n3}$  only yield less than a few percents difference in the solution of  $c_{n1}$  and  $d_{n1}$ , and  $c_{n3}$  and  $d_{n3}$  themselves are small compared to  $c_{n1}$  and  $d_{n1}$ . So if many modes are needed for good convergence and computer time is a matter of concern, one can set  $c_{n3}$  and  $d_{n3}$  to zero and solve Eqs. 3.17 and 3.18 for  $c_{n1}$  and  $d_{n1}$ .

Case B: Superharmonic Response of order 3

In order to obtain this superharmonic response, one sets  $k=1$ . Again one can set  $d_{n0}$ ,  $c_{n2}$  and  $d_{n2}$  to zero and solve the four equations, Eq. 4.17, 4.18, 4.21 and 4.22. One should note that this branch of solution is important only when the forcing frequency is around one third of that of the nature frequency of the plate with air flows over one of its surfaces. One should also note that solutions corresponding to this branch have  $c_{n3} \gg c_{n1}$ ,  $d_{n3} \gg d_{n1}$ . So one should take this fact into account when one gives the initial values for the Newton Raphson iteration.

Case C: Subharmonic Response of Order 3

This case is quite similar to case B. Only now one sets  $k=3$  and the solutions have  $c_{n1} \gg c_{n3}$  and  $d_{n1} \gg d_{n3}$ .

Case D:

For the other possible superharmonic solution, order 2 and order 3/2, and the other subharmonic solutions, order 1/2 and order 2/3, all the equations from Eq. 4.16 to Eq. 4.22 have to be used. One is referred to Tseng's<sup>46</sup> work on vibration of

beams for more detailed discussion.

In solving Eqs. 4.16 to 4.22,  $\lambda$  is assumed known. It ranges from zero to  $\lambda_c$  obtained in Chapter 2. For  $\lambda=0$ , one obtains the forced response of a plate. This solution is not good for  $\lambda \gg \lambda_c$ , because in this case, the plate already undergoes flutter and the flutter components of the response are no longer negligible. The solution given by Eq. 4.15 is not good for two reasons: first it doesn't yield response having flutter frequency, secondly, it doesn't show the effect the fluttering components on the components of the forcing response. The case of  $\lambda \gg \lambda_c$  is discussed in Section 4.4.

The nonlinear equations 4.16 to 4.22 are solved by Newton Raphson's Technique. The unknown vector is  $\tilde{x}=(d_{10}, c_{11}, d_{11}, c_{12}, d_{12}, c_{13}, d_{13}, d_{20}, \dots, d_{n3})$ . The Jacobian of these equations are given in Appendix B. The results of calculations, for different value of  $\lambda$ , are discussed in Section 5.2 and shown in figure form at the end of this thesis.

#### 4.4 Interaction of Forcing-Flutter Response

As mentioned at the end of sub-section 4.3.2, when the dynamic pressure  $\lambda$  is greater than  $\lambda_c$  (the critical dynamic pressure of a panel without forcing excitations), the plate may undergo flutter and may change the whole picture of response firstly by introducing the fluttering components and secondly by changing the magnitude of the response components having the frequency of the forcing excitations. Hence we have the whole problem of interaction between panel flutter and forcing excitations.

In order to study the interaction, one has to add a response component, having a frequency equal to that of panel flutter, to the series in Eq. 4.15. However, for simplicity, one would concentrate on the interaction between the flutter component and the first harmonic only. So one assumes

$$W_n = a_n \rho \sin \omega_1 t_1 + b_n \cos \omega_1 t_1 + C_n \rho \sin t_1 + d_n \cos t_1 \quad (4.23)$$

where  $a_n$  and  $b_n$  are the fluttering components,  $c_n$  and  $d_n$  are the forcing response components and  $\omega_1$  is the flutter frequency based on the time scale  $t_1$ .

Employing Eq. 4.23 into Eq. 4.13, balancing the four most important components  $\sin \omega_1 t_1$ ,  $\cos \omega_1 t_1$ ,  $\sin t_1$  and  $\cos t_1$ , one obtains\*

$\sin \omega_1 t_1$  terms:

$$\begin{aligned} & \sum_{n=1}^N [-\bar{M}_{mn} \omega_1^2 + \lambda E_{mn} + K_{mn}] a_n - \sum_{n=1}^N (\omega_1 \bar{G}_{mn} + G B_{mn}) b_n \\ & + \frac{1}{4} \sum_{n,p,g=1}^N C_{mnp} \{ 3a_n a_p a_g + a_n b_p b_g + b_n a_p b_g + b_n b_p a_g \\ & + 2[a_n (c_p c_g + d_p d_g) + a_p (c_n c_g + d_n d_g) + a_g (c_n c_p \\ & + d_n d_p)] \} = 0 \end{aligned} \quad (4.24)$$

$$m=1, 2 \dots N$$

---

\*Other harmonic components,  $\sin(2\omega_1 - 1)t_1$ ,  $\sin(2 - \omega_1)t_1$ , etc., have been neglected, as a first approximation. These could be included in a more accurate approximation.

$\cos \omega_1 t_1$  terms:

$$\begin{aligned} & \sum_{n=1}^N [-\omega_1^2 \bar{M}_{mn} + \lambda E_{mn} + K_{mn}] b_n + \sum_{n=1}^N (\omega_1 \bar{G}_{mn} + G B_{mn}) a_n \\ & + \frac{1}{4} \sum_{n,p,q=1}^N C_{mnpq} \{ 3b_n b_p b_q + b_n a_p a_q + a_n b_p a_q + a_n a_p b_q \\ & + 2 [b_n (C_p C_q + d_p d_q) + b_p (C_n C_q + d_n d_q) + b_q (C_n C_p \\ & + d_n d_p) ] \} = 0 \end{aligned} \quad (4.25)$$

$\sin t_1$  terms\*:

$$\begin{aligned} & \sum_{n=1}^N [-\bar{M}_{mn} + \lambda E_{mn} + K_{mn}] c_n - \sum_{n=1}^N (\bar{G}_{mn} + G B_{mn}) d_n \\ & + \frac{1}{4} \sum_{n,p,q=1}^N C_{mnpq} \{ 3c_n c_p c_q + c_n d_p d_q + d_n c_p d_q + d_n d_p c_q \\ & + 2 [c_n (a_p a_q + b_p b_q) + c_p (a_n a_q + b_n b_q) \\ & + c_q (a_n a_p + b_n b_p) ] \} = 0 \end{aligned} \quad (4.26)$$

$\cos t_1$  terms:

$$\begin{aligned} & \sum_{n=1}^N [-\bar{M}_{mn} + \lambda E_{mn} + K_{mn}] d_n + \sum_{n=1}^N (\bar{G}_{mn} + G B_{mn}) c_n \\ & + \frac{1}{4} \sum_{n,p,q=1}^N C_{mnpq} \{ 3d_n d_p d_q + d_n c_p c_q + c_n d_p c_q + c_n c_p d_q \\ & + 2 [d_n (a_p a_q + b_p b_q) + d_p (a_n a_q + b_n b_q) \\ & + d_q (a_n a_p + b_n b_p) ] \} = F_m \end{aligned} \quad (4.27)$$

---

\*The  $\tilde{\omega}$  associated with  $GB_{mn}$  in equation 4.13 is equal to  $\omega_1$  for the flutter component and equal to 1 for the forcing component, since by definition, the total work by hysteretic type structural damping is independent of the frequency of vibration.

From the above four equations, one can see that the forcing response and flutter response are coupled only through nonlinear terms. One should note that the nonlinear coupling due to forcing response add some terms linear in  $a_m$ 's and  $b_m$ 's to Eqs. 4.24 and 4.25. As one knows that linear terms determine the boundary of stability of panel flutter, the addition of these "linear" terms is going to change the boundary of stability, or  $\lambda_c$ , significantly if the components  $c_m$ 's and  $d_m$ 's are not small. One can also see that the effect of the flutter components on the forcing components is significant only when the magnitude of the flutter components are not small.

Equations 4.24 to 4.27 are solved by Newton Raphson's Technique. Since we don't know the critical dynamic pressure for a certain amplitude and frequency of forcing excitation, the unknown vector should include both  $\lambda$  and  $\omega$ . Hence one assumes  $\underline{x} = (\lambda, \omega, c_1, d_1, a_2, \dots, d_n)$ . The Jacobian of Eqs. 4.24 to 4.27 is shown in Appendix C.

Equations 4.24 to 4.27 are solved for different amplitudes and frequencies of the forcing excitation. Results are shown in figure form at the end of this thesis and the detail of interaction is discussed in Section 5.3.

CHAPTER 5

NONLINEAR INTERACTION OF PANEL FLUTTER  
AND FORCING EXCITATIONS--RESULTS

The results of nonlinear forcing-flutter interaction are discussed in this chapter. Only the case of no structural damping is given as an illustration, since in the absence of the structural damping the first two frequency coalesce at the stability boundary, so it is easier to discuss the stability boundary of the panel under forcing excitation. Because the first two modes are the most important ones in panel flutter and because only limited computer time is available, most of the results shown are two-mode solutions. A six-mode solution is given at the end of this chapter for the forced response at  $\lambda$  equal to the classical critical dynamic pressure  $\lambda_c$  for comparison. For the same reason, only one superharmonic resonance solution is shown for the  $\lambda=0$  case and nothing is done on the three-dimensional clamped-clamped plates.

Some results of direct integration on Eq. 4.13 obtained by this author are also shown to check the results from Harmonic Balance method.



## 5.1 Forced Response of Panel Below Flutter

### 5.1.1 Linear Systems

As a first step to the study of the nonlinear interaction of panel flutter and forcing excitations, the linear forced response of the panel below flutter is studied here. Fig. 33 shows the linear forced response of a panel as a function of the forcing frequency  $\Omega$  at different values of dynamic pressure  $\lambda \leq \lambda_c$ . The curve for  $\lambda=0$  is the linear forced response of a plate without airflow over its surface. Because of no damping from the air, the resonance peak at the first natural frequency  $\omega_1=9.87$  goes to infinity. However, because the forcing excitation is uniform and because of lack of coupling between modes, even modes are not present, hence there is no resonance peak at the second natural frequency,  $\omega_2=39.48$ , of the plate. When air flows over one of the faces of the plate, it causes both damping and coupling between the two modes. So the resonance peak becomes finite and the second peak comes up. As  $\lambda$  increases, the first two natural frequencies move toward each other, so do the resonance peaks. When there is more coupling between the first two modes, the effect of aerodynamic damping becomes smaller and smaller so the peaks grow higher and higher. At  $\lambda=\lambda_c$ , linear flutter analysis shows that undamped vibration exists, so the resonance peak goes to infinity as for a system of no damping.\*

---

\*For the example given here, i.e.  $g_s=g_b=0$ , the two frequencies merge together at  $\lambda=\lambda_c$ , so only one resonance peak is obtained. For  $g_s \neq 0$  and/or  $g_b \neq 0$ , two peaks may present at  $\lambda=\lambda_c$ . One peak goes to infinity while the other remains finite.

### 5.1.2 Nonlinear Systems

In this sub-section, the nonlinear forced response of a panel with air flows over one of its faces is studied. The speed of the air is limited such that the panel is not fluttering. So only the response with a frequency equal to, or a multiple of, or a fraction of the natural frequency will present.

First, look at the case of  $\lambda=0$ . Unlike the linear case, which has only one resonance peak at the first natural frequency  $\omega_1$ , we now have several resonance peaks as shown in Fig. 34. The first peak from the left corresponds to the superharmonic resonance of order 3. This branch occurs through the nonlinear coupling between the first and third harmonics. It can be obtained by giving an iterative initial value  $c_{n3} \gg c_{n1}$ ,  $d_{n3} \gg d_{n1}$ . One should note, however, that this branch exists only for the forcing frequency  $\Omega$  greater than  $1/3$  of the first natural frequency  $\omega_1$ . At this branch, the plate vibrates at its first natural frequency  $\omega_1$  instead of the forcing frequency  $\Omega$ . The forcing amplitude has little effect on response curve, so the two curves for  $F_R=40$  and  $80$  become one on the scale used here. Due to limited computer time available, this is the only superharmonic solution studied in this thesis. One is referred to Tseng<sup>49</sup> for more detailed discussion of other superharmonic and subharmonic solutions. The second peak is the simple harmonic resonance of the first mode. This response is similar to that for Duffing's equation. The third peak corresponds to the usual

resonance of the second mode. This resonance occurs through the nonlinear coupling among modes and exists only for  $\Omega$  greater than the second natural frequency  $\omega_2$ . This branch of solution can be obtained by giving iterative initial value  $c_{2r}$  and  $d_{2r}$  much greater than the other components.

Fig. 35 shows the nonlinear forced response at the dynamic pressure equal to  $3/4$  of the classical critical dynamic pressure  $\lambda_c$ . It can be seen that the solution for  $F_R=10$  is still quite linear: the peaks are not bent and the amplitude is about  $1/4$  of the linear solution shown on Fig. 33. For higher amplitude, the nonlinear terms come into play and the peaks are bent in the hard-spring fashion.

Fig. 36 shows the nonlinear forced response of a panel with dynamic pressure  $\lambda$  equal to the critical dynamic pressure  $\lambda_c$ . Recall that the linear solution yields an undamped harmonic resonance peak, i.e. with peak going to infinity at  $\Omega$  equal to the flutter frequency  $\omega=28.77$ . Instead of bending the resonance peak of a linear system to the right as for the case of  $\lambda=0$ , the nonlinear terms create two peaks. The two peaks move away from each other farther and farther as the forcing amplitude increases. In order to have a better insight into the problem, see Fig. 37 first. This figure shows the forced response at  $\lambda=\lambda_c$  but with smaller forcing amplitude. The response curve for  $F_R=.01$  behaves like linear system with a peak at  $\Omega=\omega_c$  except that the peak does not go to infinity. As  $F_R$  increases, the resonance region grows wider. For  $F_R=1.0$ , the resonance region splits and yields

two peaks. Since one knows from Figs 35 and 36 that two resonance peaks exist for sub-flutter condition, these results suggest that the nonlinear terms, which became important through forcing excitation, make the system more stable as far as flutter is concerned. The greater the forcing amplitude,  $F_R$ , the more important the nonlinear terms are, so the two peaks move farther and farther away from each other.\* This effect of the forcing excitation on the flutter stability boundary would become clearer in the discussion of the next section where both flutter component and forced response components are taken into account.

## 5.2 Forcing-Flutter Interaction

In the discussion of this section, we allow the dynamic pressure  $\lambda$  to go beyond the classical critical dynamic pressure  $\lambda_c$ . Since flutter components may present in this case, one has to include both flutter and forced response components.

Figs. 38 to 43 are the complete solutions for the forced response of the panel with  $\lambda > \lambda_c$ . Fig. 38 to 41 are the solutions for forcing-flutter interaction and Figs. 42 and 43 give the pure forcing response of the panel (no flutter components). These latter two pure forcing responses supplement the former forcing-flutter interactions.

Looking first at the forcing-flutter interaction, Fig. 38 shows the flutter stability boundaries at different forcing amplitudes. For a dynamic pressure greater than the "actual" critical dynamic pressure  $\lambda_c$ , the panel may undergo fluttering, so both forcing component and flutter component

---

\*The physical size of  $F_R$  can be visualized by noting the static deflection it causes, i.e. the  $\Omega=0$  value in Fig. 34 for  $\lambda=0$  (no airflow)

may be observed. The dotted portions of the flutter boundaries are the flutter boundaries predicted by harmonic balance method but not verified by direct numerical integration method. This region remains unclear, more discussion about this region will be given later. Fig. 39 shows the amplitude of the flutter component for different values of the forcing frequencies  $\Omega$ . The curve for  $\Omega \rightarrow 0$  is the flutter response curve without forcing excitation. For  $\Omega \leq 20$ , the response curves show the influence of the forcing excitation on the flutter boundary  $\lambda_c$ . Once  $\lambda_c$  is exceeded, the influence of forcing excitation decreases, and the response curves approach that for  $\Omega \approx 0$  rapidly. For  $\Omega = 25$ , the deviation of the flutter response from that for  $\Omega \approx 0$  is large over a greater range of  $\lambda$ . And for  $\Omega = 40$ , the deviation is very small at the beginning and becomes greater as  $\lambda$  increases. Fig. 40 shows the amplitude of the forcing component in the flutter-forcing interaction solutions. For  $\Omega \leq 20$ , the amplitude of the forcing component always decreases as  $\lambda$  increases. For  $\Omega = 25$ , it increases first then decreases. For  $\Omega = 40$ , it always increases with  $\lambda$  in the range of  $\lambda$  studied here. This variation of the forcing component may help explain the flutter response curves shown on Fig. 39. Fig. 41 shows the effect of the forcing excitation on the frequency of flutter. Forcing excitation tends to increase the flutter frequency slightly but the effect is not significant.

Looking next at the pure forcing response, Fig. 42 shows the pure forcing response for  $\lambda \geq \lambda_c$ . This figure can be better

understood if studied together with Fig. 38. At  $\lambda = \lambda_c = 274.55$ , no flutter exists for the plate under forcing excitation. The only response is the pure forcing response. The whole curve for  $\lambda = \lambda_c$  in Fig. 42, except for the two usual unstable branches, is stable. At  $\lambda = 300$ , Fig. 38 shows that the flutter component may exist for  $\Omega < 22.5$  and  $\Omega > 35.5$ . The direct integration method indicates that the pure forcing response curves for  $\lambda = 300$  in Fig. 42 are unstable for  $\Omega < 22.5$  and  $\Omega > 40.7$ , and that flutter components occur in these ranges of  $\Omega$ . Further, the direct integration method showed that in the range  $35.5 < \Omega < 40.7$ , the lower branch of the pure forcing response was unstable while the upper branch was stable. No flutter components were observed in the range  $35.5 < \Omega < 39$ . Near  $\Omega \approx 40$ , both a pure forcing response solution and a flutter-forcing interaction solution were found. Why the flutter components do not appear for  $35.5 < \Omega < 39$  as suggested by the harmonic balance method or why, if they exist, it is so difficult to obtain the flutter components by numerical integration remains to be investigated. For  $\lambda = 320, 340$  and  $370$ , again all the solid curves shown in Fig. 42 are possible pure forcing response solutions. It can be seen that this stable portion moves to the right as  $\lambda$  is increased.

Fig. 43 shows the pure forced response of the plate, at different forcing frequencies, as a function of the dynamic pressure  $\lambda$ . This is a cross plot of Figs. 34, 35, 36 and 42. But plotting  $w/h$  as a continuous function of  $\lambda$  reveals some interesting characteristics. For  $\lambda = 0$ , because there is no

structural damping, the simple harmonic resonance peak extends to infinity as shown in Fig. 34. So the upper branch of the solution at  $\lambda=0$  increases with the forcing frequency  $\Omega$  as shown in Fig. 43. With increasing  $\lambda$ , this resonance peak moves to the right, i.e. to higher frequency. Meanwhile because of the presence of aerodynamic damping, the length of the peak becomes shorter and shorter. This shortening causes the upper branch solution for  $\Omega=35$  to disappear at  $\lambda \approx 20$ , for  $\Omega=30$  to disappear at  $\lambda \approx 40$ , and for  $\Omega=25$  to disappear at  $\lambda \approx 100$ . For  $\Omega=20$ , the rightward moving of the peak overcomes the shortening effect, so we have a continuous curve. As  $\lambda$  increase, the shortening of the length of the peak slows down, and the rightward moving of the peak makes the upper branch solution for  $\Omega=25$  appear again at  $\lambda \approx 240$ , and that for  $\Omega=30$  at  $\lambda \approx 360$ . As  $\lambda$  increases, the lower branch solution for  $\Omega=20$  and 25 increases because of the rightward movement of the simple harmonic resonance peak. The one for  $\Omega=20$  disappears at  $\lambda \approx 175$  and that for  $\Omega=25$  disappears at  $\lambda \approx 265$ , when the peak passes by these two frequencies respectively. The lower branch solutions for  $\Omega=30$  and 35 increases with  $\lambda$  because of the piling up of the first and second harmonic resonance peaks. This increase continues for  $\Omega=30$  until the resonance tip passes by  $\Omega=30$  (see Fig. 42), then the response changes to the other branch and decreases in magnitude until it disappears at  $\lambda \approx 375$ .

A typical forced response of the panel for  $\Omega=20$  would be to follow the lower branch at low  $\lambda$  and jump to the higher

branch at  $\lambda \approx 175$ . Then the magnitude of vibration decreases with increasing  $\lambda$  until the flutter component comes in at  $\lambda = 291.5$ . The same pattern would be followed by the case for  $\Omega = 25$ . When one is observing the response of a panel during a flight, one is advised not to misinterpret the jump from lower branch to higher branch as the on-set of panel flutter. For  $\Omega = 30$  and  $35$ , all the curves shown here are possible solutions. It is to be noted that for  $\Omega = 30$ , no pure forced response can exist for  $\lambda > 375$ .

### 5.3 Examples of Numerical Integration

Figs. 44 to 47 show the results obtained by numerical integration for  $F_R = 40$ ,  $\Omega = 20$  and  $\lambda = 285, 292$  and  $296$  respectively. Although  $\lambda = 285 > \lambda_c$ , the integration yields a pure forced response as shown in Fig. 44. This shows that the flutter stability boundary is affected by the forcing excitation ( $\bar{\lambda}_c = 291.5$ ). For  $\lambda = 292$ , harmonic balance method gives forcing amplitude  $W_{FR} = .258$ , flutter amplitude  $W_F = .017$  and frequency ratio  $\omega_F/\Omega = 1.497$ . With the information given by Dugundji and Hore<sup>50</sup>, one can read from Fig. 45 that  $W_{FR} = .253$ ,  $W_F = .015$  and  $\omega_F/\Omega \approx 1.5$ . For  $\lambda = 296$  results from harmonic balance method shows that  $W_{FR} = .254$ ,  $W_F = .167$ ,  $\omega_F/\Omega = 1.509$ . Fig. 46 gives  $W_{FR} = .26$ ,  $W_F = .162$ , and the gradual change in the phase of the inner peaks indicate that  $\omega_F/\Omega$  is slightly off from 1.5. So the numerical results agree quite well with the results from harmonic balance method. However, if  $W_{FR}$  and  $W_F$  are both of order 1, the components with frequency  $(2\Omega - \omega_F)$  and  $(2\omega_F - \Omega)$  may become important and make the response curve



too complicated to read, thus making the comparison for the major response components very difficult. Other numerical results of the direct integration method are shown on Figs. 36, 39, 40 and 42. It can be seen that the two methods agree quite well, except for  $\Omega$  ranges from 28 to 39. Fig. 47 is an example to show the existence of both pure forced response and response with both forcing and flutter components at  $\Omega=40$ .

#### 5.4 Comparison of Two-Mode Results with Six-Mode Results

In the study of panel flutter, one knows that a six-mode solution yields good quantitative as well as qualitative representation of the exact solution. So a six-mode solution of the forcing excitation at  $\lambda=\lambda_c=344.2$  and  $F_R=40$  is given on Fig. 48 to illustrate the quantitative improvement by employing more modes. For this six-mode system, the critical flutter frequency is  $\omega_c=32.44$  as compared to  $\omega_c=28.8$  for a two-mode system. The two peaks for six-mode solution occur at  $\Omega\approx 28.5$  and  $\Omega\approx 45.2$  and those for two-mode solution occur at  $\Omega\approx 26.3$  and  $\Omega\approx 42.6$ . So the size of the resonance region is not changed much. The deflections of the two peaks for six-mode solution are  $W_{FR}=1.16$  and  $W_{FR}=.6$  and those for two-mode solution are  $W_{FR}=1.16$  and  $W_{FR}=.5$ . Thus this example shows that the most important improvement due to more modes is the accurate allocation of the resonance peaks and the other corrections are not appreciable.

## CHAPTER 6

### CONCLUSIONS

Some problems of Panel Flutter and the interaction of Panel Flutter and Forcing Excitations have been studied theoretically. In both studies, nonlinear von Karman plate theory is used to represent the elastic forces and linear Piston Theory is used to calculate the aerodynamic loadings. Harmonic Balance Method is used to find the steady state solution. Because much computer time is saved and good results are obtained as compared to straightforward direct integration, it has proved to be a good alternative to the Direct Integration Method.

Effects of some pertinent parameters on nonlinear panel flutter have been investigated. Among them, the mass ratio  $\mu/M$  is favorable both in preventing flutter and keeping the flutter amplitude low after the critical dynamic pressure is exceeded. But since the practical range of  $\mu/M$  is .01-.1, Ref. 10, its effect is quite limited unless a small amount of structural damping exists. Compressive membrane force is unfavorable because it always reduces the critical dynamic pressure hence making the panel more vulnerable to flutter. So compressive membrane force due to aerodynamic heating should be kept as low as possible. Effect of structural damping varies over a

wide range depending upon the other parameters. For small  $\mu/M$  and low  $a/b$ , a small amount of  $g_s$  has a great destabilizing effect. Presence of  $g_s$  also causes the amplitude to grow faster once  $\lambda_c$  is exceeded. So it is important for a designer to know the exact value of  $g_s$  of the material he is using. A meaningful comparison between experimental results and analytical results also requires a good knowledge of the value of  $g_s$ . In the range of  $a/b$  studied here, increase in  $a/b$  is an effective way in controlling flutter.

The study of the interaction of panel flutter and forcing excitation gives one a clearer picture of how the skin of a space vehicle will behave when external disturbance exists. The splitting of the resonance region at  $\lambda$  equal to classical  $\lambda_c$  is quite a breaking away from the response of Duffing's Equation<sup>49,51</sup>. This happens because the forcing excitation makes the already coalesced two frequencies separate again. Flutter stability boundary is increased by the forcing excitations. The amount of increase in this boundary is great for  $18 < \Omega < 38$ , but this boundary is still not clear for  $28 < \Omega < 39$ . Pure forcing excitation responses may exist well above the pure flutter stability boundary  $\lambda_c$ . For  $\Omega$  around 40 and over a certain range of dynamic pressure  $\lambda$ , coexistence of pure forcing response and forcing-flutter interaction responses have been observed.

The effect of forcing excitation on the flutter behavior is small if  $\Omega$  is less than 20. It is small first, then increases with increasing  $\lambda$  if  $\Omega$  is greater than 40.

Flutter makes the forcing component decrease with increasing  $\lambda$  if  $\Omega < 20$ , and it makes the forcing component increase with  $\lambda$  if  $\Omega > 40$ . For a given forcing frequency, as the dynamic pressure  $\lambda$  increases, large jump may occur in the panel response at  $\lambda$  well below the onset of flutter. One is advised not to misinterpret this jump as the occurrence of flutter.

For the range of dynamic pressure  $\lambda$  studied here and  $\Omega$  outside of the region of 28 to 39 the forcing-flutter results from direct integration agree quite well with those obtained by harmonic balance method. Inclusion of the components with frequencies  $2\Omega - \omega_F$  and  $2\omega_F - \Omega$  would bring improvement to the harmonic balance method used here. This improvement is significant if both flutter components and forcing components are of order 1. For all ranges of  $\Omega$  and  $\lambda$ , the pure forced response obtained by both methods always agree very well. The question of the existence of the flutter component in the frequency range  $28 < \Omega < 39$  requires more study.

Comparison of six-mode results and two-mode results shows that the prime improvement of including more modes is on the location of the resonance zone. Since the location of the resonance zone is very important practically, one has to use more modes if one wants to apply the information obtained here to practical problems.

More work should be done to study the effect of structural damping on the response characteristics. Interaction of flutter with random excitation should also be studied to

understand the effect of engine noise and random gust on the flutter response.

As one can see from the work by Morino, Kuo and Dugundji<sup>12</sup>, perturbation methods yield a convenient solution to the panel flutter problem. Since the general physical properties of forcing-flutter interaction are known through this study, one may find a proper perturbation expansion and apply this technique to obtain a convenient form for the response characteristics.

The scheme used in this work may also be applied to investigate flutter-parametric excitation interactions, as for example, may occur in the case of engine thrust variations acting together with the flutter response of missile panels.

APPENDIX A

GALERKIN'S TECHNIQUE FOR THREE-DIMENSIONAL  
CLAMPED-CLAMPED PANELS

As mentioned in sub-section 2.3.1, one of the simple forms to represent the deflection  $w$  is that expressed in Eq. 2.3.7, the derivatives of  $w$  can be written as follows

$$\frac{\partial W}{\partial \xi} = \sum_{m=1}^N W_m [(m+1)\pi \sin(m+1)\pi\xi - (m-1)\pi \sin(m-1)\pi\xi] (1 - \cos 2\pi\xi) \quad (\text{A.1.1})$$

$$\frac{\partial^2 W}{\partial \xi^2} = \sum_{m=1}^N \pi^2 W_m [(m+1)^2 \cos(m+1)\pi\xi - (m-1)^2 \cos(m-1)\pi\xi] (1 - \cos 2\pi\xi) \quad (\text{A.1.2})$$

$$\frac{\partial^4 W}{\partial \xi^4} = \sum_{m=1}^N \pi^4 W_m [(m-1)^4 \cos(m-1)\pi\xi - (m+1)^4 \cos(m+1)\pi\xi] (1 - \cos 2\pi\xi) \quad (\text{A.1.3})$$

$$\frac{\partial W}{\partial \eta} = \sum_{m=1}^N 2\pi W_m [\cos(m-1)\pi\xi - \cos(m+1)\pi\xi] \sin 2\pi\eta \quad (\text{A.1.4})$$

$$\frac{\partial^2 W}{\partial \eta^2} = \sum_{m=1}^N (2\pi)^2 W_m [\cos(m-1)\pi\xi - \cos(m+1)\pi\xi] \cos 2\pi\eta \quad (\text{A.1.5})$$

$$\frac{\partial^4 W}{\partial \eta^4} = - \sum_{m=1}^N (2\pi)^4 W_m [\cos(m-1)\pi\xi - \cos(m+1)\pi\xi] \cos 2\pi\eta \quad (\text{A.1.6})$$

$$\frac{\partial^2 W}{\partial z^2 \partial \eta} = \sum_{m=1}^N 2\pi^2 W_m [(m+1) \sin(m+1)\pi\zeta - (m-1) \sin(m-1)\pi\zeta] \sin 2\pi\eta \quad (\text{A.1.7})$$

$$\frac{\partial^4 W}{\partial z^2 \partial \eta^2} = \sum_{m=1}^N 4\pi^4 W_m [(m+1)^2 \sin(m+1)\pi\zeta - (m-1)^2 \sin(m-1)\pi\zeta] \cos 2\pi\eta \quad (\text{A.1.8})$$

Employing Eqs. A.1.2, A.1.5 and A.1.7 in Eq. 2.23 one obtains

$$\begin{aligned} \frac{\partial^4 \Phi}{\partial z^4} + 2A^2 \frac{\partial^4 \Phi}{\partial z^2 \partial \eta^2} + A^4 \frac{\partial^4 \Phi}{\partial \eta^4} = 12(1-\nu^2) DA^2 \pi^4 \sum_{p, q=1}^N W_p W_q \{ & 2p(q-p) \cos(p-q)\pi\zeta \\ & + 2p(p+q) \cos(p+q)\pi\zeta - (p+1)(p+q+2) \cos(p+q+2)\pi\zeta \\ & + (p+1)(p-q+2) \cos(p-q+2)\pi\zeta + (p-1)(p-q-2) \cos(p-q-2)\pi\zeta \\ & - (p-1)(p+q-2) \cos(p+q-2)\pi\zeta + [-2(pq+p^2+2) \cos(p-q)\pi\zeta \\ & + 2(p^2-pq+2) \cos(p+q)\pi\zeta + (p+1)(q-p) \cos(p+q+2)\pi\zeta \\ & + (p+1)(p+q) \cos(p-q+2)\pi\zeta + (p-1)(p+q) \cos(p-q-2)\pi\zeta \\ & + (p-1)(q-p) \cos(p+q-2)\pi\zeta] \times \cos 4\pi\eta \\ & - 2x[2(p^2+1) \cos(p+q)\pi\zeta - 2(p^2+1) \cos(p-q)\pi\zeta \\ & + (p+1)^2 \cos(p-q+2)\pi\zeta - (p+1)^2 \cos(p+q-2)\pi\zeta \\ & + (p-1)^2 \cos(q-p+2)\pi\zeta - (p-1)^2 \cos(p+q-2)\pi\zeta] \cos 2\pi\eta \} \end{aligned} \quad (\text{A.2})$$

Using Eqs. 2.38 and 2.39, one obtains

$$\begin{aligned}
 \Phi_p = & 12(1-\nu^2)DA^2\pi^4 \sum_{p, \delta=1}^N W_p W_\delta \left\{ \left[ (1-\delta_p^p) \frac{2p}{(\delta-p)^3} \cos(p-\delta)\pi \right] \right. \\
 & + \frac{2p}{(p+\delta)^3} \cos(p+\delta)\pi \left. \right\} - \frac{p+1}{(p+\delta+2)^3} \cos(p+\delta+2)\pi \left. \right\} + \frac{p+1}{(p-\delta+2)^3} \cos(p-\delta+2)\pi \left. \right\} \\
 & + \frac{(1-\delta_p^{\delta+2})(p-1)}{(p-\delta-2)^3} \cos(p-\delta-2)\pi \left. \right\} - \frac{(p-1)}{(p+\delta-2)^3} \cos(p+\delta-2)\pi \left. \right\} ] \\
 & + \left[ \frac{-2(p\delta+p^2+2)}{[(p-\delta)^2+16A^2]^2} \cos(p-\delta)\pi \right\} + \frac{2(p^2-p\delta+2)}{[(p+\delta)^2+16A^2]^2} \cos(p+\delta)\pi \left. \right\} \\
 & + \frac{(p+1)(\delta-p)}{[(p+\delta+2)^2+16A^2]^2} \cos(p+\delta+2)\pi \left. \right\} + \frac{(p+1)(p+\delta)}{[(p-\delta+2)^2+16A^2]^2} \cos(p-\delta+2)\pi \left. \right\} \\
 & + \frac{(p-1)(p+\delta)}{[(p-\delta-2)^2+16A^2]^2} \cos(p-\delta-2)\pi \left. \right\} + \frac{(p-1)(\delta-p)}{[(p+\delta-2)^2+16A^2]^2} \cos(p+\delta-2)\pi \left. \right\} ] \\
 & \times \cos 4\pi\eta - 2 \left[ \frac{2(p^2+1)}{[(p+\delta)^2+4A^2]^2} \cos(p+\delta)\pi \right\} - \frac{2(p^2+1)}{[(p-\delta)^2+4A^2]^2} \cos(p-\delta)\pi \left. \right\} \\
 & + \frac{(p+1)^2}{[(p-\delta+2)^2+4A^2]^2} \cos(p-\delta+2)\pi \left. \right\} - \frac{(p+1)^2}{[(p+\delta+2)^2+4A^2]^2} \cos(p+\delta+2)\pi \left. \right\} \\
 & + \frac{(p-1)^2}{[(\delta-p+2)^2+4A^2]^2} \cos(\delta-p+2)\pi \left. \right\} - \frac{(p-1)^2}{[(p+\delta-2)^2+4A^2]^2} \cos(p+\delta-2)\pi \left. \right\} ] \\
 & \times \cos 2\pi\eta \left. \right\}
 \end{aligned} \tag{A.3}$$

Comparing the coefficients of Eqs. 2.40 and A.3, one obtains



$$\begin{aligned}
 \bar{A} &= \frac{-2(p^2 + p\delta + 2)}{[(p-\delta)^2 + 16A^2]^2} & \bar{B} &= \frac{(p-1)(p+\delta)}{[(p-\delta-2)^2 + 16A^2]^2} \\
 \bar{C} &= \frac{(p+1)(p+\delta)}{[(p-\delta+2)^2 + 16A^2]^2} & \bar{D} &= \frac{2(p^2 - p\delta + 2)}{[(p+\delta)^2 + 16A^2]^2} \\
 \bar{E} &= \frac{(p-1)(\delta-p)}{[(p+\delta-2)^2 + 16A^2]^2} & \bar{F} &= \frac{(p+1)(\delta-p)}{[(p+\delta+2)^2 + 16A^2]^2} \\
 \bar{G} &= \frac{4(p^2 + 1)}{[(p-\delta)^2 + 4A^2]^2} & \bar{H} &= \frac{-2(p-1)^2}{[(p-\delta-2)^2 + 4A^2]^2} \\
 \bar{I} &= \frac{-2(p+1)^2}{[(p-\delta+2)^2 + 4A^2]^2} & \bar{J} &= \frac{-4(p^2 + 1)}{[(p+\delta)^2 + 4A^2]^2} \\
 \bar{M} &= \frac{2(p-1)^2}{[(p+\delta-2)^2 + 4A^2]^2} & \bar{N} &= \frac{2(p+1)^2}{[(p+\delta+2)^2 + 4A^2]^2} \\
 \bar{P} &= \frac{-2p}{(p-\delta)^3} (1 - S_{\delta}^p) & \bar{Q} &= \frac{(p-1)(1 - S_{\delta}^{p+2})}{(p-\delta-2)^3} \\
 \bar{R} &= \frac{(p+1)(1 - S_{\delta}^{p+2})}{(p-\delta+2)^3} & \bar{S} &= \frac{2p}{(p+\delta)^3} \\
 \bar{T} &= -\frac{(p-1)(1 - S_{\delta}^{p+\delta})}{(p+\delta-2)^3} & \bar{U} &= \frac{-(p+1)}{(p+\delta+2)^3}
 \end{aligned} \tag{A.4}$$

In order to have a complete solution for  $\bar{\Phi}$ , one assumes the homogeneous solution of  $\bar{\Phi}$  as

$$\bar{\Phi}_{\text{homo}} = \frac{1}{2} [\bar{N}_x \eta^2 + \bar{N}_{xy} \eta + \bar{N}_y \eta^2] \tag{A.5}$$

where  $\bar{N}_{xy}$ ,  $\bar{N}_x$  and  $\bar{N}_y$  are shown in Eqs. 2.42, 2.43 and 2.44.

The complete solution of  $\bar{\Phi}$  is

$$\Phi = \Phi_p + \Phi_{hom} \quad (A.6)$$

Employing Eqs. A.1.1 to A.1.8, Eqs. A.3 and Eq. A.5 in Eq. A.22 and applying Galerkin's Technique to the resulting equations, one obtains

$$\begin{aligned} & (2 + \delta_1^m) \frac{d^2 W_m}{d\tau^2} - \frac{d^2 W_{m+2}}{d\tau^2} - \frac{d^2 W_{m-2}}{d\tau^2} + \left(\frac{\mu\lambda}{M}\right)^{1/2} \left[ (2 + \delta_1^m) \frac{dW_m}{d\tau} - \frac{dW_{m-2}}{d\tau} \right. \\ & \left. - \frac{dW_{m+2}}{d\tau} \right] + \pi^4 \left\{ [(m-1)^4 + (m+1)^4 + \frac{8}{3} A^2 [(m-1)^2 + (m+1)^2] \right. \\ & \left. + \frac{16}{3} (2 + \delta_1^m) A^4 \right\} \left\{ g_a \frac{dW_m}{d\tau} + \frac{1}{\omega} g_b \frac{dW_m}{d\tau} \right\} - \pi^4 \left\{ (m-1)^4 \right. \\ & \left. + \frac{8}{3} A^2 (m-1)^2 + \frac{16}{3} A^4 \right\} \left\{ g_a \frac{dW_{m-2}}{d\tau} + \frac{1}{\omega} g_b \frac{dW_{m-2}}{d\tau} \right\} - \pi^4 \left\{ (m+1)^4 + \frac{8}{3} A^2 (m+1)^2 \right. \\ & \left. + \frac{16}{3} A^4 \right\} \left\{ g_a \frac{dW_{m+2}}{d\tau} + \frac{1}{\omega} g_b \frac{dW_{m+2}}{d\tau} \right\} + \left[ 2R_x \pi^2 (m^2 + 1) + \frac{4}{3} R_x \pi^2 A^2 (2 + \delta_1^m) \right. \\ & \left. + \pi^4 [(m-1)^4 + (m+1)^4] + \frac{8}{3} \pi^4 A^2 [(m-1)^2 + (m+1)^2] + \frac{16}{3} (2 + \delta_1^m) \pi^4 A^4 \right] W_m \\ & - \left[ R_x \pi^2 (m-1)^2 + \frac{4}{3} R_y \pi^2 A^2 + (m-1)^4 \pi^4 + \frac{8}{3} \pi^4 A^2 (m-1)^2 + \frac{16}{3} \pi^4 A^4 \right] W_{m-2} \\ & - \pi^4 \left[ (m+1)^2 R_x / \pi^2 + \frac{4}{3} A^2 R_y / \pi^2 + (m+1)^4 + \frac{8}{3} A^2 (m+1)^2 + \frac{16}{3} A^4 \right] W_{m+2} \quad (A.7) \\ & + \lambda \sum_{n=1}^N \left[ \frac{2n}{m+n} - \frac{2n}{n-m} (1 - \delta_n^m) + \frac{n+1}{n-m+2} (1 - \delta_m^{n+2}) - \frac{n-1}{n+m-2} (1 - \delta_2^{n+m}) \right. \\ & \left. - \frac{n+1}{n+m+2} + \frac{n-1}{n-m-2} (1 - \delta_{m+2}^n) \right] [1 - (-1)^{n+m}] W_n + \sum_{n,p,g=1}^N C_{mnp} g W_n W_p W_g \\ & = 0 \end{aligned}$$

$$m=1, 2, \dots, N$$

where  $C_{mnpq}$  is defined as follows

$$\begin{aligned}
 C_{mnpq} = & -16(1-\nu^2)A^4\pi^4\{[(H+\bar{A}-G-B)(n+1)^2+(\bar{A}+I-C-G) \\
 & \times (n-1)^2-2n(p-g)(G-\bar{A})-(p-g-2)(n+1)(B-H)-(p-g+2)(n-1) \\
 & \times (C-I)-(G-P-\frac{1}{2}\bar{A})(p-g)^2-\frac{1}{2}(Q+\frac{1}{2}B-H)(p-g-2)^2 \\
 & -\frac{1}{2}(R+\frac{1}{2}C-I)(p-g+2)^2][\delta_m^{p-g+n}-\delta_{-m}^{p-g+n}]+[(C+G-\bar{A}-I)(n+1)^2 \\
 & +(B+G-\bar{A}-H)(n-1)^2-2n(p-g)(G-\bar{A})-(p-g-2)(n-1)(B-H) \\
 & - (p-g+2)(n+1)(C-I)+(G-P-\frac{1}{2}\bar{A})(p-g)^2+\frac{1}{2}(Q+\frac{1}{2}B-H) \\
 & \times (p-g-2)^2+\frac{1}{2}(R+\frac{1}{2}C-I)(p-g+2)^2][\delta_m^{p-g-n}-\delta_{-m}^{p-g-n}]+[(D+M-E-J) \\
 & \times (n+1)^2+(D+N-F-J)(n-1)^2-2n(p+g)(J-D)-(p+g-2)(n+1) \\
 & \times (E-M)-(p+g+2)(n-1)(F-N)-(J-S-\frac{1}{2}D)(p+g)^2-\frac{1}{2}(U+\frac{1}{2}F-N) \\
 & \times (p+g+2)^2-\frac{1}{2}(T+\frac{1}{2}E-M)(p+g-2)^2]\delta_m^{p+g+n}+[(F+J-D-N)(n+1)^2 \\
 & +(E+J-D-M)(n-1)^2-2n(p+g)(J-D)-(p+g-2)(n-1)(E-M) \\
 & - (n+1)(p+g+2)(F-N)+(J-S-\frac{1}{2}D)(p+g)^2+\frac{1}{2}(U+\frac{1}{2}F-N)(p+g+2)^2
 \end{aligned}$$

$$\begin{aligned}
 & + \frac{1}{2}(T + \frac{1}{2}E - M)(p + \delta - 2)^2 \left[ \delta_m^{p+\delta-n} - \delta_{-m}^{p+\delta-n} \right] + [(B-H)(n+1)^2 \\
 & + (B+G-\bar{A}-H)(n-1)^2 - (p-\delta)(n-1)(\bar{A}-G) - 2n(p-\delta-2)(H-B) \\
 & + \frac{1}{2}(G-P-\frac{1}{2}\bar{A})(p-\delta)^2 + (Q+\frac{1}{2}B-H)(p-\delta-2)^2] \left[ \delta_m^{p-\delta+n-2} \right. \\
 & \left. - \delta_{-m}^{p-\delta+n-2} \right] + [(\bar{A}+H-B-G)(n+1)^2 + (H-B)(n-1)^2 - (p-\delta)(n+1)(\bar{A}-G) \\
 & - 2n(p-\delta-2)(H-B) - \frac{1}{2}(G-P-\frac{1}{2}\bar{A})(p-\delta)^2 - (Q+\frac{1}{2}B-H)(p-\delta-2)^2] \\
 & \times \left[ \delta_m^{p-\delta-n-2} - \delta_{-m}^{p-\delta-n-2} \right] + [(E-M)(n+1)^2 + (E+J-D-M)(n-1)^2 - (p+\delta)(n-1) \\
 & \times (D-J) - 2n(p+\delta-2)(M-E) + \frac{1}{2}(J-S-\frac{1}{2}D)(p+\delta)^2 + (T+\frac{1}{2}E-M) \\
 & \times (p+\delta-2)^2] \delta_m^{p+\delta+n-2} + [(D+M-E-J)(n+1)^2 + (M-E)(n-1)^2 - (p+\delta) \\
 & \times (n+1)(D-J) - 2n(p+\delta-2)(M-E) - \frac{1}{2}(J-S-\frac{1}{2}D)(p+\delta)^2 \\
 & - (T+\frac{1}{2}E-M)(p+\delta-2)^2] \left[ \delta_m^{p+\delta-n-2} - \delta_{-m}^{p+\delta-n-2} \right] + [(C+G-\bar{A}-I) \\
 & \times (n+1)^2 + (C-I)(n-1)^2 - (p-\delta)(n+1)(\bar{A}-G) - 2n(p-\delta+2)(I-C) \\
 & + \frac{1}{2}(G-P-\frac{1}{2}\bar{A})(p-\delta)^2 + (R+\frac{1}{2}C-I)(p-\delta+2)^2] \left[ \delta_m^{p-\delta+n+2} - \delta_{-m}^{p-\delta+n+2} \right] \\
 & + [(J-C)(n+1)^2 + (\bar{A}+I-C-G)(n-1)^2 - (p-\delta)(n-1)(\bar{A}-G)
 \end{aligned}$$

$$\begin{aligned}
 & -2n(p-g+2)(I-C) - \frac{1}{2}(G-P-\frac{1}{2}\bar{A})(p-g)^2 - (R+\frac{1}{2}C-I) \\
 & \times (p-g+2)^2 \left[ \delta_m^{p-g-n+2} - \delta_{-m}^{p-g-n+2} \right] + [(F+J-D-N)(n+1)^2 \\
 & + (F-N)(n-1)^2 + (p+g)(n+1)(D-J) - 2n(p+g+2)(N-F) \\
 & + \frac{1}{2}(J-S-\frac{1}{2}D)(p+g)^2 + (U+\frac{1}{2}F-N)(p+g+2)^2] \delta_m^{n+p+g+2} \\
 & + [(N-F)(n+1)^2 + (D+N-F-J)(n-1)^2 - (p+g)(n-1)(D-J) - 2n \\
 & \times (p+g+2)(N-F) - \frac{1}{2}(J-S-\frac{1}{2}D)(p+g)^2 - (U+\frac{1}{2}F-N)(p+g+2)^2] \\
 & \times \left[ \delta_m^{p+g-n+2} - \delta_{-m}^{p+g-n+2} \right] + [-(B-H)(n-1)^2 - (p-g-2)(n-1)(B-H) \\
 & + \frac{1}{2}(p-g-2)^2(H-Q-\frac{1}{2}B)] \left[ \delta_m^{p-g+n-4} - \delta_{-m}^{p-g+n-4} \right] + [(B+H)(n+1)^2 \\
 & - (p-g-2)(n+1)(B-H) - \frac{1}{2}(p-g-2)^2(H-Q-\frac{1}{2}B)] \left[ \delta_m^{p-g-n-4} - \delta_{-m}^{p-g-n-4} \right] \\
 & + [(E-M)(n+1)^2 - (p+g-2)(n+1)(E-M) + \frac{1}{2}(p+g-2)^2(M-T-\frac{1}{2}E)] \left[ \delta_m^{p+g-n-4} \right. \\
 & \left. - \delta_{-m}^{p+g-n-4} \right] + [-(E-M)(n-1)^2 - (p+g-2)(n-1)(E-M) + \frac{1}{2}(p+g-2)^2(M-T-\frac{1}{2}E)] \\
 & \times \delta_m^{p+g+n-4} + [(C-I)(n-1)^2 - (p-g+2)(n-1)(C-I) - \frac{1}{2}(m-n+2)^2(I-R-\frac{1}{2}C)] \\
 & \times \left[ \delta_m^{p-g-n+4} - \delta_{-m}^{p-g-n+4} \right] + [-(C-I)(n+1)^2 - (p-g+2)(C-I)(n+1) + \frac{1}{2}(p-g+2)^2
 \end{aligned}$$



$$F_{mn} = \left[ \frac{2n}{n+m} - \frac{2n}{n-m} (1 - \delta_n^m) + \frac{n+1}{(n-m+2)} (1 - \delta_m^{n+2}) - \frac{n-1}{n+m-2} (1 - \delta_2^{m+n}) \right. \\ \left. - \frac{n+1}{n+m+2} + \frac{n-1}{n-m-2} (1 - \delta_{m+2}^n) \right] [1 - (-1)^{n+m}] \quad (\text{A.9.5})$$

$$C_{mnpq} = \text{defined in Eq. A.8} \quad (\text{A.9.6})$$

where

$$CA(m) = \pi^4 [(m+1)^4 + (m-1)^4] + \frac{8}{3} \pi^4 A^2 [(m+1)^2 \\ + (m-1)^2] + \frac{16}{3} (2 + \delta_m^1) \pi^4 A^4 \quad (\text{A.10.1})$$

$$CB(m) = (m-1)^4 \pi^4 + \frac{8}{3} \pi^4 A^2 (m-1)^2 + \frac{16}{3} \pi^4 A^4 \quad (\text{A.10.2})$$

$$CC(m) = (m+1)^4 \pi^4 + \frac{8}{3} \pi^4 A^2 (m+1)^2 + \frac{16}{3} \pi^4 A^4 \quad (\text{A.10.3})$$

$$DA(m) = 2R_x \pi^2 (m^2 + 1) + \frac{4}{3} R_y \pi^2 A^2 (2 + \delta_m^1) + CA(m) \quad (\text{A.10.4})$$

$$DB(m) = R_x \pi^2 (m-1)^2 + \frac{4}{3} R_y \pi^2 A^2 + CB(m) \quad (\text{A.10.5})$$

$$DC(m) = R_x \pi^2 (m+1)^2 + \frac{4}{3} R_y \pi^2 A^2 + CC(m) \quad (\text{A.10.6})$$

APPENDIX B

HARMONIC BALANCE METHOD FOR FORCED RESPONSE  
BELOW FLUTTER

Concentrate on the nonlinear terms first. Rewrite  
4.15 here

$$W_n = d_{n0} + \sum_{r=1}^3 (C_{nr} \sin r t_1 + d_{nr} \cos r t_1) \quad (\text{B.1})$$

Then

$$\begin{aligned} W_n W_p W_g = & [d_{n0} + C_{n1} \sin t_1 + d_{n1} \cos t_1 + C_{n2} \sin 2t_1 + d_{n2} \cos 2t_1 \\ & + C_{n3} \sin 3t_1 + d_{n3} \cos 3t_1] \times [d_{p0} + C_{p1} \sin t_1 + d_{p1} \cos t_1 \\ & + C_{p2} \sin 2t_1 + d_{p2} \cos 2t_1 + C_{p3} \sin 3t_1 + d_{p3} \cos 3t_1] \times [d_{g0} \\ & + C_{g1} \sin t_1 + d_{g1} \cos t_1 + C_{g2} \sin 2t_1 + d_{g2} \cos 2t_1 + C_{g3} \sin 3t_1 \\ & + d_{g3} \cos 3t_1] = S_1 + S_2 \cos t_1 + S_3 \sin t_1 + S_4 \cos 2t_1 + S_5 \sin 2t_1 \\ & + S_6 \cos 3t_1 + S_7 \sin 3t_1 + S_8 \cos^2 t_1 + S_9 \cos t_1 \sin t_1 + S_{10} \sin^2 t_1 \end{aligned}$$



$$\begin{aligned} &+S_{11} \cos t, \cos 2t, +S_{12} \cos t, \sin 2t, +S_{13} \sin t, \cos 2t, +S_{14} \sin t, \sin 2t, +S_{15} \cos t, \cos 3t, \\ &+S_{16} \cos t, \sin 3t, +S_{17} \sin t, \cos 3t, +S_{18} \sin t, \sin 3t, +S_{19} \cos^2 2t, +S_{20} \cos 2t, \sin 2t, \\ &+ S_{21} \sin^2 2t, + S_{22} \cos 2t, \cos 3t, + S_{23} \cos 2t, \sin 3t, + S_{24} \sin 2t, \\ &\quad \times \cos 3t, + S_{25} \sin 2t, \sin 3t, + S_{26} \cos^2 3t, + S_{27} \cos 3t, \sin 3t, \\ &+ S_{28} \sin^2 3t, + S_{29} \cos^3 t, + S_{30} \cos^2 t, \sin t, + S_{31} \cos t, \sin^2 t, \\ &+ S_{32} \sin^3 t, + S_{33} \cos^2 t, \cos 2t, + S_{34} \cos^2 t, \sin 2t, + S_{35} \cos^2 t, \\ &\quad \times \cos 3t, + S_{36} \cos^2 t, \sin 3t, + S_{37} \cos t, \sin t, \cos 2t, + S_{38} \cos t, \\ &\quad \times \sin t, \sin 2t, + S_{39} \cos t, \sin t, \cos 3t, + S_{40} \cos t, \sin t, \\ &\quad \times \sin 3t, + S_{41} \sin^2 t, \cos 2t, + S_{42} \sin^2 t, \sin 2t, + S_{43} \sin^2 t, \\ &\quad \times \cos 3t, + S_{44} \sin^2 t, \sin 3t, + S_{45} \cos t, \cos^2 2t, + S_{46} \cos t, \\ &\quad \times \cos 2t, \sin 2t, + S_{47} \cos t, \sin^2 2t, + S_{48} \cos t, \cos 2t, \cos 3t, \\ &+ S_{49} \cos t, \cos 2t, \sin 3t, + S_{50} \cos t, \sin 2t, \cos 3t, + S_{51} \cos t, \end{aligned}$$

$$\begin{aligned} & \times \sin 2t, \cos 3t, + S_{52} \cos t, \cos^2 3t, + S_{53} \cos t, \cos 3t, \sin 3t, \\ & + S_{54} \cos t, \sin^2 3t, + S_{55} \sin t, \cos^2 2t, + S_{56} \sin t, \cos 2t, \sin 2t, \\ & + S_{57} \sin t, \sin^2 2t, + S_{58} \sin t, \cos 2t, \cos 3t, + S_{59} \sin t, \cos 2t, \\ & \times \sin 3t, + S_{60} \sin t, \sin 2t, \cos 3t, + S_{61} \sin t, \sin 2t, \sin 3t, \\ & + S_{62} \sin t, \cos^2 3t, + S_{63} \sin t, \cos 3t, \sin^2 t, + S_{64} \sin t, \sin^2 3t, \\ & + S_{65} \cos^3 2t, + S_{66} \cos^2 2t, \sin 2t, + S_{67} \cos 2t, \sin^2 2t, + S_{68} \sin^3 2t, \\ & + S_{69} \cos^2 2t, \cos 3t, + S_{70} \cos^2 2t, \sin 3t, + S_{71} \cos 2t, \sin 2t, \cos 3t, \\ & + S_{72} \cos 2t, \sin 2t, \sin 3t, + S_{73} \sin^2 2t, \cos 3t, \\ & + S_{74} \sin^2 2t, \sin 3t, + S_{75} \cos 2t, \cos^2 3t, + S_{76} \cos 2t, \\ & \times \cos 3t, \sin 3t, + S_{77} \cos 2t, \sin^2 3t, + S_{78} \sin 2t, \\ & \times \cos^2 3t, + S_{79} \sin 2t, \cos 3t, \sin 3t, + S_{80} \sin 2t, \sin^2 3t, \\ & + S_{81} \cos^3 3t, + S_{82} \cos^2 3t, \sin 3t, + S_{83} \cos 3t, \sin^2 3t, \\ & + S_{84} \sin^3 3t, \end{aligned}$$

where

$$S_1 = d_{n0} d_{p0} d_{g0}$$

$$S_2 = d_{n0} d_{p0} d_{g1} + d_{n0} d_{p1} d_{g0} + d_{n1} d_{p0} d_{g0}$$

$$S_3 = d_{n0} d_{p0} c_{g1} + d_{n0} c_{p1} d_{g0} + c_{n1} d_{p0} d_{g0}$$

$$S_4 = d_{n0} d_{p0} d_{g2} + d_{n0} d_{p2} d_{g0} + d_{n2} d_{p0} d_{g0}$$

$$S_5 = d_{n0} d_{p0} c_{g2} + d_{n0} c_{p2} d_{g0} + c_{n2} d_{p0} d_{g0}$$

$$S_6 = d_{n0} d_{p0} d_{g3} + d_{n0} d_{p3} d_{g0} + d_{n3} d_{p0} d_{g0}$$

$$S_7 = d_{n0} d_{p0} c_{g3} + d_{n0} c_{p3} d_{g0} + c_{n3} d_{p0} d_{g0}$$

$$S_8 = d_{n0} d_{p1} d_{g1} + d_{n1} d_{p0} d_{g1} + d_{n1} d_{p1} d_{g0}$$

$$S_9 = d_{n0} d_{p1} d_{g1} + d_{n0} c_{p1} d_{g1} + c_{n1} d_{p0} d_{g1} + d_{n1} d_{p0} c_{g1}$$

$$+ d_{n1} c_{p1} d_{g0} + c_{n1} d_{p1} d_{g0}$$

$$S_{10} = d_{n0} c_{p1} c_{g1} + c_{n1} d_{p0} c_{g1} + c_{n1} c_{p1} d_{g0}$$

$$S_{11} = d_{n0} d_{p1} d_{g2} + d_{n0} d_{p2} d_{g1} + d_{n1} d_{p0} d_{g2} + d_{n2} d_{p0} d_{g1}$$

$$+ d_{n1} d_{p2} d_{g0} + d_{n2} d_{p1} d_{g0}$$

$$S_{12} = d_{n0} d_{p1} C_{g2} + d_{n0} C_{p2} d_{g1} + d_{n1} d_{p0} C_{g2} + C_{n2} d_{p0} d_{g1} \\ + d_{n1} C_{p2} d_{g0} + C_{n2} d_{p1} d_{g0}$$

$$S_{13} = d_{n0} C_{p1} d_{g2} + d_{n0} d_{p2} C_{g1} + C_{n1} d_{p0} d_{g2} + d_{n2} d_{p0} C_{g1} \\ + C_{n1} d_{p2} d_{g0} + d_{n2} C_{p1} d_{g0}$$

$$S_{14} = d_{n0} C_{p1} C_{g2} + d_{n0} C_{p2} C_{g1} + C_{n1} d_{p0} C_{g2} + C_{n2} d_{p0} C_{g1} \\ + C_{n1} C_{p2} d_{g0} + C_{n2} C_{p1} d_{g0}$$

$$S_{15} = d_{n0} d_{p1} d_{g3} + d_{n0} d_{p3} d_{g1} + d_{n1} d_{p0} d_{g3} + d_{n3} d_{p0} d_{g1} \\ + d_{n1} d_{p3} d_{g0} + d_{n3} d_{p1} d_{g0}$$

$$S_{16} = d_{n0} d_{p1} C_{g3} + d_{n0} C_{p3} d_{g1} + d_{n1} d_{p0} C_{g3} + C_{n3} d_{p0} d_{g1} \\ + d_{n1} C_{p3} d_{g0} + C_{n3} d_{p1} d_{g0}$$

$$S_{17} = d_{n0} C_{p1} d_{g3} + d_{n0} d_{p3} C_{g1} + C_{n1} d_{p0} d_{g3} + d_{n3} d_{p0} C_{g1} \\ + C_{n1} d_{p3} d_{g0} + d_{n3} C_{p1} d_{g0}$$

$$S_{18} = d_{n0} C_{p1} C_{g3} + d_{n0} C_{p3} C_{g1} + C_{n1} d_{p0} C_{g3} + C_{n3} d_{p0} C_{g1} \\ + C_{n1} C_{p3} d_{g0} + C_{n3} C_{p1} d_{g0}$$

$$S_{19} = d_{n0} d_{p2} d_{g2} + d_{n2} d_{p0} d_{g2} + d_{n2} d_{p2} d_{g0}$$

$$S_{20} = d_{n0} d_{p2} C_{g2} + d_{n0} C_{p2} d_{g2} + C_{n2} d_{p0} d_{g2} + d_{n2} d_{p0} C_{g2} \\ + C_{n2} d_{p2} d_{g0} + d_{n2} C_{p2} d_{g0}$$

$$S_{21} = d_{n0} C_{p2} C_{g2} + C_{n2} d_{p0} C_{g2} + C_{n2} C_{p2} d_{g0}$$

$$S_{22} = d_{n0} d_{p2} d_{g3} + d_{n0} d_{p3} d_{g2} + d_{n2} d_{p0} d_{g3} + d_{n3} d_{p0} d_{g2} \\ + d_{n2} d_{p3} d_{g0} + d_{n3} d_{p2} d_{g0}$$

$$S_{23} = d_{n0} d_{p2} C_{g3} + d_{n0} C_{p3} d_{g2} + d_{n2} d_{p0} C_{g3} + C_{n3} d_{p0} d_{g2} \\ + d_{n2} C_{p3} d_{g0} + C_{n3} d_{p2} d_{g0}$$

$$S_{24} = d_{n0} C_{p2} d_{g3} + d_{n0} d_{p3} C_{g2} + C_{n2} d_{p0} d_{g3} + d_{n3} d_{p0} C_{g2} \\ + C_{n2} d_{p3} d_{g0} + d_{n3} C_{p2} d_{g0}$$

$$S_{25} = d_{n0} C_{p2} C_{g3} + d_{n0} C_{p3} C_{g2} + C_{n2} d_{p0} C_{g3} + C_{n3} d_{p0} C_{g2} \\ + C_{n2} C_{p3} d_{g0} + C_{n3} C_{p2} d_{g0}$$

$$S_{26} = d_{n0} d_{p3} d_{g3} + d_{n3} d_{p0} d_{g3} + d_{n3} d_{p3} d_{g0}$$

$$S_{27} = d_{n0} d_{p3} C_{g3} + d_{n0} C_{p3} d_{g3} + d_{n3} d_{p0} C_{g3} + C_{n3} d_{p0} d_{g3}$$

$$+ d_{n3} C_{p3} d_{p0} + C_{n3} d_{p3} d_{g0}$$

$$S_{28} = d_{n0} C_{p3} C_{g3} + C_{n3} d_{p0} C_{g3} + C_{n3} C_{p3} d_{g0}$$

$$S_{29} = d_{n1} d_{p1} d_{g1}$$

$$S_{30} = d_{n1} d_{p1} C_{g1} + d_{n1} C_{p1} d_{g1} + C_{n1} d_{p1} d_{g1}$$

$$S_{31} = C_{n1} C_{p1} d_{g1} + C_{n1} d_{p1} C_{g1} + d_{n1} C_{p1} C_{g1}$$

$$S_{32} = C_{n1} C_{p1} C_{g1}$$

$$S_{33} = d_{n1} d_{p1} d_{g2} + d_{n1} d_{p2} d_{g1} + d_{n2} d_{p1} d_{g1}$$

$$S_{34} = d_{n1} d_{p1} C_{g2} + d_{n1} C_{p2} d_{g1} + C_{n2} d_{p1} d_{g1}$$

$$S_{35} = d_{n1} d_{p1} d_{g3} + d_{n1} d_{p3} d_{g1} + d_{n3} d_{p1} d_{g1}$$

$$S_{36} = d_{n1} d_{p1} C_{g3} + d_{n1} C_{p3} d_{g1} + C_{n3} d_{p1} d_{g1}$$

$$S_{37} = d_{n2} d_{p1} C_{g1} + d_{n2} C_{p1} d_{g1} + d_{n1} d_{p2} C_{g1} + C_{n1} d_{p2} d_{g1} \\ + d_{n1} C_{p1} d_{g2} + C_{n1} d_{p1} d_{g2}$$

$$S_{38} = C_{n2} d_{p1} C_{g1} + C_{n2} C_{p1} d_{g1} + d_{n1} C_{p2} C_{g1} + C_{n1} C_{p2} d_{g1}$$

$$+d_{n1} C_{p1} C_{g2} + C_{n1} d_{p1} C_{g2}$$

$$S_{39} = d_{n3} d_{p1} C_{g1} + d_{n3} C_{p1} d_{g1} + d_{n1} d_{p3} C_{g1} + C_{n1} d_{p3} d_{g1}$$

$$+ d_{n1} C_{p1} d_{g3} + C_{n1} d_{p1} d_{g3}$$

$$S_{40} = C_{n3} d_{p1} C_{g1} + C_{n3} C_{p1} d_{g1} + d_{n1} C_{p3} C_{g1} + C_{n1} C_{p3} d_{g1}$$

$$+ d_{n1} C_{p1} C_{g3} + C_{n1} d_{p1} C_{g3}$$

$$S_{41} = C_{n1} C_{p1} d_{g2} + C_{n1} d_{p2} C_{g1} + d_{n2} C_{p1} C_{g1}$$

$$S_{42} = C_{n1} C_{p1} C_{g2} + C_{n1} C_{p2} C_{g1} + C_{n2} C_{p1} C_{g1}$$

$$S_{43} = C_{n1} C_{p1} d_{g3} + C_{n1} d_{p3} C_{g1} + d_{n3} C_{p1} C_{g1}$$

$$S_{44} = C_{n1} C_{p1} C_{g3} + C_{n1} C_{p3} C_{g1} + C_{n3} C_{p1} C_{g1}$$

$$S_{45} = d_{n2} d_{p2} d_{g1} + d_{n2} d_{p1} d_{g2} + d_{n1} d_{p2} d_{g2}$$

$$S_{46} = d_{n1} C_{p2} d_{g2} + d_{n1} d_{p2} C_{g2} + C_{n2} d_{p1} d_{g2} + d_{n2} d_{p1} C_{g2}$$

$$+ C_{n2} d_{p2} d_{g1} + d_{n2} C_{p2} d_{g1}$$

$$S_{47} = C_{n2} C_{p2} d_{g1} + C_{n2} d_{p1} C_{g2} + d_{n1} C_{p2} C_{g2}$$

$$S_{48} = d_{n1} d_{p2} d_{g3} + d_{n1} d_{p3} d_{g2} + d_{n2} d_{p1} d_{g3} + d_{n3} d_{p1} d_{g2}$$

$$+ d_{n2} d_{p3} d_{g1} + d_{n3} d_{p2} d_{g1}$$

$$S_{49} = d_{n1} d_{p2} C_{g3} + d_{n1} C_{p3} d_{g2} + d_{n2} d_{p1} C_{g3} + C_{n3} d_{p1} d_{g2}$$

$$+ d_{n2} C_{p3} d_{g1} + C_{n3} d_{p2} d_{g1}$$

$$S_{50} = d_{n1} C_{p2} d_{g3} + d_{n1} d_{p3} C_{g2} + C_{n2} d_{p1} d_{g3} + d_{n3} d_{p1} C_{g2}$$

$$+ C_{n2} d_{p3} d_{g1} + d_{n3} d_{p2} d_{g1}$$

$$S_{51} = d_{n1} C_{p2} C_{g3} + d_{n1} C_{p3} C_{g2} + C_{n2} d_{p1} C_{g3} + C_{n3} d_{p1} C_{g2}$$

$$+ C_{n2} C_{p3} d_{g1} + C_{n3} C_{p2} d_{g1}$$

$$S_{52} = d_{n3} d_{p3} d_{g1} + d_{n3} d_{p1} d_{g3} + d_{n1} d_{p3} d_{g3}$$

$$S_{53} = d_{n1} C_{p3} d_{g3} + d_{n1} d_{p3} C_{g3} + C_{n3} d_{p1} d_{g3} + d_{n3} d_{p1} C_{g3}$$

$$+ C_{n3} d_{p3} d_{g1} + d_{n3} C_{p3} d_{g1}$$

$$S_{54} = C_{n3} C_{p3} d_{g1} + C_{n3} d_{p1} C_{g3} + d_{n1} C_{p3} C_{g3}$$

$$S_{55} = d_{n2} d_{p2} C_{g1} + d_{n2} C_{p2} d_{g2} + C_{n1} d_{p2} d_{g2}$$

$$S_{56} = C_{n1} C_{p2} d_{g2} + C_{n1} d_{p2} C_{g2} + C_{n2} C_{p1} d_{g2} + d_{n2} C_{p1} C_{g2}$$



$$+ C_{n2} d_{p2} C_{g1} + d_{n2} C_{p2} C_{g1}$$

$$S_{57} = C_{n2} C_{p2} C_{g1} + C_{n2} C_{p1} C_{g2} + C_{n1} C_{p2} C_{g2}$$

$$S_{58} = C_{n1} d_{p2} d_{g3} + C_{n1} d_{p3} d_{g2} + d_{n2} C_{p1} d_{g3} + d_{n3} C_{p1} d_{g2}$$

$$+ d_{n2} d_{p3} C_{g1} + d_{n3} d_{p2} C_{g1}$$

$$S_{59} = C_{n1} d_{p2} C_{g3} + C_{n1} C_{p3} d_{g2} + d_{n2} C_{p1} C_{g3} + C_{n3} C_{p1} d_{g2}$$

$$+ d_{n2} C_{p3} C_{g1} + C_{n3} d_{p2} C_{g1}$$

$$S_{60} = C_{n1} C_{p2} d_{g3} + C_{n1} d_{p3} C_{g2} + C_{n2} C_{p1} d_{g3} + d_{n3} C_{p1} C_{g2}$$

$$+ C_{n2} d_{p3} C_{g1} + d_{n3} C_{p2} C_{g1}$$

$$S_{61} = C_{n1} C_{p2} C_{g3} + C_{n1} C_{p3} C_{g2} + C_{n2} C_{p1} C_{g3} + C_{n3} C_{p1} C_{g2}$$

$$+ C_{n2} C_{p3} C_{g1} + C_{n3} C_{p2} C_{g1}$$

$$S_{62} = C_{n1} d_{p3} d_{g3} + d_{n3} C_{p1} d_{g3} + d_{n3} d_{p3} C_{g1}$$

$$S_{63} = C_{n1} C_{p3} d_{g3} + C_{n1} d_{g3} C_{p3} + C_{n3} C_{p1} d_{g3} + d_{n3} C_{p1} C_{g3}$$

$$+ C_{n3} d_{p3} C_{g1} + d_{n3} C_{p3} C_{g1}$$

$$S_{64} = C_{n1} C_{p3} C_{g3} + C_{n3} C_{p1} C_{g3} + C_{n3} C_{p3} C_{g1}$$

$$S_{65} = d_{n2} d_{p2} d_{g2}$$

$$S_{66} = d_{n2} d_{p2} C_{g2} + d_{n2} C_{p2} d_{g2} + C_{n2} d_{p2} d_{g2}$$

$$S_{67} = C_{n2} C_{p2} d_{g2} + C_{n2} d_{p2} C_{g2} + d_{n2} C_{p2} C_{g2}$$

$$S_{68} = C_{n2} C_{p2} C_{g2}$$

$$S_{69} = d_{n2} d_{p2} d_{g3} + d_{n2} d_{p3} d_{g2} + d_{n3} d_{p2} d_{g2}$$

$$S_{70} = d_{n2} d_{p2} C_{g3} + d_{n2} C_{p3} d_{g2} + C_{n3} d_{p2} d_{g2}$$

$$S_{71} = d_{n2} C_{p2} d_{g3} + d_{n2} d_{p3} C_{g2} + C_{n2} d_{p2} d_{g3} + d_{n3} d_{p2} C_{g2} \\ + C_{n2} d_{p3} d_{g2} + d_{n3} C_{p2} C_{g2}$$

$$S_{72} = d_{n2} C_{p2} C_{g3} + d_{n2} C_{p3} C_{g2} + C_{n2} d_{p2} C_{g3} + C_{n3} d_{p2} C_{g2} \\ + C_{n2} C_{p3} d_{g2} + C_{n3} C_{p2} d_{g2}$$

$$S_{73} = C_{n2} C_{p2} d_{g3} + C_{n2} d_{p3} C_{g2} + d_{n3} C_{p2} C_{g2}$$

$$S_{74} = C_{n2} C_{p2} C_{g3} + C_{n2} C_{p3} C_{g2} + C_{n3} C_{p2} C_{g2}$$

$$S_{75} = d_{n2} d_{p3} d_{g3} + d_{n3} d_{p2} d_{g3} + d_{n3} d_{p3} d_{g2}$$

$$S_{76} = d_{n2} d_{p3} C_{g3} + d_{n2} C_{p3} d_{g3} + d_{n3} d_{n2} C_{g3}$$

$$+ C_{n3} d_{n2} d_{g3} + d_{n3} C_{p3} d_{g2} + C_{n3} d_{p3} d_{g2}$$

$$S_{77} = d_{n2} C_{p3} C_{g3} + C_{n3} d_{p2} C_{g3} + C_{n3} C_{p3} d_{g2}$$

$$S_{78} = C_{n2} d_{p3} d_{g3} + d_{n3} C_{p2} d_{g3} + d_{n3} d_{p3} C_{g2}$$

$$S_{79} = C_{n2} d_{p3} C_{g3} + C_{n2} C_{p3} d_{g3} + d_{n3} C_{p2} d_{g3}$$

$$+ C_{n3} C_{p2} d_{g3} + d_{n3} C_{p3} C_{g2} + C_{n3} d_{p3} C_{g2}$$

$$S_{80} = C_{n2} C_{p3} C_{g3} + C_{n3} C_{p2} C_{g3} + C_{n3} C_{p3} C_{g2}$$

(B.3)

$$S_{81} = d_{n3} d_{p3} d_{g3}$$

$$S_{82} = d_{n3} d_{p3} C_{g3} + d_{n3} C_{p3} d_{g3} + C_{n3} d_{p3} d_{g3}$$

$$S_{83} = C_{n3} C_{p3} d_{g3} + C_{n3} d_{p3} C_{g3} + d_{n3} C_{p3} C_{g3}$$

$$S_{84} = C_{n3} C_{p3} C_{g3}$$

Reducing the products of sine and cosine functions to the sums of sine and cosine functions, one obtains

$$W_n W_p W_q = P_1 + P_2 \sin t_1 + P_3 \cos t_1 + P_4 \sin 2t_1 + P_5 \cos 2t_1 + P_6 \sin 3t_1 + P_7 \cos 3t_1 \quad (\text{B.4})$$

where

$$P_1 = S_1 + \frac{1}{2} S_8 + \frac{1}{2} (S_{10} + S_{19} + S_{21} + S_{26} + S_{28}) + \frac{1}{4} (S_{33} + S_{38} - S_{41} + S_{48} + S_{51} + S_{59} - S_{60}) \quad (\text{B.5.1})$$

$$P_2 = S_3 + \frac{1}{2} (S_{12} - S_{13} + S_{23} - S_{24} + S_{55} + S_{57} + S_{62} + S_{64}) + \frac{1}{4} (S_{30} + 3S_{32} + S_{36} - S_{39} - S_{44} - S_{70} + S_{71} + S_{74}) \quad (\text{B.5.2})$$

$$P_3 = S_2 + \frac{1}{2} (S_{11} + S_{14} + S_{22} + S_{25} + S_{45} + S_{47} + S_{52} + S_{54}) + \frac{1}{4} (3S_{29} + S_{31} + S_{35} + S_{40} - S_{43} + S_{69} + S_{72} - S_{78}) \quad (\text{B.5.3})$$

$$P_4 = S_5 + \frac{1}{2} (S_9 + S_{16} - S_{17} + S_{34} + S_{78} + S_{80}) + \frac{1}{4} (S_{42} + S_{49} - S_{50} + S_{58} + S_{61} + S_{66} + 3S_{68}) \quad (\text{B.5.4})$$

$$P_3 = S_4 + \frac{1}{2}(S_8 - S_{10} + S_{15} + S_{18} + S_{33} + S_{41} + S_{75} + S_{77}) + \frac{1}{4}(S_{48} + S_{51} - S_{59} + S_{60} + 3S_{65} + S_{67}) \quad (\text{B.5.5})$$

$$P_6 = S_7 + \frac{1}{2}(S_{12} + S_{13} + S_{36} + S_{44} + S_{70} + S_{74}) + \frac{1}{4}(S_{30} - S_{32} + S_{46} - S_{55} + S_{57} + S_{82} + 3S_{84}) \quad (\text{B.5.6})$$

$$P_7 = S_6 + \frac{1}{2}(S_{11} - S_{14} + S_{35} + S_{43} + S_{69} + S_{73}) + \frac{1}{4}(S_{29} - S_{31} + S_{45} - S_{47} + S_{56} + 3S_{81} + S_{83}) \quad (\text{B.5.7})$$

Employing Eqs. 4.15 and B.4 in Eq. 4.13 and balancing terms up to third harmonic, one obtains constant terms:

$$f_{m1} = \sum_{n=1}^N (\lambda E_{mn} + K_{mn}) d_{n0} + \sum_{n,\beta,\gamma=1}^N C_{mnp\beta\gamma} P_1 = 0 \quad (\text{B.6})$$

sin  $t_1$  terms

$$f_{m2} = \sum_{n=1}^N [(-\bar{M}_{mn} + \lambda E_{mn} + K_{mn}) C_{n1} - (\bar{G}_{mn} + GB_{mn}) d_{n1}] + \sum_{n,\beta,\gamma=1}^N C_{mnp\beta\gamma} P_2 = 0 \quad (\text{B.7})$$

cos  $t_1$  terms

$$f_{m3} = \sum_{n=1}^N [(-\bar{M}_{mn} + \lambda E_{mn} + K_{mn}) d_{n1} + (\bar{G}_{mn} + GB_{mn}) C_{n1}] + \sum_{n,\beta,\gamma=1}^N C_{mnp\beta\gamma} P_3 - F_m S_i^k = 0 \quad (\text{B.8})$$

sin  $2t_1$  terms

$$f_{m4} = \sum_{n=1}^N [(-4\bar{M}_{mn} + \lambda E_{mn} + K_{mn}) C_{n2} - (2\bar{G}_{mn} + GB_{mn}) d_{n2}] + \sum_{n,p,q=1}^N C_{mnpq} P_4 = 0 \quad (B.9)$$

cos  $2t_1$  terms

$$f_{m5} = \sum_{n=1}^N [(-4\bar{M}_{mn} + \lambda E_{mn} + K_{mn}) d_{n2} - (2\bar{G}_{mn} + GB_{mn}) C_{n2}] + \sum_{n,p,q=1}^N C_{mnpq} P_5 - F_m S_2^k = 0 \quad (B.10)$$

sin  $3t_1$  terms

$$f_{m6} = \sum_{n=1}^N [(-9\bar{M}_{mn} + \lambda E_{mn} + K_{mn}) C_{n3} - (3\bar{G}_{mn} + GB_{mn}) d_{n3}] + \sum_{n,p,q=1}^N C_{mnpq} P_6 = 0 \quad (B.11)$$

cos  $3t_1$  terms:

$$f_{m7} = \sum_{n=1}^N [(-9\bar{M}_{mn} + \lambda E_{mn} + K_{mn}) d_{n3} + (3\bar{G}_{mn} + GB_{mn}) C_{n3}] + \sum_{n,p,q=1}^N C_{mnpq} P_7 - F_m S_3^k = 0 \quad (B.12)$$

Let the unknown vector  $x = (b_{10}, a_{11}, b_{11}, a_{12}, b_{12}, a_{13}, b_{13}, a_{21}, b_{21}, \dots, b_{N3})$ , and write Eqs. B.6 to B.12 as

$$f(\underline{x}) = \begin{pmatrix} f_{11} \\ f_{12} \\ f_{13} \\ f_{14} \\ f_{15} \\ f_{16} \\ f_{17} \\ f_{21} \\ \vdots \end{pmatrix} \quad (B.13)$$

one obtains  $7 \times N$  equations with  $7 \times N$  unknowns. Let

$$\begin{aligned}
 m_a &= 7(m-1)+1 & l_a &= 7(l-1)+1 \\
 m_b &= m+1 & l_b &= l+1 \\
 m_c &= m+2 & l_c &= l+2 \\
 m_d &= m+3 & l_d &= l+3 \\
 m_e &= m+4 & l_e &= l+4 \\
 m_f &= m+5 & l_f &= l+5 \\
 m_g &= m+6 & l_g &= l+6
 \end{aligned}
 \tag{B.14}$$

Then Jacobian of these equations are

$$\begin{aligned}
 J_{m_a, l_a} &= \lambda F_{m,l} + K_{m,l} + \sum_{n,p,q=1}^N C_{mnpq} \frac{\partial P_i}{\partial d_{e0}} \\
 J_{m_a, l_b} &= \sum_{n,p,q=1}^N C_{mnpq} \frac{\partial P_i}{\partial c_{e1}} \\
 J_{m_a, l_c} &= \sum_{n,p,q=1}^N C_{mnpq} \frac{\partial P_i}{\partial d_{e1}} \\
 J_{m_a, l_d} &= \sum_{n,p,q=1}^N C_{mnpq} \frac{\partial P_i}{\partial c_{e2}} \\
 J_{m_a, l_e} &= \sum_{n,p,q=1}^N C_{mnpq} \frac{\partial P_i}{\partial d_{e2}} \\
 J_{m_a, l_f} &= \sum_{n,p,q=1}^N C_{mnpq} \frac{\partial P_i}{\partial c_{e3}} \\
 J_{m_a, l_g} &= \sum_{n,p,q=1}^N C_{mnpq} \frac{\partial P_i}{\partial d_{e3}}
 \end{aligned}$$

$$J_{mb,la} = \sum_{n,p,q=1}^N C_{mnpq} \frac{\partial P_2}{\partial d_{e0}}$$

$$J_{mb,lb} = -\bar{M}_{me} + \lambda E_{me} + K_{me} + \sum_{n,p,q=1}^N C_{mnpq} \frac{\partial P_2}{\partial c_{e1}}$$

$$J_{mb,lc} = -\bar{G}_{me} - GB_{me} + \sum_{n,p,q=1}^N C_{mnpq} \frac{\partial P_2}{\partial d_{e1}}$$

$$J_{mb,ld} = \sum_{n,p,q=1}^N C_{mnpq} \frac{\partial P_2}{\partial c_{e2}}$$

$$J_{mb,le} = \sum_{n,p,q=1}^N C_{mnpq} \frac{\partial P_2}{\partial d_{e2}}$$

$$J_{mb,lf} = \sum_{n,p,q=1}^N C_{mnpq} \frac{\partial P_2}{\partial c_{e3}}$$

$$J_{mb,lg} = \sum_{n,p,q=1}^N C_{mnpq} \frac{\partial P_2}{\partial d_{e3}}$$

$$J_{mc,la} = \sum_{n,p,q=1}^N C_{mnpq} \frac{\partial P_3}{\partial d_{e0}}$$

$$J_{mc,lb} = -\bar{G}_{me} - GB_{me} + \sum_{n,p,q=1}^N C_{mnpq} \frac{\partial P_3}{\partial c_{e1}}$$

$$J_{mc,lc} = -\bar{M}_{me} + \lambda E_{me} + K_{me} + \sum_{n,p,q=1}^N C_{mnpq} \frac{\partial P_3}{\partial d_{e1}}$$

$$J_{mc,ld} = \sum_{n,p,q=1}^N C_{mnpq} \frac{\partial P_3}{\partial c_{e2}}$$

$$J_{mc,le} = \sum_{n,p,q=1}^N C_{mnpq} \frac{\partial P_3}{\partial d_{e2}}$$

$$J_{mc,lf} = \sum_{n,p,q=1}^N C_{mnpq} \frac{\partial P_3}{\partial c_{e3}}$$



$$J_{mc,eq} = \sum_{n,p,q=1}^N C_{mnpq} \frac{\partial P_3}{\partial d_{e3}}$$

$$J_{md,ea} = \sum_{n,p,q=1}^N C_{mnpq} \frac{\partial P_4}{\partial d_{e0}}$$

$$J_{md,eb} = \sum_{n,p,q=1}^N C_{mnpq} \frac{\partial P_4}{\partial c_{e1}}$$

$$J_{md,ec} = \sum_{n,p,q=1}^N C_{mnpq} \frac{\partial P_4}{\partial d_{e1}}$$

$$J_{md,ed} = -4\bar{M}_{me} + \lambda E_{me} + K_{me} + \sum_{n,p,q=1}^N C_{mnpq} \frac{\partial P_4}{\partial c_{e2}}$$

$$J_{md,ee} = -2\bar{G}_{me} - G_{B_{me}} + \sum_{n,p,q=1}^N C_{mnpq} \frac{\partial P_4}{\partial d_{e2}}$$

$$J_{md,ef} = \sum_{n,p,q=1}^N C_{mnpq} \frac{\partial P_4}{\partial c_{e3}}$$

$$J_{md,eg} = \sum_{n,p,q=1}^N C_{mnpq} \frac{\partial P_4}{\partial d_{e3}}$$

$$J_{me,ea} = \sum_{n,p,q=1}^N C_{mnpq} \frac{\partial P_5}{\partial d_{e0}}$$

$$J_{me,eb} = \sum_{n,p,q=1}^N C_{mnpq} \frac{\partial P_5}{\partial c_{e1}}$$

$$J_{me,ec} = \sum_{n,p,q=1}^N C_{mnpq} \frac{\partial P_5}{\partial d_{e1}}$$

$$J_{me,ed} = -2\bar{G}_{me} - G_{B_{me}} + \sum_{n,p,q=1}^N C_{mnpq} \frac{\partial P_5}{\partial c_{e2}}$$

$$J_{me,ee} = -4\bar{M}_{me} + \lambda E_{me} + K_{me} + \sum_{n,p,q=1}^N C_{mnpq} \frac{\partial P_5}{\partial d_{e2}}$$

$$J_{me,ef} = \sum_{n,p,g=1}^N C_{mnpq} \frac{\partial P_5}{\partial c_{e3}}$$

$$J_{me,lg} = \sum_{n,p,g=1}^N C_{mnpq} \frac{\partial P_5}{\partial d_{e3}}$$

$$J_{mf,la} = \sum_{n,p,g=1}^N C_{mnpq} \frac{\partial P_6}{\partial d_{e0}}$$

$$J_{mf,lb} = \sum_{n,p,g=1}^N C_{mnpq} \frac{\partial P_6}{\partial c_{e1}}$$

$$J_{mf,lc} = \sum_{n,p,g=1}^N C_{mnpq} \frac{\partial P_6}{\partial d_{e1}}$$

$$J_{mf,ld} = \sum_{n,p,g=1}^N C_{mnpq} \frac{\partial P_6}{\partial c_{e2}}$$

$$J_{mf,le} = \sum_{n,p,g=1}^N C_{mnpq} \frac{\partial P_6}{\partial d_{e2}}$$

$$J_{mf,lf} = -9 \bar{M}_{me} + \lambda E_{me} + K_{me} + \sum_{n,p,g=1}^N C_{mnpq} \frac{\partial P_6}{\partial c_{e3}}$$

$$J_{mf,lg} = -3 \bar{G}_{me} - G_{B_{me}} + \sum_{n,p,g=1}^N C_{mnpq} \frac{\partial P_6}{\partial d_{e3}}$$

$$J_{mg,la} = \sum_{n,p,g=1}^N C_{mnpq} \frac{\partial P_7}{\partial d_{e0}}$$

$$J_{mg,lb} = \sum_{n,p,g=1}^N C_{mnpq} \frac{\partial P_7}{\partial c_{e1}}$$

$$J_{mg,lc} = \sum_{n,p,g=1}^N C_{mnpq} \frac{\partial P_7}{\partial d_{e1}}$$

$$J_{mg,ed} = \sum_{n,p,q=1}^N C_{mnpq} \frac{\partial P_7}{\partial C_{d2}}$$

$$J_{mg,le} = \sum_{n,p,q=1}^N C_{mnpq} \frac{\partial P_7}{\partial d_{e2}}$$

$$J_{mg,lf} = 3 \bar{G}_{me} + G_{B_{me}} + \sum_{n,p,q=1}^N C_{mnpq} \frac{\partial P_7}{\partial C_{d3}}$$

(B.15)

$$J_{mg,lg} = -9 \bar{M}_{me} + \lambda E_{me} + K_{me} + \sum_{n,p,q=1}^N C_{mnpq} \frac{\partial P_7}{\partial d_{l3}}$$

where

$$\begin{aligned} \frac{\partial P_i}{\partial d_{e0}} = & [d_{p0}d_{g0} + \frac{1}{2}(d_{p1}d_{g1} + C_{p1}C_{g1} + d_{p2}d_{g2} + C_{p2}C_{g2} \\ & + d_{p3}d_{g3} + C_{p3}C_{g3})] S_e^n + P.T. \end{aligned}$$

where P.T. means permutation terms, i.e.,  $n \rightarrow p$ ,  $p \rightarrow q$ ,  $q \rightarrow n$  and so on

$$\begin{aligned} \frac{\partial P_i}{\partial C_{d1}} = & [\frac{1}{2}(d_{p0}C_{g1} + C_{p1}d_{g0}) + \frac{1}{4}(C_{p2}d_{g1} + d_{p1}C_{g2} - C_{p1}d_{g2} - d_{p2}C_{g1} \\ & + d_{p2}C_{g3} + C_{p3}d_{g2} - C_{p2}d_{g3} - d_{p3}C_{g2})] S_e^n + P.T. \end{aligned}$$

$$\begin{aligned} \frac{\partial P_i}{\partial d_{l1}} = & [\frac{1}{2}(d_{p0}d_{g1} + d_{p1}d_{g0}) + \frac{1}{4}(d_{p1}d_{g2} + d_{p2}d_{g1} + C_{p2}C_{g1} + C_{p1}C_{g2} \\ & + d_{p2}d_{g3} + d_{p3}d_{g2} + C_{p2}C_{g3} + C_{p3}C_{g2})] S_e^n + P.T. \end{aligned}$$

$$\frac{\partial P_1}{\partial C_{e2}} = \left[ \frac{1}{2} (d_{p0} C_{g2} + C_{p2} d_{g0}) + \frac{1}{4} (d_{p1} C_{g1} + C_{p1} d_{g1} + d_{p1} C_{g3} + C_{p3} d_{g1} - C_{p1} d_{g3} - d_{p3} C_{g1}) \right] S_e^n + P.T.$$

$$\frac{\partial P_1}{\partial C_{e2}} = \left[ \frac{1}{2} (d_{p0} d_{g2} + d_{p2} d_{g0}) + \frac{1}{4} (d_{p1} d_{g1} - C_{p1} C_{g1} + d_{p1} d_{g3} + d_{p3} d_{g1} + C_{p1} C_{g3} + C_{p3} C_{g1}) \right] S_e^n + P.T.$$

$$\frac{\partial P_1}{\partial C_{e3}} = \left[ \frac{1}{2} (d_{p0} C_{g3} + C_{p3} d_{g0}) + \frac{1}{4} (d_{p1} C_{g2} + C_{p2} d_{g1} + C_{p1} d_{g2} + d_{p2} C_{g1}) \right] S_e^n + P.T.$$

$$\frac{\partial P_1}{\partial C_{e3}} = \left[ \frac{1}{2} (d_{p0} d_{g3} + d_{p3} d_{g0}) + \frac{1}{4} (d_{p1} d_{g2} + d_{p2} d_{g1} - C_{p1} C_{g2} + C_{p2} C_{g1}) \right] S_e^n + P.T.$$

$$\frac{\partial P_2}{\partial C_{e0}} = \left[ d_{p0} C_{g1} + C_{p1} d_{g0} + \frac{1}{2} (d_{p1} C_{g2} + C_{p2} d_{g1} - C_{p1} d_{g2} - d_{p2} C_{g1} + d_{p2} C_{g3} + C_{p3} d_{g2} - C_{p2} d_{g3} - d_{p3} C_{g2}) \right] S_e^n + P.T.$$

$$\frac{\partial P_2}{\partial C_{e1}} = \left[ d_{p0} d_{g0} + \frac{1}{2} (d_{p0} d_{g2} + d_{p2} d_{g0} + d_{p2} d_{g2} + C_{p2} C_{g2} + d_{p3} d_{g3} + C_{p3} C_{g3}) + \frac{1}{4} (d_{p1} d_{g1} + 3C_{p1} C_{g1} + d_{p3} d_{g1} - d_{p1} d_{g3} - C_{p1} C_{g3} - C_{p3} C_{g1}) \right] S_e^n + P.T.$$

$$\frac{\partial P_2}{\partial C_{e1}} = \left[ \frac{1}{2} (d_{p0} C_{g2} + C_{p2} d_{g0}) + \frac{1}{4} (d_{p1} C_{g1} + C_{p1} d_{g1} + d_{p1} C_{g3} + C_{p3} d_{g1} - d_{p3} C_{g1} - C_{p1} d_{g3}) \right] S_e^n + P.T.$$

$$\frac{\partial P_2}{\partial C_{l_2}} = \left[ \frac{1}{2} (d_{p_0} d_{g_1} + d_{p_1} d_{g_0} - d_{p_0} d_{g_3} - d_{p_3} d_{g_0} + C_{p_2} C_{g_1} + C_{p_1} C_{g_2}) \right. \\ \left. + \frac{1}{4} (d_{p_2} d_{g_3} + d_{p_3} d_{g_2} + C_{p_2} C_{g_3} + C_{p_3} C_{g_2}) \right] \delta_{\ell}^n + P. T.$$

$$\frac{\partial P_2}{\partial d_{l_2}} = \left[ \frac{1}{2} (d_{p_0} C_{g_3} + C_{p_3} d_{g_0} - d_{p_0} C_{g_1} - C_{p_1} d_{g_0} + d_{p_2} C_{g_1} + C_{p_1} d_{g_2}) \right. \\ \left. + \frac{1}{4} (C_{p_2} d_{g_3} + d_{p_3} C_{g_2} - d_{p_2} C_{g_3} - C_{p_3} d_{g_2}) \right] \delta_{\ell}^n + P. T.$$

$$\frac{\partial P_2}{\partial C_{l_3}} = \left[ \frac{1}{2} (d_{p_0} d_{g_2} + d_{p_2} d_{g_0} + C_{p_1} C_{g_3} + C_{p_3} C_{g_1}) + \frac{1}{4} (d_{p_1} d_{g_1} \right. \\ \left. - d_{p_2} d_{g_2} + C_{p_2} C_{g_2}) \right] \delta_{\ell}^n + P. T.$$

$$\frac{\partial P_2}{\partial d_{l_3}} = \left[ \frac{1}{2} (C_{p_1} d_{g_3} + d_{p_3} C_{g_1} - d_{p_0} C_{g_2} - C_{p_2} d_{g_0}) + \frac{1}{4} (d_{p_2} C_{g_2} \right. \\ \left. + C_{p_2} d_{g_2} - d_{p_1} C_{g_1} - C_{p_1} d_{g_1}) \right] \delta_{\ell}^n + P. T.$$

$$\frac{\partial P_3}{\partial d_{l_0}} = \left[ (d_{p_0} d_{g_1} + d_{p_1} d_{g_0}) + \frac{1}{2} (d_{p_1} d_{g_2} + d_{p_2} d_{g_1} + C_{p_1} C_{g_2} + C_{p_2} C_{g_1} \right. \\ \left. + d_{p_2} d_{g_3} + d_{p_3} d_{g_2} + C_{p_2} C_{g_3} + C_{p_3} C_{g_2}) \right] \delta_{\ell}^n + P. T.$$

$$\frac{\partial P_3}{\partial C_{l_1}} = \left[ \frac{1}{2} (d_{p_0} C_{g_2} + C_{p_2} d_{g_0}) + \frac{1}{4} (C_{p_1} d_{g_1} + d_{p_1} C_{g_1} + C_{p_3} d_{g_1} \right. \\ \left. + d_{p_1} C_{g_3} - C_{p_1} d_{g_3} - d_{p_3} C_{g_1}) \right] \delta_{\ell}^n + P. T.$$

$$\begin{aligned} \frac{\partial P_3}{\partial d_{e1}} = & [d_{p0}d_{g0} + \frac{1}{2}(d_{p0}d_{g2} + d_{p2}d_{g0} + d_{p2}d_{g2} + C_{p2}C_{g2} + d_{p3}d_{g3} \\ & + C_{p3}C_{g3}) + \frac{1}{4}(3d_{p1}d_{g1} + C_{p1}C_{g1} + d_{p1}d_{g3} + d_{p3}d_{g1} + C_{p3}C_{g1} \\ & + C_{p1}C_{g3})] \delta_{\ell}^n + P.T. \end{aligned}$$

$$\begin{aligned} \frac{\partial P_3}{\partial d_{e2}} = & [ \frac{1}{2}(d_{p0}C_{g1} + C_{p1}d_{g0} + d_{p0}C_{g3} + C_{p3}d_{g0} + C_{p2}d_{g1} + d_{p1}C_{g2}) \\ & + \frac{1}{4}(d_{p2}C_{g3} + C_{p3}d_{g2} - C_{p2}d_{g3} - d_{p3}C_{g2}) ] \delta_{\ell}^n + P.T. \end{aligned}$$

$$\begin{aligned} \frac{\partial P_3}{\partial d_{e2}} = & [ \frac{1}{2}(d_{p0}d_{g1} + d_{p1}d_{g0} + d_{p0}d_{g3} + d_{p3}d_{g0} + d_{p2}d_{g1} + d_{p1}d_{g2}) \\ & + \frac{1}{4}(d_{p2}d_{g3} + d_{p3}d_{g2} + C_{p2}C_{g3} + C_{p3}C_{g2}) ] \delta_{\ell}^n + P.T. \end{aligned}$$

$$\begin{aligned} \frac{\partial P_3}{\partial d_{e3}} = & [ \frac{1}{2}(d_{p0}C_{g2} + C_{p2}d_{g0} + C_{p3}d_{g1} + d_{p1}C_{g3}) + \frac{1}{4}(d_{p1}C_{g1} \\ & + C_{p1}d_{g1} + d_{p2}C_{g2} + C_{p2}d_{g2}) ] \delta_{\ell}^n + P.T. \end{aligned}$$

$$\begin{aligned} \frac{\partial P_3}{\partial d_{e3}} = & [ \frac{1}{2}(d_{p0}d_{g2} + d_{p2}d_{g0} + d_{p3}d_{g1} + d_{p1}d_{g3}) + \frac{1}{4}(d_{p1}d_{g1} \\ & - C_{p1}C_{g1} + d_{p2}d_{g2} - C_{p2}C_{g2}) ] \delta_{\ell}^n + P.T. \end{aligned}$$

$$\begin{aligned} \frac{\partial P_4}{\partial d_{e6}} = & [ (d_{p0}C_{g2} + C_{p2}d_{g0}) + \frac{1}{2}(d_{p1}C_{g1} + C_{p1}d_{g1} + d_{p1}C_{g3} \\ & + C_{p3}d_{g1} - C_{p1}d_{g3} + d_{p3}C_{g1}) ] \delta_{\ell}^n + P.T. \end{aligned}$$

$$\frac{\partial P_2}{\partial C_{e1}} = \left[ \frac{1}{2} (d_{p0} d_{g1} + d_{p1} d_{g0} - d_{p0} d_{g3} - d_{p3} d_{g0}) + \frac{1}{4} (C_{p1} C_{g2} + C_{p2} C_{g1} + d_{p2} d_{g3} + C_{p2} C_{g3} + C_{p3} C_{g2}) \right] \delta_{\ell}^n + P.T.$$

$$\frac{\partial P_4}{\partial d_{e1}} = \left[ \frac{1}{2} (d_{p0} C_{g1} + C_{p1} d_{g0} + d_{p0} C_{g3} + C_{p3} d_{g0} + d_{p1} C_{g2} + C_{p2} d_{g1}) + \frac{1}{4} (d_{p2} C_{g3} + C_{p3} d_{g2} - C_{p2} d_{g3} - d_{p3} C_{g2}) \right] \delta_{\ell}^n + P.T.$$

$$\frac{\partial P_4}{\partial C_{e2}} = \left[ d_{p0} d_{g0} + \frac{1}{2} (d_{p1} d_{g1} + C_{p1} C_{g1} + C_{p3} C_{g3} + d_{p3} d_{g3}) + \frac{1}{4} (d_{p2} d_{g2} + 3 C_{p2} C_{g2} - d_{p1} d_{g3} - d_{p3} d_{g1} + C_{p1} C_{g3} + C_{p3} C_{g1}) \right] \delta_{\ell}^n + P.T.$$

$$\frac{\partial P_4}{\partial d_{e2}} = \frac{1}{4} [d_{p1} C_{g3} + C_{p3} d_{g1} + C_{p1} d_{g3} + d_{p3} C_{g1} + d_{p2} C_{g2} + C_{p2} d_{g2}] \delta_{\ell}^n + P.T.$$

$$\frac{\partial P_4}{\partial C_{e3}} = \left[ \frac{1}{2} (d_{p0} d_{g1} + d_{p1} d_{g0} + C_{p2} C_{g3} + C_{p3} C_{g2}) + \frac{1}{4} (d_{p1} d_{g2} + d_{p2} d_{g1} + C_{p1} C_{g2} + C_{p2} C_{g1}) \right] \delta_{\ell}^n + P.T.$$

$$\frac{\partial P_4}{\partial d_{e3}} = \left[ \frac{1}{2} (C_{p2} d_{g3} + d_{p3} C_{g2} - d_{p0} C_{g1} - C_{p1} d_{g0}) + \frac{1}{4} (C_{p1} d_{g2} + d_{p2} C_{g1} - d_{p1} C_{g2} - C_{p2} d_{g1}) \right] \delta_{\ell}^n + P.T.$$

$$\frac{\partial P_5}{\partial d_{e0}} = \left[ d_{p0} d_{g2} + d_{p2} d_{g0} + \frac{1}{2} (d_{p1} d_{g1} + d_{p1} d_{g3} + d_{p3} d_{g1} + C_{p1} C_{g3} + C_{p3} C_{g1} - C_{p1} C_{g1}) \right] \delta_{\ell}^n + P.T.$$

$$\frac{\partial P_5}{\partial C_{e1}} = \left[ \frac{1}{2} (d_{p0} C_{g3} + C_{p3} d_{g0} - d_{p0} C_{g1} - C_{p1} d_{g0} + C_{p1} d_{g2} + d_{p2} C_{g1}) \right. \\ \left. + \frac{1}{4} (C_{p2} d_{g3} + d_{p3} C_{g2} - d_{p2} C_{g3} - C_{p3} d_{g2}) \right] S_e^n + P. T.$$

$$\frac{\partial P_5}{\partial d_{e1}} = \left[ \frac{1}{2} (d_{p0} d_{g1} + C_{p1} d_{g0} + d_{p0} d_{g3} + d_{p3} d_{g0} + d_{p1} d_{g2} + d_{p2} d_{g1}) \right. \\ \left. + \frac{1}{4} (d_{p2} d_{g3} + d_{p3} d_{g2} + C_{p2} C_{g3} + C_{p3} C_{g2}) \right] S_e^n + P. T.$$

$$\frac{\partial P_5}{\partial C_{e2}} = \frac{1}{4} [d_{p1} C_{g3} + C_{p3} d_{g1} + C_{p1} d_{g3} + d_{p3} C_{g1} + C_{p2} d_{g2} + d_{p2} C_{g2}] S_e^n + P. T.$$

$$\frac{\partial P_5}{\partial d_{e2}} = [d_{p0} d_{g0} + \frac{1}{2} (d_{p1} d_{g1} + C_{p1} C_{g1} + d_{p3} d_{g3} + C_{p3} C_{g3}) + \frac{1}{4} (C_{p2} C_{g2} \\ + 3d_{p1} d_{g2} + d_{p1} d_{g3} + d_{p3} d_{g1} - C_{p1} C_{g3} - C_{p3} C_{g1})] S_e^n + P. T.$$

$$\frac{\partial P_5}{\partial C_{e3}} = \left[ \frac{1}{2} (d_{p0} C_{g1} + C_{p1} d_{g0} + d_{p2} C_{g3} + C_{p3} d_{g2}) + \frac{1}{4} (d_{p1} C_{g2} \right. \\ \left. + C_{p2} d_{g1} - C_{p1} d_{g2} - d_{p2} C_{g1}) \right] S_e^n + P. T.$$

$$\frac{\partial P_5}{\partial d_{e3}} = \left[ \frac{1}{2} (d_{p0} d_{g1} + d_{p1} d_{g0} + d_{p2} d_{g3} + d_{p3} d_{g2}) + \frac{1}{4} (d_{p1} d_{g2} \right. \\ \left. + d_{p2} d_{g1} + C_{p1} C_{g2} + C_{p2} C_{g1}) \right] S_e^n + P. T.$$

$$\frac{\partial P_5}{\partial d_{e0}} = [d_{p0} C_{g3} + C_{p3} d_{g0}] + \frac{1}{2} (d_{p1} C_{g2} + C_{p2} d_{g1} + C_{p1} d_{g2} \\ + d_{p2} C_{g1})] S_e^n + P. T.$$



$$\frac{\partial P_6}{\partial c_{e1}} = \left[ \frac{1}{2} (d_{p0} d_{g2} + d_{p2} d_{g0} + C_{p1} C_{g3} + C_{p3} C_{g1}) + \frac{1}{4} (d_{p1} d_{g1} - C_{p1} C_{g1} - d_{p2} d_{g2} + C_{p2} C_{g2}) \right] S_{\ell}^n + P. T.$$

$$\frac{\partial P_6}{\partial d_{e1}} = \left[ \frac{1}{2} (d_{g0} C_{p2} + C_{g2} d_{p0} + d_{p1} C_{g3} + C_{p3} d_{g1}) + \frac{1}{4} (d_{p1} C_{g1} + C_{p1} d_{g1} + C_{p2} d_{g2} + d_{p2} C_{g2}) \right] S_{\ell}^n + P. T.$$

$$\frac{\partial P_6}{\partial c_{e2}} = \left[ \frac{1}{2} (d_{p0} d_{g1} + d_{p1} d_{g0} + C_{p2} C_{g3} + C_{p3} C_{g2}) + \frac{1}{4} (d_{p1} d_{g2} + d_{p2} d_{g1} + C_{p2} C_{g1} + C_{p1} C_{g2}) \right] S_{\ell}^n + P. T.$$

$$\frac{\partial P_6}{\partial d_{e2}} = \left[ \frac{1}{2} (d_{p0} C_{g1} + C_{p1} d_{g0} + d_{p2} C_{g3} + C_{p3} d_{g2}) + \frac{1}{4} (d_{p1} C_{g2} + C_{p2} d_{g1} - d_{p2} C_{g1} - C_{p1} d_{g2}) \right] S_{\ell}^n + P. T.$$

$$\frac{\partial P_6}{\partial c_{e3}} = \left[ d_{p0} d_{g0} + \frac{1}{2} (C_{p1} C_{g1} + d_{p1} d_{g1} + C_{p2} C_{g2} + d_{p2} d_{g2}) + \frac{1}{4} (3 C_{p3} C_{g3} + d_{p3} d_{g3}) \right] S_{\ell}^n + P. T.$$

$$\frac{\partial P_6}{\partial d_{e3}} = \frac{1}{4} (d_{p3} C_{g3} + C_{p3} d_{g3}) S_{\ell}^n + P. T.$$

$$\frac{\partial P_7}{\partial d_{e0}} = \left[ (d_{p0} d_{g3} + d_{p3} d_{g0}) + \frac{1}{2} (d_{p1} d_{g2} + d_{p2} d_{g1} - C_{p1} C_{g2} - C_{p2} C_{g1}) \right] S_{\ell}^n + P. T.$$

$$\frac{\partial P_7}{\partial C_{e1}} = \left[ \frac{1}{2} (C_{p1} d_{g3} + d_{p3} C_{g1} - d_{p0} C_{g2} - C_{p2} d_{g0}) + \frac{1}{4} (C_{p2} d_{g2} + d_{p2} C_{g2} - C_{p1} d_{g1} - d_{p1} C_{g1}) \right] \delta_e^n + P.T.$$

$$\frac{\partial P_7}{\partial d_{e1}} = \left[ \frac{1}{2} (d_{p0} d_{g2} + d_{p2} d_{g0} + d_{p1} d_{g3} + d_{p3} d_{g1}) + \frac{1}{4} (d_{p1} d_{g1} - C_{p1} C_{g1} + d_{p2} d_{g2} - C_{p2} C_{g2}) \right] \delta_e^n + P.T.$$

$$\frac{\partial P_7}{\partial C_{e2}} = \left[ \frac{1}{2} (C_{p2} d_{g3} + d_{p3} C_{g2} - d_{p0} C_{g1} - C_{p1} d_{g0}) + \frac{1}{4} (C_{p1} d_{g2} + d_{p2} C_{g1} - C_{p2} d_{g1} - d_{p1} C_{g2}) \right] \delta_e^n + P.T.$$

$$\frac{\partial P_7}{\partial d_{e2}} = \left[ \frac{1}{2} (d_{p0} d_{g1} + d_{p1} d_{g0} + d_{p2} d_{g3} + d_{p3} d_{g2}) + \frac{1}{4} (d_{p2} d_{g1} + d_{p1} d_{g2} + C_{p1} C_{g2} + C_{p2} C_{g1}) \right] \delta_e^n + P.T. \quad (B.16)$$

$$\frac{\partial P_7}{\partial C_{e3}} = \frac{1}{4} (C_{p3} d_{g3} + d_{p3} C_{g3}) \delta_e^n + P.T.$$

$$\frac{\partial P_7}{\partial d_{e3}} = \left[ d_{p0} d_{g0} + \frac{1}{2} (d_{p1} d_{g1} + C_{p1} C_{g1} + d_{p2} d_{g2} + C_{p2} C_{g2}) + \frac{1}{4} (3d_{p3} d_{g3} + C_{p3} C_{g3}) \right] \delta_e^n + P.T.$$

APPENDIX C

HARMONIC BALANCE METHOD FOR FORCING-FLUTTER  
INTERACTION

As mentioned in Section 4.4, only the two most important responses, forcing response and flutter response, are considered. So, employing Eq. 4.23 in Eq. 4.13 and balancing terms with frequencies one and  $\omega_1$ , one obtains

$\sin \omega_1 t_1$

$$\begin{aligned}
 f_{m_1} = & \sum_{n=1}^N [-\bar{M}_{mn} \omega_1^2 + \lambda E_{mn} + K_{mn}] a_n - \sum_{n=1}^N (\omega_1 \bar{G}_{mn} + GB_{mn}) b_n \\
 & + \frac{1}{4} \sum_{n,p,g=1}^N C_{mnpq} \{3a_n a_p a_g + a_n b_p b_g + a_p b_n b_g + a_g b_n b_p \\
 & + 2 [a_n (c_p c_g + d_p d_g) + a_p (c_n c_g + d_n d_g) + a_g (c_n c_p + d_n d_p)]\} = 0
 \end{aligned} \tag{C.1}$$

$\cos \omega_1 t_1$  terms:

$$\begin{aligned}
 f_{m_2} = & \sum_{n=1}^N [(-\bar{M}_{mn} \omega_1^2 + \lambda E_{mn} + K_{mn}) b_n + (\omega_1 \bar{G}_{mn} + GB_{mn}) a_n \\
 & + \frac{1}{4} \sum_{n,p,g=1}^N C_{mnpq} \{3b_n b_p b_g + b_n a_p a_g + a_n b_p a_g + a_n a_p b_g \\
 & + 2 [b_n (c_p c_g + d_p d_g) + b_p (c_n c_g + d_n d_g) + b_g (c_n c_p + d_n d_p)]\} = 0
 \end{aligned} \tag{C.2}$$

sin  $t_1$  terms:

$$\begin{aligned}
 f_{m3} = & \sum_{n=1}^N [(-\bar{M}_{mn} + \lambda E_{mn} + K_{mn}) C_n - (\bar{G}_{mn} + G B_{mn}) d_n \\
 & + \frac{1}{4} \sum_{n,p,q=1}^N C_{mnpq} \{ 3 C_n C_p C_q + C_n d_p d_q + d_n C_p d_q + d_n d_p C_q \\
 & + 2 [ C_n (a_p a_q + b_p b_q) + C_p (a_n a_q + b_n b_q) + C_q (a_n a_p + b_n b_p) ] \} = 0
 \end{aligned} \quad (C.3)$$

cos  $t_1$  terms:

$$\begin{aligned}
 f_{m4} = & \sum_{n=1}^N [(-\bar{M}_{mn} + \lambda E_{mn} + K_{mn}) d_n + (\bar{G}_{mn} + G B_{mn}) C_n \\
 & + \frac{1}{4} \sum_{n,p,q=1}^N C_{mnpq} \{ 3 d_n d_p d_q + d_n C_p C_q + C_n d_p C_q + C_n C_p d_q \\
 & + 2 [ d_n (a_p a_q + b_p b_q) + d_p (a_n a_q + b_n b_q) + d_q (a_n a_p \\
 & + b_n b_p) ] \} - F_m = 0
 \end{aligned} \quad (C.4)$$

Let

$$\tilde{f}(\tilde{x}) = \begin{pmatrix} f_{11} \\ f_{12} \\ f_{13} \\ f_{14} \\ f_{21} \\ \vdots \\ f_{Na} \end{pmatrix} = 0 \quad (C.5)$$

and the unknown vector  $x = (\lambda, w, c_1, d_1, a_2, b_2, c_2, d_2, \dots, d_N)$ , then the Jacobian of Eq. C.5 is

$$J_{ma,1} = \sum_{n=1}^N [ E_{mn} a_n - \frac{1}{2} \omega_i \lambda^{-1/2} \tilde{G}_{mn} b_n ]$$

$$J_{ma,2} = \sum_{n=1}^N [ -2 \bar{M}_{mn} \omega_i a_n - \bar{G}_{mn} b_n ]$$

$$J_{ma,ea} = -\omega_i^2 \bar{M}_{me} + \lambda E_{me} + K_{me} + \frac{1}{4} \sum_{n,p,g=1}^N C_{mnpq} \{ [3a_p a_g + b_p b_g + 2c_p c_g + 2d_p d_g] \delta_e^n + [3a_n a_g + b_n b_g + 2c_n c_g + 2d_n d_g] \delta_e^p + [3a_n a_p + b_n b_p + 2c_n c_p + 2d_n d_p] \delta_e^g \}$$

$$J_{ma,eb} = -\omega_i \bar{G}_{me} - G_{me} + \frac{1}{4} \sum_{n,p,g=1}^N C_{mnpq} \{ (a_p b_g + a_g b_p) \delta_e^n + (a_n b_g + a_g b_n) \delta_e^p + (a_n b_p + a_p b_n) \delta_e^g \}$$

$$J_{ma,ec} = \frac{1}{2} \sum_{n,p,g=1}^N C_{mnpq} \{ (a_p c_g + a_g c_p) \delta_e^n + (a_n c_g + a_g c_n) \delta_e^p + (a_n c_p + a_p c_n) \delta_e^g \}$$

$$J_{ma,ed} = \frac{1}{2} \sum_{n,p,g=1}^N C_{mnpq} \{ (a_p d_g + a_g d_p) \delta_e^n + (a_n d_g + a_g d_n) \delta_e^p + (a_n d_p + a_p d_n) \delta_e^g \}$$

$$J_{mb,1} = \sum_{n=1}^N [E_{mn} b_n + \frac{1}{2} \omega_i \lambda^{-1/2} \bar{G}_{mn} a_n]$$

$$J_{mb,2} = \sum_{n=1}^N [-2\omega_i \bar{M}_{mn} b_n + \bar{G}_{mn} a_n]$$

$$J_{mb,ea} = \omega_i \bar{G}_{mn} + G_{mn} + \frac{1}{4} \sum_{n,p,g=1}^N C_{mnpq} \{ (a_p b_g + a_g b_p) \delta_e^n + (a_n b_g + a_g b_n) \delta_e^p + (a_n b_p + a_p b_n) \delta_e^g \}$$

$$\begin{aligned}
 J_{mb,lb} &= [-\omega_i^2 \bar{M}_{me} + \lambda E_{me} + K_{me}] + \frac{1}{4} \sum_{n,p,g=1}^N C_{mnpq} \{ (3b_p b_g \\
 &+ a_p a_g + 2c_p c_g + 2d_p d_g) \delta_e^n + (3b_n b_g + a_n a_g + 2c_n c_g \\
 &+ 2d_n d_g) \delta_e^p + (3b_n b_p + a_n a_p + 2c_n c_p + 2d_n d_p) \delta_e^g \} \\
 J_{mb,lc} &= \frac{1}{2} \sum_{n,p,g=1}^N C_{mnpq} \{ (b_p c_g + b_g c_p) \delta_e^n + (b_n c_g + b_g c_n) \delta_e^p \\
 &+ (b_n c_p + b_p c_n) \delta_e^g \} \\
 J_{mb,ld} &= \frac{1}{2} \sum_{n,p,g=1}^N C_{mnpq} \{ (b_p d_g + b_g d_p) \delta_e^n + (b_n d_g + b_g d_n) \delta_e^p \\
 &+ (b_n d_p + b_p d_n) \delta_e^g \}
 \end{aligned}$$

$$J_{mc,1} = 0$$

$$J_{mc,2} = 0$$

$$\begin{aligned}
 J_{mc,la} &= \frac{1}{2} \sum_{n,p,g=1}^N C_{mnpq} \{ (a_p c_g + a_g c_p) \delta_e^n + (a_n c_g + a_g c_n) \delta_e^p \\
 &+ (a_n c_p + a_p c_n) \delta_e^g \}
 \end{aligned}$$

$$\begin{aligned}
 J_{mc,lb} &= \frac{1}{2} \sum_{n,p,g=1}^N C_{mnpq} \{ (b_p c_g + b_g c_p) \delta_e^n + (b_n c_g + b_g c_n) \delta_e^p \\
 &+ (b_n c_p + b_p c_n) \delta_e^g \}
 \end{aligned}$$

$$J_{mc,ec} = -\bar{M}_{me} + \lambda F_{me} + K_{me} + \frac{1}{4} \sum_{n,p,g=1}^N C_{mnpq} \{ (3C_p C_g + d_p d_g + 2a_p a_g + 2b_p b_g) \delta_e^n + (3C_n C_g + d_n d_g + 2a_n a_g + 2b_n b_g) \delta_e^p + (3C_n C_p + d_n d_p + 2a_n a_p + 2b_n b_p) \delta_e^g \}$$

$$J_{mc,ed} = -\bar{G}_{me} - G_{Bme} + \frac{1}{4} \sum_{n,p,g=1}^N C_{mnpq} \{ (C_p d_g + C_g d_p) \delta_e^n + (C_n d_g + C_g d_n) \delta_e^p + (C_n d_p + C_p d_n) \delta_e^g \}$$

$$J_{md,1} = 0$$

$$J_{md,2} = 0$$

$$J_{md,ea} = \frac{1}{2} \sum_{n,p,g=1}^N C_{mnpq} [ (a_p d_g + a_g d_p) \delta_e^n + (a_n d_g + a_g d_n) \delta_e^p + (a_n d_p + a_p d_n) \delta_e^g ]$$

$$J_{md,eb} = \frac{1}{2} \sum_{n,p,g=1}^N C_{mnpq} [ (b_p d_g + b_g d_p) \delta_e^n + (b_n d_g + b_g d_n) \delta_e^p + (b_n d_p + b_p d_n) \delta_e^g ]$$

$$J_{md,ec} = \bar{G}_{me} + G_{Bme} + \frac{1}{4} \sum_{n,p,g=1}^N C_{mnpq} \{ (C_p d_g + C_g d_p) \delta_e^n + (C_n d_g + C_g d_n) \delta_e^p + (C_n d_p + C_p d_n) \delta_e^g \}$$

$$\begin{aligned}
 J_{md,ed} = & -\bar{M}_{me} + \lambda E_{me} + K_{me} + \frac{1}{4} \sum_{n,p,q=1}^N C_{mnpq} \{ (3d_p d_q + C_p C_q \\
 & + 2a_p a_q + 2b_p b_q) S_e^n + (3d_n d_q + C_n C_q + 2a_n a_q + 2b_n b_q) S_e^p \\
 & + (3d_n d_p + C_n C_p + 2a_n a_p + 2b_n b_p) S_e^q \}
 \end{aligned}$$

where

$$m_a = 4x(m-1) + 1$$

$$m_b = m_a + 1$$

$$m_c = m_a + 2$$

$$m_d = m_a + 3$$

$$\text{for } m = 1, 2, \dots, N$$

$$l_a = 4x(l-1) + 1$$

$$l_b = l_a + 1$$

$$l_c = 4x(l-1) + 3$$

$$l_d = l_c + 1$$

$$\text{for } l = 2, 3, \dots, N$$

$$\text{for } l = 1, 2, \dots, N$$



TABLE 1  
 EFFECTS OF APPLIED MEMBRANE FORCE  $R_y$  ON PANEL FLUTTER\*

| $R_y = 0$ |       | $R_y = -2\pi^2$ |       |
|-----------|-------|-----------------|-------|
| $\lambda$ | Amp.  | $\lambda$       | Amp.  |
| 900.9     | .061  | 898.7           | .061  |
| 924.3     | .303  | 922.2           | .303  |
| 995.7     | .600  | 993.4           | .600  |
| 1110.5    | .891  | 1108.1          | .891  |
| 1267.9    | 1.177 | 1265.3          | 1.177 |

---

\*This table is for the three-dimensional, clamped-clamped plate with  $a/b = 1$ ,  $R_x = 0$ ,  $\mu/M = .1$ ,  $g_s = 0$ ,  $g_b = 0$ .

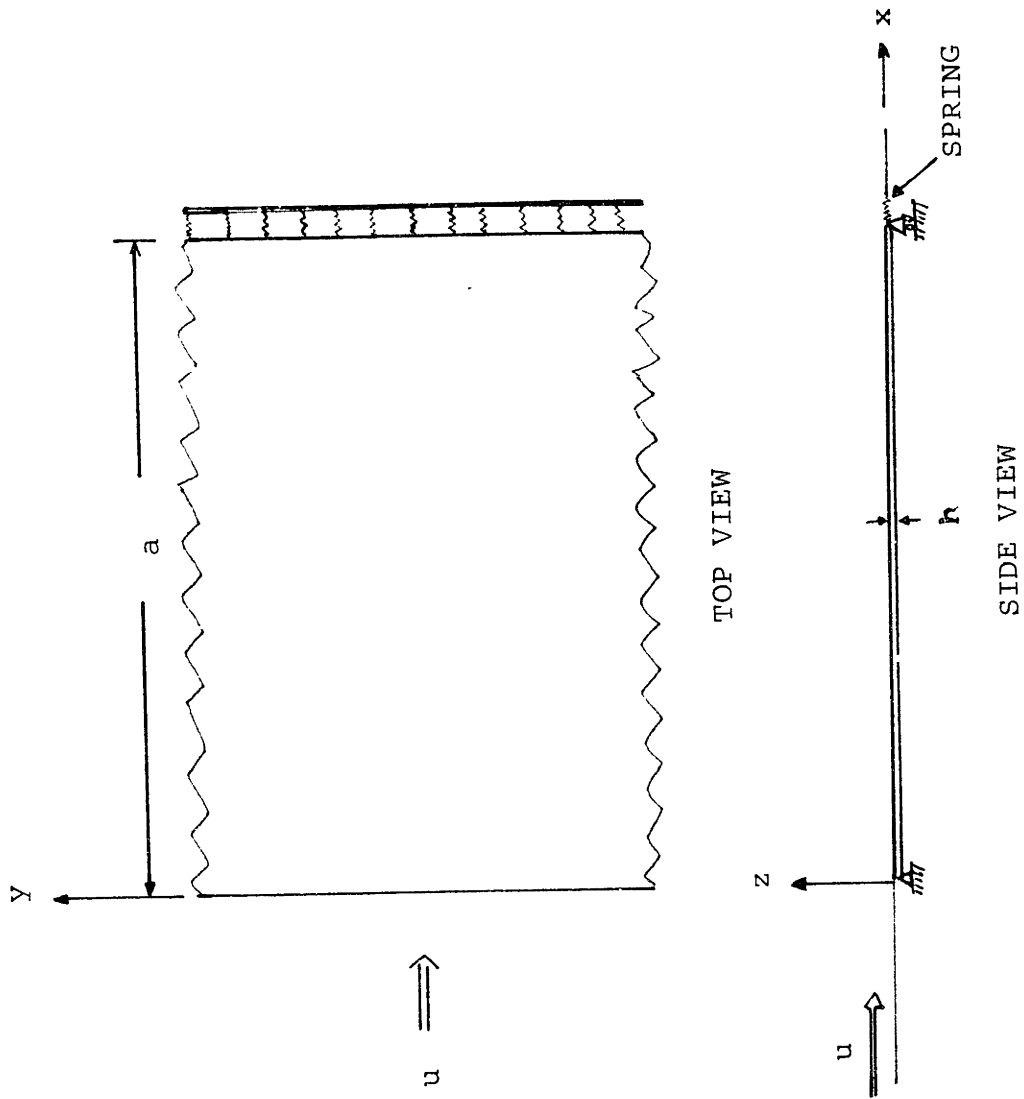


FIG. 1 TWO-DIMENSIONAL PANEL CONFIGURATION FOR A SIMPLY-SUPPORTED PLATE

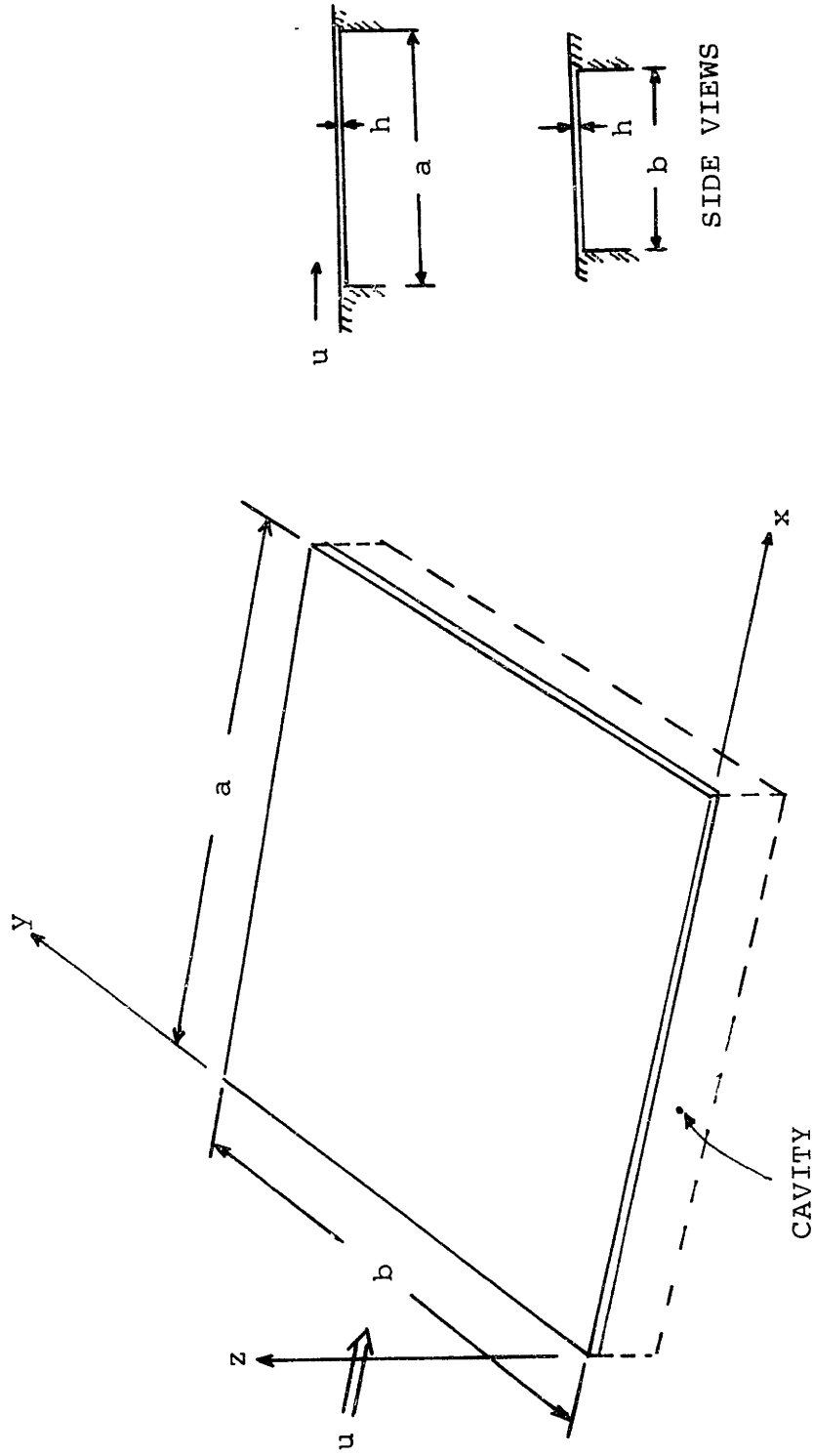


FIG. 2 THREE-DIMENSIONAL PANEL CONFIGURATION WITH CLAMPED EDGES

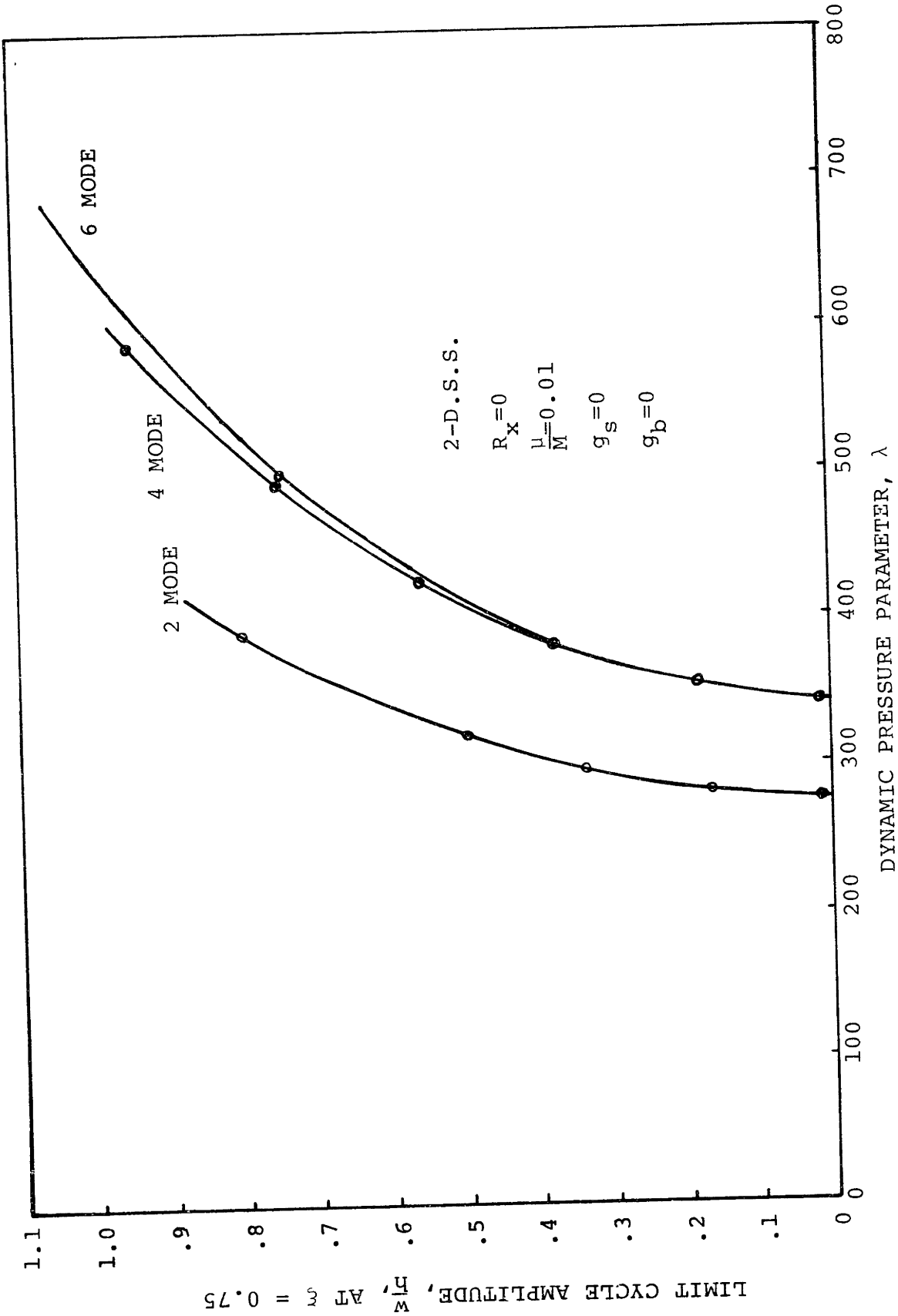


FIG. 3 CONVERGENCE OF HARMONIC BALANCE SOLUTIONS FOR A TWO-DIMENSIONAL SIMPLY-SUPPORTED FLAT PLATE

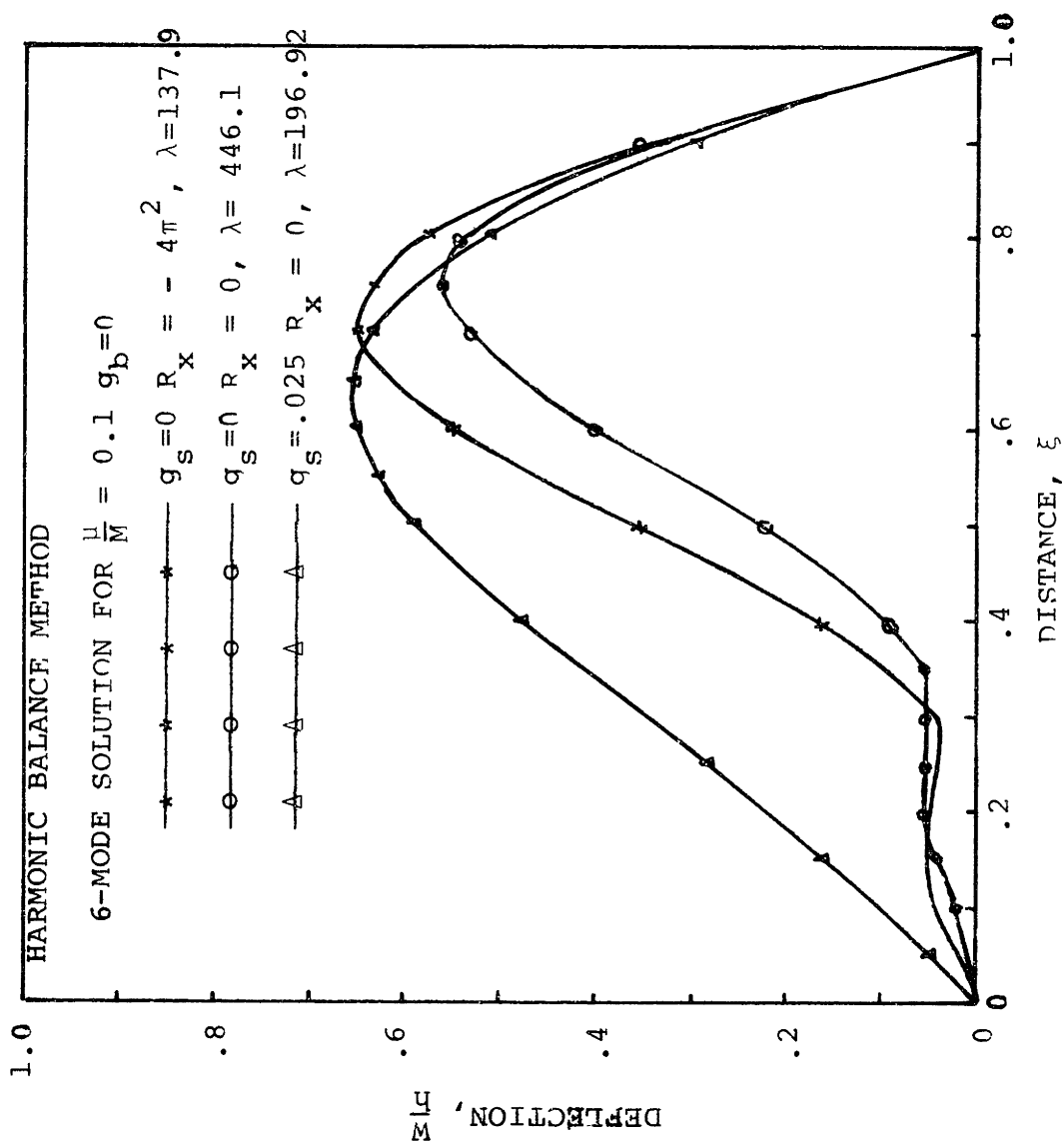


FIG. 4 COMPARISON OF LIMIT-CYCLE DEFLECTION VS. DISTANCE FOR A

TWO-DIMENSIONAL SIMPLY-SUPPORTED FLAT PLATE

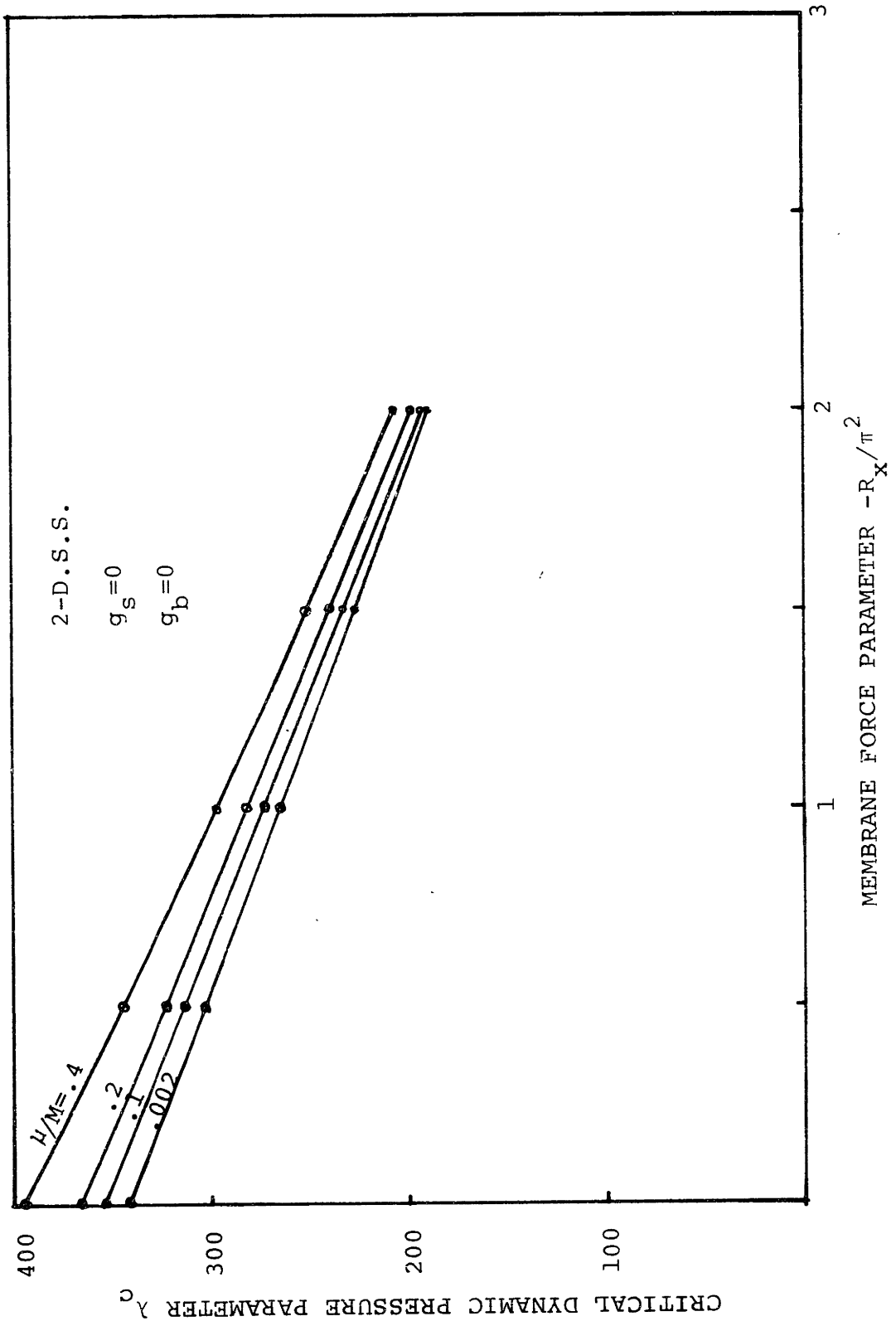


FIG. 5 EFFECT OF MEMBRANE FORCE  $R_x$  AND MASS RATIO  $\mu/M$  ON THE CRITICAL DYNAMIC PRESSURE  $\lambda_c$  FOR TWO-DIMENSIONAL SIMPLY-SUPPORTED PLATES

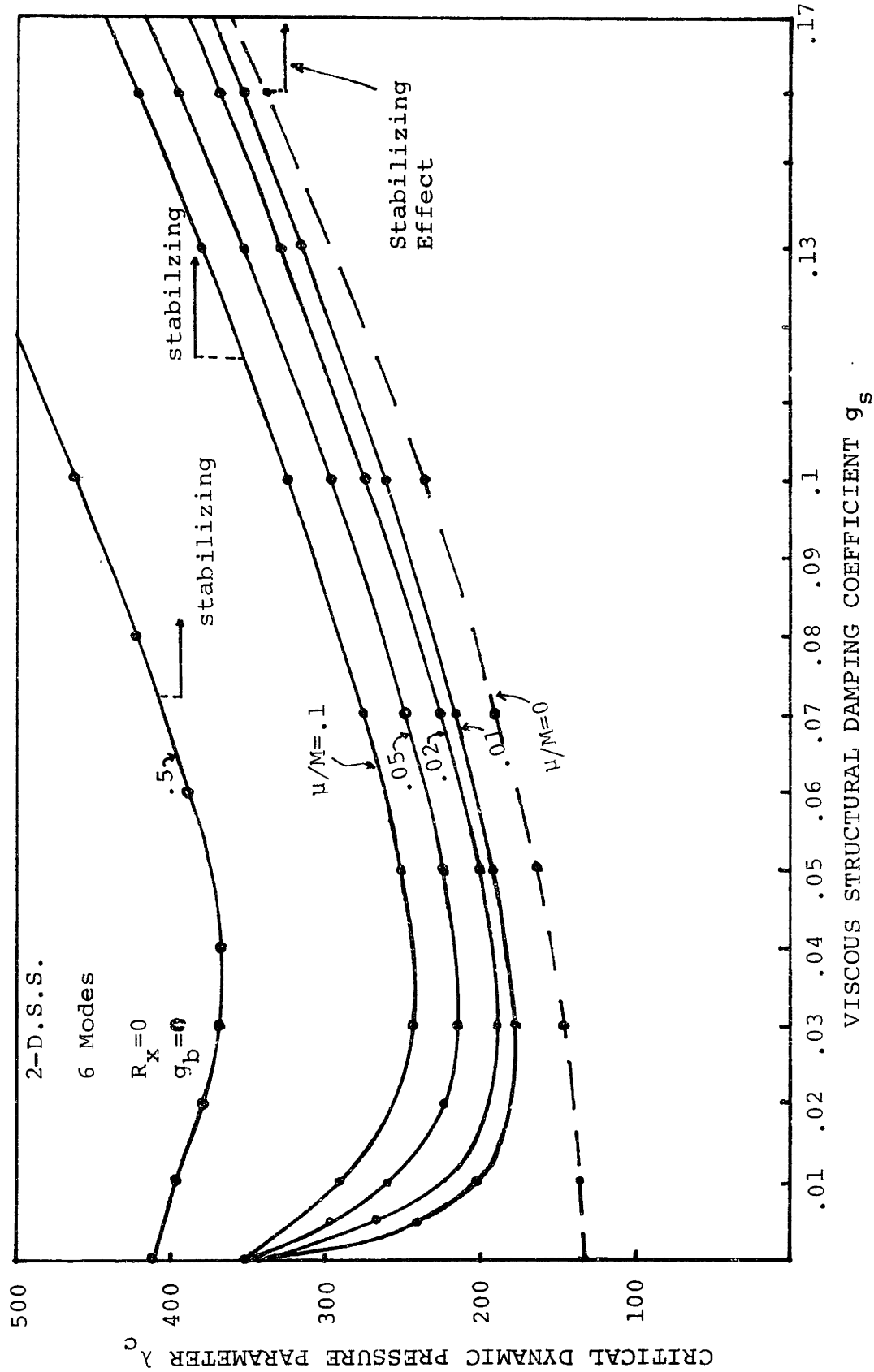


FIG. 6 EFFECT OF THE VISCOUS TYPE STRUCTURAL DAMPING  $g_s$  ON THE CRITICAL DYNAMIC PRESSURE  $\lambda_c$  OF TWO-DIMENSIONAL SIMPLY-SUPPORTED PLATES

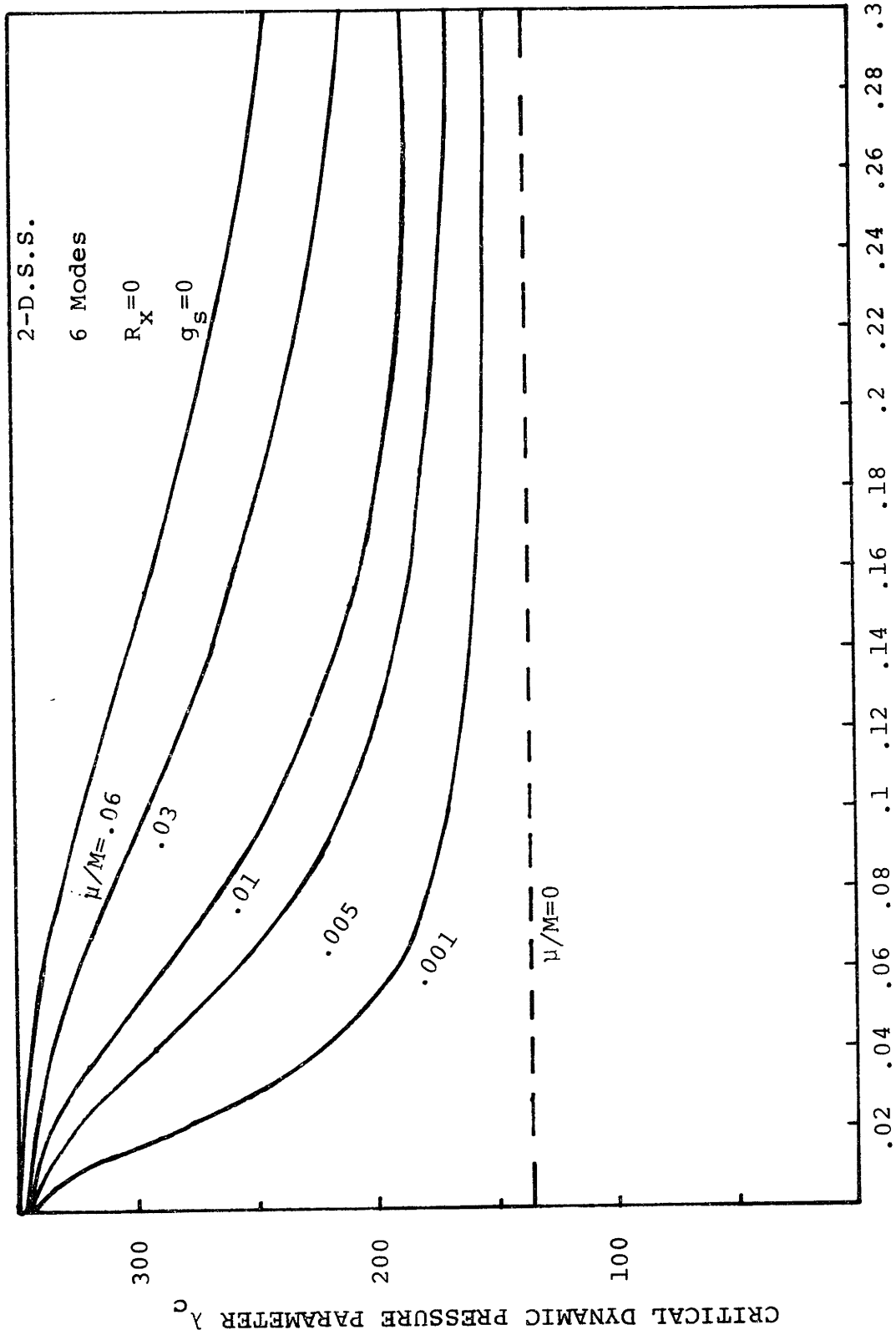


FIG. 7 EFFECT OF THE HYSTERETIC TYPE STRUCTURAL DAMPING  $g_s$  ON THE CRITICAL DYNAMIC PRESSURE  $\lambda_c$  FOR TWO-DIMENSIONAL SIMPLY-SUPPORTED PANELS



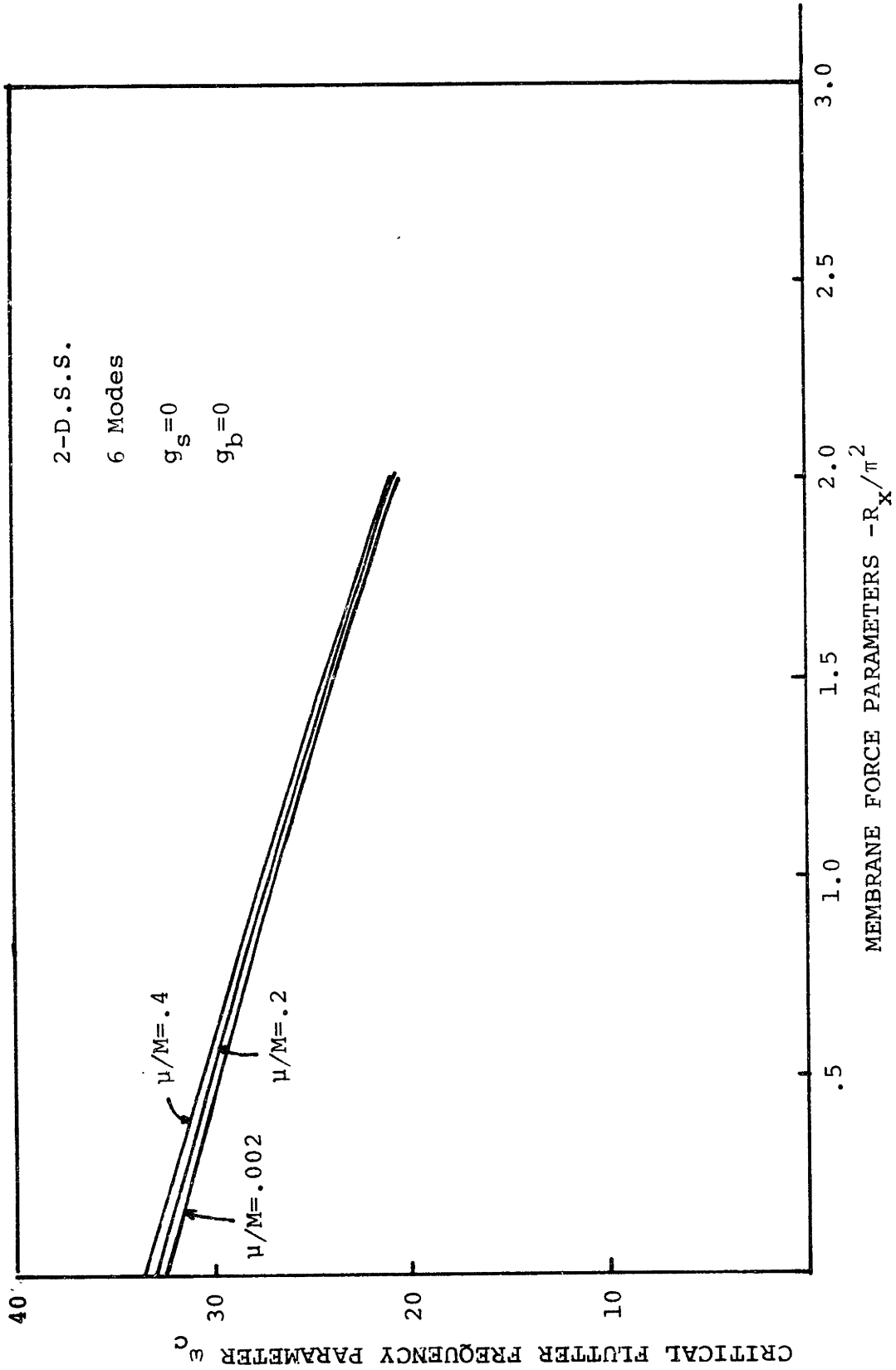


FIG. 8 EFFECT OF THE MEMBRANE FORCE  $R_x$  AND MASS RATIO  $\mu/M$  ON THE CRITICAL FLUTTER FREQUENCY  $\omega_c$  FOR TWO-DIMENSIONAL SIMPLY-SUPPORTED PLATES

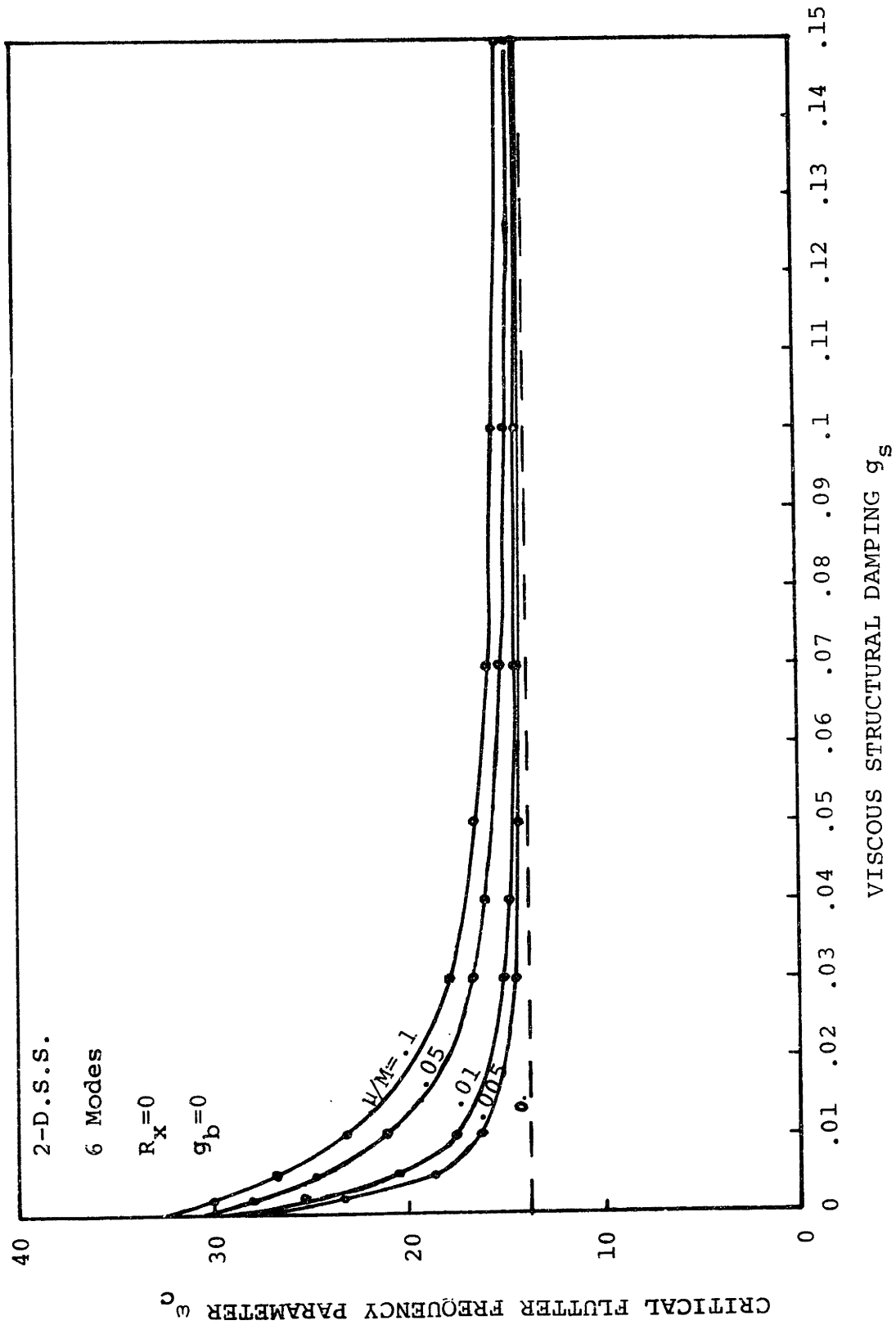


FIG. 9 EFFECT OF THE VISCOUS TYPE STRUCTURAL DAMPING  $g_s$  ON THE CRITICAL FLUTTER FREQUENCY  $\omega_c$  FOR TWO-DIMENSIONAL SIMPLY-SUPPORTED PLATES AT DIFFERENT VALUES OF  $\mu/M$

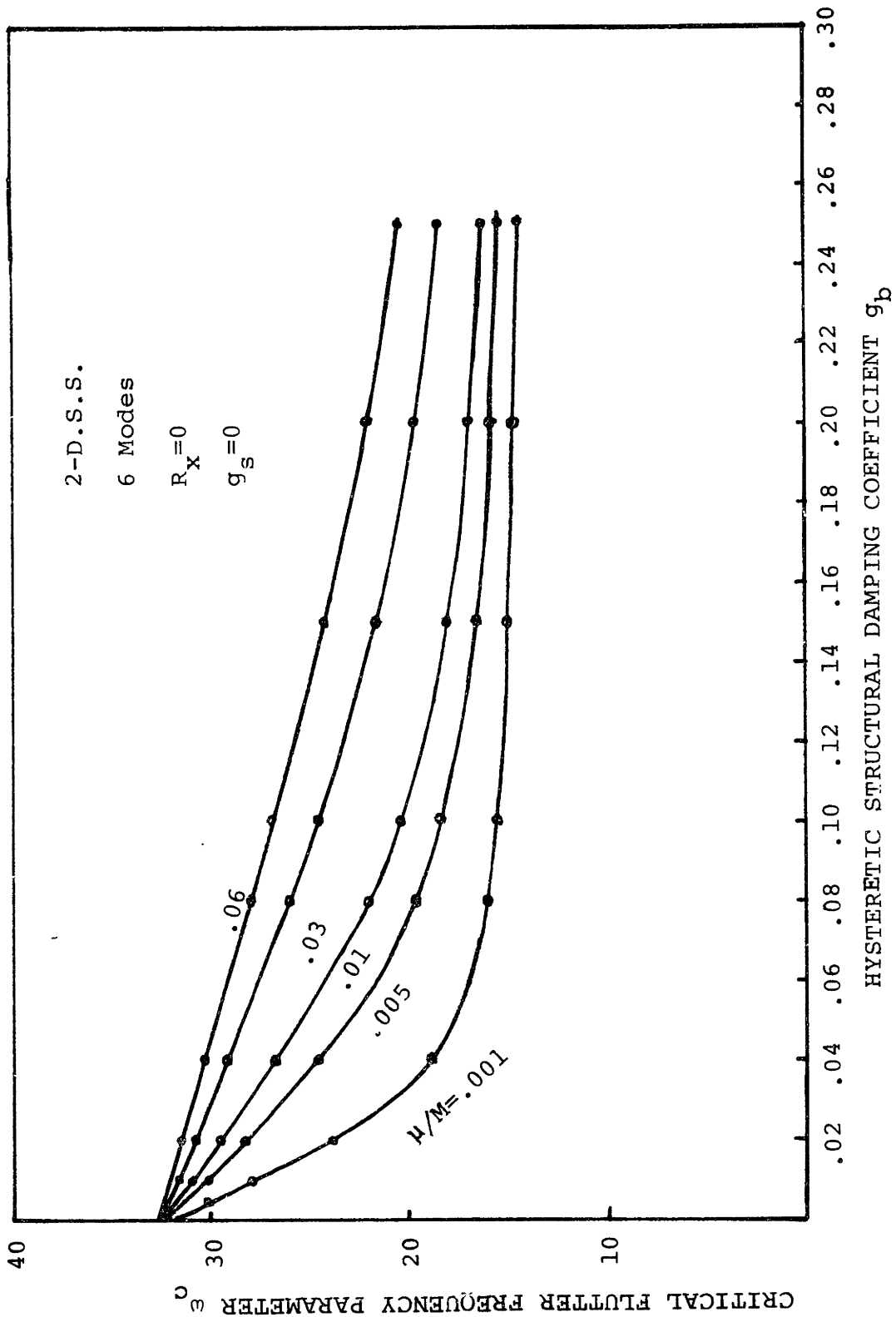


FIG. 10 EFFECT OF THE HYSTERETIC TYPE STRUCTURAL DAMPING  $g_b$  ON THE CRITICAL FLUTTER FREQUENCY  $\omega_c$  FOR TWO-DIMENSIONAL SIMPLY-SUPPORTED PLATES AT DIFFERENT VALUES OF  $\mu/M$

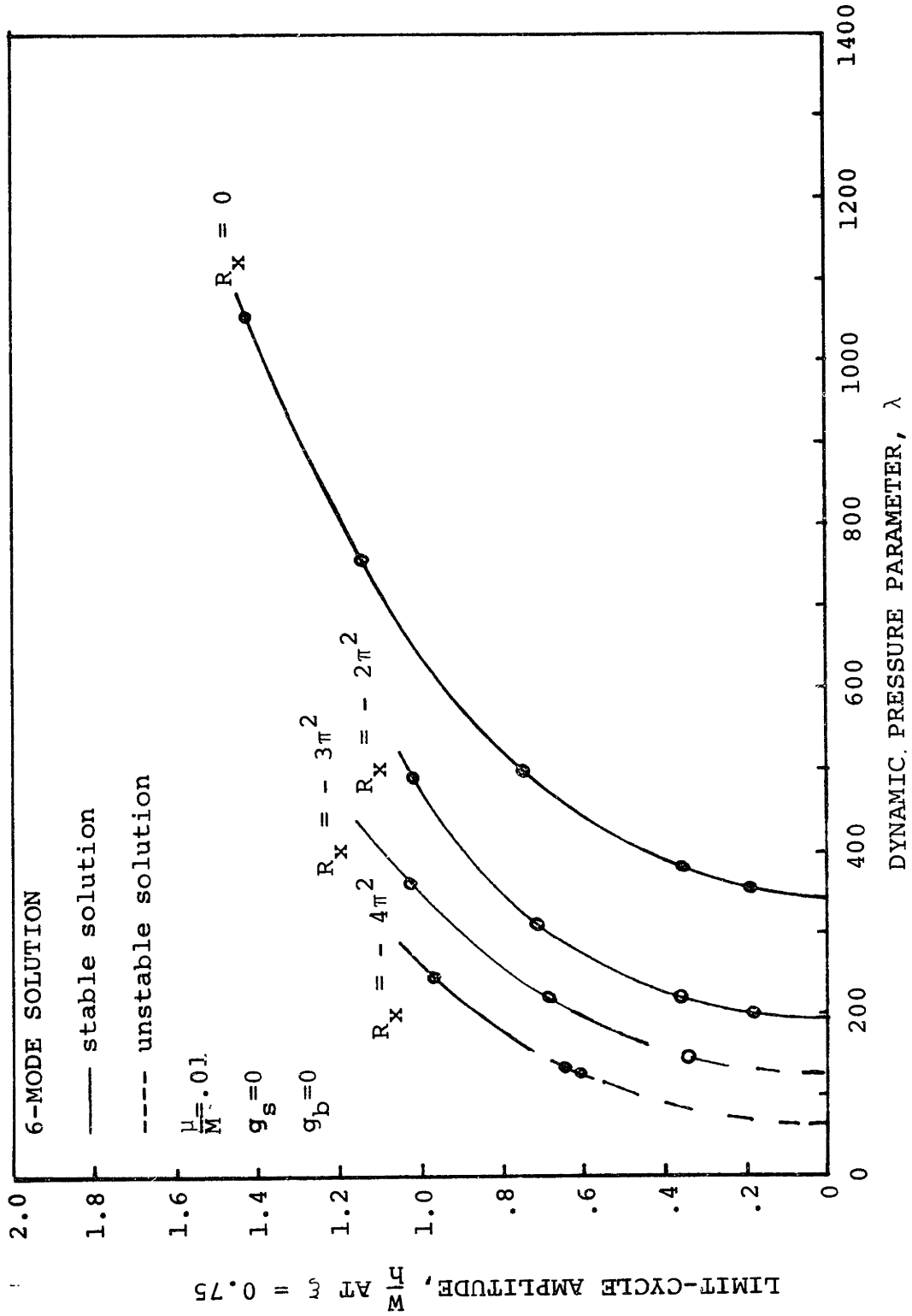


FIG. 11 EFFECT OF APPLIED MEMBRANE FORCE  $R_x$  ON THE LIMIT-CYCLE AMPLITUDES OF TWO-DIMENSIONAL SIMPLY-SUPPORTED FLAT PLATES

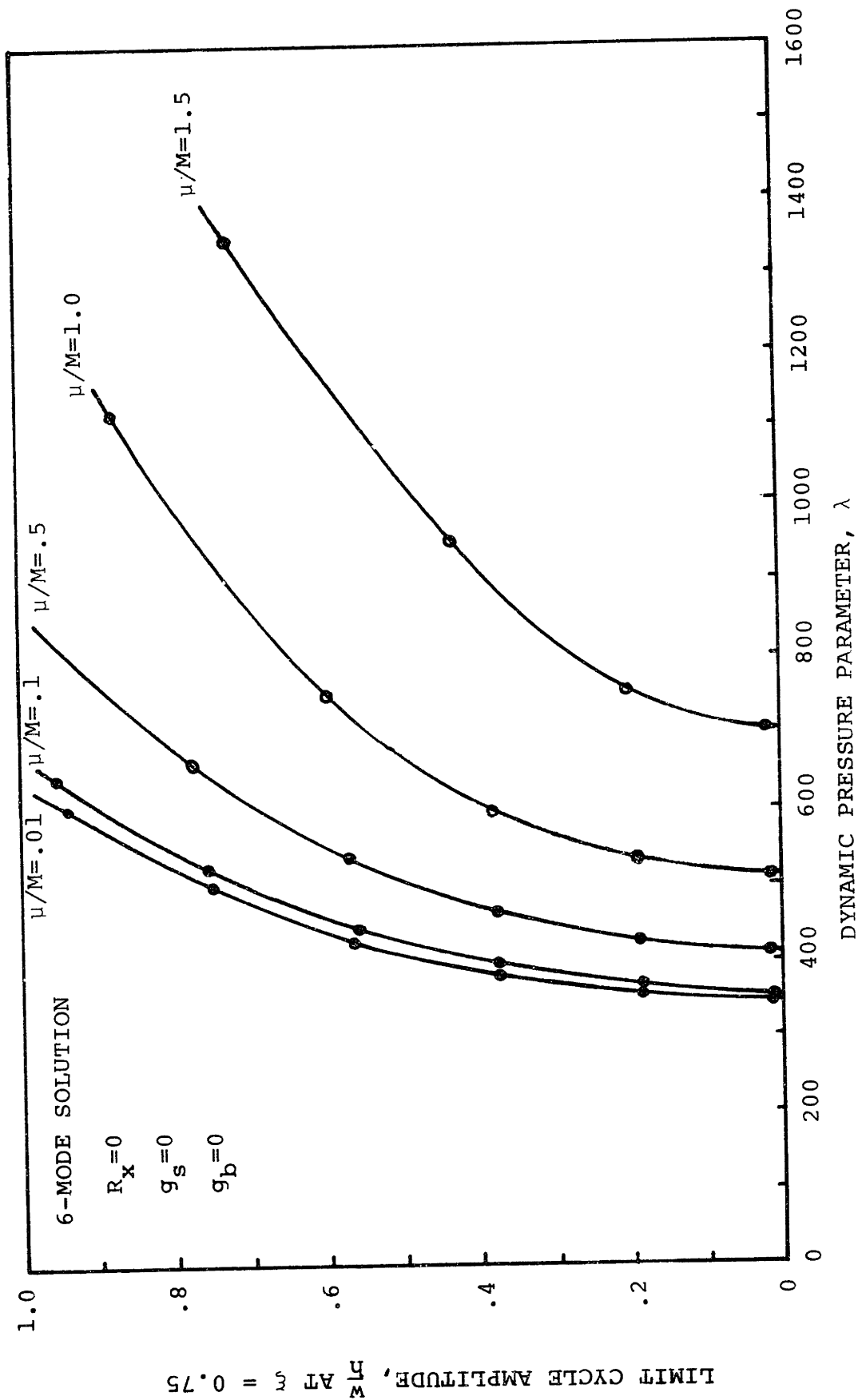


FIG. 12 EFFECT OF MASS RATIO  $\mu/M$  ON THE LIMIT-CYCLE AMPLITUDES OF TWO-DIMENSIONAL SIMPLY-SUPPORTED FLAT PLATES

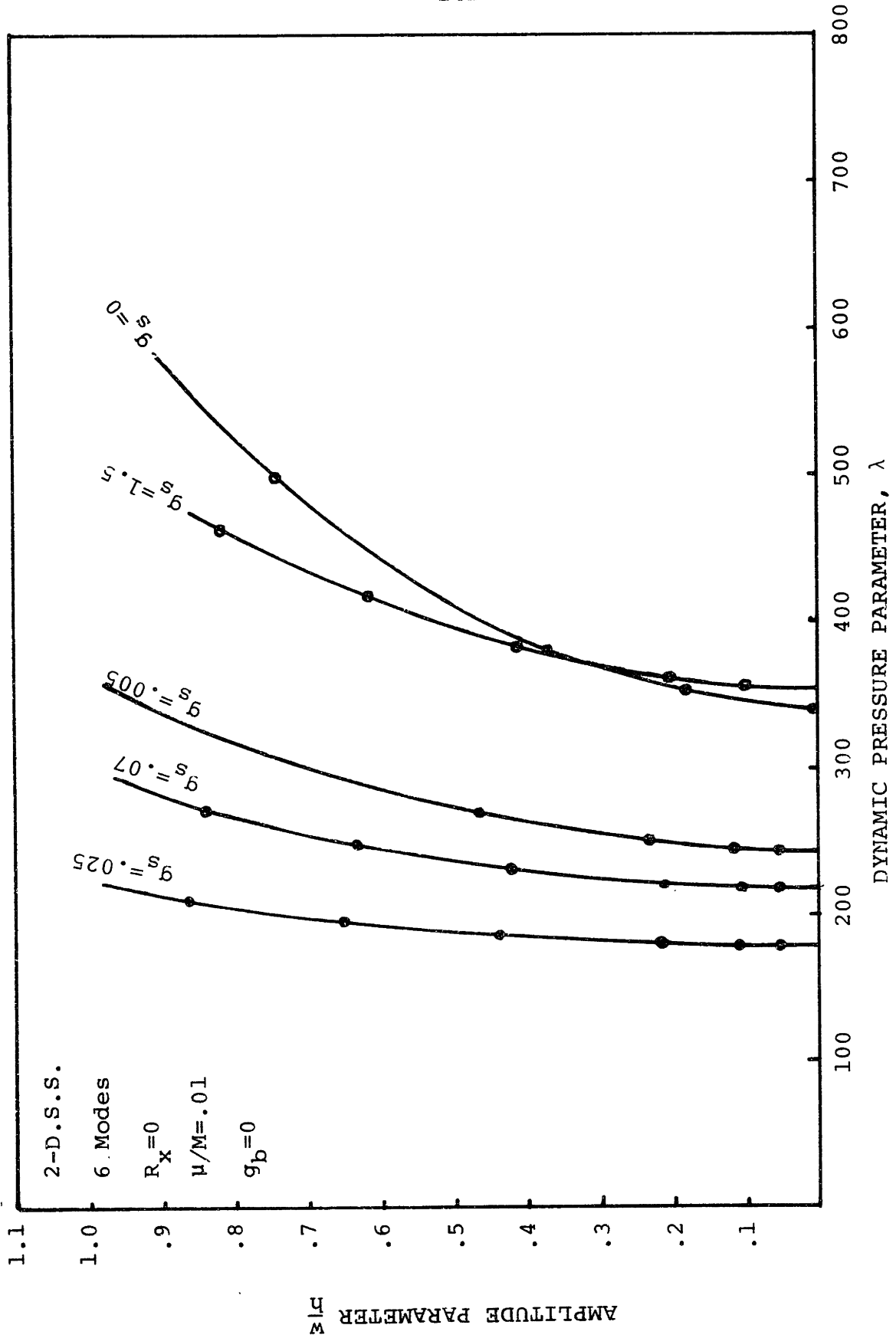


FIG. 13 EFFECT OF VISCOUS STRUCTURAL DAMPING ON THE LIMIT-CYCLE AMPLITUDES OF TWO-DIMENSIONAL SIMPLY-SUPPORTED PLATES

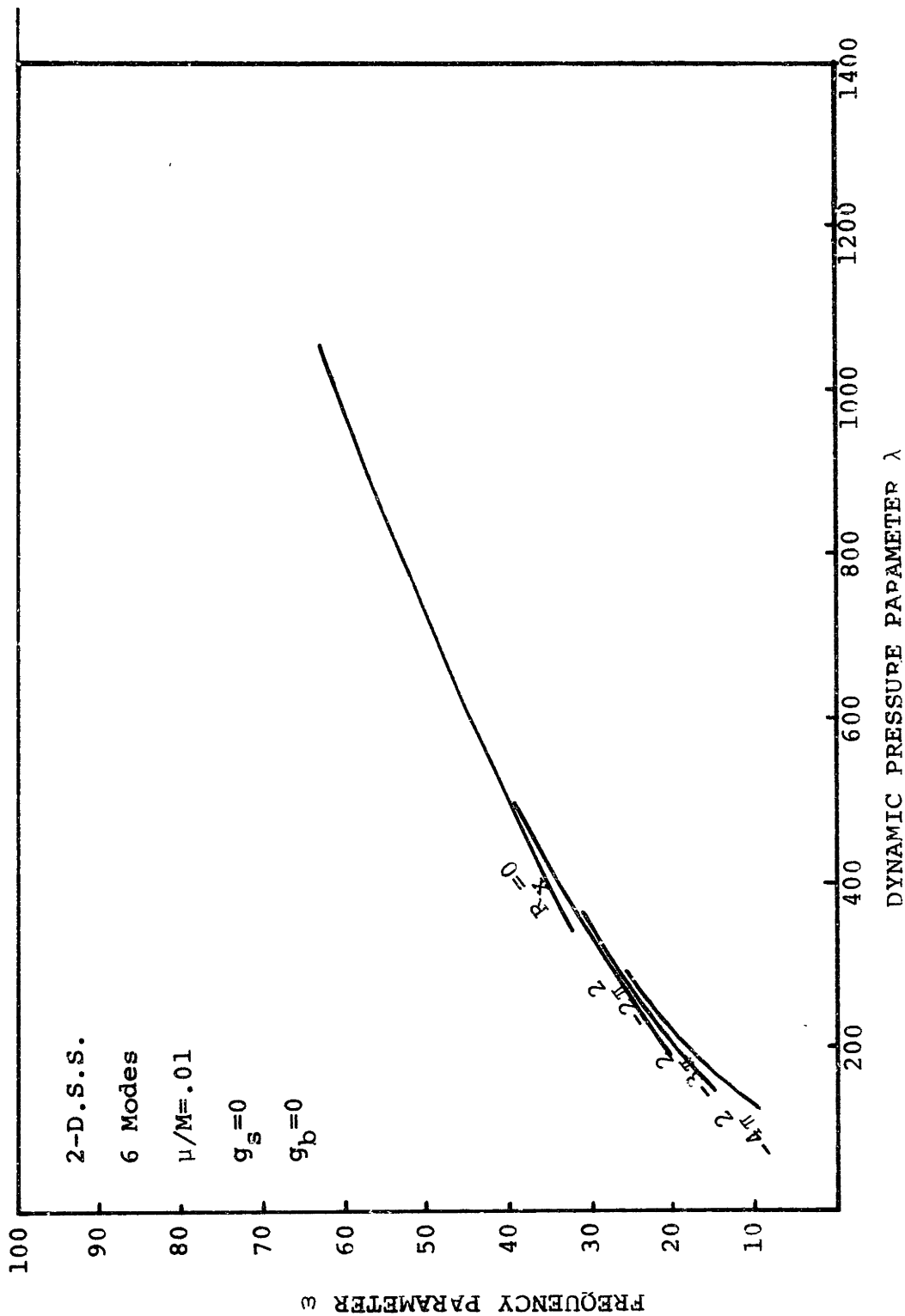


FIG. 14 VARIATION OF FLUTTER FREQUENCY  $\omega$  WITH DYNAMIC PRESSURE  $\lambda$  AT DIFFERENT VALUES OF MEMBRANE FORCE  $R_x$  FOR A TWO-DIMENSIONAL SIMPLY-SUPPORTED PLATE

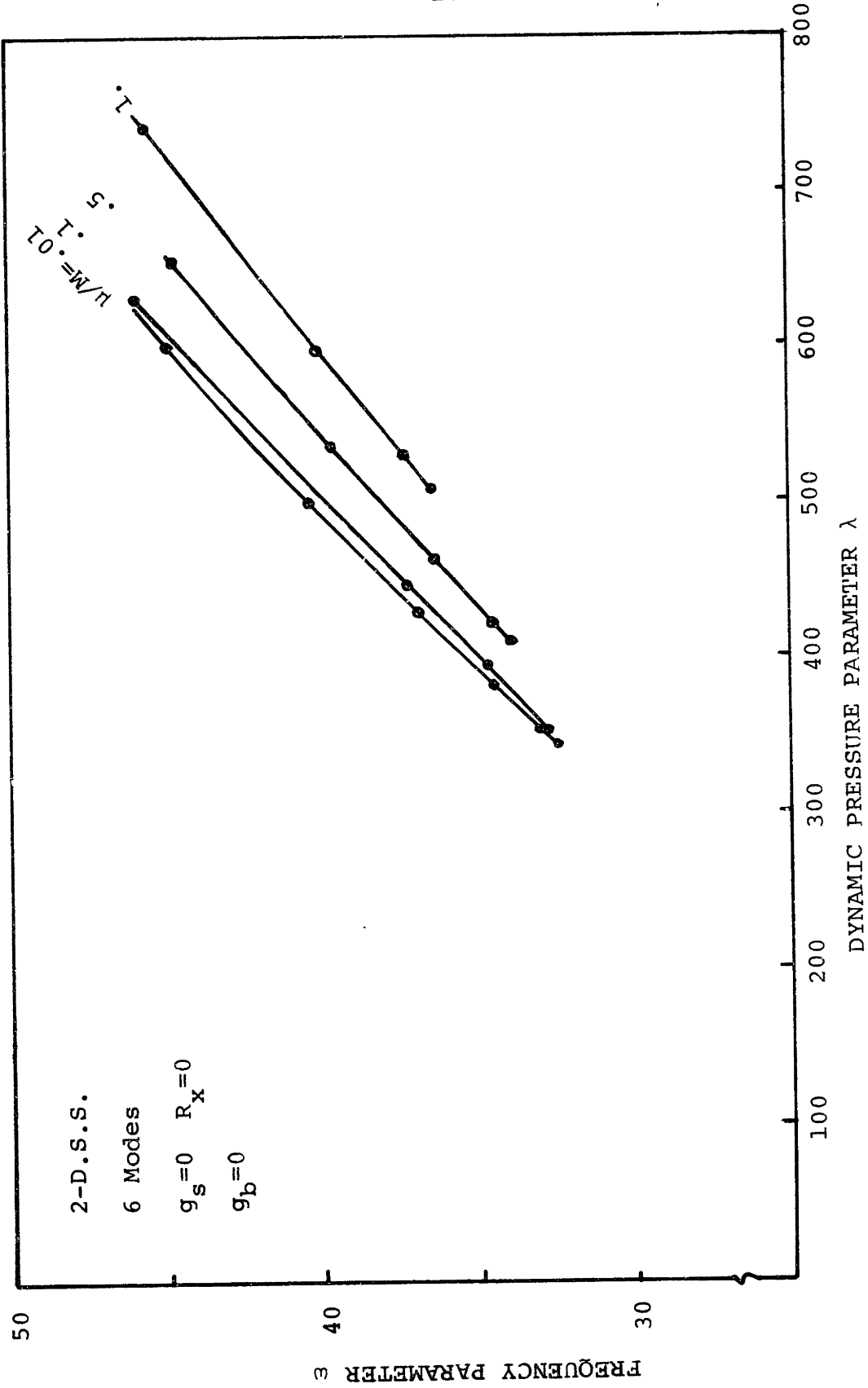


FIG. 15 VARIATION OF FLUTTER FREQUENCY  $\omega$  WITH DYNAMIC PRESSURE  $\lambda$  AT DIFFERENT VALUES OF  $\mu/M$  FOR A TWO-DIMENSIONAL SIMPLY-SUPPORTED PLATE



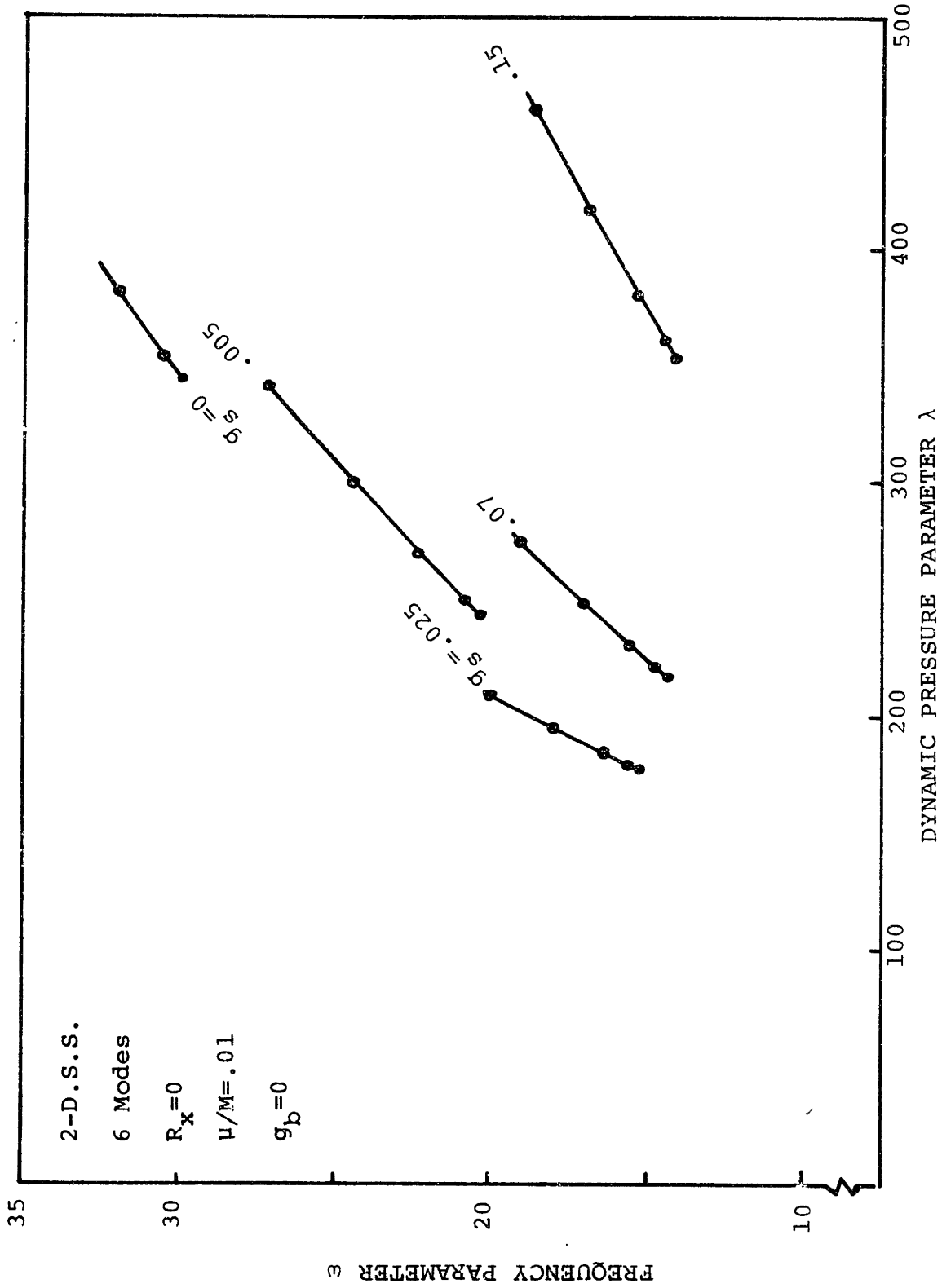


FIG. 16 VARIATION OF FLUTTER FREQUENCY  $\omega$  WITH DYNAMIC PRESSURE  $\lambda$  AT DIFFERENT VALUES OF  $\mu/M$  FOR A TWO-DIMENSIONAL SIMPLY-SUPPORTED PLATE

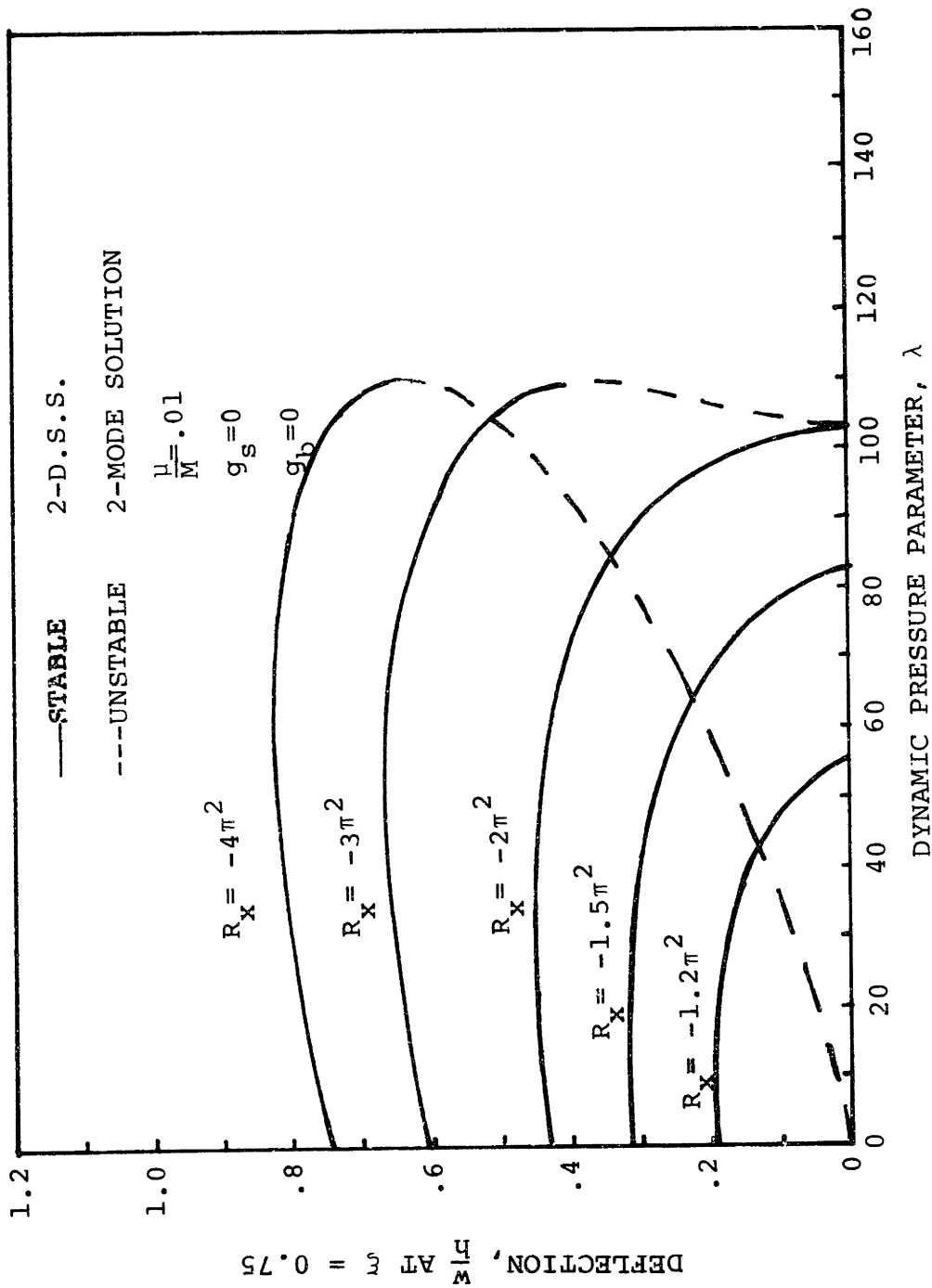


FIG. 17 STATIC BUCKLING SOLUTIONS FOR TWO-DIMENSIONAL SIMPLY-SUPPORTED FLAT PLATES

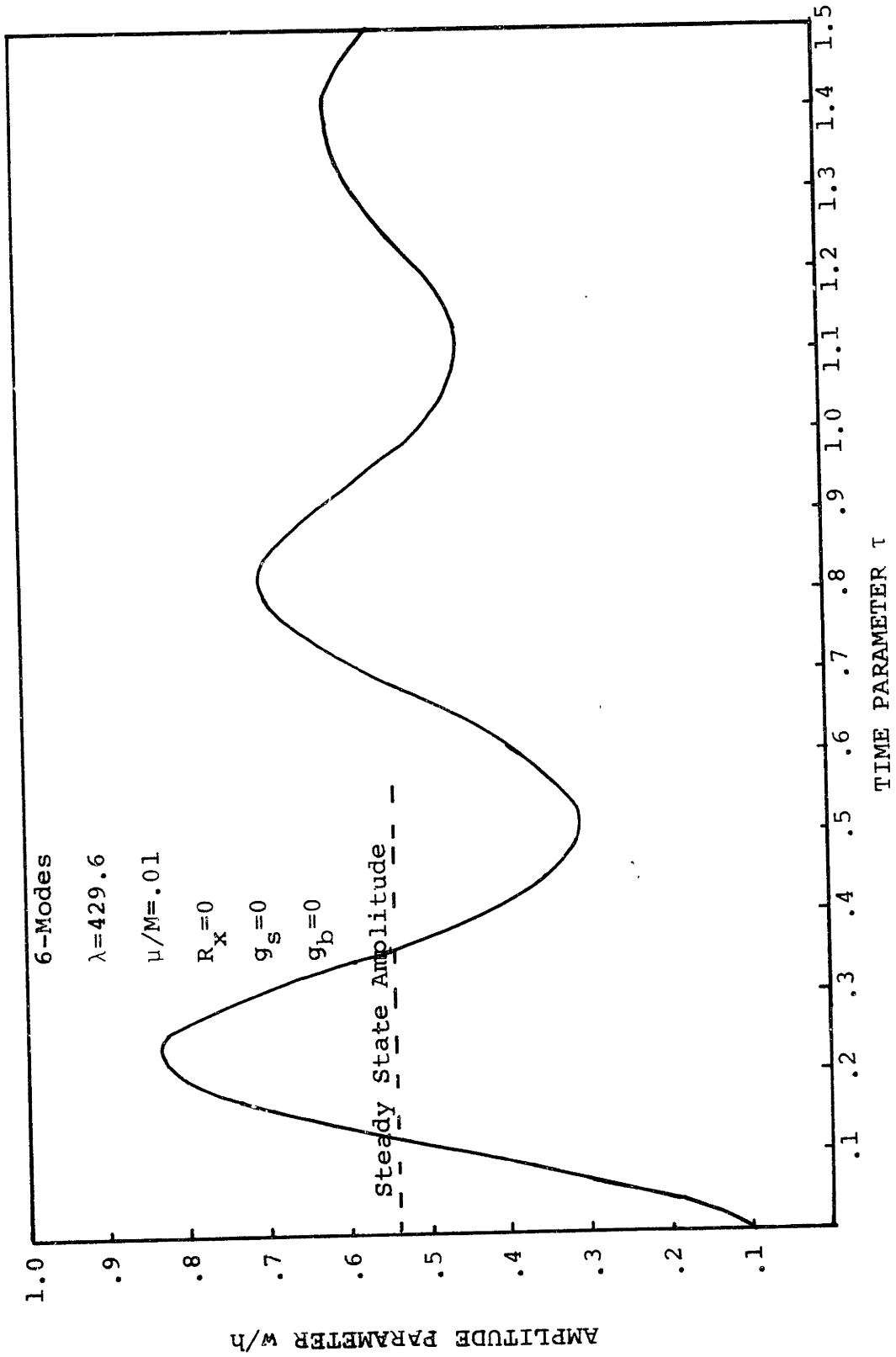


FIG. 18 EXAMPLE ENVELOPE OF TRANSIENT RESPONSE FOR A TWO-DIMENSIONAL SIMPLY-SUPPORTED FLAT PLATE

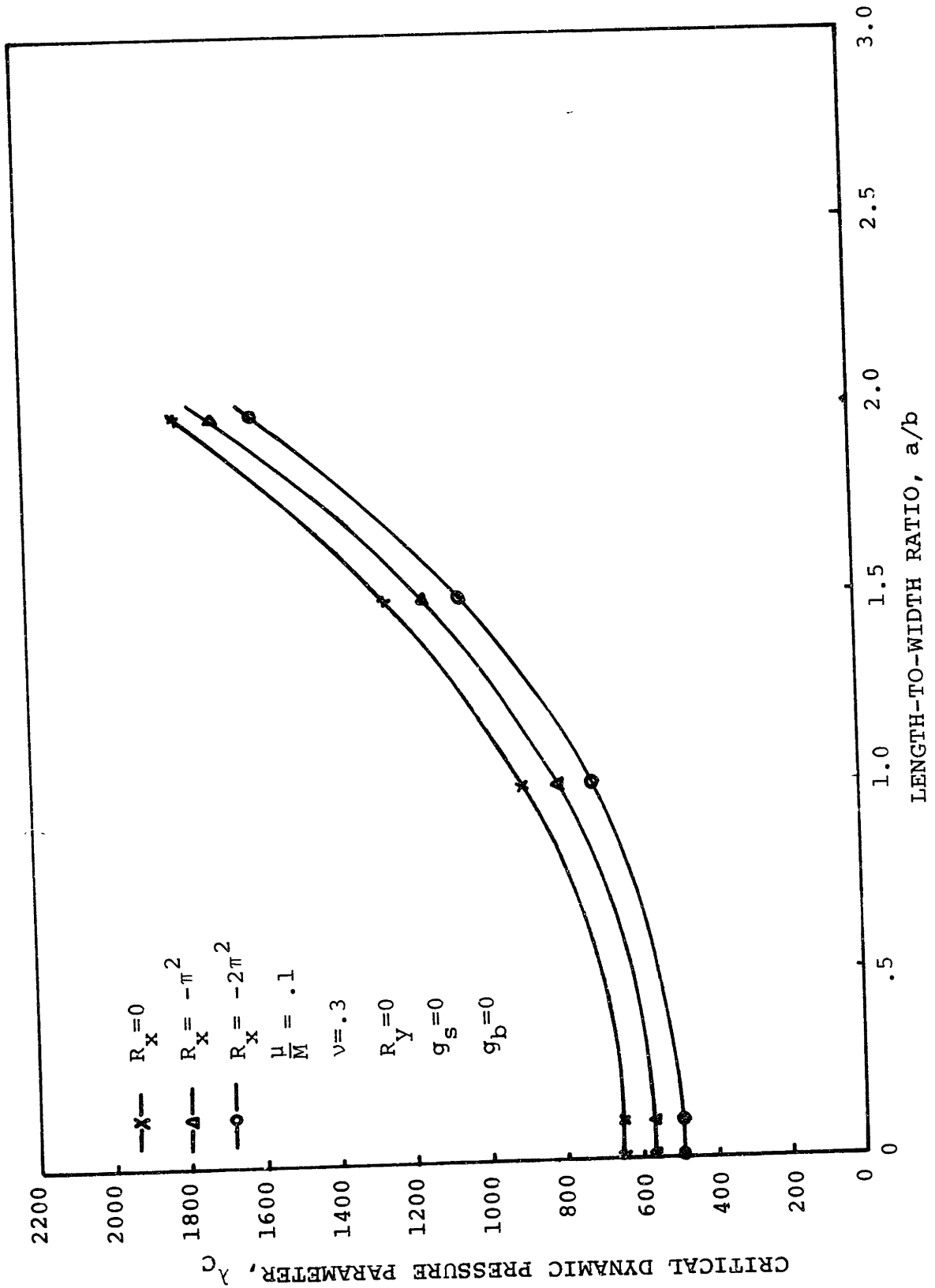


FIG. 19 EFFECTS OF VARYING  $a/b$  AND  $R_x$  UPON THE CRITICAL DYNAMIC PRESSURE TO PRODUCE FLUTTER OF A THREE-DIMENSIONAL CLAMPED-CLAMPED FLAT PLATE

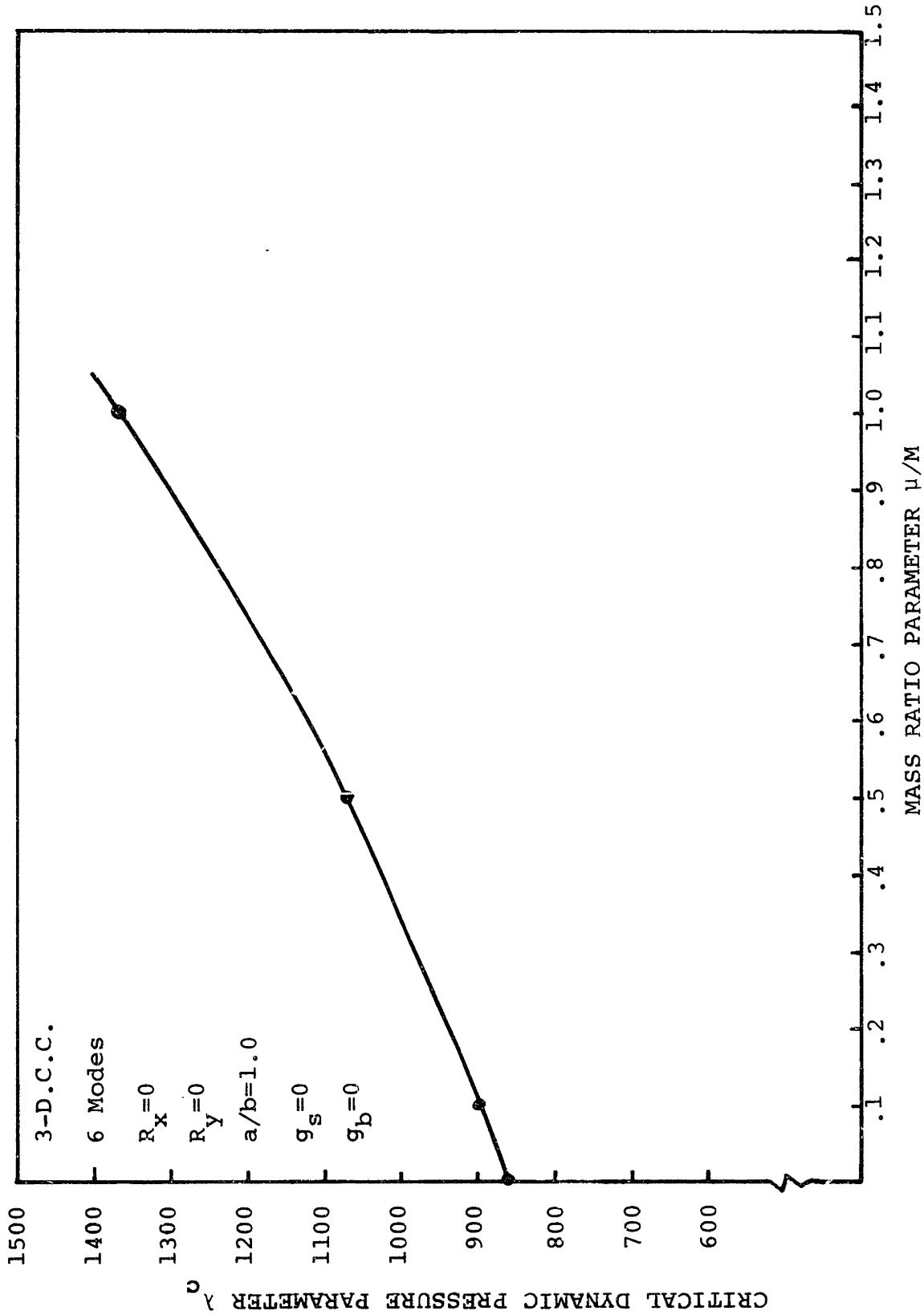


FIG. 20 EFFECT OF  $\mu/M$  ON  $\lambda_c$  FOR THREE-DIMENSIONAL CLAMPED-CLAMPED

PANEL WITH  $a/b=1.0$

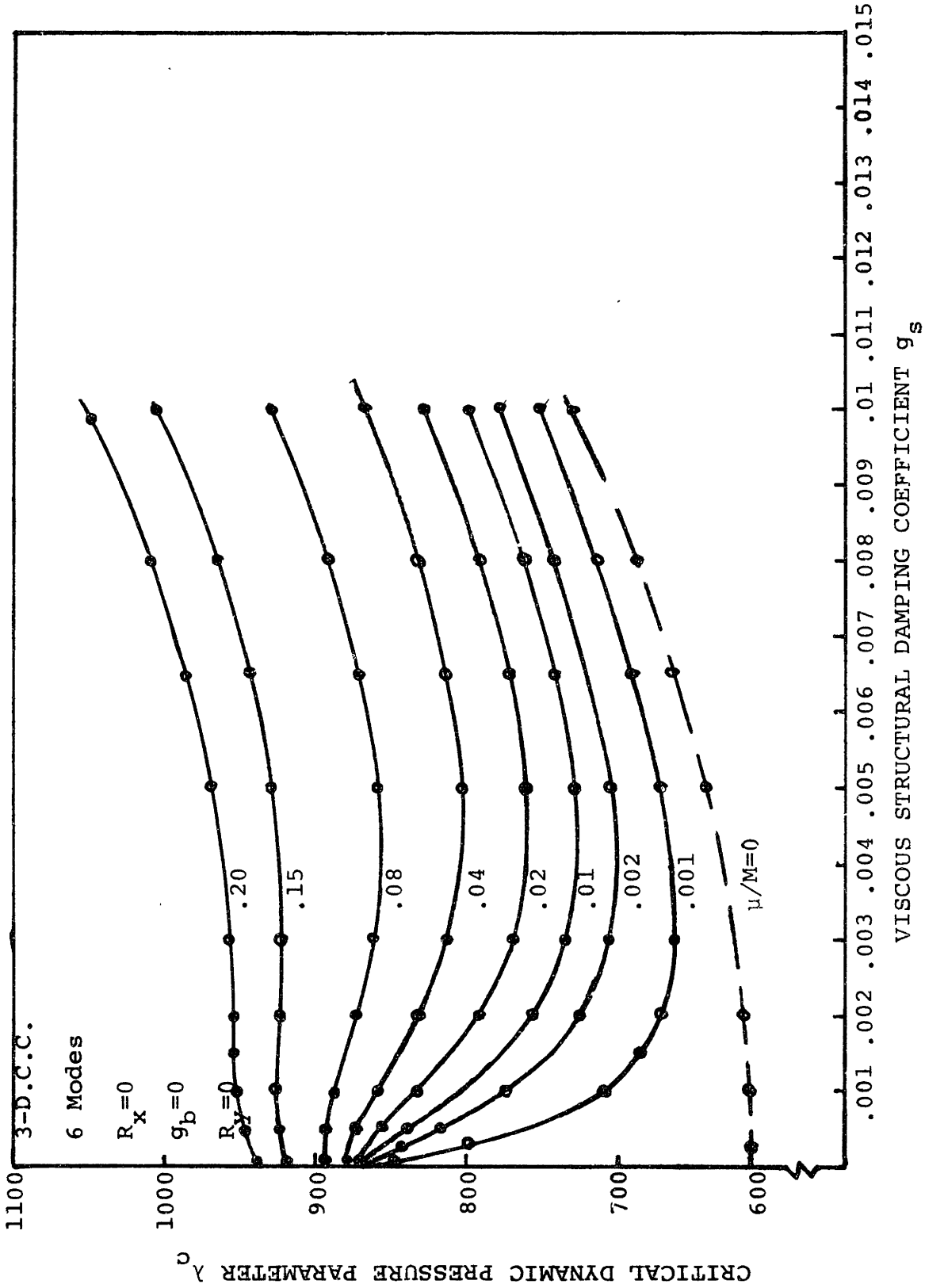


FIG. 21 EFFECT OF THE VISCOUS TYPE DAMPING  $g_s$  ON THE CRITICAL DYNAMIC PRESSURE  $\lambda_c$  FOR THREE-DIMENSIONAL CLAMPED-CLAMPED PANEL WITH  $a/b=1.0$  AND DIFFERENT VALUES OF  $\mu/M$

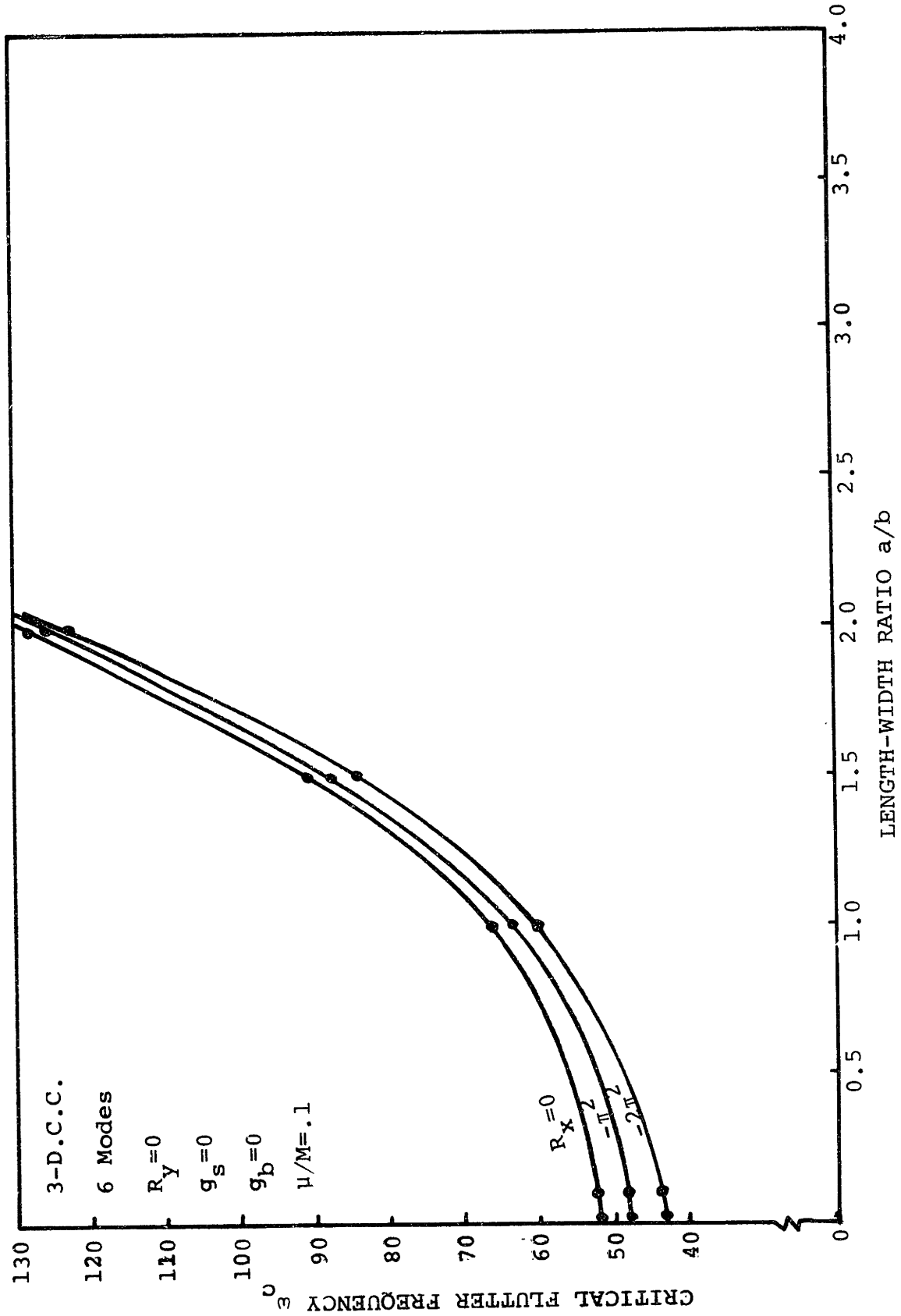


FIG. 22 EFFECT OF MEMBRANE FORCE  $R_x$  AND LENGTH-TO-WIDTH RATIO  $a/b$  ON THE CRITICAL FLUTTER FREQUENCY  $\omega_c$  FOR THREE-DIMENSIONAL CLAMPED-CLAMPED PANEL

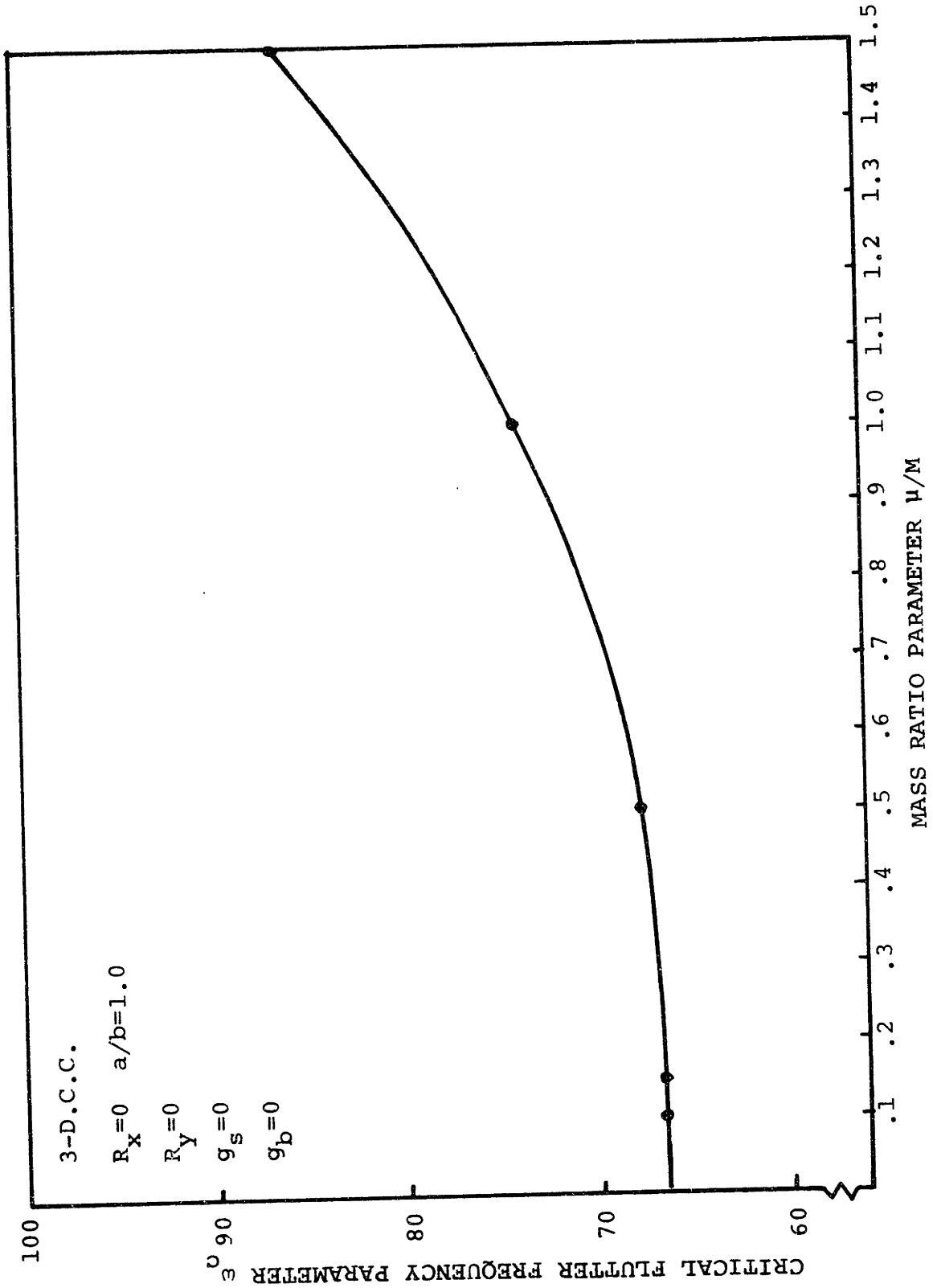


FIG. 23 EFFECT OF  $M/M$  ON  $\omega_c$  FOR THREE-DIMENSIONAL PANELS WITH  $a/b=1.0$  AND VARIOUS VALUES OF  $g_s$



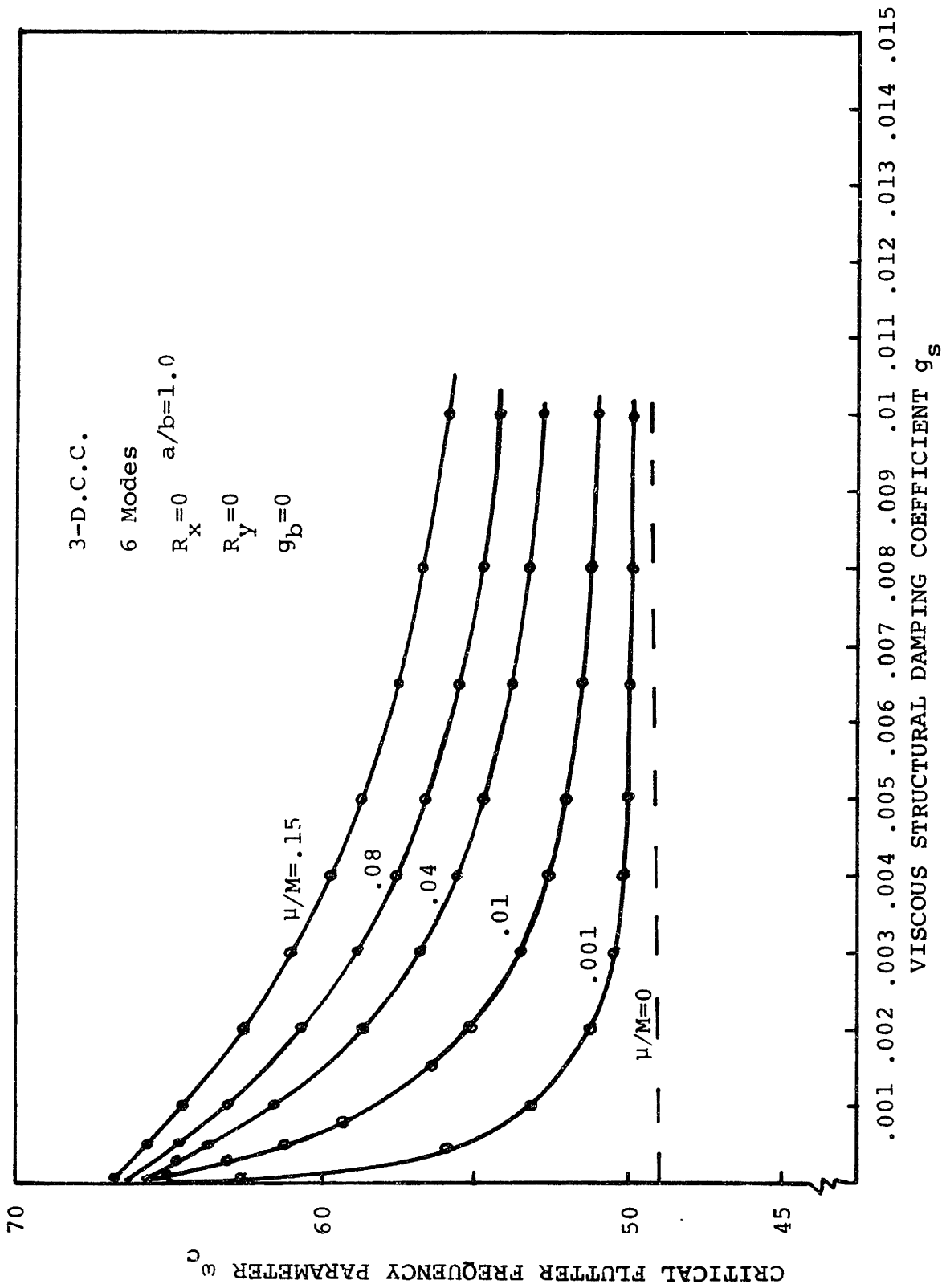


FIG. 24 EFFECT OF VISCOUS TYPE STRUCTURAL DAMPING  $g_s$  ON THE CRITICAL FLUTTER FREQUENCY  $\omega_c$  FOR THREE-DIMENSIONAL CLAMPED-CLAMPED PANELS WITH DIFFERENT VALUES OF  $\mu/M$

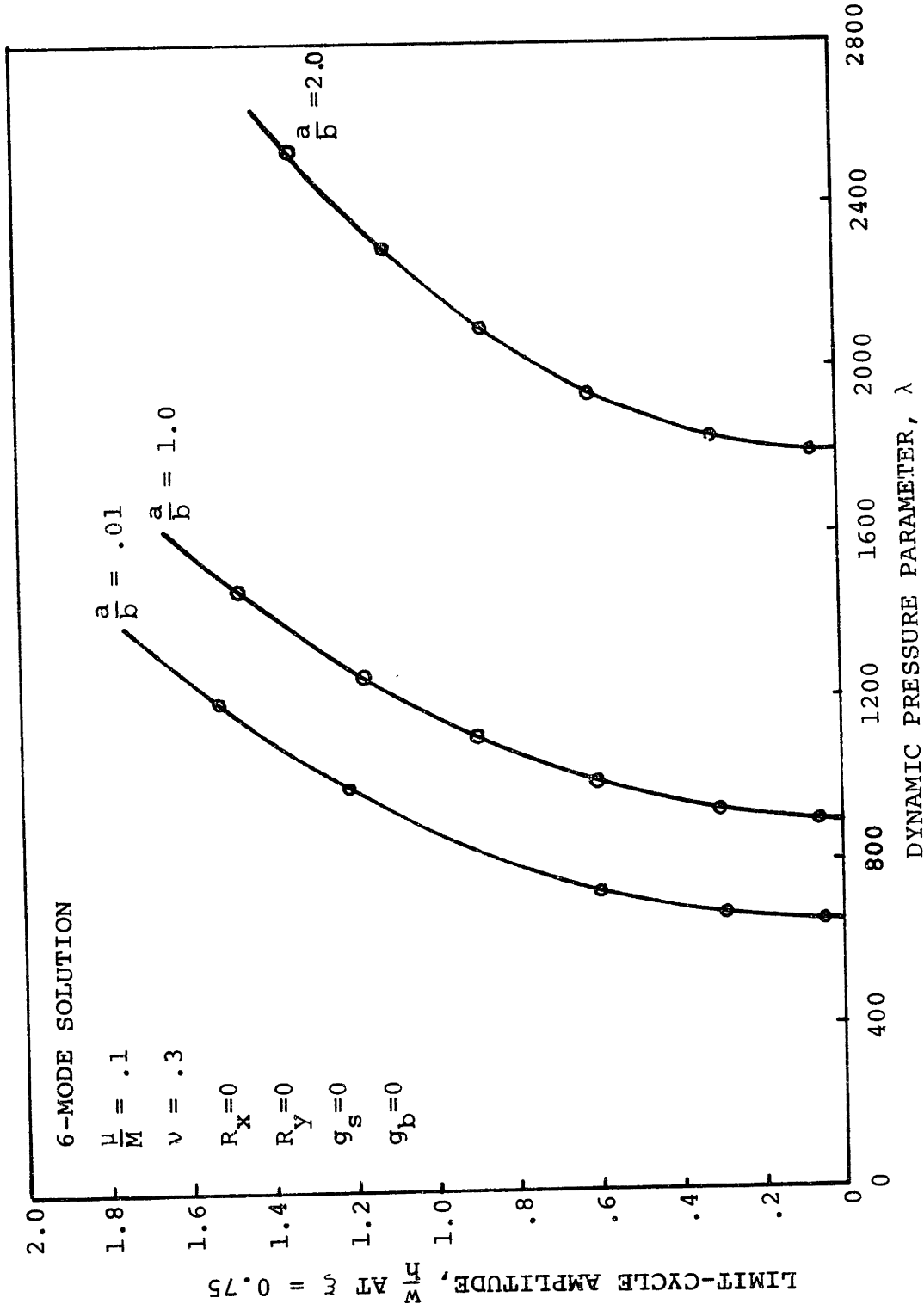


FIG. 25 EFFECT OF LENGTH-TO-WIDTH RATIO  $a/b$  ON THE LIMIT-CYCLE AMPLITUDE FOR A THREE-DIMENSIONAL CLAMPED-CLAMPED FLAT PLATE WITH  $R_x = R_y = 0$

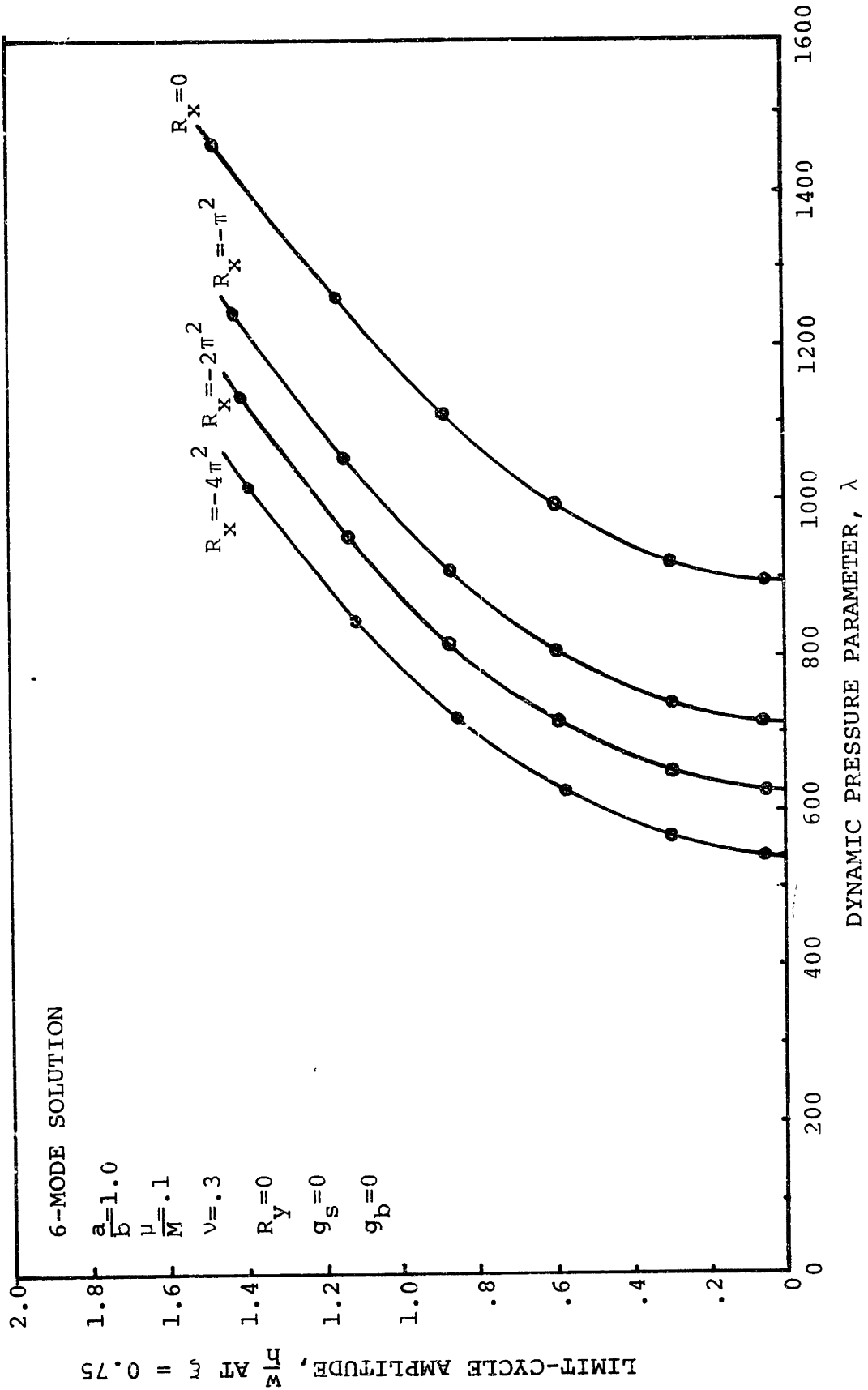


FIG. 26 EFFECT OF APPLIED MEMBRANE FORCE  $R_x$  (FOR  $R_y = 0$ ) ON THE LIMIT-CYCLE AMPLITUDE OF A THREE-DIMENSIONAL CLAMPED-CLAMPED FLAT PLATE WITH  $a/b = 1.0$

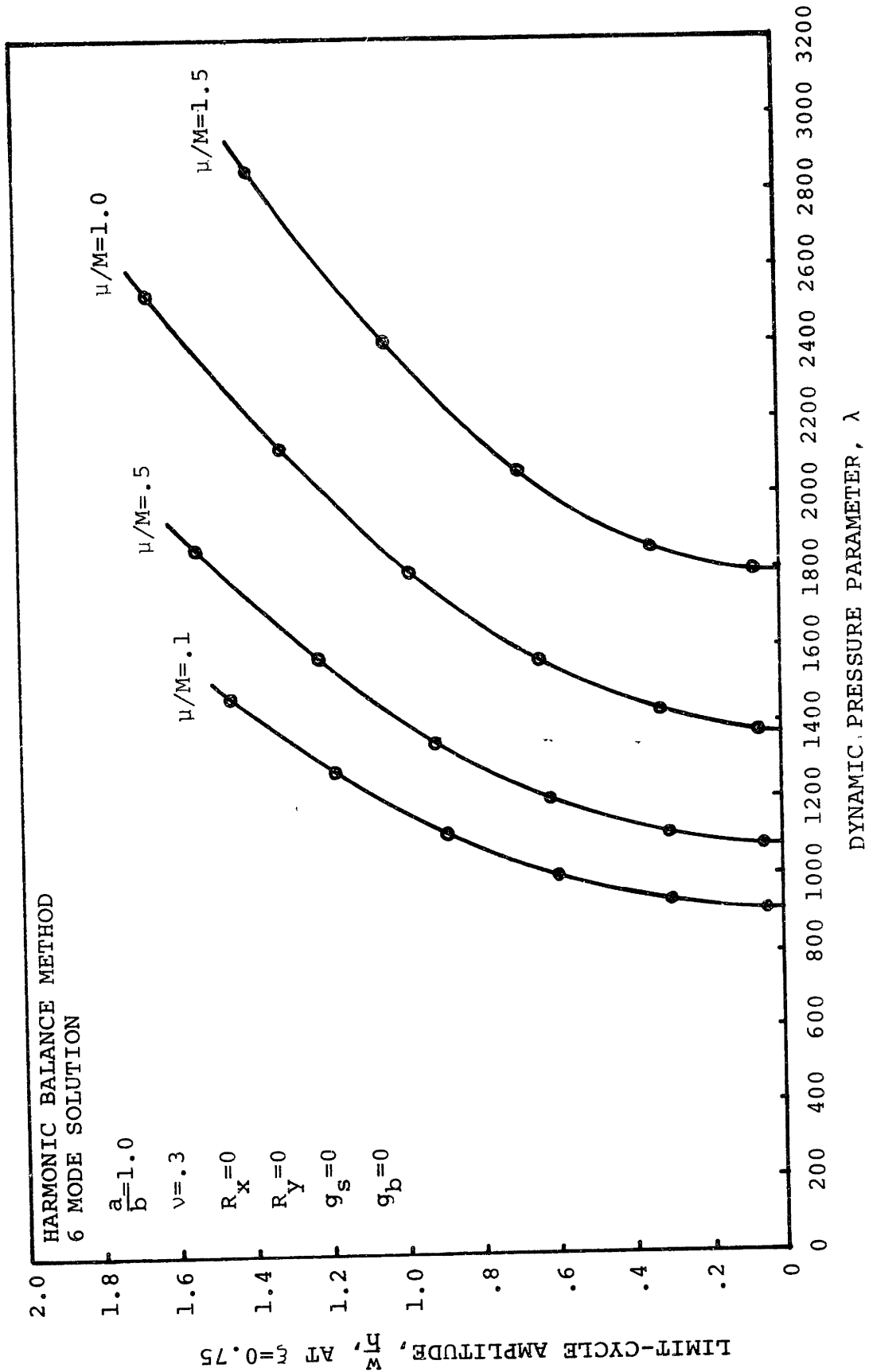


FIG. 27 EFFECT OF MASS RATIO  $\mu/M$  ON THE LIMIT-CYCLE AMPLITUDE FOR A THREE-DIMENSIONAL CLAMPED-CLAMPED FLAT PLATE WITH  $R_x = R_y = 0$ .

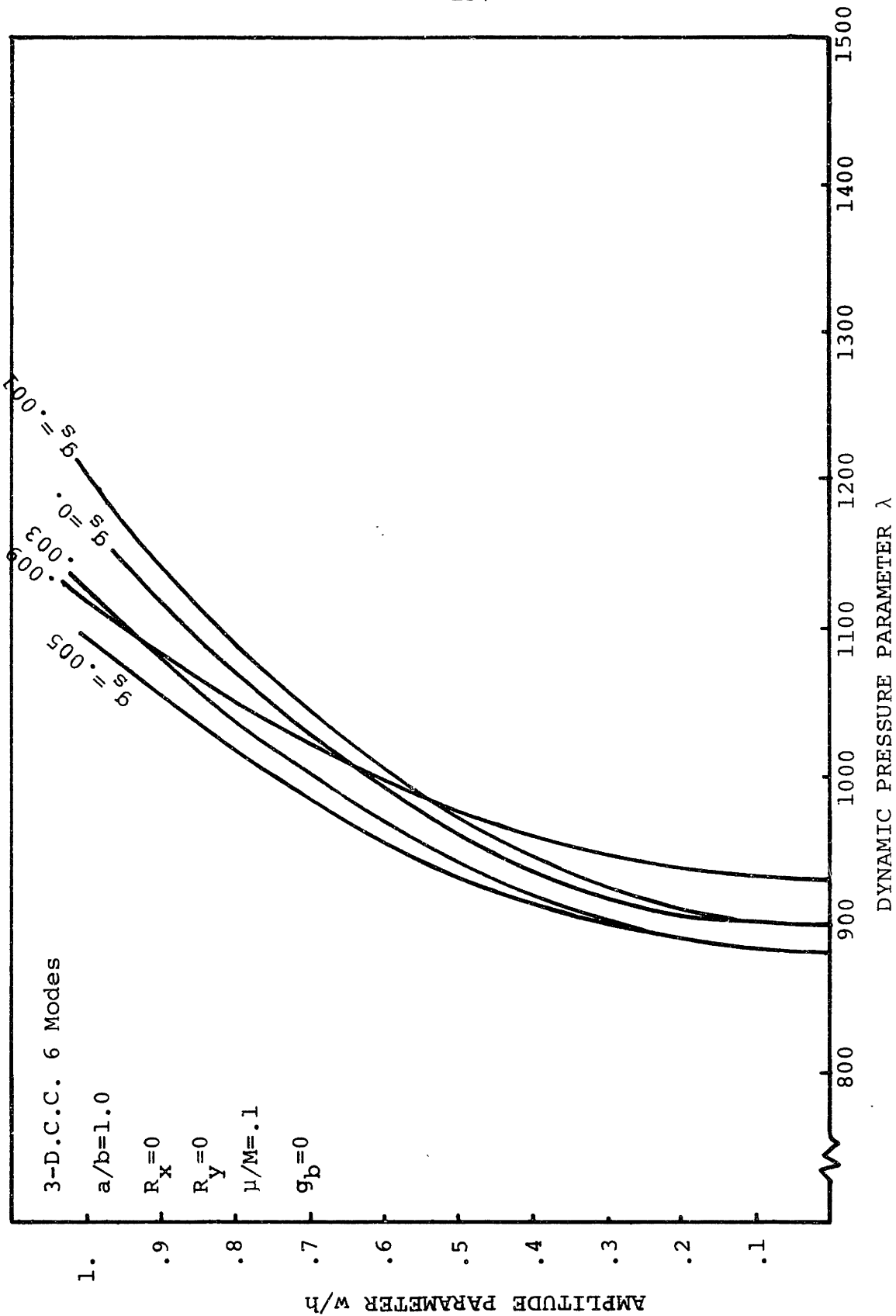


FIG. 28 EFFECT OF VISCOUS STRUCTURAL DAMPING  $g_s$  ON THE LIMIT-CYCLE AMPLITUDE OF THREE-DIMENSIONAL PANELS WITH  $a/b=1.0$

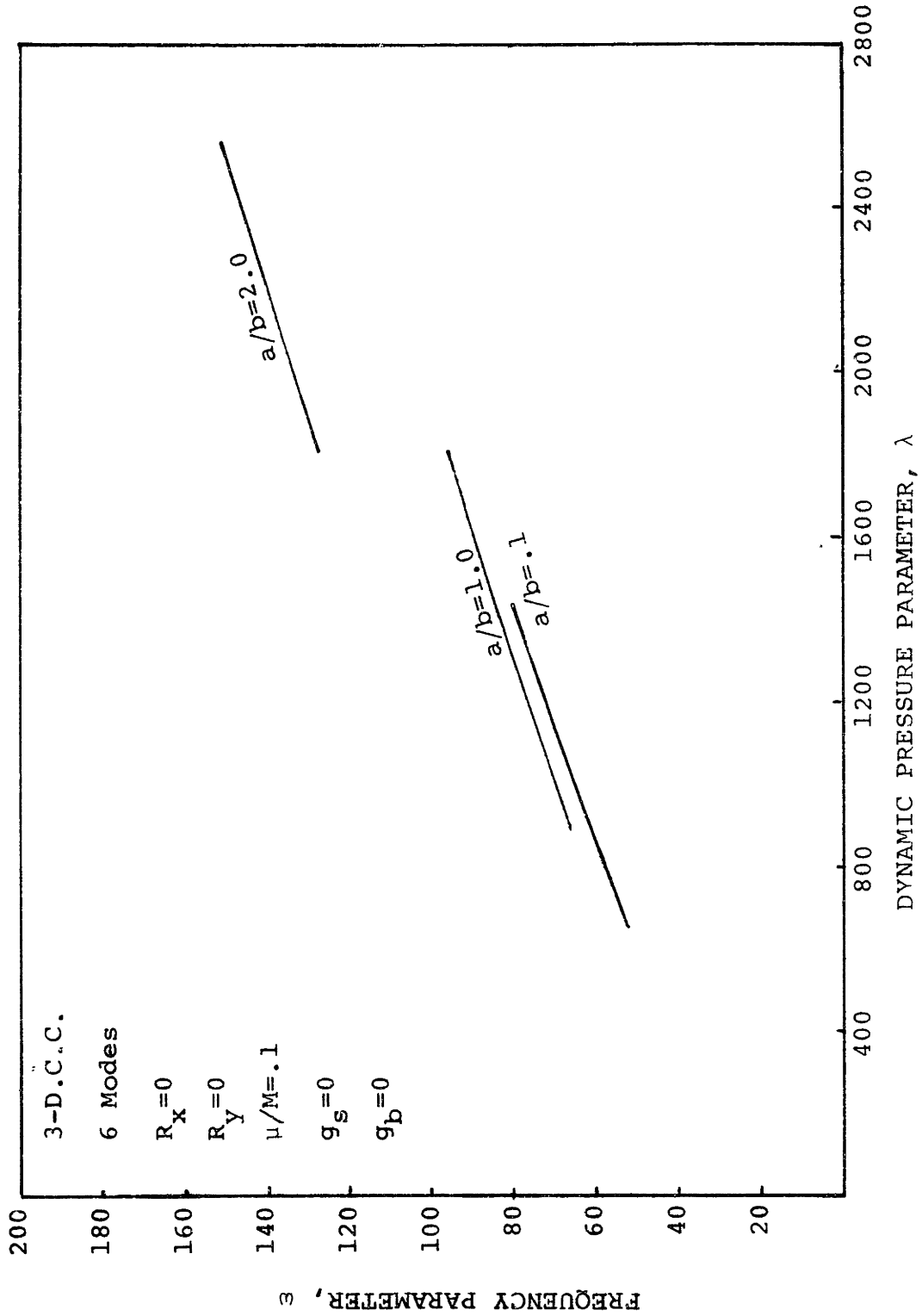


FIG. 29 VARIATION OF FLUTTER FREQUENCY  $\omega$  WITH DYNAMIC PRESSURE  $\lambda$  FOR THREE-DIMENSIONAL CLAMPED-CLAMPED PLATES WITH DIFFERENT VALUES OF  $a/b$

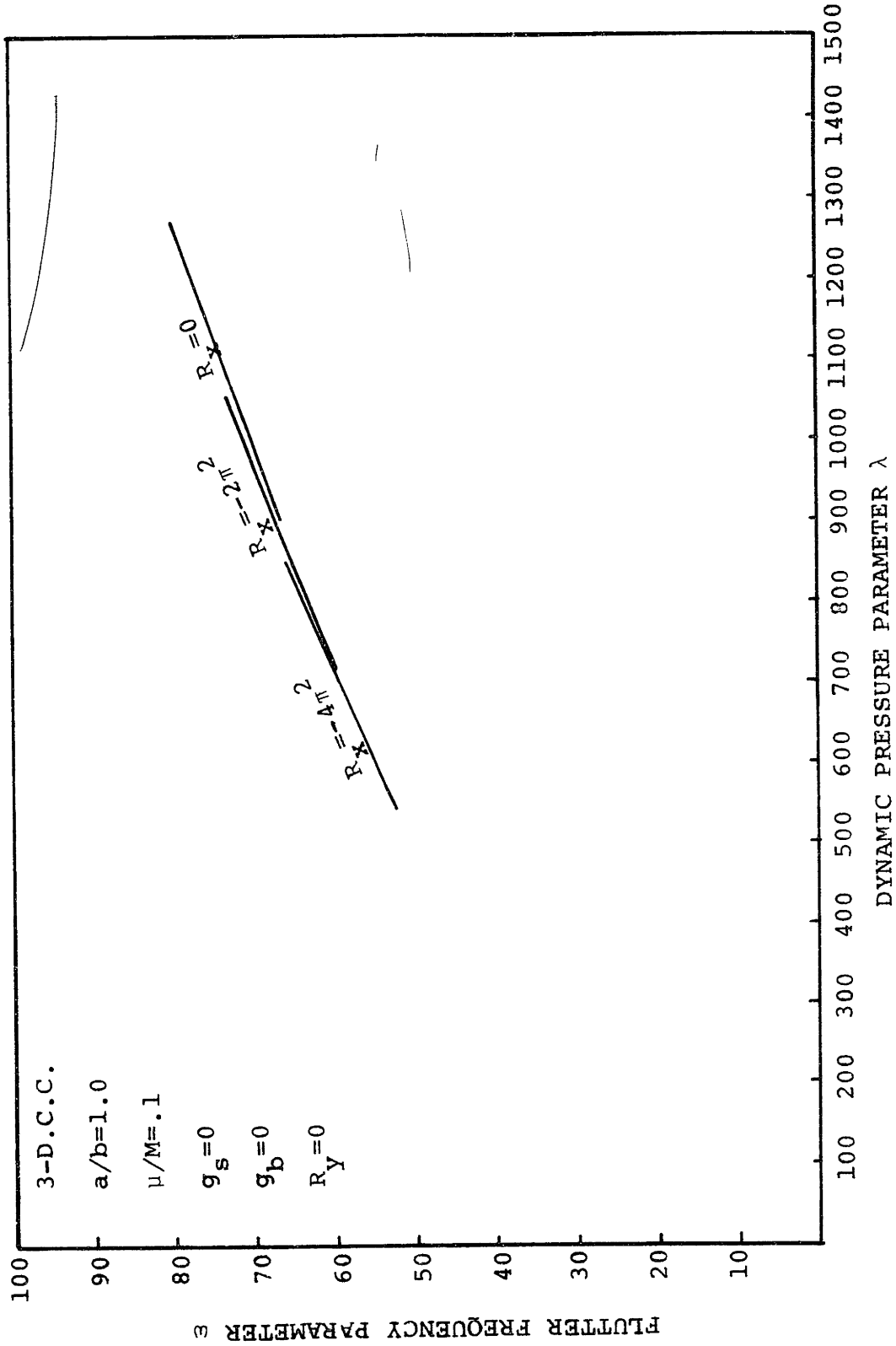


FIG. 30 VARIATION OF FLUTTER FREQUENCY  $\omega$  WITH DYNAMIC PRESSURE  $\lambda$  FOR A THREE-DIMENSIONAL CLAMPED-CLAMPED PLATE AT DIFFERENT VALUES OF MEMBRANE FORCE  $R_x$

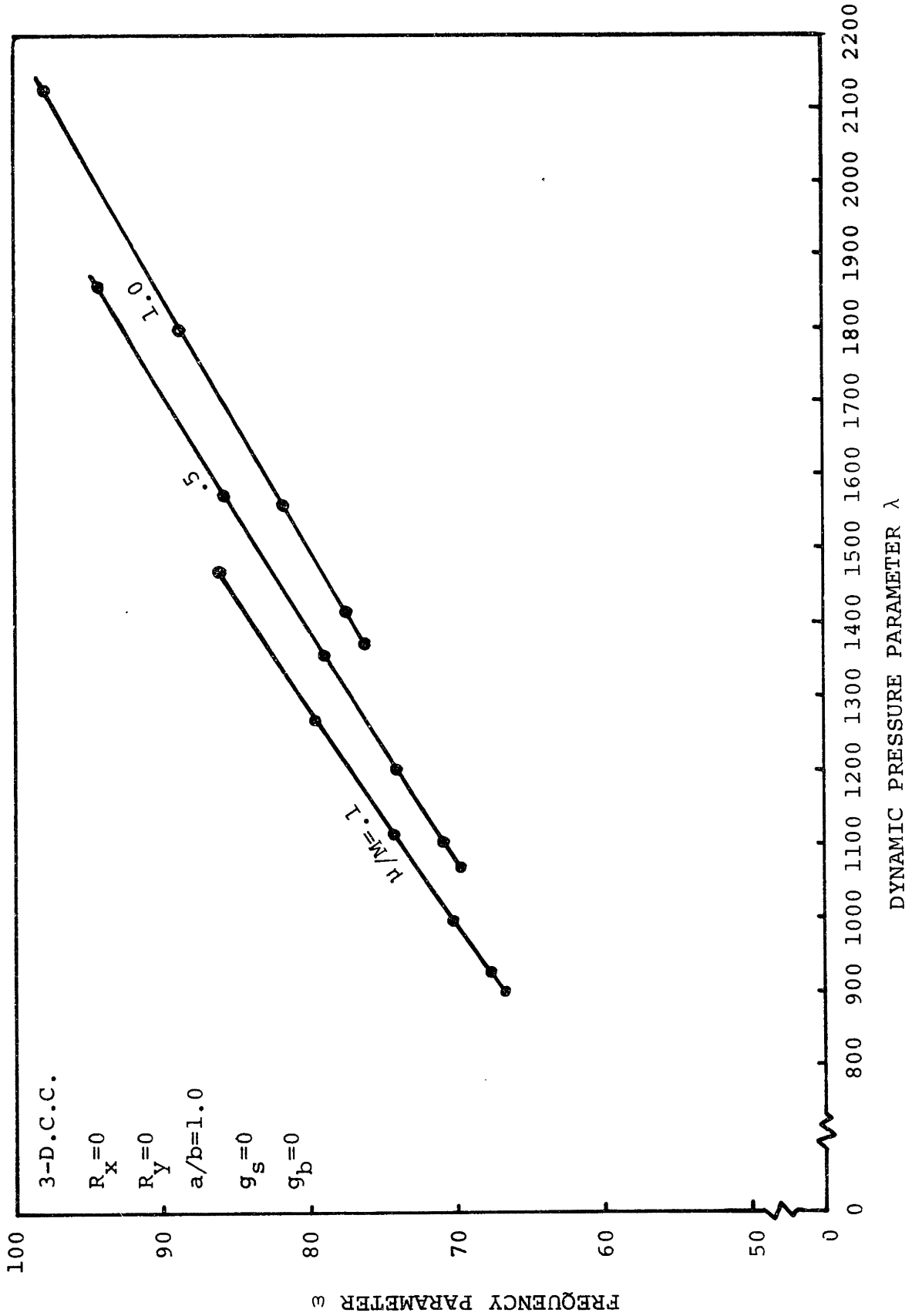


FIG. 31 VARIATION OF FLUTTER FREQUENCY  $\omega$  WITH DYNAMIC PRESSURE  $\lambda$  FOR THREE-DIMENSIONAL PLATES WITH  $a/b=1.0$  AND VARIOUS VALUES OF  $\mu/M$



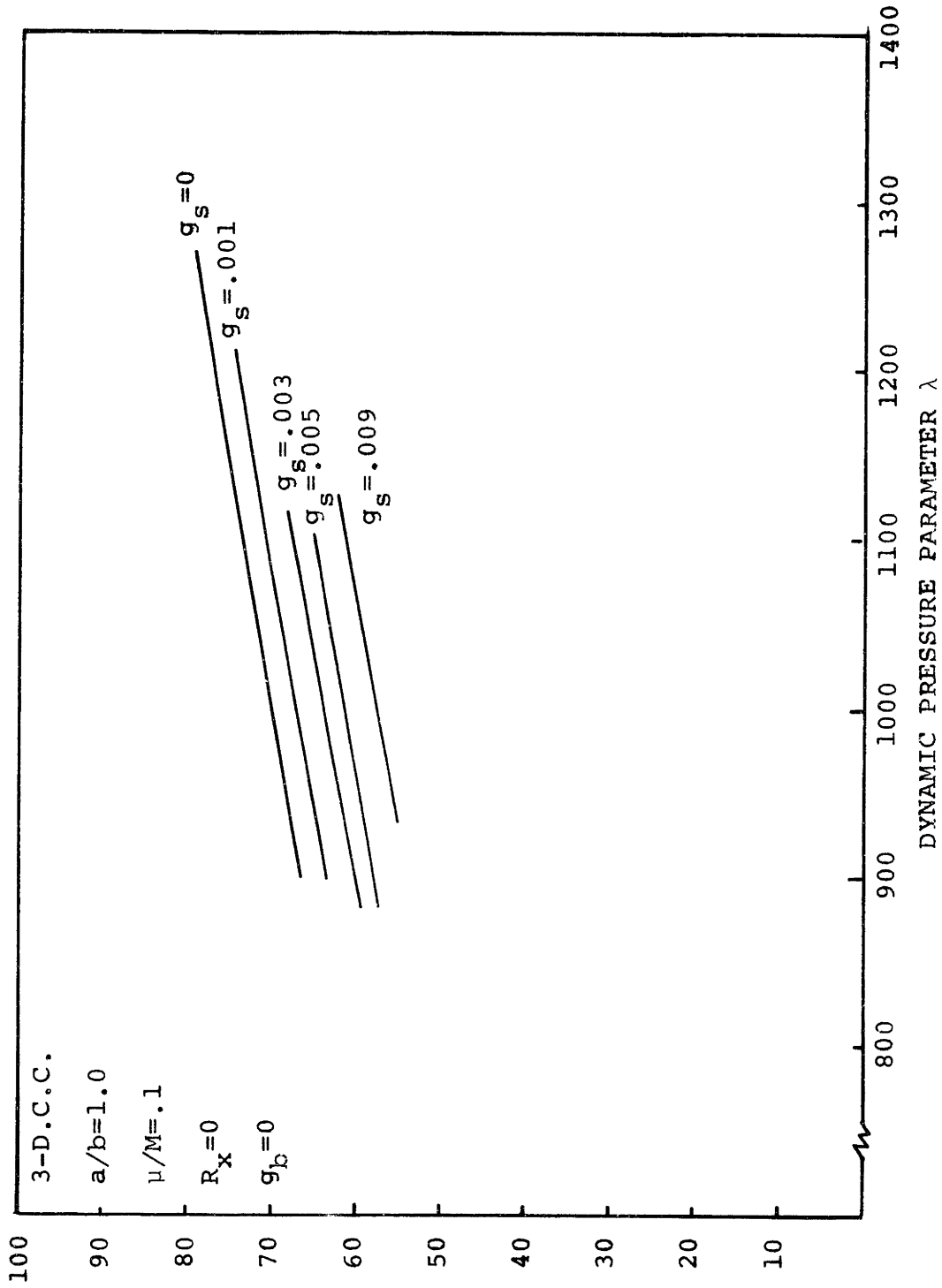


FIG. 32 VARIATION OF FLUTTER FREQUENCY  $\omega$  WITH DYNAMIC PRESSURE  $\lambda$  FOR A THREE-DIMENSIONAL CLAMPED-CLAMPED PLATE AT DIFFERENT VALUES OF VISCOUS STRUCTURAL DAMPING  $g_s$

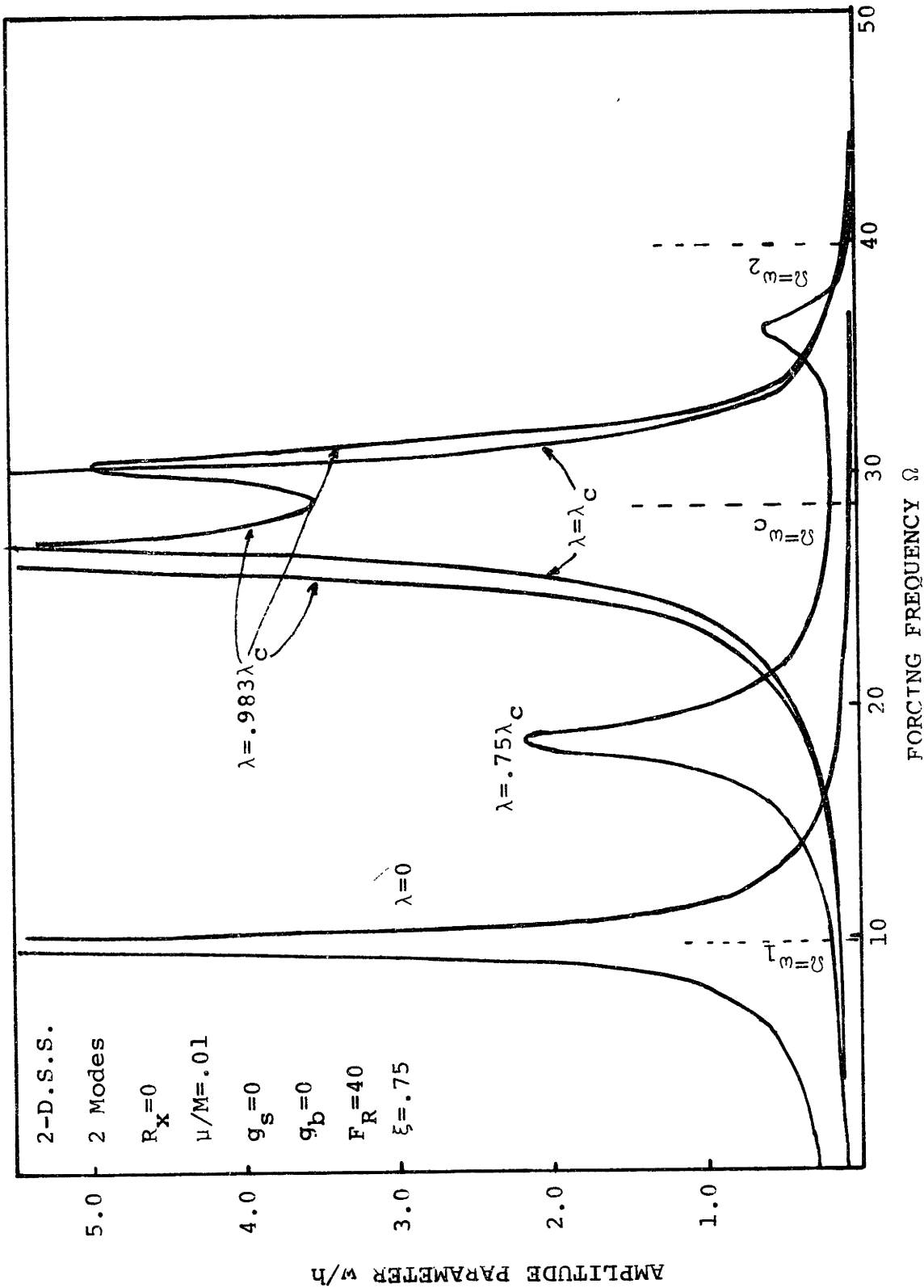


FIG. 33 LINEAR FORCED RESPONSE OF PANEL BELOW FLUTTER

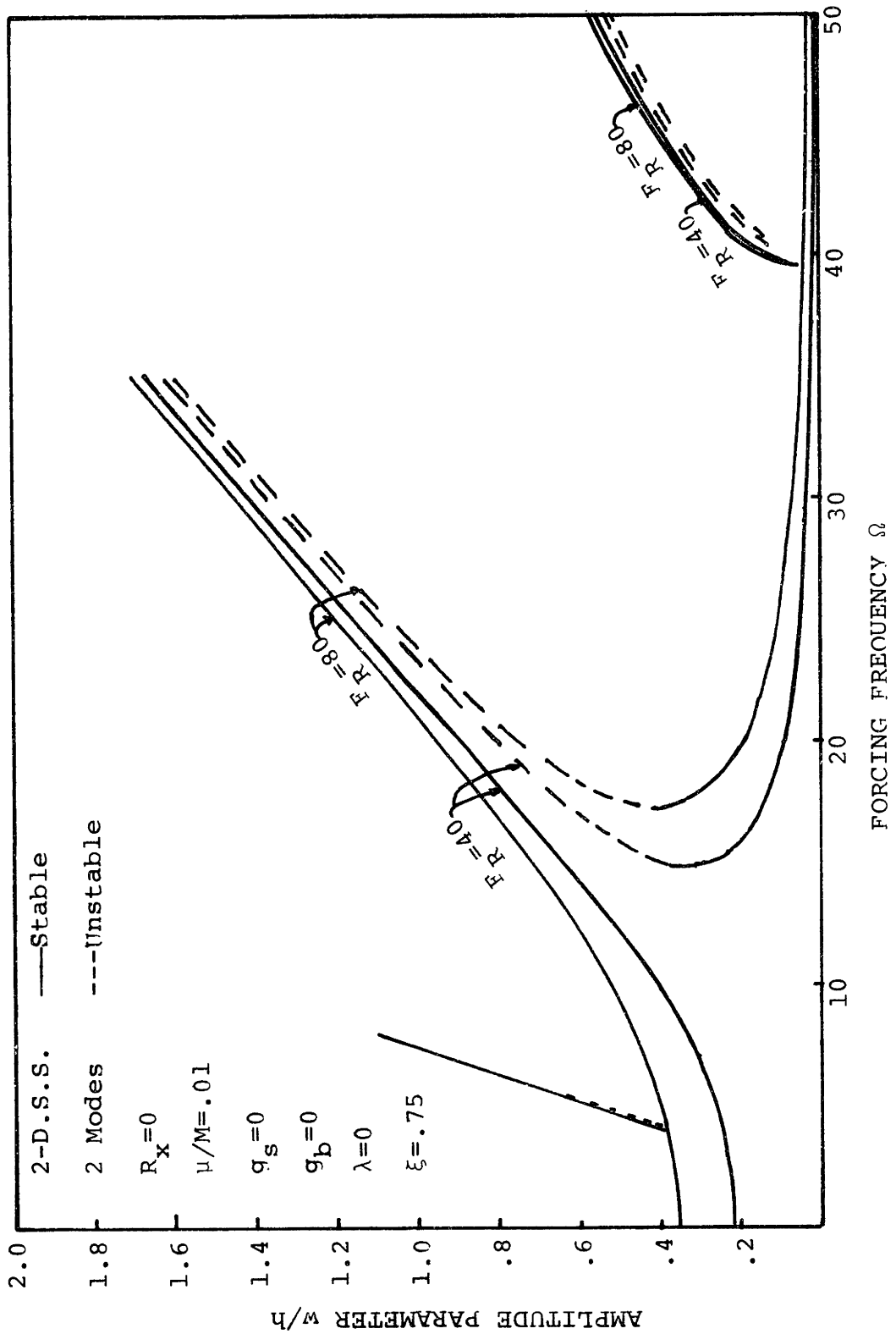


FIG. 34 NONLINEAR FORCED RESPONSE OF A PLATE WITHOUT AIR FLOW,  $\lambda=0$

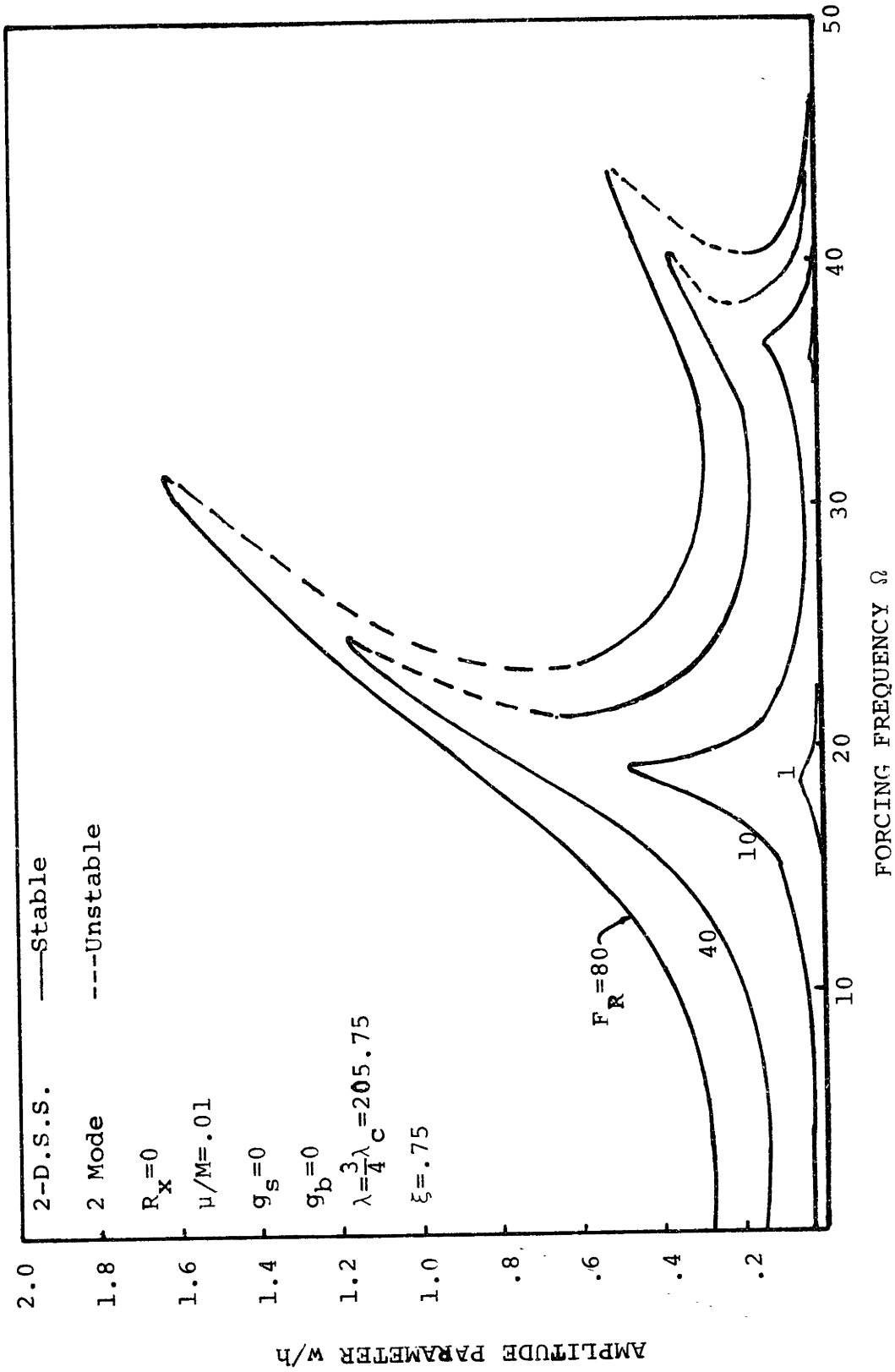


FIG. 35 NONLINEAR FORCED RESPONSE OF A PLATE AT  $\lambda = \frac{3}{4} \lambda_c$

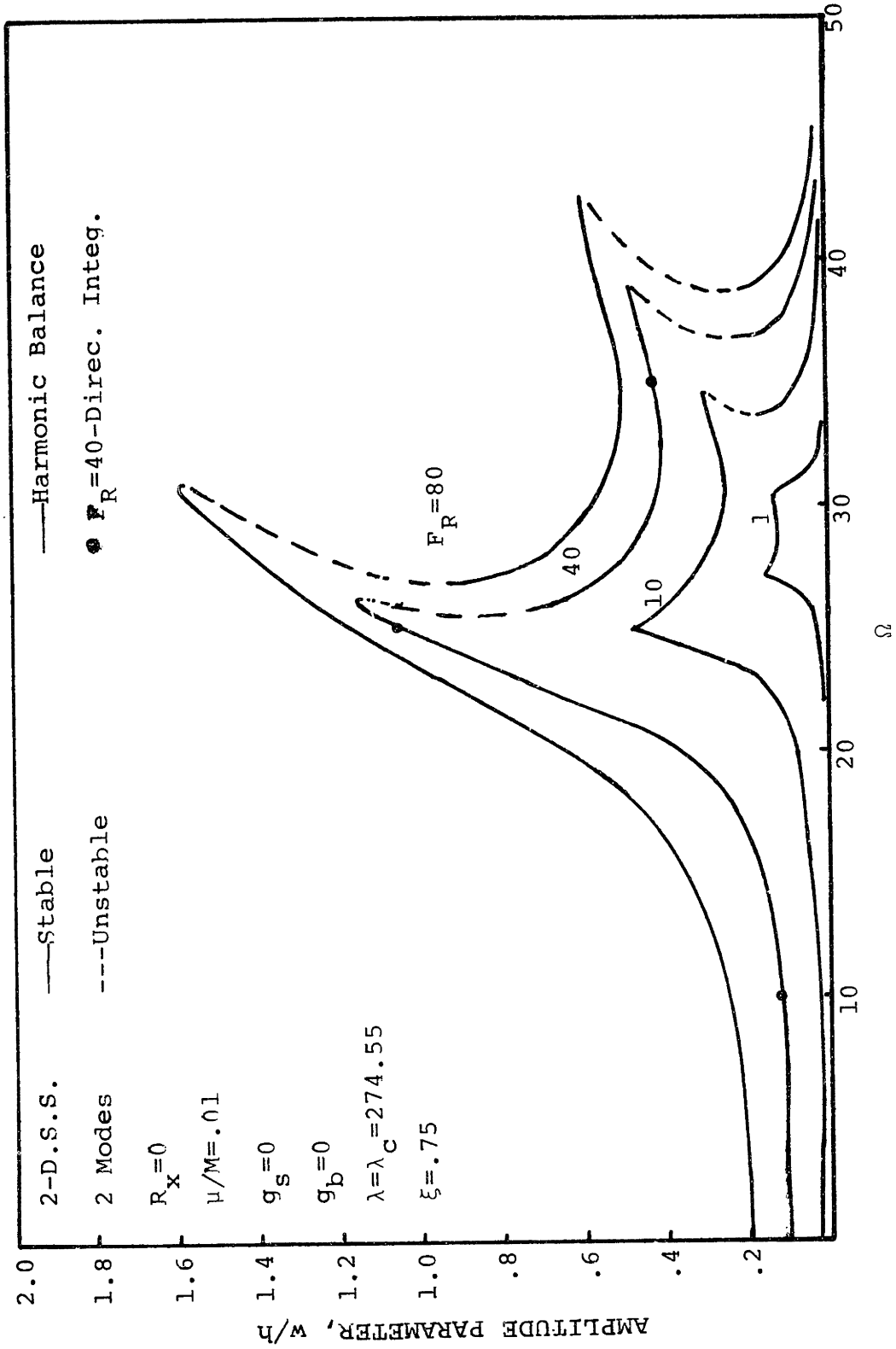


FIG. 36 NONLINEAR FORCED RESPONSE OF A PLATE AT  $\lambda=\lambda_C$  WITH LARGE FORCING EXCITATION

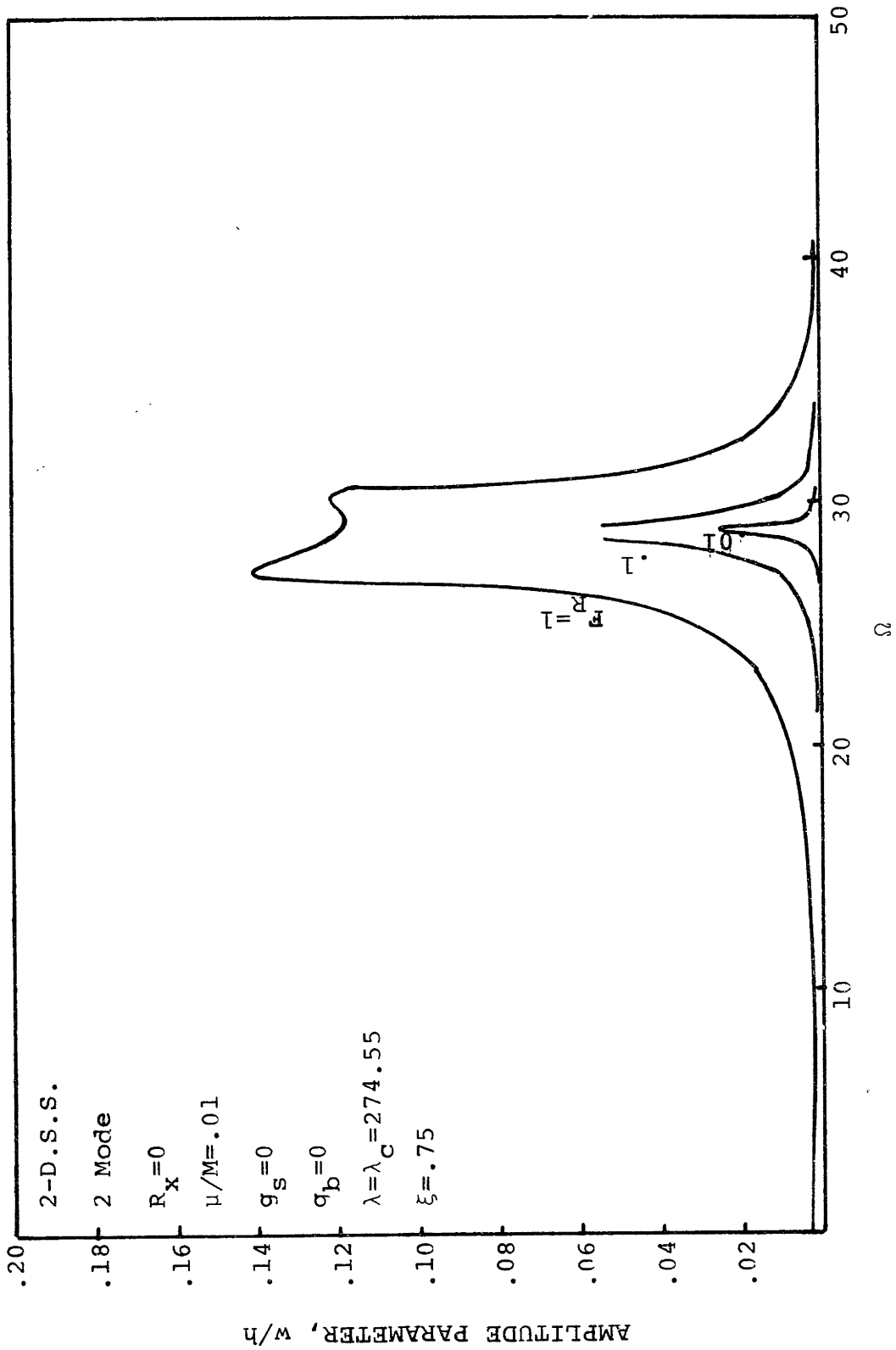


FIG. 37 NONLINEAR FORCED RESPONSE OF A PANEL AT  $\lambda=\lambda_c$  WITH SMALL FORCING EXCITATIONS

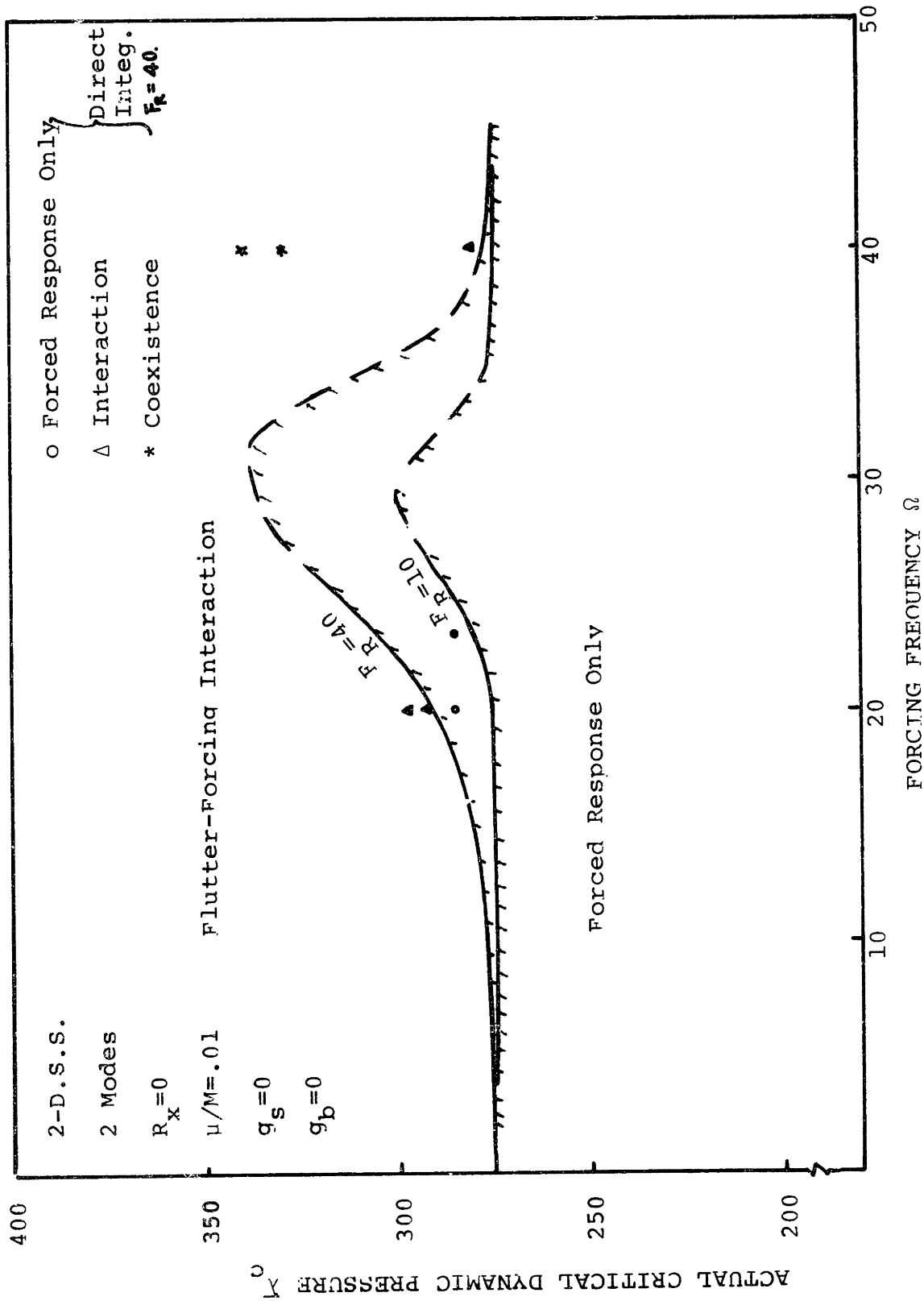


FIG. 38 ACTUAL CRITICAL DYNAMIC PRESSURE  $\lambda_c$  AT DIFFERENT FORCING AMPLITUDES

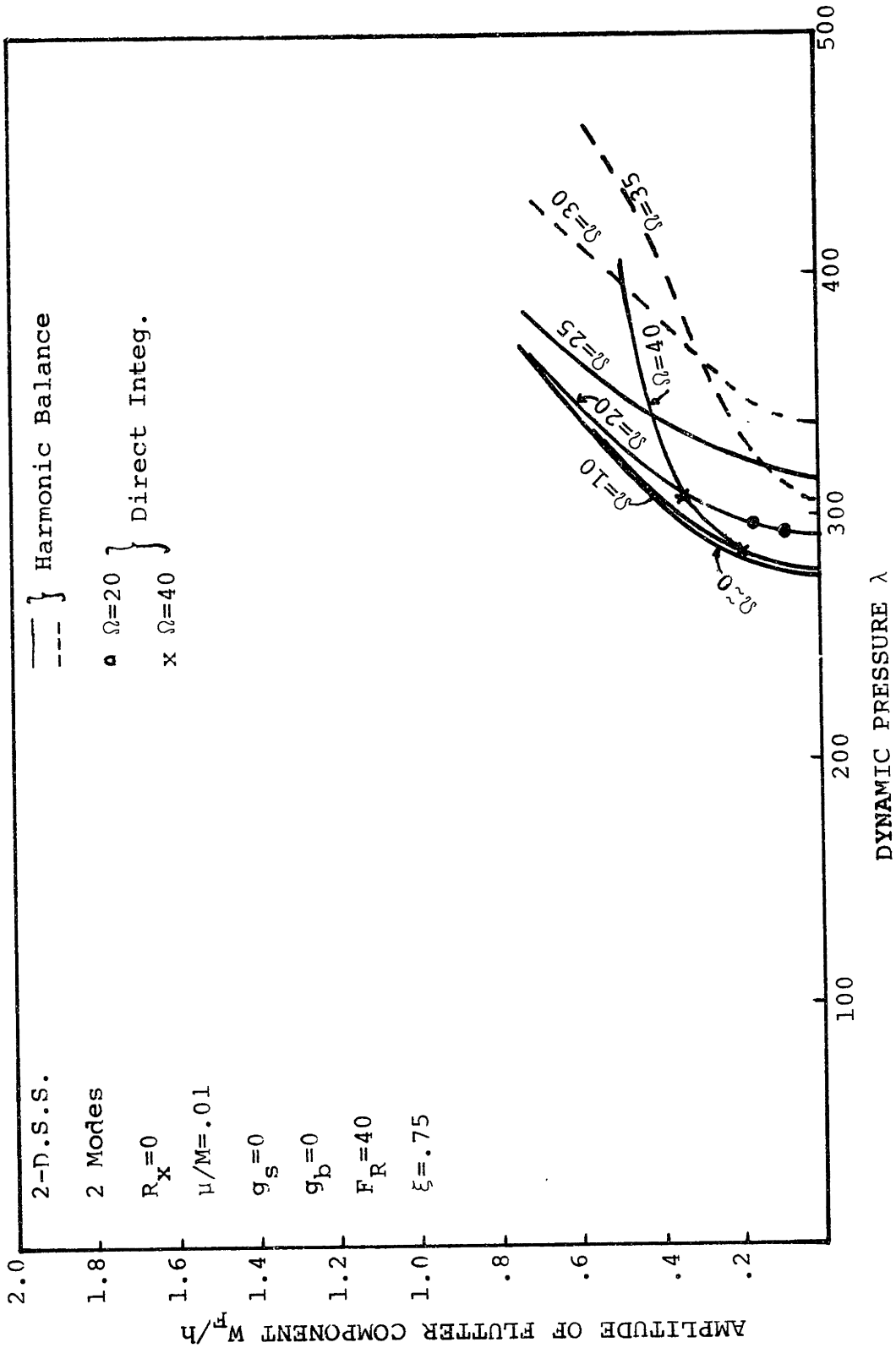


FIG. 39 FORCING-FLUTTER INTERACTION--AMPLITUDE OF THE FLUTTER COMPONENT FOR DIFFERENT VALUES OF FORCING FREQUENCY  $\Omega$



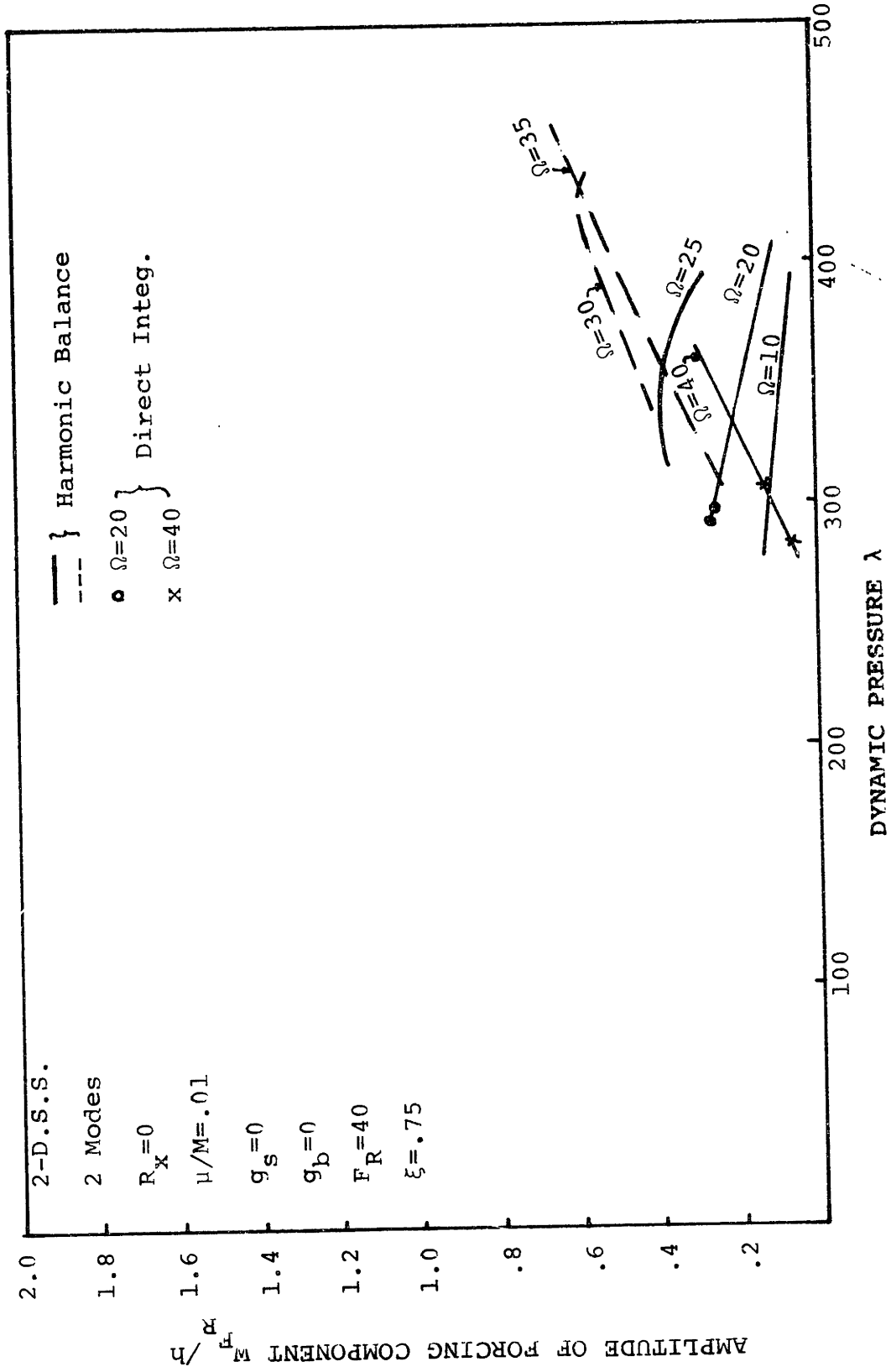


FIG. 40 FORCING-FLUTTER INTERACTION--AMPLITUDE OF FORCING COMPONENT FOR DIFFERENT VALUES OF FORCING FREQUENCY  $\Omega$

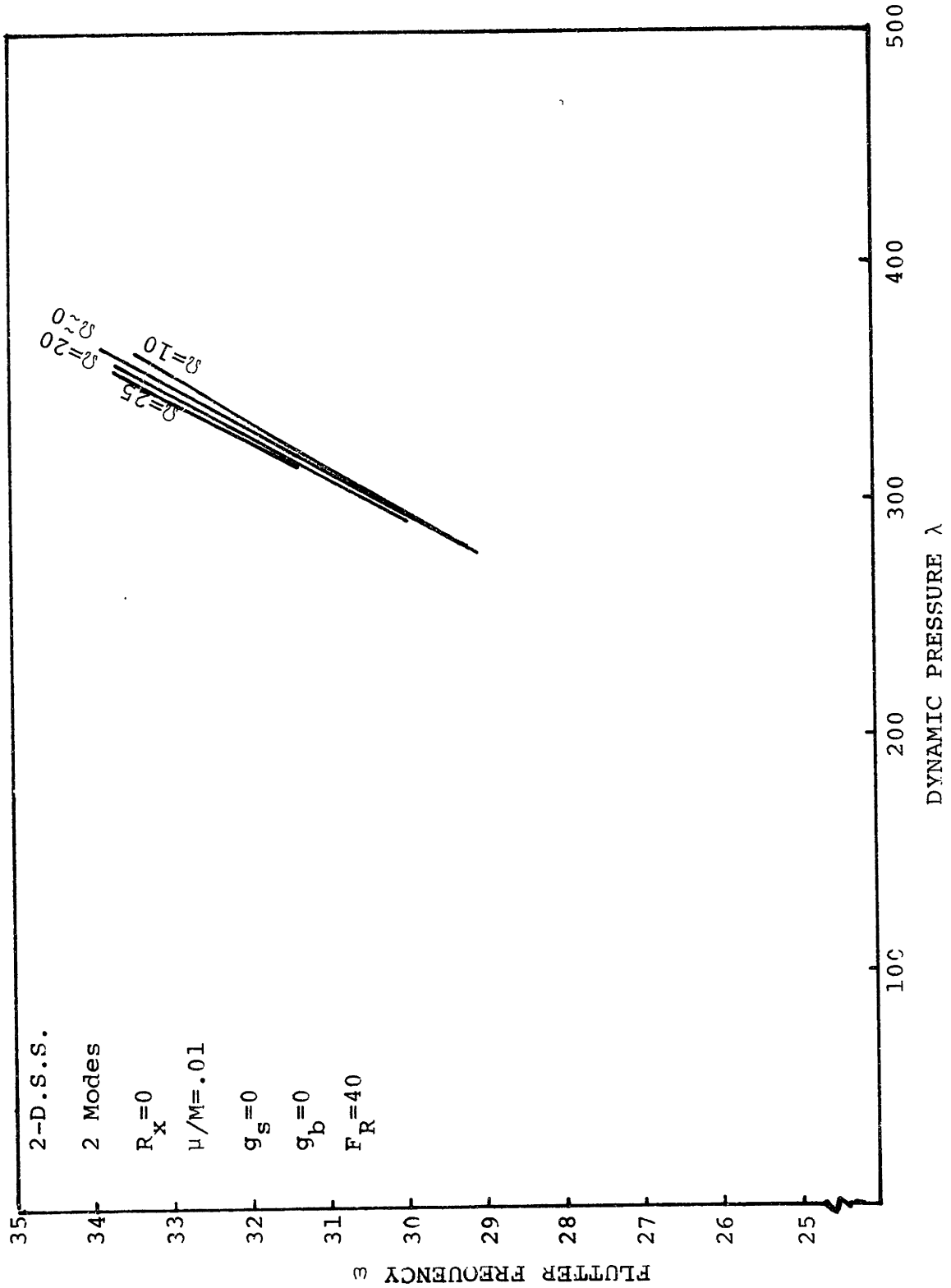


FIG. 41 FORCING FLUTTER INTERACTION--VARIATION OF FLUTTER FREQUENCY WITH DYNAMIC PRESSURE FOR DIFFERENT FORCING FREQUENCY  $\Omega$

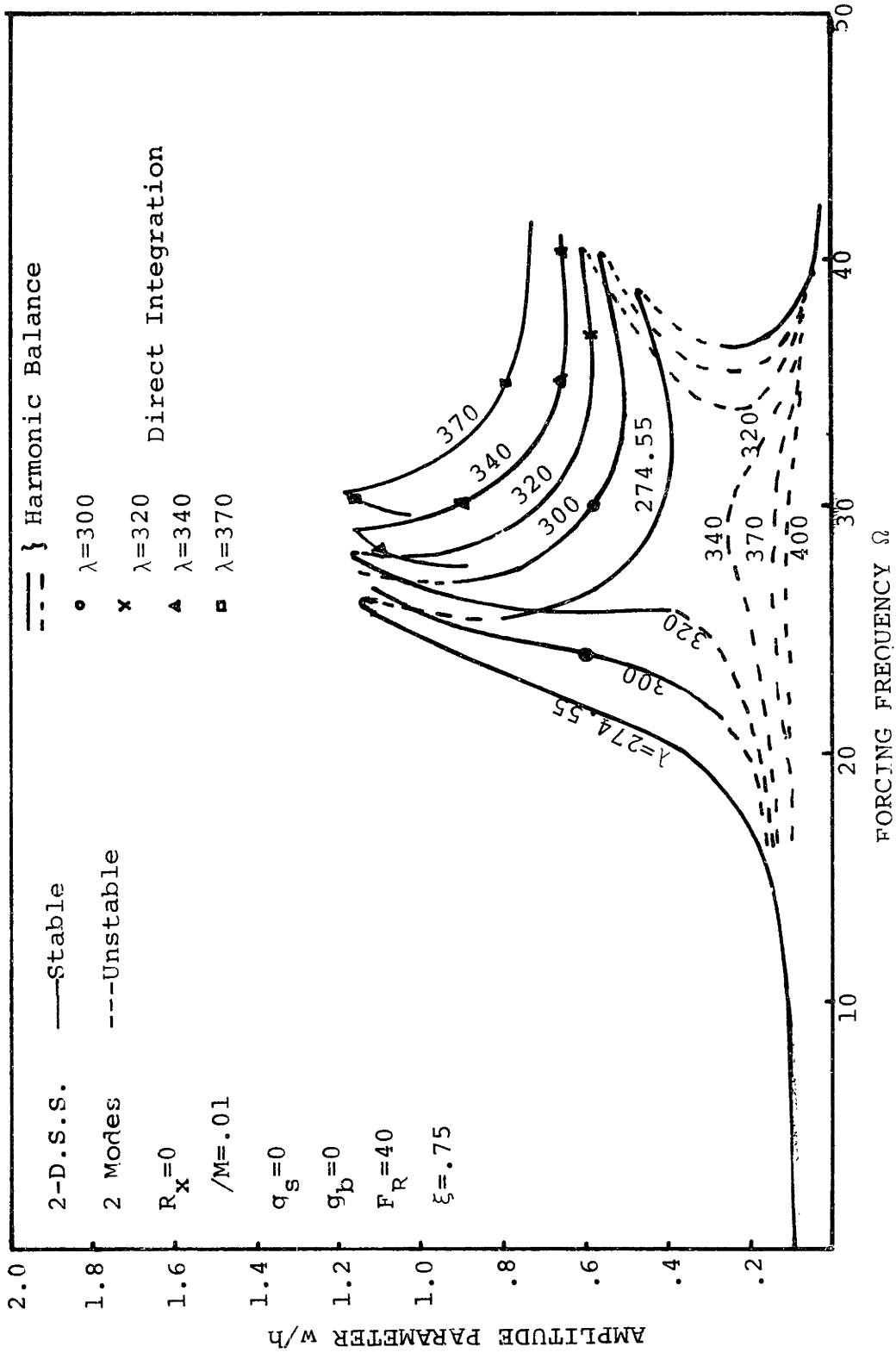


FIG. 42 NONLINEAR FORCED RESPONSE OF A PANEL AT  $\lambda \geq \lambda_c$

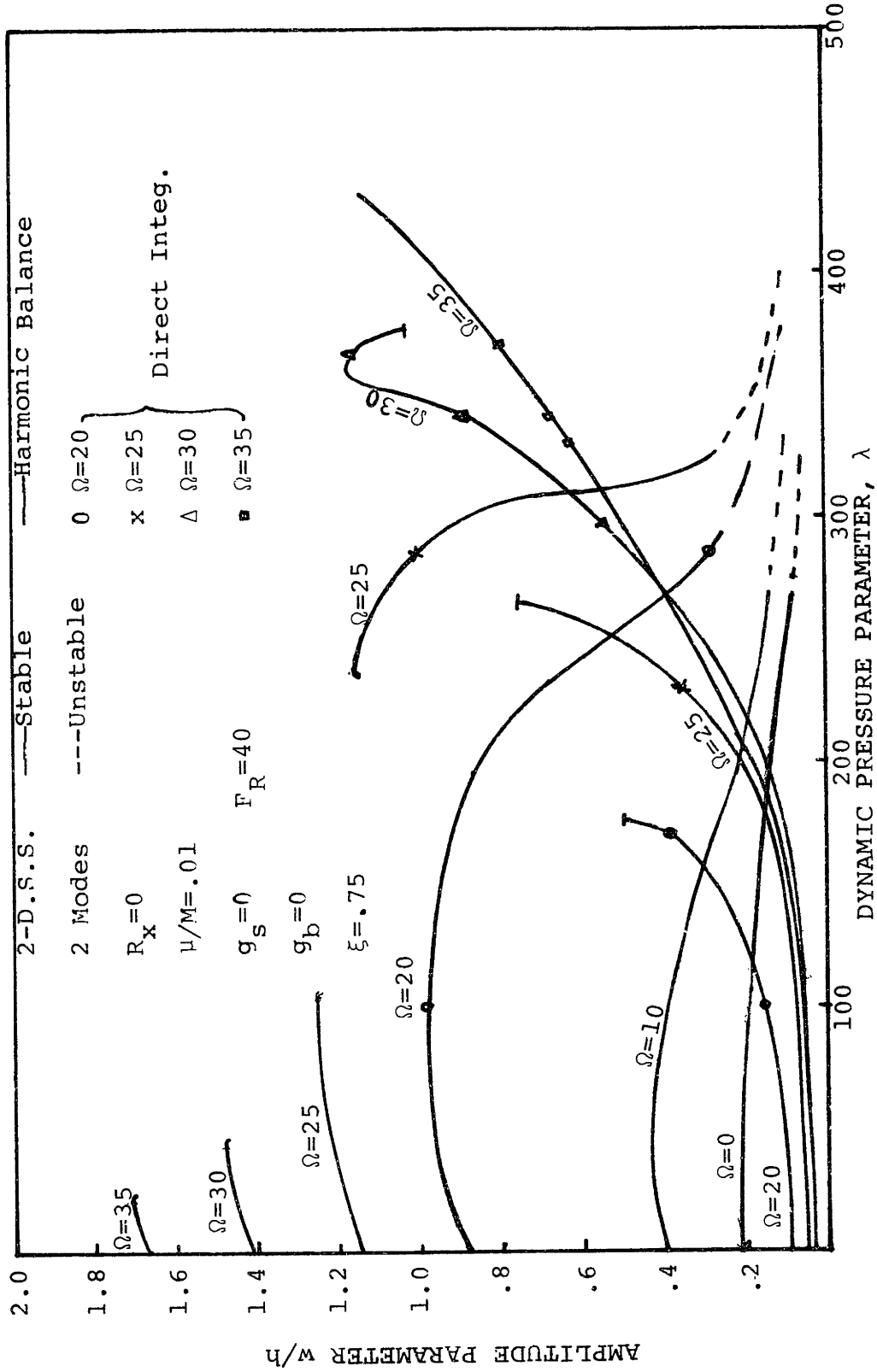


FIG. 43 NONLINEAR FORCED RESPONSE OF A PANEL AT DIFFERENT

FORCING FREQUENCIES

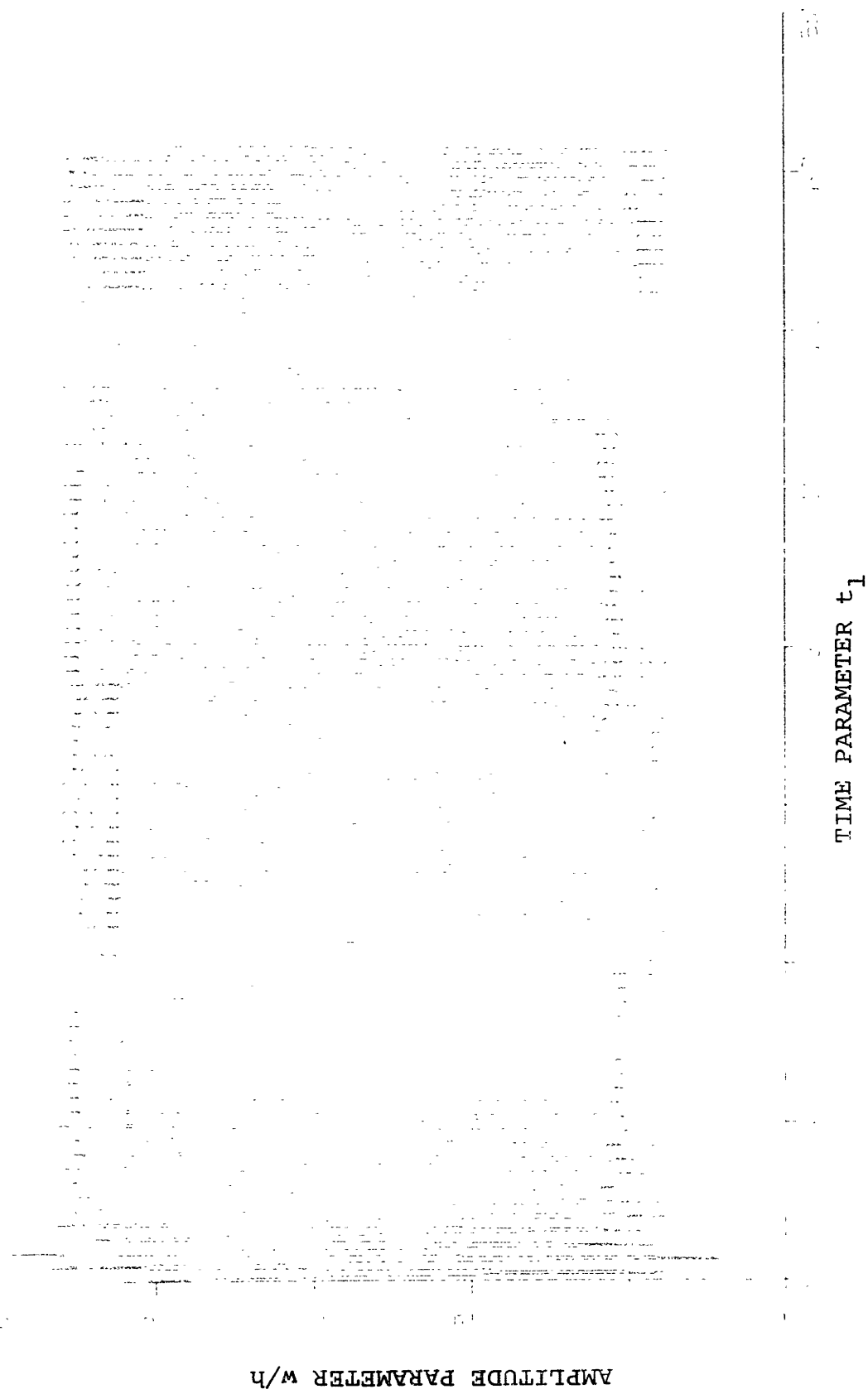
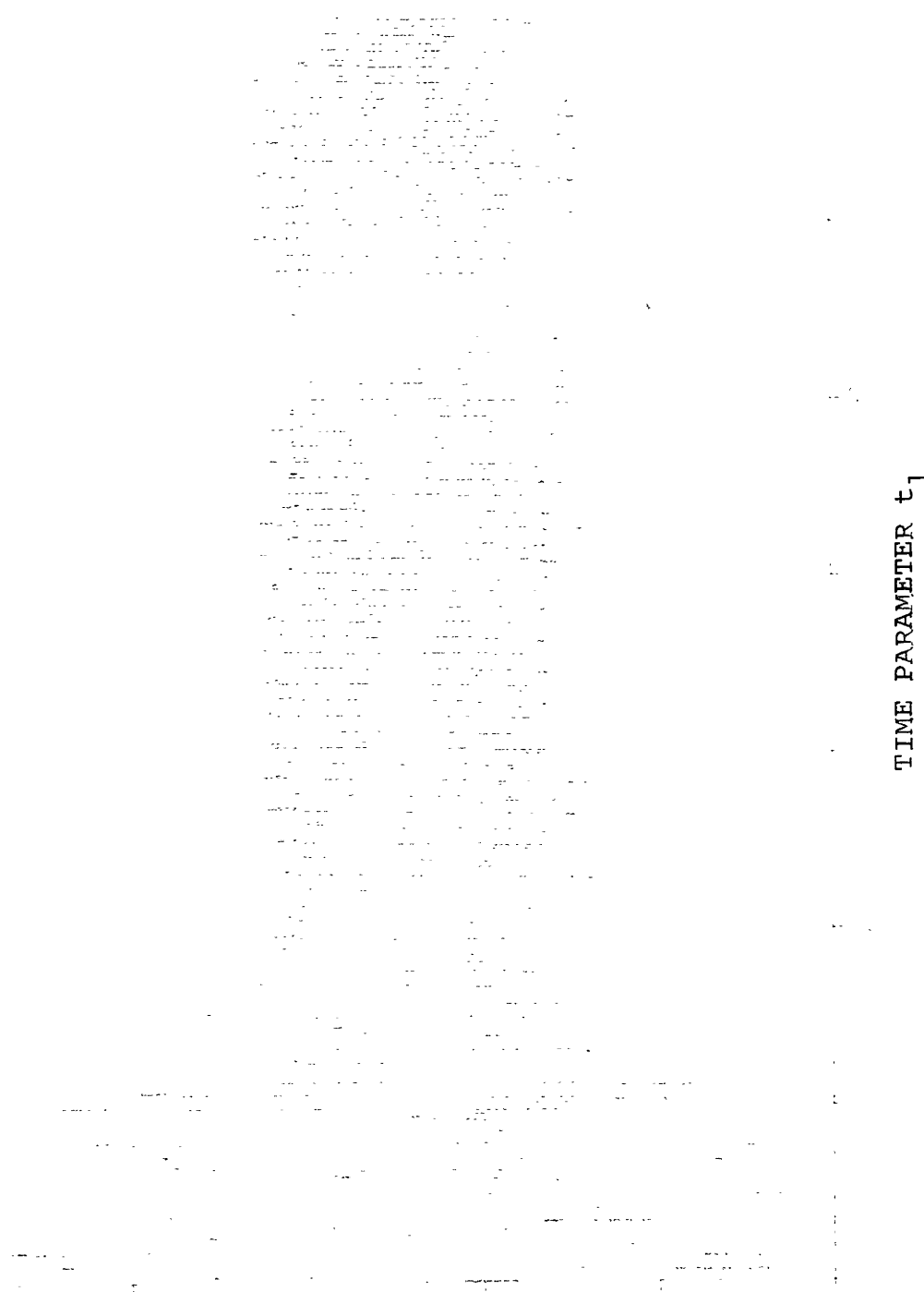


FIG. 44 DIRECT INTEGRATION--PURE FORCED RESPONSE AT  $\lambda=285$ ,  $\Omega=20$ ,  $F_R=40$

AMPLITUDE PARAMETER w/h

TIME PARAMETER  $t_1$



AMPLITUDE PARAMETER

TIME PARAMETER  $t_1$

FIG. 45 DIRECT INTEGRATION--FORCING FLUTTER INTERACTION AT  $\lambda=292$ ,  $\Omega=20$ ,  $F_R=40$

AMPLITUDE PARAMETER  $w/h$



TIME PARAMETER  $t_1$

FIG. 46 DIRECT INTEGRATION--FORCING-FLUTTER INTERACTION AT  $\lambda=295.9$ ,  $\Omega=20$ ,  $F_R=40$

AMPLITUDE  $w/h$

TIME PARAMETER  $t_1$   
(a) PURE FORCING RESPONSE

AMPLITUDE  $w/h$

TIME PARAMETER  $t_1$   
(b) FORCING-FLUTTER INTEGRATION

FIG. 47 DIRECT INTEGRATION--COEXISTENCE OF PURE FORCED RESPONSE AND FORCING-FLUTTER INTERACTION AT  $\lambda = 340$ ,  $\Omega = 40$ ,  $F_R = 40$



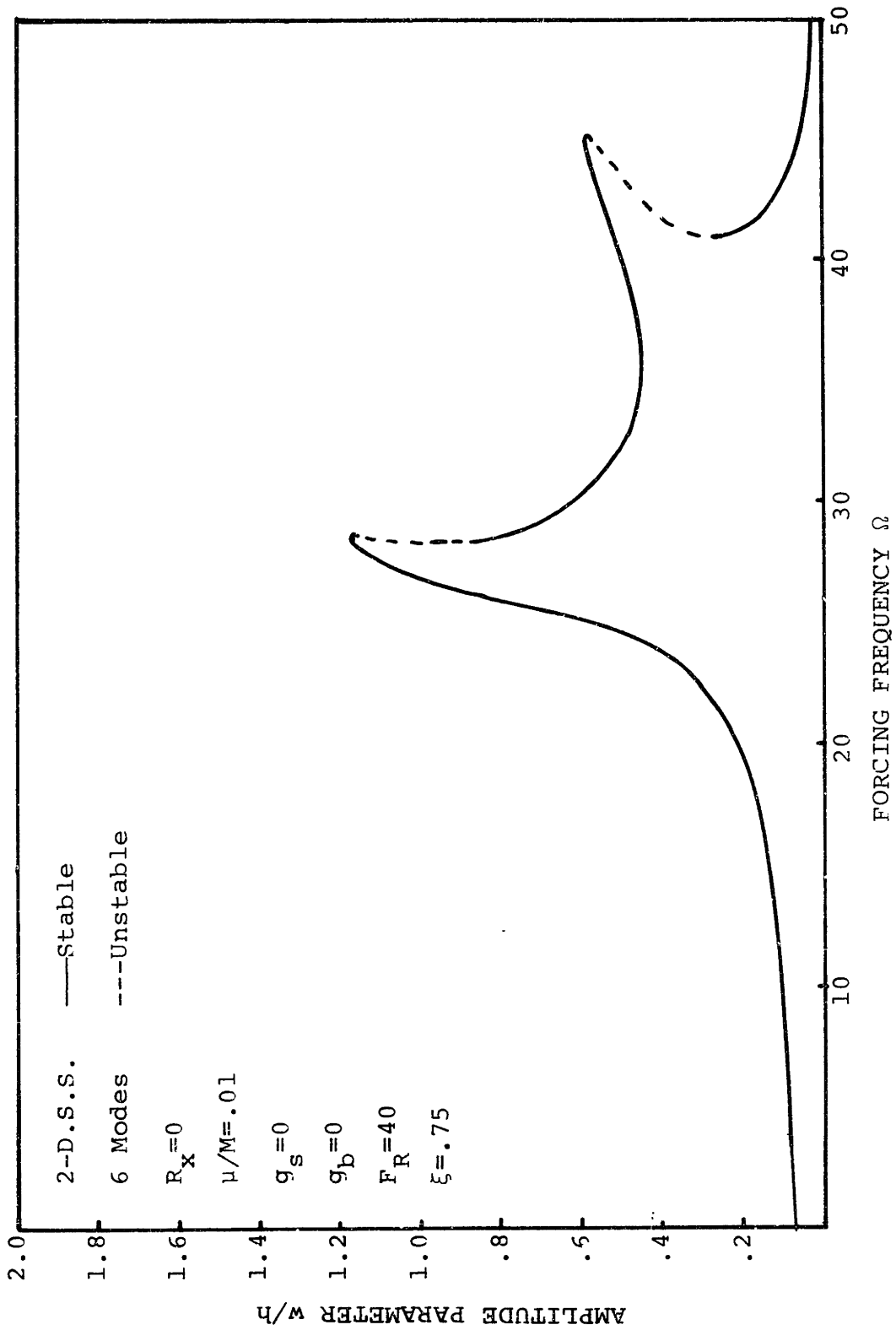


FIG. 48 A SIX-MODE EXAMPLE OF FORCED RESPONSE OF A PANEL AT  $\lambda=\lambda_c=344.2$

REFERENCES

1. Miles, J. W., "Dynamic Chordwise Stability at Supersonic Speeds," North American Aviation Report AL-1140, 1950.
2. Shen, S. F., Flutter of a Two-Dimensional Simply-Supported Uniform Panel in a Supersonic Stream., M.I.T. Aeroelastic and Structures Research Laboratory Report on Contract N5-ori-07833, 1952.
3. Goland, M., and Luke, Y. L., "A Exact Solution for two-dimensional Linear Panel Flutter at Supersonic Speed," J. Aero. Sciences, Vol. 21, No. 4, pp. 275-276, 1954.
4. Easley, J. G., "The Flutter of Rectangular Simply Supported Panels in Supersonic Flow" AFOSR T.N. 55-236, 1955.
5. Nelson, H. C. and Cunningham, H. J., "Theoretical Investigation of Flutter of Two-Dimensional Flat Panels With One Surface Exposed to Supersonic Potential Flow" NACA Report 1280, 1956.
6. Hedgepeth, J. M., "Flutter of Rectangular Simply-Supported Panels at High Supersonic Speeds," Journal of the Aeronautical Sciences, Vol. 24, No. 8, Aug. 1957, pp. 563-573 and p. 586.
7. Dugundji, J., "Theoretical Considerations of Panel Flutter at High Supersonic Mach Numbers," AIAA Journal, Vol. 4, No. 7, July 1966, pp. 1257-1266.

8. Bolotin, V. V. Nonconservative Problems of the Theory of Elastic Stability, MacMillan Co., New York, 1963, pp. 274-312.
9. Kobayashi, S., "Flutter of Simply-Supported Rectangular Panels in a Supersonic Flow--Two-Dimensional Panel Flutter, I--Simply Supported Panel, II--Clamped Panel" Transactions of Japan Society of Aeronautical and Space Sciences, Vol. 5, 1962, pp. 79-118.
10. Dowell, E. H., "Nonlinear Oscillations of a Fluttering Plate I" AIAA Journal, Vol. 4, No. 7, July 1966, pp. 1267-1275.
11. Dowell, E. H., "Nonlinear Oscillations of a Fluttering Plate II," AIAA Journal, Vol. 5, No. 10, Oct. 1967, pp. 1856-1862.
12. Morino, L., Kuo, C. C., Dugundji, J., Perturbation and Harmonic Balance Methods for Nonlinear Panel Flutter, ASRL TR-164-1, Aeroelastic and Structures Research Lab., Dept. of Aeronautics and Astronautics, M.I.T., Cambridge, Mass.
13. Ashley, H. and Zartarian, G. "Piston Theory--A New Aerodynamic Tool for the Aeroelastician," Journal of The Aeronautical Science, Vol. 23, No. 12, Dec., 1956.
14. Cunningham, H. J. "Flutter Analysis of Flat Rectangular Panels Based on Three-Dimensional Supersonic Potential Flow" AIAA Journal, Vol. 1, No. 8, August 1963, pp. 1795-1801.

15. Dowell, E. H. and Voss, H. M., "Experimental and Theoretical Panel Flutter Studies in Mach Number Range 1.0 to 5.0" AIAA Journal, Vol. 3, No. 12, Dec. 1965, pp. 2292-2304.
16. Cunningham, H. J., "Flutter Analysis of Flat Rectangular Panels Based on Three-Dimensional Supersonic Unsteady Potential Flow" TR T-256, 1967 NASA.
17. Dixon, S. C., "Comparison of Panel Flutter Results from Approximate Aerodynamic Theory with Results from Exact Inviscid Theory and Experiment" TND-3649 NASA.
18. Fung, Y. C., "The Flutter of a Buckled Plate in a Supersonic Flow," AFOSR-TN-55-237, July 1955.
19. Fung, Y. C., "On Two-Dimensional Panel Flutter," Journal of the Aeronautical Sciences, Vol. 25, No. 3, March 1958, pp. 145-160.
20. Eisely, J. G. "The Flutter of a Two-Dimensional Buckled Plate with Clamped Edges in a Supersonic Flow," OSR-TN-56-296, Guggenheim Aeronautical Lab., California Institute of Technology, July 1956.
21. Houbolt, J. C., "A Study of Several Aerothermoelastic Problems of Aircraft Structures," Mitteilung aus dem Institute fur Flugzeugstatik und Leichbau, Nr. 5, E.T.H. Zurich, 1958.
22. Fralich, R. W., "Postbuckling Effects on the Flutter of Simply Supported Rectangular Panels at Supersonic Speeds," NASA TN D-1615, March 1965.

23. Olson, M. D. and Fung, Y. C., "Supersonic Flutter of Circular Cylindrical Shells Subject to Internal Pressure and Axial Compression," AIAA Journal, Vol. 4, No. 5, May 1966, pp. 858-864.
24. Evensen, D. A. and Olson, M. D., "Nonlinear Flutter of a Circular Cylindrical Shell in Supersonic Flow," TN D-4265, 1967, NASA.
25. Dowell, E. H., "Nonlinear Analysis of the Flutter of Plates and Shells," ASME Fluid-Solid Interaction Symposium, 1967.
26. Dowell, E. H., "Nonlinear Flutter of Curved Plates II," AIAA Journal, Vol. 8, No. 2, Feb. 1970, pp. 261-263.
27. Kordes, E. E. and Noll, R. B., "Theoretical Flutter Analysis of Flat Rectangular Panels in Uniform Coplanar Flow With Arbitrary Direction" NASA TN D-1156, 1962.
28. Friedmann, P. and Hanin, M. "Supersonic Nonlinear Flutter of Orthotropic or Isotropic Panels with Arbitrary Flow Direction" Israel Journal of Technology, Vol. 6, No. 1-2, 1968, pp. 46-57.
29. Dowell, E. H., "Generalized Aerodynamic Forces on a Flexible Plate Undergoing Transient Motion in a Shear Flow with an Application to Panel Flutter," AIAA Journal, Vol. 9, No. 5, May 1971, pp. 834-841.
30. Johns, D. J., "The Present Status of Panel Flutter," Rept. 486, 1961, Advisory Group for Aeronautical Research and Development.

31. Johns, D. J., "A Survey on Panel Flutter," Advisory Rept. 1, Nov. 1965, Advisory Group for Aeronautical Research and Development.
32. Fung, Y. C., "A Summary of the Theories and Experiments on Panel Flutter," AFOSR TN-60-224, May 1960, Guggenheim Aeronautical Lab., California Institute of Technology, Pasadena, Calif.
33. Fung, Y. C., "Some Recent Contribution to Panel Flutter" I.A.S. Paper No. 63-26.
34. Dowell, E. H., "Panel Flutter: A Review of the Aeroelastic Stability of Plates and Shells" AIAA Journal, Vol. 8, No. 3, March 1970.
35. Sylvester, M. A. and Baker, J. W. "Some Experimental Studies of Panel Flutter at Mach Number 1.3" NACA TN-3914, 1957 (Supersedes NACA RM L52116).
36. Dixon, S. C., "Experimental Investigation at Mach Number 3.0 of Effects of Thermal Stress and Buckling on Flutter Characteristics of Flat Single-Bay Panels of Length-Width Ratio 0.96," NASA TN D-1485, 1962.
37. Stearman, R. G., Lock, M. H. and Fung, Y. C., "Ames Tests on the Flutter of Cylindrical Shells," Structural Dynamics Rept., SM 62-37, 1962, Graduate Aero. Lab., Calif. Inst. of Tech., Pasadena, Calif.
38. Anderson, W. J., "Experiments on the Flutter of Flat and Slightly Curved Panels at  $M=2.18$ ," AFOSR TN 2996, 1962, Guggenheim Aeronautical Lab., California Institute of Technology, Pasadena, Calif.

39. Kappus, H. P., Lemley, C. E. and Zimmerman, N. H., "An Experimental Investigation of High Amplitude Panel Flutter" NASA CR-1837, May 1971.
40. Ventres, C. S. Nonlinear Flutter of Clamped Plates, Ph.D. Thesis, Department of Aerospace and Mechanical Sciences, Princeton University, 1969.
41. Estep, F. E. and McIntosh, S. C., "The Analysis of Nonlinear Panel Flutter and Response Under Random Excitation or Nonlinear Aerodynamic Loading," AIAA/ASME 11th Structures, Structural Dynamics, and Materials Conference, Denver, Colo., April 22-24, 1970, pp. 36-47.
42. Olson, M. D. and Fung, Y. C., "Comparing Theory and Experiment for the Supersonic Flutter of Circular Cylindrical Shells," AIAA Journal, Vol. 5, No. 10, Oct. 1967, pp. 1849-1856.
43. Morino, L., "A Perturbation Method for Treating Nonlinear Panel Flutter Problems," AIAA Journal, Vol. 7, No. 3, March 1969, pp. 405-411.
44. Morino, L. and Kuo, C. C., Detailed Extensions of Perturbation Methods for Nonlinear Panel Flutter, ASRL TR 164-2, Aeroelastic and Structures Research Lab., Dept. of Aeronautics and Astronautics, M.I.T., Cambridge, Mass.
45. Librescu, L., "Aeroelastic Stability of Orthotropic Heterogeneous Thin Panels in the Vicinity of the Flutter Critical Boundary," Journal de Mechanique, 4, 1, 1965, pp. 51-76.

46. Dzygadło, Z., "Local Analysis of Nonlinear Forced Vibrations of a Plate of Finite Length in Plane Supersonic Flow" Proceedings of Vibration Problems, 4, 11 (1970), Warsaw.
47. Duncan, W. J., "Galerkin's Method in Mechanics and Differential Equations," British A.R.C., R and M, 1798-1937.
48. Dowell, E. H., "Fatigue Life Estimation of Fluttering Panels" AIAA Journal, Vol. 8, No. 10, Oct. 1970, pp. 1879-1881.
49. Tseng, W. Y., Nonlinear Vibrations of Straight and Buckled Beams Under Harmonic Excitation, M.I.T. Aeroelastic and Structures Research Lab Report TR 159-1, Air Force Office of Scientific Research AFOSR 69-2157 TR, November 1969.
50. Dugundji, J. and Hore, P. Brief Handbook For the Sum of Two Harmonics, AFOSR 70-2515 TR, ASRL TR-159-2, Aeroelastic and Structures Research Lab., Dept. of Aeronautics and Astronautics, M.I.T.
51. Stoker, J. J., Nonlinear Vibrations in Mechanical and Electrical Systems, Interscience Publishers, Inc., New York, 1954.



BIOGRAPHICAL NOTE

Ching-Chiang Kuo, chinese original name 郭清江, was born on December 28, 1942, at Chu Nan, Taiwan. He received his B.S. degree in Civil Engineering from Cheng Kung University, Taiwan, in 1965. He served in the Chinese Air Force as a Second Lieutenant from July 1965 to July 1966. He entered the University of Iowa at Iowa City in September 1966 and obtained his M.S. degree in February 1968. He came to the department of Aeronautics and Astronautics at M.I.T. as a doctoral candidate in September 1968.

Mr. Kuo is married to the former Ju-pi Chen of Tao-yen, Taiwan.